The Structure, Mechanism and Inhibition of Dihydropteroate synthase from *Streptococcus pneumoniae*.

Helen G. Vinnicombe

Declaration

A thesis submitted to the University of Manchester Institute of Science and Technology for the degree of Doctor of Philosophy. September 1997.

No portion of the work referred to in this thesis has been submitted in support of an application for another degree or qualification of this or any other university, or institute of learning.

Acknowledgements.

The author wishes to thank Dr. J. P. Derrick for his continued advice and guidance, also for his help during the preparation of this thesis. Thanks are also due to Benjamin Stapley for circular dicroism measurements and to my colleagues for their many discussions.

The use of the facilities of the Biochemistry Department of the University of Manchester Institute of Science and Technology, the SRS at Daresbury, Cheshire and financial support from the BBSRC are all gratefully acknowledged.

Finally the author wishes to thank Dr. F. Amini and her family for their patience, encouragement and support during the past three years.

Abbreviations.

The following abbreviations have been used:-

p-ABA	*para* - Aminobenzoic acid
Bis	N, N'- methylenebisacrylamide
BSA	Bovine serum albumin
bp	base pair
Ci	Curies
cpm	counts per minute
DEAE-Sephacel	Diethylaminoethyl - Sephacel
DHFR	Dihydrofolate reductase
DHFS	Dihydrofolate synthase
DHNA	Dihydroneopterin aldolase
DHPS	Dihydropteroate synthase
Dihydrofolate	Dihydropteroyl-L-Glutamic acid
Dihydropteroate	2-Amino-4-hydroxy-6-pyrophosphorylmethyl-7,8-dihydropteridine
DMSO	Dimethylsulphoxide
DTT	Dithiothreitol
EDTA	Ethylene diaminetetra-acetate
Folate	Pteroylglutamic Acid
FPLC	Fast protein liquid chromatography
HEPES	(N-[2-Hydroxyethyl]piperazine-N'-[2-ethanesulfonic acid])
HPPK	6-hydroxymethyl-7,8-dihydropterin pyrophosphokinase
IPTG	Isopropanol β-D-thiogalactopyranoside
kDa.	kilodalton
MES	(2-[N-Morpholino] ethanesulphonic acid)
MOPS	(3-[N-Morpholino] propanesulphonic acid)
MPD	2-Methyl-2,4-pentane diol
MTX	Methotrexate [(+) Amethopterin]

PBP	Penicillin binding protein
PCR	Polymerase chain reaction
PEG	Polyethylene glycol
PEI	Polyethylenimine
Pterine	2-Amino-4-hydroxylpteridine
Pterin pyrophosphate	7,8-dihydroxy-6-methylpterin pyrophosphate
rpm	revolutions per minute
SA	Sulphanilamide
SAA	Sulphanilic Acid
SDS	Sodium dodecylsulphate
SDS-PAGE	Sodium dodecylsulphate polyacrylamide gel electrophoresis
SMX	Sulphamethoxazole
SP	Sulphaphenazole
STZ	Sulphathiazole
SQ	Sulphaquinoxaline
TEMED	N, N, N', N' - tetramethylethylenediamine
Tetrahydrofolate	5,6,7,8-Tetrahydropteroyl-L-Glutamic Acid
Tris	2-Amino-2-hydroxymethylpropane-1,3-diol

Abstract.

Dihydropteroate synthase (DHPS; E.C. 2.5.1.15) catalyses the condensation of 7,8-dihydroxy-6-methylpterin pyrophosphate with *para*-Aminobenzoic acid (pABA); a key step in the folate biosynthesis pathway. It is also the target for inhibition by the sulphonamide class of antimicrobial drugs. Recombinant DHPS from *Streptococcus pneumoniae* has been expressed in *E. coli*, purified to homogeneity in milligram quantities and confirmed as a dimer with a monomeric molecular weight of 34kDa. Crystals of the DHPS apoprotein have been grown using macroseeding techniques. The crystals diffract beyond 2.8Ang and are of spacegroup $P2_12_12_1$ or an enantiomorph. (a=47.58, b=90.3 & c=138.42Ang.) Further crystallisation experiments established different sets of conditions for the crystallisation of binary complexes with each of the two substrates, 7,8-dihydroxy-6-methylpterin pyrophosphate and pABA, a sulphonamide (sulphamethoxazole) and sodium pyrophosphate. Ternary complex crystals of 7,8-dihydroxy-6-methylpterin pyrophosphate and benzoic acid as an analogue of *para*-aminobenzoic acid have also been grown.

A novel binding assay has been developed using immobilised DHPS to obtain equilibrium binding constants for pABA, dihydropteroate, pyrophosphate and a range of sulphonamides. The results of the equilibrium binding experiments show that the binding of pABA to DHPS is absolutely dependent on the presence of pyrophosphate, which can be used as an analogue of the real second substrate 7,8-dihydroxy-6-methylpterin pyrophosphate. K_d values of 830nM and 115μM were obtained for pABA and pyrophosphate respectively. The binding affinity for dihydropteroate was similar to pABA, with a K_d of 510nM. The K_ds for a range of sulphonamides were determined by competition with pABA and were shown to lie in the range of 490nM (sulphaphenoxazole) to 38.9μM (sulphanilamide). Hummel and Dreyer equilibrium binding experiments confirmed these results and a fixed order has been proposed for the binding of substrates by *S. pneumoniae* DHPS with 7,8-dihydroxymethylpterin pyrophosphate binding first and pABA second. The release of products is proposed to occur in a random manner.

The steady state kinetics of DHPS were investigated: the K_m for pABA was independent of the concentration of 7,8-dihydroxy-6-methylpterin pyrophosphate and vice versa. The kinetic data were better described by a random order-type mechanism, rather than the fixed order indicated by the equilibrium binding studies. Possible reasons are discussed. The inhibition properties of a range of sulphonamides were investigated and in each case inhibition was competitive with respect to pABA. Lower K_i values were obtained using sulphonamides with larger substituents on the sulphate group, in agreement with the equilibrium binding experiments. The inhibition of DHPS by a range of other pABA and folate analogues was also studied. The results show that the current assumption of a random order kinetic mechanism for DHPS may only pertain under certain conditions, and that a fixed order of substrate addition, with 7,8-dihydroxy-6-methylpterin pyrophosphate binding first, can also occur. It is also clear that different substituents on the sulphate group play an important part in the bindng of sulphonamides to DHPS. These results, combined with the recent crystal structures of DHPS from *E. coli* and *Staphylococcus aureus*, pave the way for a more rational approach to the design of folate-based antimicrobial drugs.

Contents.

List of Figures.

List of Tables.

Chapter 1 Introduction.

Medical advances in the form of vaccines, effective public health programs and improvements in living standards, sanitation, hygiene and nutrition have been instrumental in reducing the incidence of infectious diseases. Exploitation of antigenic components of microbes have yielded improved, safer vaccines and their secondary metabolites have provided countless different antibiotics, sometimes after modification to improve the pharmacokinetic properties, safety or potency for human and animal use. There are now thirteen main classes of antibacterial/antibiotic agents which affect bacterial growth and reproduction in a variety of different ways. In 1969, it was wrongly believed that hospital wards containing patients with bacterial infections were a thing of the past. [Bloom, 1992)] In America between 1910-1920 one person in every 1000 died from infection with *Mycobacterium tuberculosis*. However, even today this bacterial species alone continues to kill an estimated three million people each year, mainly in the third world. [Brickner, (1997)]

Penicillin, the most well known of the antibiotics, inhibits the synthesis of bacterial cell walls, whilst others prevent bacterial protein synthesis by interfering with the activity of the 50S ribosomal subunit (e.g. Erythromycin, a macrolide) or the 30S ribosomal subunit (e.g. Tetracycline and the aminoglycosides). [Wingard, (1991)] Trimethoprim and the sulphonamides are antibacterial agents that specifically inhibit folic acid metabolism in micro-organisms and not in animals. Fluoroquinolones, more recently developed, comprise a class of totally synthetic antibacterial agents that inhibit DNA gyrase preventing the replication of the bacterial genome. [Thomson, *et al.* (1997)]

Infectious diseases, despite the vast array of antibiotics and antibacterial drugs, remain the largest cause of death in the world, greater than cancer or cardiovascular disease. The World Health Organisation estimated in 1991 there were 4.3 million deaths in children from acute respiratory diseases alone. [Neu, (1992), Cohen, (1992)]

1.1 Problems of widespread antibiotic resistance.

Despite the successes of the past 50 years, the introduction of each new drug was often quickly followed only a few years later by the appearance of resistant organisms. Previously there have always been newer and more effective drugs to use.

In the last 10 years or so however, the frequency of resistance to antibiotics and the spectrum of resistant infections has increased in both the hospitals and the community at large. This increased frequency has been blamed on a combination of bacterial evolution, selective pressure on bacteria due to antimicrobial use and over-use, and changes within society which have increased the transmission of these drug resistance organisms.

1.1.1 Microbial evolution.

Bacteria have devised numerous ways to defeat antibiotic action. By developing the capability to hydrolyse, acetylate or phosphorylate the drug, bacteria can render it inactive; examples of this are the expression of β-lactamase and aminoglycoside-inactivating enzymes in the periplasmic space of bacteria. [Neu, (1997)] The target site for the antimicrobial agent can be altered or the intracellular concentration of the drug can be reduced by actively pumping the drug out of the cell or decreasing the permeability of the cell membrane. One or several of these adaptations can evolve in bacteria by point mutations in the chromosome, e.g. the single amino acid alterations in the dihydrofolate reductase gene decreases the sensitivity of the expressed enzyme for the folate synthesis drug trimethoprim [Dale, *et al.* (1997)], or the induction of a previously latent chromosomal or plasmid-encoded gene. [Radstrom & Swedberg, (1988)] Resistance can also develop by the transfer of DNA via transduction (infection with a bacteriophage), transformations (exchange of DNA between bacteria of the same species) or conjugation by plasmids. Transposons may also transmit plasmid or chromosomal genes to bacteria of different species. It is thought that some antibiotics can actually induce the transfer of resistant, plasmid-encoded genes. [Brickner, (1997)] Gram positive species of bacteria can transfer resistance to Gram negative species, but the reverse is uncommon due to the presence of the peptidoglycan layer. [Wingard, (1991)]

Neisseria meningitidis is believed to have acquired new penicillin binding proteins (PBPs) by gene transfer and β-lactamase production encoded on plasmids from commensal organisms. [Neu, (1992)]

1.1.2 Selection pressures.

Drug-resistant strains are believed to be as virulent as sensitive strains. In some cases however, prior antimicrobial exposure is an important risk factor in the ability of resistant strains to cause disease.

One of the most important consequences of resistance to antimicrobial drugs is that the resistance itself can lead to an increase in the incidence of disease. A patient infected with a multidrug-resistant strain of a disease who is improperly treated continues to present a risk of transmission. A susceptible strain similarly treated would present no further opportunity for transmission. [Neu, (1992)] Another serious effect of administration of antimicrobial drugs to a patient carrying a resistant organism is that the drug provides a selective advantage to that resistant organism by killing off all other competing organisms in the host. [Bloom, *et al.* (1992), Cohen, (1992)] Consequently resistant organisms are also excreted in the faeces of patients in larger numbers, for longer periods and have more time and opportunity for transmission to another animal host.

1.1.3 Societal changes.

A series of changes within society have provided enhanced opportunity for the transmission of certain organisms. Improvements in travel now enable the transport of food and people from one continent to another in a matter of hours and this includes the import/export of resistant organisms. Little improvement in sanitation and hygiene in the developing world increases the frequency of infection by resistant organisms from developed countries, along with the lack of readily available antibiotics. In the developed world, demographic changes show an increasingly aging population at risk of infection along with a rise in immunocompromised patients e.g. AIDS patients and those undergoing chemotherapy. For example, *Pseudomonas aeruginosa* is a major cause of infection in patients with reduced white cell counts as a result of chemotherapy. All *P. aeruginosa* strains contain inducible, chromosomally-mediated cephalosporinases. [Neu, (1992)]

Aminoglycosidase-inactivating enzymes are also common. This makes the treatment of these infections very difficult. Economic changes, whilst improving general standards of sanitation, hygiene and nutrition have also created distinct reservoirs for infections in situations of over-crowding and homelessness.

Cholera is currently a major problem in South and Central America where some bacterial isolates have been found to be resistant to most available antibiotics. In some countries, specifically the US, the closure of centres for the treatment of infectious diseases like tuberculosis has been implicated in the increasing incidences of this disease and others where treatment is largely community, rather than hospital-based. [Bloom, (1992)] A sudden increase in the transmission of sexually-transmitted diseases followed the changes in sexual behaviour in the 1960s and soon after to the emergence of drug-resistant organisms. Penicillin was the drug of choice for the treatment of gonorrhea but as a result of a chromosomal mutation reducing the affinity of the drug for PBPs, the dosage had to be increased. [Wingard, (1991)] In 1992 in the Phillipines and Thailand, over 90% of *Neisseria gonorrhea* species produce β-lactamases, and in New York 42% of these organisms are resistant to penicillin. [Neu, (1992)] Nowadays the concentrations of cephalosporins necessarily administered to cure infection are on the increase.

From the 1980s the increased transmission of certain infectious diseases have been linked to the increased use of cocaine. Methicillin-resistant *Staphylococcus aureus* (MRSA) became a problem in the US in day-care centres amongst habitual drug users. [Neu, (1992)] The recent rapid rise in the incidence of multiple antibiotic-resistant pathogens is now a serious concern around the world, arising from the evolutionary capabilities of bacterial populations. Bacteria can evolve markedly within a single human lifetime. The sudden appearance of new bacterial clones means that in just 50 years the chromosomal DNA sequence of a representative pathogen can change significantly from those seen historically to those seen at the present day.

In 1941, almost all strains of *S. aureus* worldwide were susceptible to antibiotics, specifically penicillin G. By 1944, *S. aureus* had evolved the capability to produce a β-lactamase and today over 95% of clinical isolates are resistant to penicillins. [Neu, (1992)]

MRSA is now resistant to all β-lactam antibiotics- penicillins, cephalosporins and carbapenems. Vancomycin, a glycopeptide which inhibits late stages of bacterial cell wall peptidoglycan synthesis, was then used as the only effective treatment for infections. Now vancomycin-resistant enterococci have appeared, presumably as a consequence of overexposure to this drug. [Brickner, (1997)]

Streptococcus pyogenes has remained largely susceptible to penicillins although the concentrations required to kill the organism have risen over the past 20 years. [Neu, (1992)] β-lactamase-producing Enterococci are also now found in many parts of Europe and the US and consequently high levels of resistance. Aminoglycosides are now used in combination with penicillins to try to defeat these organisms. [Brickner, (1997)]

It is clear that the very drugs once believed capable of erradicating serious microbial infections have contributed to the evolution of resistance, to some extent, in most bacterial pathogens. The main factors in this evolution have been the inappropriate prescription of antibiotics for viral infections or when they are not necessary and the incompletion of the full course of treatment producing conditions that select for drug-resistance in a bacterial population. [Bloom & Murray, (1992)]

Ways to stem the tide of resistance include hygienic practices to prevent the spread to multidrug-resistant bacteria within hospitals, efforts to decrease the unnecessary use of antimicrobial drugs both in humans and animal feeds and the rapid diagnosis of infections to direct the use of narrow-range antibiotics rather than broad-spectrum antibiotics currently used. These methods all aim to disrupt the transmission of infectious organisms and to preserve the dwindling arsenal of drugs still available for the treatment of present diseases. However one of the best ways to prevent infection and stop evolution of resistance mechanisms is the development of effective vaccines, especially for those infections which are currently difficult to treat. However this method is made very difficult in some organisms by their capacity for antigenic variation and is an extremely time-consuming procedure. The need for new antimicrobial therapies is now more important than ever, together with the necessity for a comprehensive understanding of the effect of the drug on its target.

The rapid development of molecular biology techniques now allows the interactions of the drug with its target molecule to be studied in detail permitting a more rational approach to synthetic drug design. [Neu, (1992), Cohen, (1992)] One new approach to the study of microbial pathogenesis is the use of genomics. [Strauss & Falkow, (1997)] There are an increasing number of complete microbial gene sequences which can be compared and the minimum gene set required for cellular activity compiled. This type of list represents the metabolic core of reactions for cells living in similar environments. When this type of analysis is carried out with pathogenic organisms, the resulting gene set, subtracted from the complete genome, should reveal distinct genotypic characteristics that include virulence factors. Many such factors are found as discrete genes often displaying a distinct codon usage and / or a different overall base composition from the core chromosomal genes which are absent from non-pathogenic members of the same species. Some pharmaceutical companies have begun to channel their efforts in this direction in an attempt to discover novel genes enabling bacterial pathogens to circumvent the host immune system. [Strauss & Falkow, (1997)]

1.2 *Streptococcus pneumoniae* - role in microbial pathogenesis.

S. pneumoniae are gram-positive bacteria normally present at low levels in the upper respiratory tract. Rapid multiplication of these bacteria in the alveolar spaces of the lungs causes lobar pneumonia. This microorganism is also responsible for other invasive diseases including septicaemia, bacteraemia, arthritis and otitis media. Although these diseases can affect people of all ages, they are most common in the elderly or very young. Diagnosis is by culture, chest X-ray and treatment has commonly been penicillin G. Of all respiratory diseases described as pneumonia, 60-80% are caused by this single organism alone which translates into over 300 000 cases in the U.S. per year and 40 000 deaths. [Wingard, (1991), Brickner, (1997)] Resistance of *S. pneumoniae* to antibiotics was first noted in South Africa in 1977 and the fast rising prevalence of penicillin resistant *S. pneumoniae* infections is now a real problem. The administration of 40 000 units of penicillin per day cured patients of pneumococcal pneumonia in 1941. By 1992 the administration of 24 million units was no guarantee of survival from the disease. [Neu, (1992), Cohen (1992)

One of the worst situations is in Hungary where 70% of the *S. pneumoniae* isolates from children tested between 1988-1989 were resistant to penicillin. [Marton, *et al.* (1991)] The mechanism of penicillin resistance in *S. pneumoniae* often involves the development of altered forms of penicillin-binding proteins (PBPs) which have a lower affinity for the β-lactam class of antibiotics. [Sifaoui, *et al.* (1996), Pares, *et al.* (1996)] There has also been a significant rise in the number of *S. pneumoniae* isolates resistant to antibiotic treatment in Canada [Simor, *et al.* (1996)] France, Belgium and the U.K. [Neu, (1996) Thomson, *et al.* (1997)] Pneumococci can be serotyped and some are more commonly resistant than others. The spread of resistance can be monitored and a serotype 23F strain which caused outbreaks of pneumococcal disease in Spain has recently been recognised in certain parts of America. This has implications for the treatment of disease because the strains resistant to penicillin are also less susceptible to broad-spectrum cephalosporins. Moreover the resistance of *S. pneumoniae* to the macrolide group of antibiotics is increasing due to the production of a plasmid-mediated enzyme which methylates an important adenine residue in the 23S rRNA. [Neu, (1992)] This prevents the binding of erythromycin and other macrolides. This group of antibiotics have not been widely administered in the US so far, which may explain the current susceptibility of strains of *S. pneumoniae*. However the newly developed macrolides - azithromycin, clarithromycin and roxithromycin are likely to increase macrolide-resistant *S. pneumoniae* in the US in the coming years.

S. pneumoniae is also a major cause of bacterial meningitis together with *Neisseria meningitidis* and *Haemophilus influenzae*, type B. Carriers and active cases of meningitis can transmit bacteria through air by respiratory secretions. The bacteria colonise the nasopharynx area, cross the mucosa and enter the bloodstream. When they reach the cerebrospinal fluid, the bacteria produce inflammation of the meninges. Within hours of the first sign of symptoms, meningococcal disease can develop into meningitis or septicaemia with the subsequent risk of death. [Peltola, (1983)] Current treatment relies upon the swift diagnosis and administration of broad-spectrum antibiotic - cephalosporin. [Viladrich, *et al.* (1996) Kristiansen, *et al.* (1986), (1991), (1995)]

A three-year study of paediatric meningitis showed that meningitis occurred in 76% of all infections by *N. meningitidis*, 16% of all infections by *S. pneumoniae* and 56% of all infections by *H. influenzae*. [Dagan, *et al.* (1994)] Meningococcal disease is endemic and epidemic in many parts of the world. Unlike *S. pneumoniae*, *N. meningitidis* and *H. influenzae* are gram-negative cocci. The first indications of reduced sensitivity of *N. meningitidis* to sulphonamides were seen soon after their introduction in 1932 and an increase in resistance was observed during the epidemics of World War II. [Peltola, (1983)]

H. influenzae is an obligate parasite which occupies the mucus membranes and as such causes chronic bronchitis, sinusitis, conjunctivitis and otitis media as well as meningitis. Meningitis caused by *Haemophilus influenzae* was successfully treated with ampicillin until the mid-1970s when a plasmid-mediated β-lactamase first appeared. In 1986, data indicated that 32% of *H. influenzae* isolates were resistant to ampicillin. [Cohen, (1992)] Resistance to rifampin has developed in patients receiving the drug for the prevention of meningococcal meningitis. In the US most *H. influenzae* are still susceptible to TMP/SMX (folate biosynthesis inhibitors) and certain cephalosporins with iminomethoxy or propyl carboxy moieties on the β-acyl side chain. [Neu, (1992)] Like *S. pyogenes*, most strains of *N. meningitidis* remain susceptible to penicillin but the concentrations needed to kill meningococci have increased. [Peltola, (1983)]

The recent rapid rise in multiple-resistant bacterial infection worldwide has highlighted the need for a better understanding of bacterial drug targets and the mechanism of drug action on target molecules. There is a fast-growing requirement for new pharmacological agents with greater specificity and potency.

1.3 Elucidation of the folate biosynthesis pathway.

All cells require reduced folate cofactors for the synthesis of a variety of essential nutrients. Folate compounds can be captured from the diet or environment by all mammals and most micro-organisms using membrane-associated folate transport proteins. [Henderson & Huennekens (1986)]

However folate is biosynthesised in all plants and micro-organisms with the exception of the methanogenic bacteria which utilise tetrahydromethanopterin instead of tetrahydrofolate as the carrier of one-carbon fragments. For this reason, enzymes of the folate biosynthetic pathway have been and still are potential targets for antibacterial drugs.

The folate pathway was gradually revealed when *para*-aminobenzoic acid (pABA) was found to reverse the inhibitory effects of sulphanilamide on bacterial cell growth. [Woods, (1940) Fildes, (1940) Selbie, (1940)] Extracts from *Lactobacillus arabinosus* were found to contain enzymes which, with ATP, could form pteroic acid (from pABA) or folic acid (from *para*-aminobenzoylglutamic acid), using different pteridine precursors. [Shiota, *et al.* (1959)] In the same year, pteroic acid was postulated to be an intermediate in the biosynthesis of folate in *E. coli.* [Brown, *et al.* (1959)] The first scheme for the biosynthesis of dihydrofolic acid was published two years later. [Brown, *et al.* (1961)] Enzymes from cell-free extracts were separated into two fractions by chromatography. Fraction A contained an enzyme which catalysed the formation of an intermediate compound from ATP and pteridine. Fraction B contained an enzyme which would react with pABA to convert the intermediate into dihydropteroic acid. [Weisman & Brown (1964)] The activity in Fraction A was later named hydroxymethyl-dihydropteridine pyrophosphokinase (HPPK) and the intermediate was the pyrophosphate ester of hydroxymethylpteridine. [Disraely & McCann (1964)] Fraction B was named dihydropteroate synthase (DHPS). [Shiota, *et al.* (1964), Richey & Brown (1969)] See Figure 1.1. At the head of the pathway, a guanosine nucleotide was proposed as a direct precursor of pteridine compounds. [Reynolds & Brown (1964)] Guanosine triphosphate (GTP) was later confirmed as that precursor molecule. [Mathis & Brown (1970)] GTP cyclohydrolase I (GTPCH) is now known to catalyse the first committed step in the biosynthesis of tetrahydrofolate compounds in bacteria. It catalyses the formation of dihydroneopterin triphosphate from GTP. An as yet unidentified phosphatase is believed to remove the phosphate residues to form dihydropteridine, and dihydroneopterin aldolase (DHNA) catalyses the loss of glycoaldehyde to form hydroxymethyl-dihydropteridine. [Lopez, *et al.* (1993)]

Figure 1.1 The folate biosynthesis pathway.

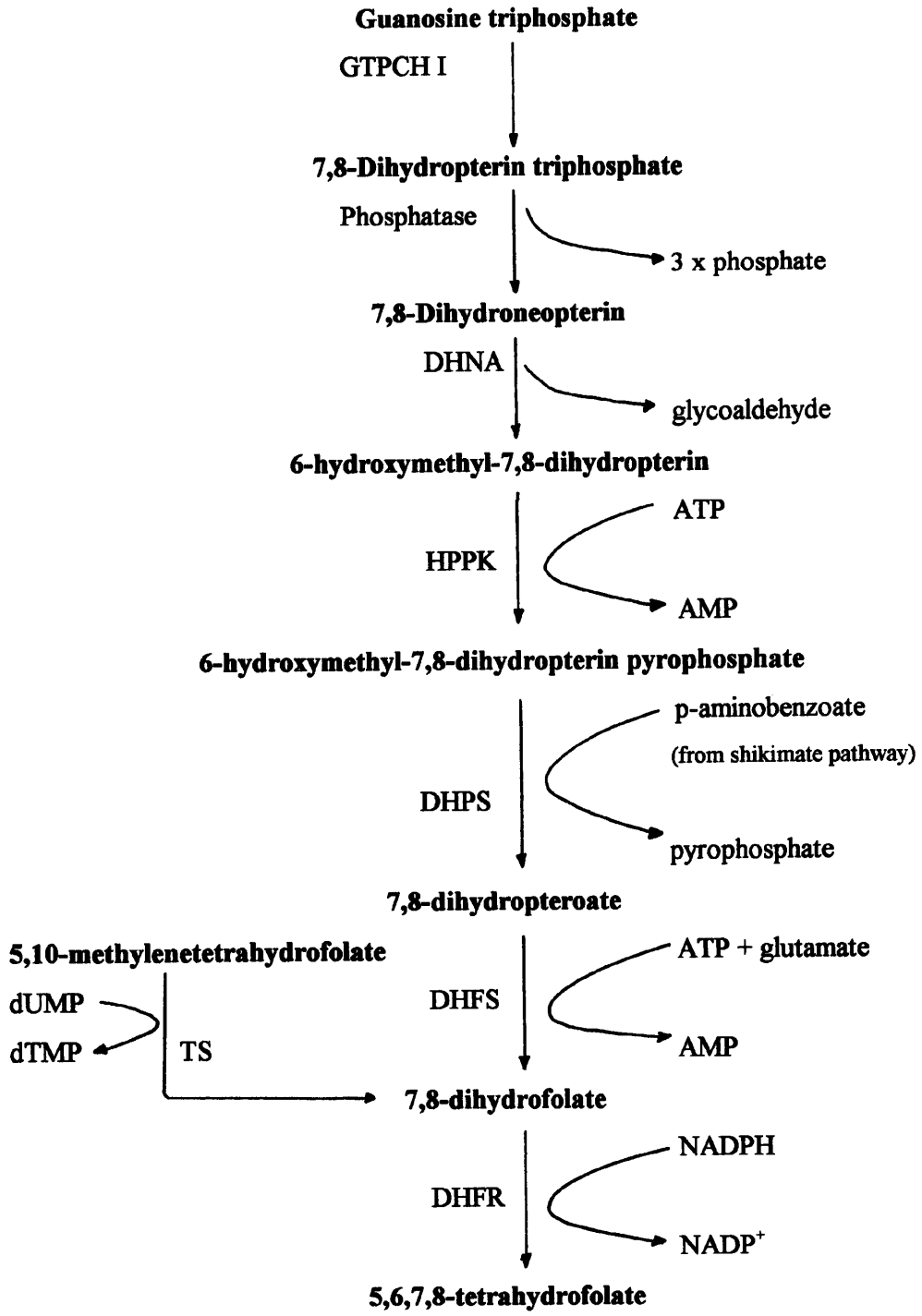

GTP cyclohydrolase I occurs in mammals for the biosynthesis of tetrahydrobiopterin, a cofactor in the hydroxylation of aromatic amino acids and possibly the cytokine-mediated proliferation of T-lymphocytes. [Meining, *et al.* (1995)] Further steps were elucidated with dihydrofolate synthase (DHFS) catalysing the addition of glutamate to dihydropteroic acid forming dihydrofolate. [Webb & Ferone (1976)] Dihydrofolate is also formed in the reaction catalysed by thymidylate synthase (TS). [Friedkin, (1963), Blakley & Benkovic (1984)] Dihydrofolate reductase (DHFR) catalyses the reduction of dihydrofolate to tetrahydrofolate using NADPH. [Blakley, (1969), Dale, *et al.* (1995)] Aside from the folate pathway, TS and DHFR also catalyse sequential reactions in the synthesis of thymidine 5'-monophosphate for DNA synthesis. [Basco, *et al.* (1995), Trujillo, *et al.* (1996), Pawelczak, *et al.* (1993), Foote, *et al.* (1990)]
By 1964 the formation of di- and tri-glutamate derivatives of pteroic acid had been revealed. [Griffin & Brown (1964)] Tetrahydrofolate-polyglutamate compounds are important cofactors for a variety of enzymes catalysing one-carbon metabolic reactions. [Mahler & Cordes (1966)] As a result, a number of other pathways such as those involved in the metabolism of methionine, serine, glycine, purine and thymidylate are all dependent on a continuous supply of these cofactors. [Bognar, *et al.* (1985), (1987) Pelletier & Mackenzie (1995)] Therefore when folate biosynthesis is inhibited, bacterial cell growth is halted. [Wingard, (1991)]

1.4 Dihydropteroate synthase (DHPS, E.C. 2.5.1.15)

DHPS catalyses the formation of a carbon-nitrogen bond between pterin pyrophosphate and pABA by displacement of pyrophosphate to create dihydropteroate. [Figure 1.2]
The *S. pneumoniae* DHPS gene *SulA* has been cloned, sequenced and shown to constitute dihydropteroate synthase by enzyme activity measurements, amino-terminal sequencing of the polypeptide product and expression in minicells of *Bacillus subtilis*. The gene was cloned into an *E. coli* expression vector, shown to encode a 34kDa. polypeptide and the enzyme purified. [Lopez, *et al.* (1987)] Native streptococcal DHPS is believed to be a homodimer or trimer. A mutant dihydropteroate synthase (*sul-d*) gene was isolated which contained an insertion of a six bp segment (Ile-Glu) at position 68 of the wild type sequence (*sul-s*). [Figure 1.3]

Figure 1.2 The DHPS reaction.

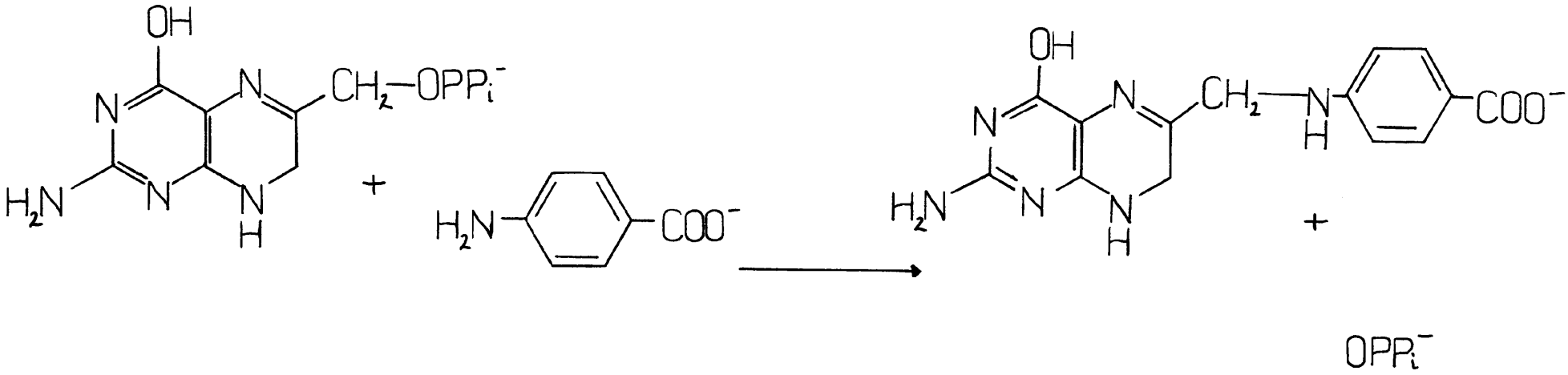

6-hydroxymethyl-7,8-dihydropterin + *para*-aminobenzoic acid ⟶ 7,8-dihydropteroate + pyrophosphate

pyrophosphate

Dihydropteroate synthase (DHPS)

Figure 1.3: Sequence alignment of *dhps* amino acid sequences.

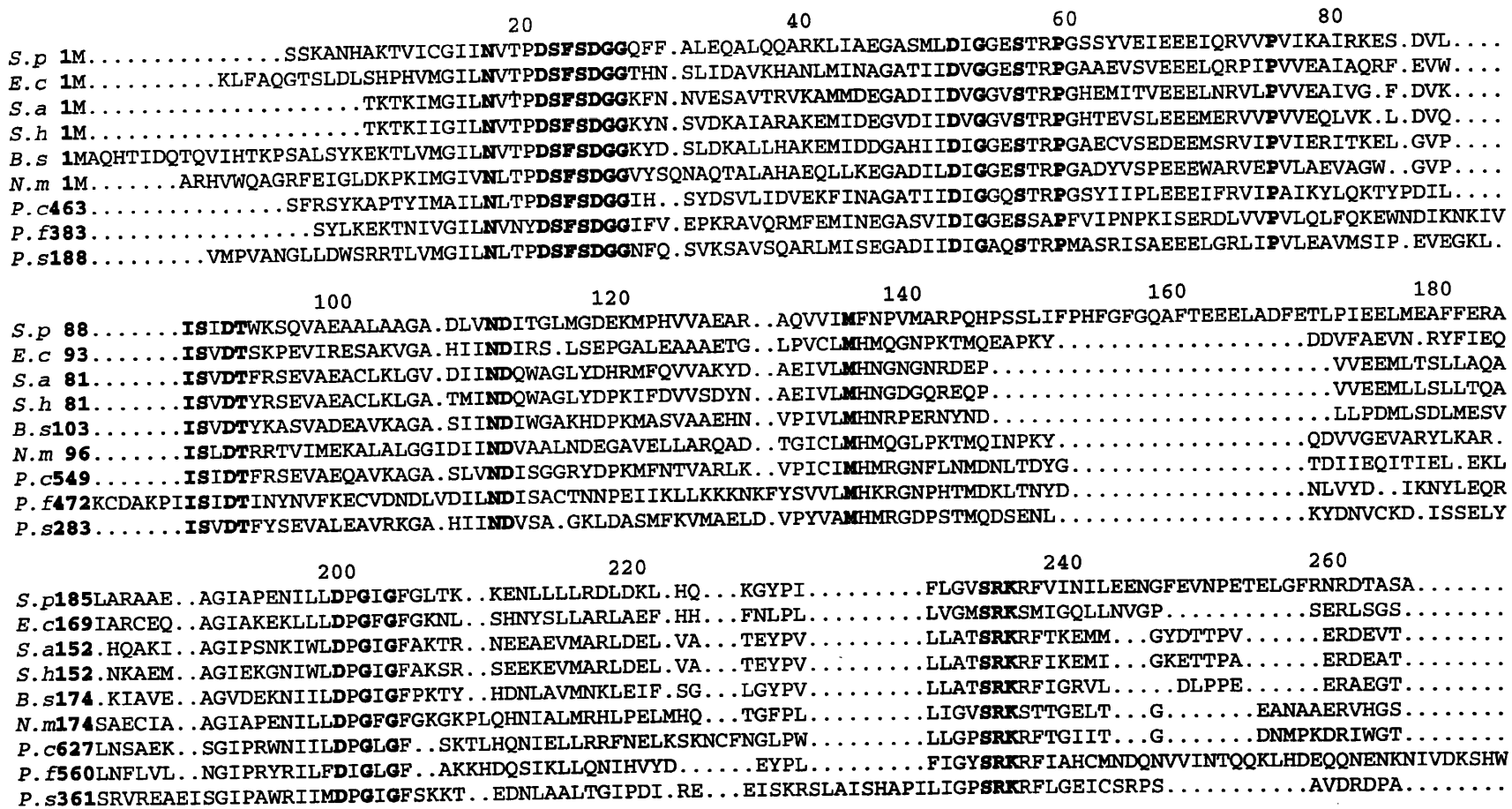

```
                                        280                 300
S.p  268.....................AHVTSIAARQ.GVEVVRVHDVASHRMAVEIASAIRLADEAENLDLKQYK  315
E.c  240.....................LACAVIAAMQ.GAHIIRVHDVKETVEAMRVVEATLSAKENKRYE.....  282
S.a  224.....................AATTAYGIMK.GVRAVRVHNV...ELNAKLAKGIDFLKENENARHNFS.  267
S.h  224.....................AATTVYGIMK.GIQAVRVHNV...DLNVKLAQSIDFLKENEHERHHLS.  267
B.s  244.....................GATVCLGIQK.GCDIVRVHDV...KQIARMAKMMDAMLNKGGVHHG...  286
N.m  251.....................VAAALASVAR.GAQIVRVHDVKATADALKVWEALGINL.............  287
P.c  673.....................VAAVVASISG.GCDIIRVHDVYEMYKISKMSDAIWKEIY.........  710
P.f  649MFQMNYMRKDKDQLLYQKNICGGLAIASYSYYK.KVDLIRVHDVLETKSVLDVLTKIDQV..........  707
P.s  443.....................TIASVTAGVLCGANIVRVHNVKDNLDAVKLCDAILKQKSSPIKFKQ...  488
```

The completely conserved amino acids are shown in bold type. The abbreviations used are: *S.p, Streptococcus pneumoniae* [Lopez, *et al.* (1987)], *E.c, Escherichia coli* [Dallas, *et al.* (1992)], *S.a, Staphylococcus aureus* [Hampele, *et al.* (1997)], *S.h, Staphylococcus haemolyticus* [Kellam, *et al.* (1995)], *B.s, Bacillus subtilis* [Slock, *et al* (1990)], *N.m, Neisseria meningitidis* [Cowman, *et al.* (1988)], *P.c, Pneumocystis carinii*, [Volpe, *et al.* (1992)], *P.f, Plasmodium falciparum* [Brooks, *et al.* (1994)] and *P.s, Pisum sativum* [Rebeille, *et al.* (1997)]. The numbering above the sequence alignment corresponds to the *S. pneumoniae* DHPS sequence only.

Figure 1.3a: Amino acid sequence alignments indicating likely secondary structure assignment.

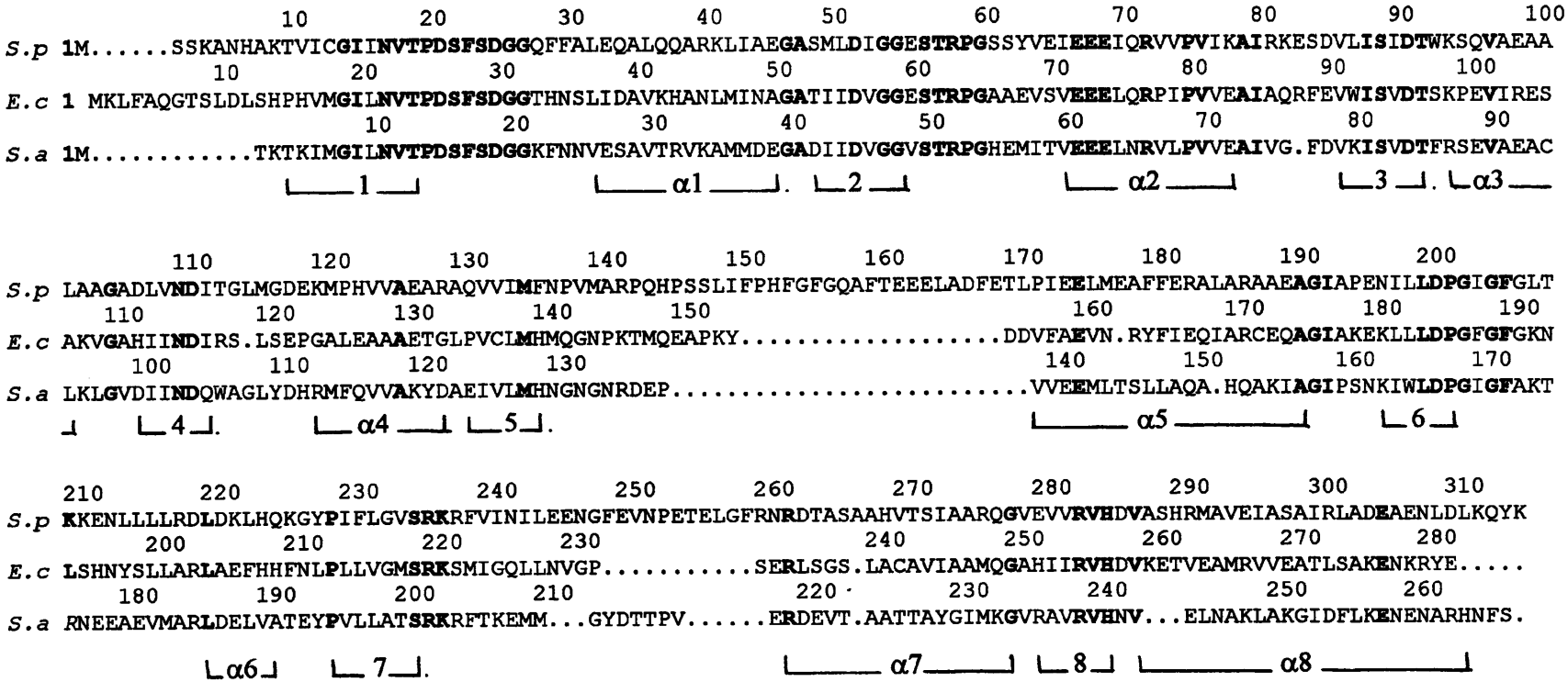

The completely conserved amino acids are shown in bold type. The abbreviations used are: *S.p, Streptococcus pneumoniae* [Lopez, *et al.* (1987)], *E.c, Escherichia coli* [Dallas, *et al.* (1992)], *S.a, Staphylococcus aureus* [Hampele, *et al.* (1997)] α-helices are labelled α1to α8 and β-strands are consecutively numbered according to Hampele, *et al.* (1997)The numbering above the sequences correspond to the respective DHPS sequences as published.

This *sul-d* mutation arose after prolonged selection with sulphanilamide. The two codon insertion into the wild type sequence is not in a region of sequence conservation.
The resulting protein had only a slightly altered affinity for pABA (2-fold higher K_m) and sulphanilamide (7-fold higher K_i) compared with the wild type enzyme. The effect of this mutation on pABA affinity was small but predicted to cause an alteration in the tertiary structure of the protein.
There are now several published *dhps* gene sequences from different bacteria - *E. coli* [Dallas, *et al.* (1992), Talarico, *et al* (1992)], *S. aureus* [Hampele, *et al.* (1997)], *S. haemolyticus* [Kellam, *et al.*(1995)], *B. subtilis* [Slock, *et al.* (1990)], *N. meningitidis* [Radstrom, *et al.* (1992)], protozoa - *P. falciparum* [Brooks, *et al.* (1994), Triglia & Cowman, (1994)], sporozoa - *P. carinii* [Volpe, *et al.* (1992)] and recently the higher plant - *P. sativum* [Rebeille, *et al.* (1997)] These DHPS sequences have all been aligned relative to that of *S. pneumoniae* in Figure 1.3.
The *E. coli dhps* gene from the strain MC4100, designated *folP*, was cloned and sequenced by Dallas, *et al.* (1992). [Figure 1.4] The protein was shown to be a homodimer similar to *S. pneumoniae* DHPS comprising two 30kDa. subunits. A temperature-sensitive mutant MC4100ts3 was also isolated. It was reasoned that a mutation in the *dhps* gene caused by selecting for resistance to the sulphonamide STZ might also have increased the thermolability of the enzyme. This mutant carried a point mutation which caused a change in a conserved phenylalanine residue Phe28 to leucine. In contrast to the *sul-d* mutant of *S. pneumoniae*, MC4100ts3 had a dramatic effect on the K_m for pABA (300-fold higher than the wild type) and the K_i for STZ (2000-fold higher than wild type). The pterin pyrophosphate substrate affinity for DHPS was unchanged. [Table 1.1a]
The *dspA* gene from *S. aureus*, coding for DHPS, has recently been cloned and sequenced in a PCR method similar to that used by Brooks, *et al.* in the cloning of the *P. falciparum* gene. [Hampele, *et al.* (1997)] Sulphonamide resistance in nine clinical isolates was postulated to be due to mutations in the chromosomal *dspA* gene, as strains remained resistant even when cured of plasmids. Seven of the nine isolates were different when compared to the wild type sensitive strain by at least thirteen residues, whereas the other two isolates had only two amino acid substitutions.

Figure 1.4 The arrangement of the folate biosynthesis genes in different species.

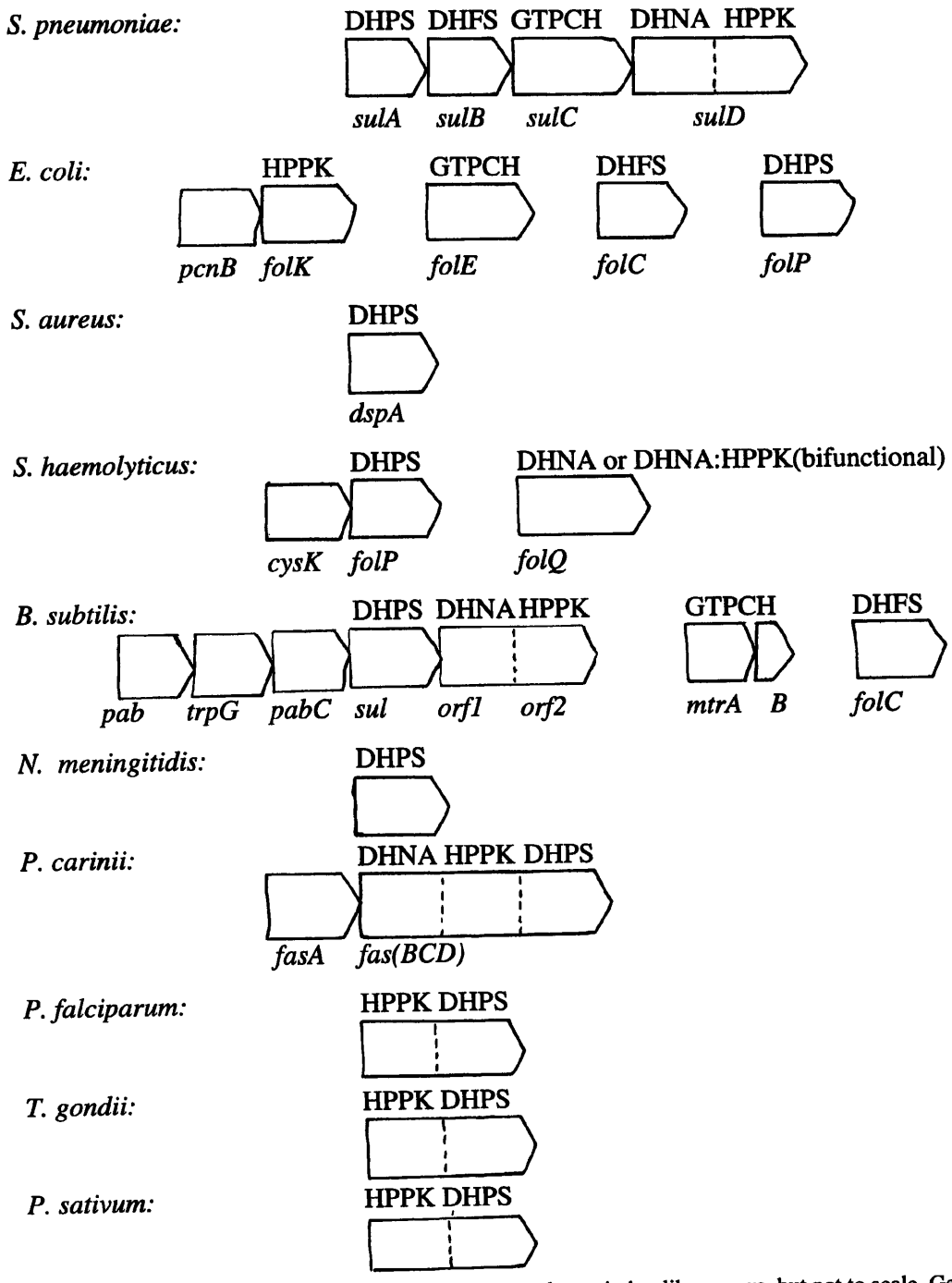

Genes or gene segments corresponding to enzymes are drawn in boxlike arrows, but not to scale. Genes not shown adjacent are far apart in the genome. Gene designations are given below the arrows and enzyme designations above the arrows.

Table 1.1a: Mutations in the *dhps* genes of laboratory strains of different micro-organisms.

Organism.	Chromosomal alteration.	Mutation.	Effect of mutant (if measured)
S. pneumoniae *sul-d* [Lopez, *et al.* (1987)]	6bp insertion	Ile-Glu after Glu67	K_m (pABA) increased 2-fold and K_i for SMX increased 7-fold.
E.coli MC4100ts3 [Dallas, *et al.* (1992)]	Temperature-sensitive, point mutation.	Phe28 (conserved) → Leu28	K_m (pABA) increased 300-fold and K_i for STZ increased 2000-fold.
B. subtilis [Slock, *et al.* (1990), Brooks, *et al.* (1994)]	Possible point mutation	Pro195	A sulphonamide resistant strain was sequenced.

The sequence numbering system is specific to each organism - see Figure 1.3.

Five of the nine isolates have a two amino acid insertion at the C terminal end of the protein due to an insertion of six bp as observed with the *S. pneumoniae sul-d* mutation and that of *N. meningitidis.*[See Table 1.1b]

S. haemolyticus dhps gene sequences were cloned by their ability to support the growth of the MC4100ts3 mutant used in the *E. coli* study, under non-permissive conditions. [Kellam, *et al.* (1995)] The plasmid contained a *S. haemolyticus* DNA insert of 1.7kb and the fragment contained one complete open reading frame for a protein with 49% homology to the *S. pneumoniae dhps* gene.

An entire 4.9kb fragment of the *B. subtilis* chromosome containing the seventh *trp* gene (not located in the *trpEDCFBA* operon) and the *sul* gene (for sulphonamide resistance) was sequenced by Slock, *et al.* (1990). Genes identified included *pab, trpG* and *pabC* for the synthesis of pABA. *trpG* encoded an enzyme which was also required in the synthesis of anthranilate, an intermediate in the tryptophan biosythetic pathway. The *Sul* gene was found to have greatest sequence homology to the *SulA* gene of *S. pneumoniae*. This sulphonamide resistant *Sul* gene had a proline residue at position 581 which, although not a conserved residue, corresponds to an alanine residue mutated in *P. falciparum* to a glycine residue, known to encode sulphonamide resistance. [Table 1.1b] [Brooks, *et al.* (1994)]

A 3.9kb fragment of a B:15 meningococcus (MO 035), selected from a genomic library, was shown by complementation experiments to express a sulphonamide resistant dihydropteroate synthase. [Radstrom, *et al.* (1992)] A 1.2kb *SspI* fragment was used as a DNA probe to isolate *dhps* genes from eight strains of *N. meningitidis* from serogroups A, B and C. *dhps* genes from three sulphonamide resistant strains (MO 035, MO 124 and 418) contained identical central regions of 424bp, which compared to sulphonamide sensitive strains, included an insert of six bp at position 230, (Ser-Gly) between two highly conserved residues. A fourth resistant strain had the preceding glycine230 residue mutated to a cysteine, where sensitive strains and other DHPS proteins have a conserved glycine residue.

Table 1.1b: Major mutations in *dhps* genes of clinical isolates of different micro-organisms.

Organism.	Chromosomal alteration.	Mutation.
S. aureus [Hampele, *et al.* (1997)]	point mutations	Phe17→Leu, Val30→Ile, Thr31→Asn, Met37→Ile, Ile58→Val, Thr59→Ser, Val60→Leu, Leu64→Met, Ile101→Met, Val117→Ile, Val126→Ile, Phe266→Leu, Thr51→Met, Glu208→Lys.
	6bp insertion	Lys-Glu at position 257.
N. meningitidis		
Strains MO035, MO124, 418	6bp insertion	Ser-Gly at position 195.
Strain BT227 [Fermer, *et al.* (1995)]	point mutation	Gly194→ Cys
P.falciparum		
Strains V1/S, WS, SL/D6	coupled point mutations	Ser436 → Phe with Ala613 → Ser/Thr
Strain K1 [Brooks, *et al.* (1994)]	point mutation	Ala581 → Gly
Pseudomonas [Brooks, *et al.* (1994)]	plasmid-encoded *dhps* 6bp insertions	Phe-Leu at a position equivalent to Ala581 of *P. falciparum*.

The sequence numbering system is specific to each organism - see Figure 1.3.

The *dhps* gene from *Pneumocystis carinii* was cloned by Volpe, *et al.* (1992). Degenerate oligonucleotides based on two conserved regions of the DHPS proteins from *S. pneumoniae* and *B. subtilis* were synthesised, taking into account the codon bias of *P. carinii*. A cDNA library was extracted from *P. carinii* grown in rats, and this library was searched using the oligonucleotides described. A single clone was identified which hybridised to a specific fragment of *P. carinii* genomic DNA. A 3.4kb insert was cloned and sequenced and contained the *Fas* gene and three introns in the central coding region. FasD, the domain at the C terminus of the Fas polypeptide, aligned optimally with the *Sul* gene of *B. subtilis* and *SulA* of *S. pneumoniae*.

The *Plasmodium falciparum dhps* gene was cloned by Triglia & Cowman in 1994. Oligonucleotides corresponding to two conserved regions of *dhps* genes from other organisms were used to amplify the *dhps* gene from the genomic DNA of the NF7 isolate of *P. falciparum*. As a result, a region of 3077bp has now been sequenced. All sulphadoxine-resistant mutations in the *dhps* genes of *P. falciparum* clinical isolates mapped to non-conserved residues, but were close to highly conserved residues. [Table 1.1b] The *dhps* gene of the higher plant *Pisum sativum* has recently been sequenced and the enzyme purified. [Rebeille, *et al.* (1997)] Sulphonamide-resistant bacterial species e.g. *Enterobacter* and *Pseudomonas* frequently contain a plasmid encoding alternative DHPS proteins from *SulI* or *SulII* genes. [Radstrom, *et al.* (1988)] Both genes possess a dipeptide insertion (Phe-Leu) at position 581 - similar to the K1 isolate of *P. falciparum*. *Mycobacterium*, *Haemophilus* and yeast *dhps* gene sequences have also been determined. [See Protein database on www.ncbl.nlm.nih.gov/biotech inform]

1.5 DHPS amino acid sequence homologies.

The five genes encoding enzymes of the folate pathway (GTPCH, DHNA, HPPK, DHPS and DHFS) are clustered together on the chromosome to a greater extent in *S. pneumoniae* than from other organisms, presumably to help regulate their expression. This single gene cluster encodes DHPS from *sulA*, DHFS from *sulB*, GTPCH from *sulC* and *sulD* supports both HPPK and DHNA activities. Figure 1.4 shows the arrangement of these genes in different species.

It is possible that *sulA, B* or *C* might also harbour another activity in the form of the phosphatase required to convert the 7,8-dihydroneopterin triphosphate product of GTPCH to 7,8-dihydroneopterin. [Lacks, *et al.* (1995), Lopez, *et al.* (1993)]

The three genes encoding DHNA, HPPK and DHPS are similarly close in *B. subtilis* alongside a *trpG* gene which is involved in the synthesis of aromatic compounds and two genes for pABA synthesis *pab* and *pabC*. [Slock, *et al.* (1990)] However the *B. subtilis* genes encoding GTPCH and DHFS, *mtrA* and *folC*, are found separately elsewhere on the chromosome. Notably the *mtrA* gene is part of an operon with another gene *mtrB*. The protein product of this gene acts as a repressor of the tryptophan operon and also possibly as a repressor of translation of *trpG*, regulating its expression from the operon housing the *sul* gene of DHPS. [Babitzke, *et al.* (1992)] *E.coli* encodes the GTPCH, HPPK, DHPS and DHFS polypeptides on separate genes, *folE, folK, folP* and *folC* respectively. [Talarico, *et al.* (1992), (1991), Dallas, *et al.* (1993)] The possibility of a linked gene encoding DHNA activity, as is the case for *S. pneumoniae,* cannot occur as the DNA upstream of *folK* encodes a poly(A)polymerase gene, *pcnB*. [Liu & Parkinson, (1989), Cao & Sarkar, (1992)] *N. meningitidis* is known to encode the DHPS polypeptide on a single gene. [Radstrom, *et al.* (1992).]

In general the DHPS in prokaryotes is monofunctional whilst other enzymes of the folate biosynthesis pathway may be monofunctional or bifunctional. In eukaryotes the picture is somewhat different with HPPK and DHPS activities often found associated. The DHPS coding sequence of *P. falciparum* forms part of a longer sequence on chromosome 8, which also specifies HPPK at the 5' end. [Triglia, *et al.* (1994), Brooks, *et al.* (1994).] This situation also occurs in *Toxoplasma gondii*. [Allegra, *et al.* (1990)] In the sporozoa *P. carinii*, three sequential enzymes of the pathway are encoded by a single *fas* gene. This gene encodes a single 69kDa. polypeptide with DHNA, HPPK and DHPS activities. [Volpe, *et al.* (1993).] Antibodies to *P. carinii* DHPS have now been developed but the genes for GTPCH and DHFS activities have not been located. [Voeller & Allegra (1994)] The recent work on the mitochondrial pea DHPS revealed that it too is encoded on a single bifunctional gene which also harbours HPPK activity. [Rebeille, *et al.* (1997)]

Preliminary kinetic studies on the purified HPPK/DHPS protein revealed low K_m values of less than 1μM for 6-hydroxymethyl-7,8-dihydropterin and pABA but a higher K_m value of 30-40μM for 6-hydroxymethyl-7,8-dihydropterin pyrophosphate. The kinetics of the DHPS reaction fitted a random bireactant mechanism which was subject to strong product inhibition from dihydropteroate, with a K_i value of 7-11μM with respect to pterin pyrophosphate and 5-8μM with respect to pABA. Maximal DHPS activity was recorded at a temperature of 50°C and the optimum pH for the reaction was about 9. Sequence identities between *dhps* genes from *S. pneumoniae* and other species are 33% with *E. coli*, 43% with *S. aureus*, 49% with *S. haemolyticus*, 33% with *B. subtilis*, 36% with *N. meningitidis*, 35% with *P. carinii*, 25% with *P. falciparum* and 28% with *P. sativum*. [Figure 1.3]

1.6 DHPS crystal structures.

The crystal structures of the *S. aureus* DHPS apoenzyme and a binary complex with a substrate analogue - oxidised pterin pyrophosphate - were determined to 2.2Angstroms and 2.4Angstroms respectively. [Hampele, *et al.* (1997)] The *S. aureus* DHPS protein, like *S. pneumoniae*, is a homodimer. Each monomer consisted of a single polypeptide domain which folded into an eight-stranded α/β-barrel of approximately 35 x 40 x 40 Angstroms. In all other known α/β-barrel enzymes, the active site has been located at the C-terminal end of the β-barrel fold (the sequence direction of the α-helices stacked around the outside of an inner distorted cylinder of parallel β-strands defines the poles of the cylinder as N- or C-terminal.) [Farber & Petsko, (1990), Banner, *et al.* (1975)] From the comparison of sequences from other DHPS proteins, almost all the conserved residues are located in α-helices or β-sheets.There are however two highly conserved regions which are not involved in either of those two types of tertiary structures. These loop regions of amino acids PDSFSDGG (14-21) and STRPG (50-54) connect the first β-sheet and α-helix (β1α1) and the second β-sheet and α-helix (β2α2). These two regions were proposed as the pABA-binding site. Sulphonamide-resistant mutations in the clinical isolates studied neither confirmed nor disproved this hypothesis as the altered residues were varied and mapped to many different locations on the DHPS molecule.

From a comparison of the crystal structures of the apo-enzyme and the binary complex with oxidised pterin pyrophosphate and Mn^{2+} bound, the residues involved in the binding of the substrate were revealed. Initially it was noted that although the availability of the active site of each monomer appeared to be very similar, the ligand had bound to only one of the monomers. This supported kinetic results suggesting half-of-sites reactivity in the dimer. The pterin part of the molecule did not cause any major structural changes within the DHPS molecule on binding but displaced five water molecules from the active site.

The pterin binding site was formed by residues Asn103, Val126, Asp167 and Leu197 and an estimated 80% of the surface of the molecule was in contact with conserved side- or main-chain amino acids. The residues involved in hydrogen bonds to the pterin pyrophosphate are summarised in Table 1.2.

The sulphonamide-resistant isolates had a variety of different mutations within their primary sequences. In six of the nine isolates, a conserved Phe17 was mutated to a leucine residue and this was the equivalent mutation seen in *E. coli* (Phe28 → Leu) and in *N. meningitidis* (Phe31 → Ile). Five of the nine isolates had an insertion of two amino acids near the C-terminus resulting from a duplication of 6bp (Lys-Glu at position 256) as seen in *S. pneumoniae* (Ile-Glu) and *N. meningitidis* (Ser-Gly). When the position of this duplication in *S. aureus* was mapped to the protein molecule, it appeared towards the C-terminal end of the eigth and final α-helix (α8). This structure, along with α-helix α7 from the binding monomer, and α-helices α6' and α7' from the non-binding monomer form the dimer interface. The total buried surface area is approximately 3000 square Angstroms - comparable with other α/β-barrel or 'TIM'-barrel proteins.

The *E. coli* DHPS crystal structure has been solved to 2.0 Angstrom resolution, together with a 2.5 Angstrom resolution of a binary complex of DHPS with its true substrate - reduced pterin pyrophosphate, and a 2.0 Angstrom resolution of a ternary complex with a substrate analogue dihydroxymethylpterin and a sulphonamide, sulphanilamide. [Achari, *et al.* (1997)] As with the *S. aureus* structure, *E. coli* DHPS is a dimer with each monomer forming an eight stranded α/β-barrel structure of approximately 49 x 48 x 48 Angstroms.

Table 1.2 Summary of the DHPS amino acid residues involved in the binding of pterin pyrophosphate.

Pterin pyrophosphate	*S. aureus* residues	*E.coli* residues	Corresponding *S.p* residue
Pterin atoms:	**Hydrogen bonds**		
N1	Lys203		Lys237
N4	Asp84	Asp96	Lys78
N5	Asn103	Asn115	Asn110
N6	Asn103	Asn115	Asn110
	Asp167	Asp96	Asp201
N7	Asp167	Asp185	Asp201
O8	Lys203	Lys221	Lys237
		1 H_2O	
α-phosphate atoms:	Arg52	Arg63 (main chain)	Arg58
	1H_2O	Thr62 (main & side chain)	Thr57
β-phosphate atoms:	His241	His257	His285
	Arg239	Arg255	Arg283
	Asn11	Asn22	Asn17
		Arg63	Arg58
Pterin ring:	**Van der Waals interactions**		
	Phe172	Phe190	Phe206
	Arg239	Arg255	Arg283
	Met128	Met139	Met135
		Ile117	Ile88
		Phe188	Ile204
		Gly217	Gly233
		Lys221	Lys237

S. pneumoniae. (S. p)

The dimer interface was proposed to be a shallow area of each monomer, about 37 x 27 Angstroms formed by hydrophobic interactions between the final three α-helices, α6, α7 and α8 and the four C-terminal residues. The same helices formed the dimer interface in the *S. aureus* DHPS crystal structure. Analysis of the binary complex revealed that pterin pyrophosphate was bound in a deep cleft towards the C-terminal end of the β-barrel. Intermolecular interactions are made at the pterin, β-phosphate and α-phosphate binding sites but there was no detectable difference between the positions of the main-chain residues on binding the substrate.

On binding to DHPS, pterin pyrophosphate displaced eight water molecules compared with the apo-enzyme - seven bound at the pterin ring pocket and one at the β-phosphate pocket. Four residues Asp96, Asn115, Asp185 and Lys221 form a narrow binding pocket for the pterin ring. The residues involved in hydrogen bonds with the pterin pyrophosphate are summarised in Table 1.2. The authors reported that attempts to generate a binary complex of DHPS with sulphanilamide by soaking the DHPS crystals in ligand showed no binding. Soaking apoenzyme crystals with 6-hydroxymethyl-7,8-dihydropterin, pyrophosphate and sulphanilamide produced crystals showing electron density in the pterin binding site, the β-phosphate site and also a more open region closer to the surface of the DHPS molecule bounded by the residues Phe190 and Pro61. There was some doubt as to whether the pyrophosphate had bound as there was no detectable electron density in the α-phosphate region. This is not surprising as there would be insufficient space in the pterin pyrophosphate binding pocket to accommodate the hydroxyl- group of the dihydropterin *and* the oxygen atom of the pyrophosphate moiety. The sulphanilamide had bound between the main chain of Arg220 and the side chain of Lys221 on one side and the side chain of Arg63 on the other. The conditions used to crystallise *E. coli* DHPS were 42% ammonium sulphate, 50mM Tris/HCl, pH 8.4. Consequently the β-phosphate pocket is occupied by a sulphate ion in the native DHPS crystal structure. Stabilising hydrogen bonds occur from the hydroxyl group of Ser219 to the amide NH_2 group of sulphanilamide, and one of the sulphanilamide oxygen atoms accepts a hydrogen bond from the guanidinium group of Arg63. The carbonyl group of Thr62, as well as the side-chains of Phe190 and His257 could all make Van der Waals contacts with the benzene ring of the ligand.

The distance from the aniline NH_2 group of sulphanilamide and the hydroxymethyl-group of the pterin pyrophosphate at approximately 3.5 Angstroms appears to be too long for a readily reactive complex and suggests that some rearrangement of pABA must occur before the reaction to form dihydropteroate can occur.

The relevance of Phe190 becomes apparent with the elucidation of the pABA-binding site. The residue immediately after this conserved residue is often mutated e.g. Ala581→ Gly in *P. falciparum* or Gly195 → Cys in *N.meningitidis.* Addition of two amino acids, Phe-Leu can occur immediately after this residue. This would severely affect the position of the two main-chain loops at the C-terminal end of the β-barrel, the first loop forming part of the pABA/sulphonamide-binding site. A disruption of this nature would prevent the binding of sulphonamides by DHPS making the enzyme appear sulphonamide-resistant.

The nature of the pterin pyrophosphate binding site seems to be highly conserved across both prokaryotic and eukaryotic species. [Achari, et al. (1997)] Where alterations in the residues occur, they are usually conservative changes and the side chain points away from the main-chain leaving the binding pocket largely intact, e.g. a leucine residue in *E.coli* DHPS (position 21) is conserved across five other species but the corresponding residue in *S. pneumoniae* DHPS is isoleucine and in *N. meningitidis* is valine. The sulphonamide/pABA binding site on the other hand appeared to be less well conserved e.g.Ser222 is a serine residue in *N. meningitidis* but in other species is an arginine residue.

There is now also a crystal structure of the GTPCH I decamer enzyme complex from *E. coli* resolved to 3 Angstroms. [Meining, *et al.* (1995)]

1.7 Sulphonamide drugs.

The DHPS reaction has been the target of the sulphonamide drugs since the 1930s but the mechanism of the DHPS reaction is still unknown and how these drugs inhibit the reaction is not clear. Much more structural, functional and mechanistic information is needed to fully understand this enzyme and the mode of inhibition.

The introduction of antibacterials (the so-called sulpha-drugs) into clinical medicine marked the beginning of microbial chemotherapy.

In the 1930s, German chemists showed that an industrial dye known as prontosil was metabolised to sulphonamide. This was the active antibacterial which protected mice infected with streptococci. The sulphonamides, amides of sulphonic acids, are the successors of those original sulpha drugs. [Barton & Ollis (1979)] The *para*-NH_2 group of sulphonamides is critical for antibacterial activity; ortho- and meta- substituents are inactive. [Woods, (1940)] The -SO_2NH_2 group can be substituted but there must be a direct sulphur-carbon link to the benzene ring. [Wingard, (1991)] [Figure 1.5]

The availability of antibiotics, the development of sulphonamide-resistant bacteria, and side-effects such as nausea, rash and jaundice meant that demand for sulphonamides declined sharply. These drugs are, however, still in clinical use; sulphamethoxazole is often used in combination with trimethoprim, a DHFR inhibitor in the drug Co-trimoxazole. [Huovinen, *et al.* (1995)] They reach high concentrations in the urine and so are particularly useful in treating urinary tract infections in humans; also treating infections of the respiratory tract, gastrointestinal tract, skin and ear. [Guide to Medicines and Drugs, British Medical Association.]

Sulphonamides are one of the few effective drugs for the treatment of pneumocystis pneumonia (which has become a very important disease for AIDS patients), prostatitis and gonorrhea and is commonly used to combat chloroquine-resistant malaria. [Wang, *et al.* (1995)] It is widely used in veterinary medicine. [van Duijkeren & van Miert (1994)]

Although sulphonamides are structurally similar to pABA, there is very little direct evidence that the sulphonamides are competitive inhibitors of DHPS with respect to p-ABA. There is evidence however that DHPS is capable of using sulphonamides as substrates, although poorly, producing sulpha-pterin analogues and depleting the cell of pteridine. [Swedberg, *et al.* (1979) , Roland, *et al.* (1979).]

If the mechanism of inhibition of the DHPS reaction were better understood, the problems of resistance could be approached more rationally and there would be potential for development of more effective drugs in the future.

Figure 1.5 Structures of the sulphonamide drugs used in this work.

pABA

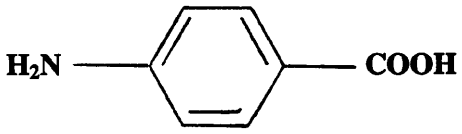

Sulphanilic acid (SAA)

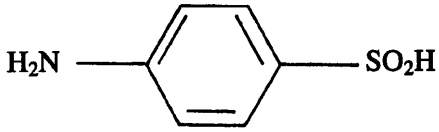

Sulphanilamide (SA)

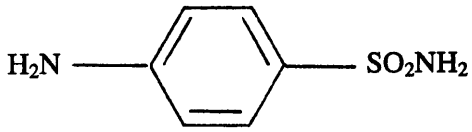

Sulphamethoxazole (SMX)

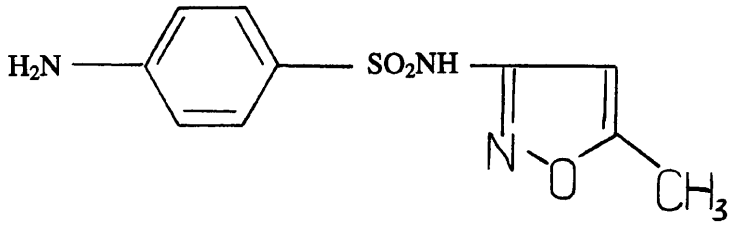

Sulphaquinoxaline (SQ)

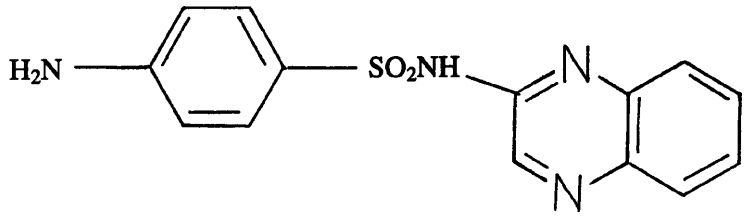

Sulphaphenoxazole (SP)

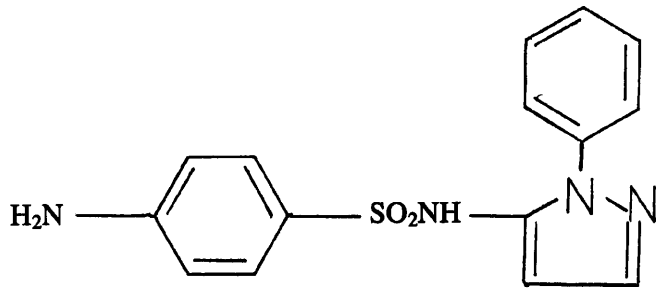

1.8 The possible modes of inhibition of *S. pneumoniae* DHPS by sulphonamides.

There are a variety of ways in which the sulphonamides can inhibit the DHPS reaction. The possibilities are summarised below using a classification by Dixon & Webb (1966).

Type Ia

Here the inhibitor and substrate bind at the same site on the enzyme. At any one time the enzyme can be in combination with its substrate or the inhibitor but never both.

This can be shown by the model below which assumes that the EI complex undergoes no further reaction and an EIS complex cannot be formed. This is the competitive inhibition assumed to occur with DHPS - it can bind pABA or a sulphonamide but not both.

$$E + S \underset{}{\overset{K_I}{\rightleftharpoons}} ES \overset{k}{\rightleftharpoons} E + P$$

$$+$$

$$I$$

$$\Updownarrow K_i$$

$$EI + S \not\longrightarrow \text{No Reaction}$$

Where $K_I = K_m/(1 + [I] / K_i)$

The steady state rate - v is described by the expression:

$$v = \frac{V_{max}}{1 + K_m/[S](1 + [I]/K_i)}$$

where [S] is the substrate concentration and [I] is the inhibitor concentration.

From this equation it is clear that the effect of a competitive inhibitor of this nature is to produce an apparent increase in the effective K_m for the competing substrate by a factor $(1 + [I]/K_i)$, which increases without limit as [I] increases.

Type Ib.

In this case the inhibitor is assumed not to bind at the substrate-binding site on the enzyme but one which is sufficiently close to it to reduce the affinity of the enzyme for the substrate. The enzyme can combine with both substrate and inhibitor at the same time, but the effects are still competitive. The model differs from that for Type Ia as the EIS complex can now exist. The inhibition affects only the substrate's affinity and not the overall V_{max} so the complexes ES and EIS must break down at the same rate. The new EI complex has a different affinity for the substrate than free E. The expression for the overall velocity of the reaction is given as the sum of these two reactions. It is difficult to distinguish between Types Ia and Ib graphically. Varying [I] at fixed [S] can be used to distinguish Type Ib because the inhibition does not increase indefinitely on increasing [I] but approaches a limit when all the enzyme is combined with inhibitor and the amount of EI can increase no more.

Type IIa.

Here the EIS complex does not break down at all so the velocity of the reaction is dependent only on the breakdown of the ES complex. This has an effect similar to a reduction in the amount of the active enzyme. The effect of inhibitor on the expression for the velocity of the reaction is to divide V_{max} by the factor $1 + [I]/K_i$ leaving K_1 unaffected.

Type IIb

The other main possibility is that the EIS complex can break down at a different rate than the ES complex. Then the velocity of the reaction is dependent on both rates. In the presence of an excess of substrate, the velocity of the reaction falls to a defined limit and not to zero.

A **mixed** type of inhibition may occur with the inhibitor having an effect on both the V_{max} and the effective K_m. This produces a mixture of competitive and non-competitive effects. e.g. Type Ib with IIa or Ib with IIb. Type Ia cannot combine with any of the others because there is no EIS complex and effects on its breakdown considered by the other cases would be meaningless. Inhibition can also be produced by an inhibitor which combines with a substrate cofactor or metal activator leaving them unavailable for the enzyme.

The concentration of the inhibitor must be of the same order as the substrate or cofactor and addition of more substrate would abolish the inhibitory effects. Competitive inhibition with respect to the substrate or cofactor would be observed. The modes of inhibition with regard to DHPS are discussed in more detail in Chapter 6.

1.9 Bisubstrate-biproduct enzyme mechanisms.

There are several potential mechanisms which DHPS could adopt. More detailed descriptions of bisubstrate biproduct reactions can be found in Mahler & Cordes (1966), Gutfreud (1965) and Dixon & Webb (1964).

A general equation for a reversible, bisubstrate biproduct reaction is:

$$A + B \rightleftharpoons P + Q$$

The assumptions on which the theory is based are similar to single substrate reactions. Variation of initial velocity (v) measured as a function of the concentration of the substrate (A) is given by the Michaelis-Menten equation:

$$v = \frac{V_{max} \cdot [A]}{K_m + [A]}$$ provided that

1) the concentration of A is much higher than the enzyme concentration and the concentration of B is fixed (not necessarily saturating) compared to A to become kinetically insignificant,

2) the rate of change of the concentration of all enzyme-substrate complexes is zero,

3) v is measured using different initial concentrations of A and the product concentrations are set to zero,

4) all other variables like temperature, buffer (with respect to pH, composition and ionic strength etc.) are constant throughout. [Dalziel, (1957)]

For two substrate reactions, the general random order kinetic equation requires five parameters - V_{max}, K_A, K_B, $K_BK_{\bar{A}}$ and $K_AK_{\bar{B}}$ - which can be expressed in many ways, where

K_A = the dissociation constant for substrate A from EA, (EA $\rightleftharpoons$ E + A)

K_B = the dissociation constant for substrate B from EB, (EB $\rightleftharpoons$ E + B)

$K_AK_{\bar{B}}$ = the dissociation constant from the ternary complex EAB, (EAB $\rightleftharpoons$ EA + B)

$K_BK_{\bar{A}}$ = the dissociation constant from the ternary complex EAB, (EAB $\rightleftharpoons$ EB + A)

The three most common mechanisms used by enzymes studied to date are presented in summary below.

1.9.1 The Ping-Pong mechanism.

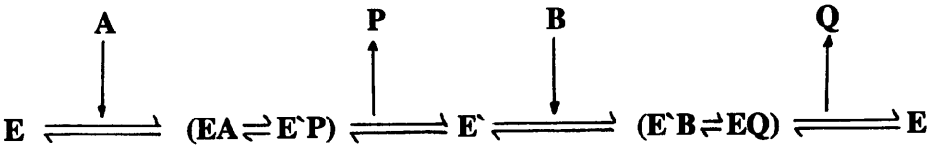

The first product (P) is formed before the conversion of the enzyme from a form E to E` and a reaction with the second substrate (B). The equilibria involved are shown in the scheme below:

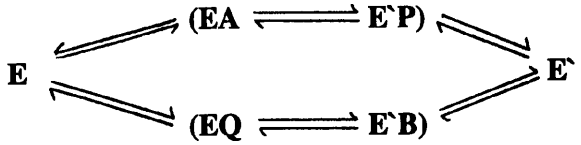

The pyridoxal phosphate-requiring transaminases and the dehydrogenase reactions catalysed by some flavoproteins use this mechanism. [Mahler & Cordes, (1966)]

1.9.2 The ordered mechanism.

In this case one of the substrates (A) must be bound by the enzyme before the second substrate (B) can bind, and one of the products (P) must leave before the other (Q).

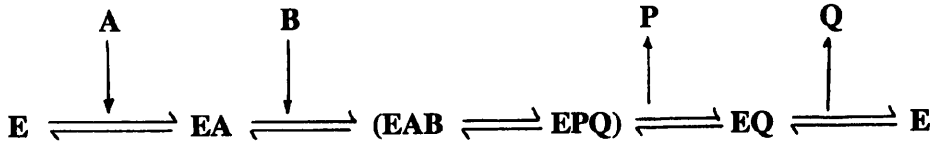

The equilibria involved are shown in the scheme below:

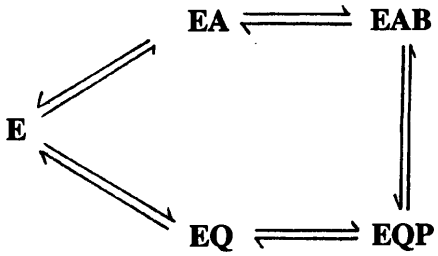

Due to the symmetry of this reaction pattern it is not always clear which substrate is A i.e. the `leading` substrate which must interact with the enzyme before the reaction can proceed. This identification can usually be accomplished by binding studies.
The NAD- and NADP-requiring dehydrogenases are the classic example of enzymes utilising this mechanism. [Dalziel, K (1957), Mahler & Cordes (1966)]

1.9.3 The random mechanism.

In this case both possible binary enzyme-substrate complexes can be formed rapidly and reversibly. Theoretically the magnitude of any dissociation constant for a substrate is unaffected by the prior attachment of another substrate to the enzyme. However there is more commonly a preferential binding route adopted by the enzyme, which is not a compulsory binding order, and the dissociation constant for one of the substrates may be affected by the prior binding of the other substrate. The slow step is the interconversion of the two ternary complexes EAB and EPQ and the equilibria are shown in the model below:

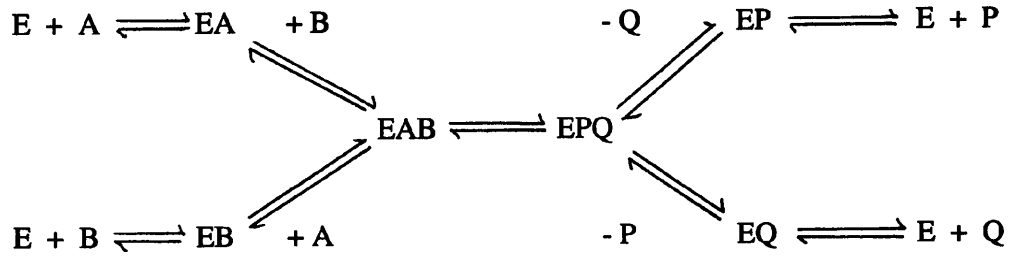

Many phosphotransferases like Creatine kinase use a random mechanism.

There are other less common reaction patterns such as the Theorell-Chance, Avion and Nordlie but these will not be described here. The DHPS mechanism will be discussed in more detail in Chapter 5.

1.10 Dihydrofolate reductase - a model study.

Dihydrofolate reductase catalyses the reduction of 7,8-dihydrofolate to 5,6,7,8-tetrahydrofolate by NADPH:-

$$NADPH + H^+ + \text{Dihydrofolate} \rightleftharpoons NADP^+ + \text{Tetrahydrofolate.}$$

It is the most studied enzyme involved in folate metabolism and one of the best understood enzyme structures. Interest in DHFR and its biological role was stimulated by the discovery that several inhibitors are clinically useful in the treatment of a variety of disease states. [Figure 1.6] Crystals of DHFR from *E. coli* and *Lactobacillus casei* were grown and the structures solved to 1.7Angstrom resolution. [Bolin, *et al.* (1982), Filman, *et al.* (1982)] Crystals of DHFR complexed with a variety of different ligands including two inhibitors - trimethoprim and methotrexate have also been grown. [Martorell, *et al.* (1994), Bystroff, *et al.* (1990), Hyunsook, *et al.* (1996)] The ternary complex structure of DHFR (with NADPH and trimethoprim) from *P. carinii* has been resolved to 1.9 Angstroms along with a ternary complex of NADPH and piritrexim, another inhibitor. [Champness, *et al.* (1994)] Crystal structures of DHFR revealed the backbone structure, the active site and binding of the substrate NADPH, together with binding of the inhibitors. [Blakley, (1984)] The active site is a cavity, about 15Angstroms deep across one face of DHFR. It is lined mainly with hydrophobic side chains indicating that much of the substrate and inhibitor binding is due to hydrophobic and Van der Waals interactions.

Dissociation constants of binary complexes of dihydrofolate, methotrexate and trimethoprim with DHFR from various sources were determined by fluorescence titrations at 25°C and provided important information about the affinity of substrates and inhibitors and the order of their binding to the enzyme. [Blakley, (1984) Birdsall, *et al.* (1980a & b) (1983), Jeong & Gready (1993)]

Figure 1.6 Structures of some DHFR inhibitors used in this work.

Methotrexate
(MTX)

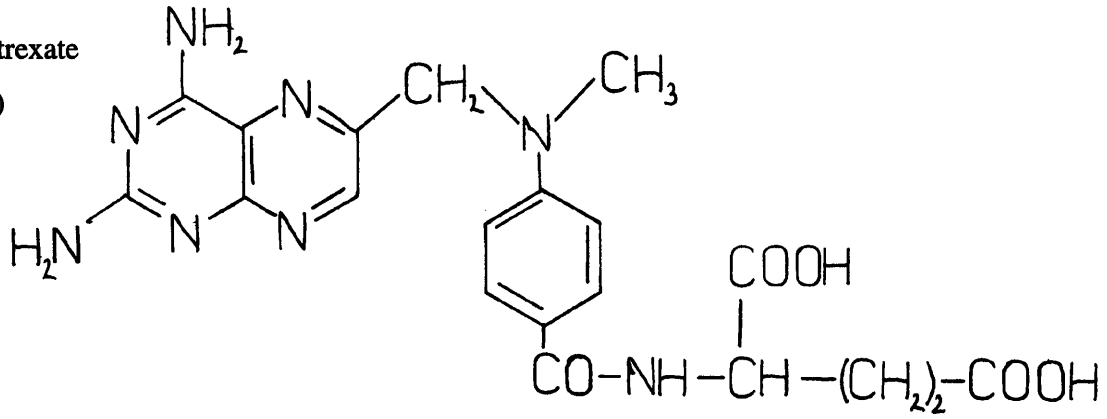

Trimethoprim
(TMP)

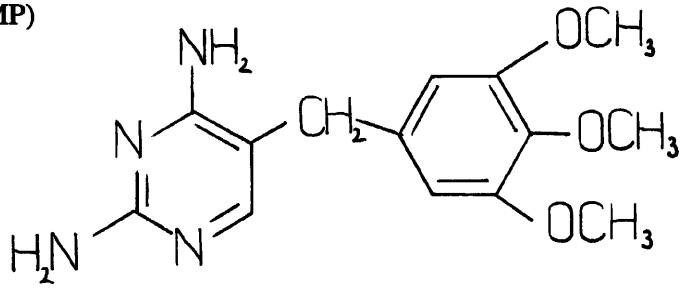

Pyrimethamine
(PMM)

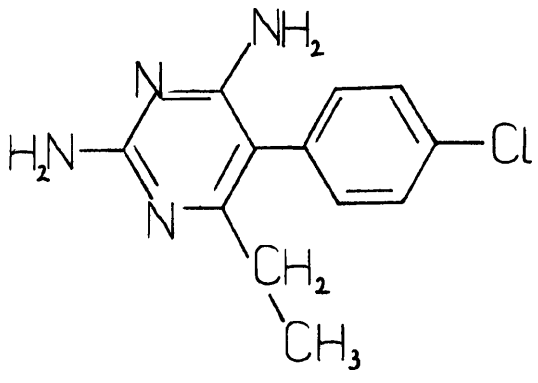

In an analogous fashion, equilibrium constants for the binding of substrates and/or inhibitors to *S. pneumoniae* DHPS can be measured. These measurements could help to determine the order of binding of substrates in binary and *pseudo*-ternary complexes and possibly the reaction pattern of the DHPS mechanism. The behaviour of sulphonamides in those equilibrium binding experiments could provide information regarding their likely binding site on the DHPS molecule e.g. whether they displace pABA or pterin pyrophosphate. As mentioned earlier in the chapter, steady-state kinetic analysis of DHPS from different organisms has been the sole means of ascribing a mechanism. No other method has been used to date in conjunction with kinetic measurements to verify the results obtained.

1.11 Summary of aims and objectives.

The solution of the three-dimensional structure of *S. pneumoniae* DHPS, as the apoenzyme and complexed with substrates and inhibitors, is a vital step in identifying the detailed molecular mechanism of the enzyme. A clear knowledge of the catalytic mechanism of the enzyme and its inhibition by the sulphonamides, together with the amino acid residues involved at the sulphonamide binding site, would also help to map mutations which cause sulphonamide resistance and would be critical in the development of novel inhibitors.

The three main objectives of this work are:

1. To crystallise *S. pneumoniae* DHPS as the apoenzyme, in a binary complex with each substrate and a sulphonamide. Crystal trials will also be attempted by generating *pseudo*-ternary complexes using one substrate and an analogue of the second substrate. Once these crystallisation conditions have been established, the aim is to grow the crystals to a sufficient size for X-ray analysis, with the eventual aim of solving the structure of *S. pneumoniae* DHPS.

2. To study the mechanism of the DHPS reaction using a combination of steady-state kinetic analyses and equilibrium binding experiments to determine dissociation constants for substrates and substrate analogues. Knowledge of the mechanism of the reaction may also be gleaned from a study of its pH dependence.

3. To determine the mode of inhibition of DHPS by sulphonamides and other inhibitors using a combination of steady-state kinetic analysis of sulphonamide inhibition and equilibrium binding experiments to determine the corresponding dissociation constants.

Chapter 2: Materials and Methods.

Materials

2.1 Chemicals.

All basic chemicals used were of analytical grade. Certain chemicals were of higher purity and are listed below.

para-Aminobenzoic acid, [3,5-^{3}H]. Moravek Biochemicals Inc. MT-599. (Specific activity 41.9Ci/mmole, Concentration 1.0mCi/ml.)

para-Aminobenzoic acid, [carboxyl-^{14}C] ICN. 1704583 (Specific activity 60mCi/mmole, Concentration 100μCi/ml.)

di-Ammonium hydrogen orthophosphate. Fisons Specified Lab. Reagent. A/5320/53.

Ammonium sulphate. Fisons Bioscience Grade. A/6485/53.

DEAE-Sephacel. Sigma. I-6505.

Folin and Ciocalteu's phenol reagent. Fison's laboratory reagent. J/4100/08

Ecoscint A. National Diagnostics. LS-273

HEPES. Sigma Ultra. H-7523.

6-Hydroxymethylpterin. Sigma. H-8512

6-Hydroxymethylpterin pyrophosphate. lithium salt. Dr. B. Schircks laboratories.

Imidazole (glyoxaline) extra pure. Fisons Specified Lab. Reagent. I/0012/53.

Isopropyl- β-D-thiogalactopyranoside (IPTG, dioxane free). Sigma. I-6758.

2-Methyl-2,4-pentane diol (MPD). gold label. Aldrich Chemical Co. Ltd. 23,955-0.

Phenylmethylsulphonyl fluoride (PMSF) Sigma. P-7626

Polyethyleneimine (PEI, 50% [w/v] aqueous solution) Sigma. P-3143.

Polyethylene glycol 6000 (PEG). Hampton Research. HR-P6K500.

Pterine. Fluka. 82551.

SDS-PAGE Molecular Weight Standards. low range. Bio-Rad Laboratories. 161-0304.

Sodium hydrosulphite. Sigma. S-9251

Sodium pyrophosphate decahydrate. ACS Reagent. Sigma. S-9515.

2.2 Inhibitors.

Aniline. Sigma. A-9880

Benzoic Acid. Sigma. B-7521

Dihydrofolate. Sigma. D-7006

Folate. Sigma. F-7876

Methotrexate. Sigma. A-6770

Pyrimethamine. Sigma. P-7771.

Sulfanilamide. Sigma. S-9251

Sulfamethoxazole. sodium salt. Sigma. S-7507.

Sulfaquinoxaline. sodium salt. Sigma. S-7382.

Tetrahydrofolate. Sigma. T-3125

Trimethoprim. Sigma. T-7883

2.3 Equipment.

CNBr-Activated Sepharose 4B. Pharmacia Biotech AB. 17-0430-01.

Exmire Microsyringe (10/0.1µl) Philip Harris Scientific. S95-764

28-well Microdialysis system. Life Technologies. 91200-022

Linbro tissue culture multi-well plates with covers. Flow Laboratories Inc. 17-033-05.

Mono-P HR 5/20 pre-packed Chromatofocusing column. Pharmacia Biotech AB. 17-0548-01

Mono-Q HR 10/10 pre-packed anion exchange column. Pharmacia Biotech AB. 17-0556-01.

Pipette Tips, large orifice. Fisher. PQP-225-0105.

Solid phase extraction column. ODS Octadecyl 5% Cartridge Type. Whatman. 6804-0005

Syringe filters (0.2µm pore size), Sterile Acrodisc, Gelman Sciences Ltd. 6224192

Superdex 200 HR 10/30 pre-packed Size exclusion column. Pharmacia Biotech AB. 17-1088-01.

Wizard Minicolumns. Promega. A7211.

2.4 Genotype of *E.coli* XL1-Blue.

The *E.coli* strain used throughout this work was XL1-Blue. Its genotype is given below.

supE 44 *hsd R*17 *rec* A1 *end A*1 *gyr* A46 *thi* F' [*pro*AB^{+} *lacI*^{q} *lac* ZΔ M15 Tn / O(*tet*^{r})]

See Section 2.6 for details.

Methods.

2.5 *E.coli* Media. (Adapted from Sambrook *et al.*,1995)

LB (Luria-Bertani) Medium.

Per litre:	Bacto-tryptone	10g
	Bacto-yeast extract	5g
	NaCl	10g

2 x YT Medium.

Per litre:	Bacto-tryptone	16g
	Bacto-yeast extract	10g
	NaCl	5g

The pH of the medium was corrected up to pH 7.0 using a few drops of sodium hydroxide before autoclaving.

2.6 DHPS expression vector system.

Isolation and cloning of the *dhps* gene was carried out by Dr. J. Derrick (Unpublished results).

Briefly, the gene encoding DHPS was isolated from *Streptococcus pneumoniae* chromosomal DNA by PCR using the following primers:

5'- CGCGCGAATTCAGGAGGTATCGATTATGTCAAGTAAAGCCAATCAT - 3'

EcoRI site ClaI site

5'- AATTTAGATTTAAAACAATATAAATAACTGCAGGCGCG - 3'

PstI site

The design of the oligonucleotide sequences was based on the sequence of the *dhps* gene, published previously by Lopez and Lacks [Lopez, *et al.* (1987)]. The linear DNA fragment was digested with *EcoRI* and *PstI* and inserted into these sites within the polylinker for the expression vector pKK223-3 (Pharmacia).

The construct is designed to produce inducible expression of DHPS on addition of IPTG from the tac promoter (a hybrid trp-lac promoter), in an appropriate *LacI*^{q} *E.coli* strain. pKK223-3, containing the *dhps* gene, was transformed into XL1-Blue and maintained on LB agar plates in the presence of 10µg/ml. tetracycline and 100µg/ml. ampicillin. The DNA sequence of the DHPS coding sequence was confirmed to be identical to that reported by Lopez *et al* (1987) by automated dideoxy-DNA sequencing.

2.7 Production of competent *E. coli* XL1-Blue cells.

The method of Chung *et al.* (1989) was used; briefly an overnight culture of XL1-Blue cells were grown in LB medium. A 1:100 dilution was used to inoculate a fresh culture of LB which was grown to an optical density of 0.2-0.4 (approximately 2 hours). The cells were cooled on ice for 15-20 minutes, then centrifuged at 3300rpm for 10 minutes at 4°C. The cell pellet was resuspended in 10 ml of ice-cold buffer comprising:

85% (v/v) LB medium

10% (v/v) PEG 3350

5% (v/v) DMSO

0.05M $MgCl_2$, pH 6.5

200µl aliquots of this solution were placed into sterile eppendorf tubes and snap-frozen in a dry-ice/ethanol bath. The tubes were stored at -80°C.

2.8 Transformation of *E. coli* XL1-Blue cells with pKK/DHPS.

100µl of competent cells were transferred to sterile eppendorf tubes. 1.0µg (1.0µl) of pKK/DHPS DNA was added to one tube and 1µl of sterile water added to the other tube as a control. The tubes were mixed well and kept on ice for 15 minutes. The tubes were transferred to a rack in a circulating water bath which had been pre-heated to 42°C, were incubated for 2 minutes, then quickly returned to the ice bath. The cells were cooled for several minutes on ice then 400µl of LB medium was added. The cultures were incubated for a further 30 minutes at 37°C to allow the bacterial cells to proliferate. A sterile pipette was used to transfer 100µl of transformed cells onto the surface of 2 x YT agar plates containing 100µg/ml ampicillin and 10µg/ml tetracycline as selection.

The cells were spread gently over the surface of the agar plates and they were placed at 37°C. Colonies of XL1-Blue/pKK/DHPS appeared on the experimental plate after 12-16 hours and the control plate remained clear with no colonies.

2.9 Lowry Method of Protein Determination.

Stock reagents were:

A	1% (w/v) copper sulphate ($CuSO_4 . 5H_2O$)
B	2% (w/v) sodium potassium tartrate
C	0.2M sodium hydroxide
D	4% (w/v) sodium carbonate

These reagents are stable at room temperature. To make 100ml of reagent E, 49ml of D were added to 49ml of reagent C followed by 1ml of reagent A and 1ml of reagent B. This copper-alkali solution was unstable at room temperature and was prepared fresh when required. The Folin-Ciocalteau reagent was diluted with an equal volume of water prior to use (reagent F).

0.5ml samples containing up to 0.5mg of protein were used in this assay. 2.5ml of reagent E was added to each sample, mixed well and left to stand for 10 mintues. 0.25ml of reagent F was added, mixed well and the blue colour allowed to develop for 30 minutes. The absorbance at 750nm of each sample was measured against a blank of 0.5ml of sample buffer which had been processed in the same way. The assay was calibrated using BSA solutions whose concentrations had been standardised by dry weight.

2.10 Trichloroacetic acid precipitation of proteins.

This method was used to concentrate a protein solution prior to loading samples onto acrylamide gels. The proteins were precipitated in a final concentration of 10% [w/v] TCA, the solution was mixed well and left on ice for 10 minutes. The solution was centrifuged at 11 300g for 5 minutes, the majority of the supernatant removed then centrifuged again before the final traces of supernatant were removed with a fine pipette. The pellet washed once with 1ml. of cold acetone. The tubes were left open on the bench for 5 minutes to let the acetone evaporate. 10µl. of sample buffer was added before the solutions were loaded onto gels.

2.11 SDS-PAGE.

The following solutions were used for the preparation of 12.5% SDS-PAGE gels:

Separating Gel

1.5M Tris/HCl, pH 8.8	0.625ml
30% Acrylamide / 0.8% Bis	2.1ml
Ammonium persulphate (10%, w/v)	25µl
TEMED	5µl
Deionised water	2.24ml

Stacking Gel.

0.5M Tris/HCl, pH 6.8	1.25ml
30% Acrylamide/ 0.8% Bis	0.325ml
Ammonium persulphate (10%, w/v)	12µl
TEMED	2.5µl
Deionised water	0.91ml

The Tris buffers are stable at 4°C for up to 1 month. The ammonium persulphate must be prepared fresh before each gel is poured.

Electrode Reservoir Running Buffer.

For 1 litre of 10x strength buffer:	Tris base	30g
	Glycine	144g
	SDS	10g

were dissolved in deionised water. This solution was diluted prior to each electrophoretic run.

Sample Solubilising Buffer.

For 10ml:	10% (w/v) SDS solution	3ml
	0.5M Tris/HCl, pH 6.8	2ml
	Glycerol	2ml
	Saturated Bromophenol Blue solution	0.4ml
	1.0M Dithiothreitol	50µl
	Deionised Water	2.55ml

If the bromophenol blue was added as a solid, 1.0-2.0mg. was added to the solution and mixed well to disperse.

The amount of deionised water added was then adjusted to 2.95ml. The solution was stored at 4°C and was stable for several months. The solution was allowed to warm to room temperature and shaken to fully dissolve the SDS before use.

Gel Staining Solution.

For 1 litre, 1g of Coomassie Brilliant Blue dye was dissolved in 400ml of methanol under a fume hood. 100ml of glacial acetic acid and 500ml of deionised water were added and the solution mixed well.

Gel Destaining Solution.

For 1 litre, 100ml methanol and 100ml glacial acetic acid were dissolved in 800ml of deionised water in the fume hood.

2.12 Preparation of reduced pterin compounds.

6-hydroxymethylpterin.

The protocol for the reduction of 6-hydroxymethylpterin to 7,8-dihydro-6-hydroxymethylpterin as described by Futterman (1957) was adopted.

Briefly, 10mg (52 µmoles) of 6-hydroxymethylpterin were dissolved in 200µl of 1.0M sodium hydroxide and quickly diluted with 2.0ml. of distilled water. 3.0ml of 0.4M potassium ascorbate/KOH, pH 5.0 were added and the solution cooled on ice. 200mg (1.2 mmoles) of sodium dithionite were added, with stirring, to the solution and it was cooled again on ice, shielded from light for 15 minutes. Aliquots were placed into sealed tubes and stored under a nitrogen atmosphere at -70°C.

The reduction was followed spectrophotometrically by a relative change in absorption at 365nm. and 340nm. as the pterin ring is reduced. The absorption measured and peak clearly seen at 365nm. due to the 6-hydroxymethylpterin was no longer visible after reduction but a large peak subsequently appeared at 340nm. A 10mg/ml. solution of oxidised pterin pyrophosphate in 0.4M potassium ascorbate, pH 5.0 gave an A_{365}/A_{340} reading of 0.7. On reduction with sodium dithionite, the reading decreased to less than 0.1.

Pterin.

The above protocol was also used to reduce pterin to 7,8-dihydropterin.

6-Hydroxymethylpterin pyrophosphate.

6-hydroxymethylpterin pyrophosphate was obtained commercially. DHPS can only utilise the reduced form, 7,8-dihydro-6-hydroxymethylpterin pyrophosphate. A modified version of the protocol described above was used to reduce this molecule because the pyrophosphate group is highly susceptible to degradation. The solubility of the molecule is improved by the presence of the pyrophosphate group. For this reason, 9.0mg (24μmoles) were dissolved directly into 1.0ml of the potassium ascorbate buffer described earlier, 50mg. (292 μmoles) of sodium dithionite was added, with stirring to the solution and it was left to stand at room temperature for 10 minutes shielded from light. The solution was cooled on ice and aliquots were stored under an oxygen-free nitrogen atmosphere at -70°C in sealed tubes.

2.13 Preparation of tetrahydrofolate and dihydrofolate.

Solutions of tetrahydro- and dihydrofolate, uncontaminated with the other folate species were required for kinetic work. Commercially obtained tetrahydrofolate dissolves in water with the addition of one drop of 1M Tris base. However, on immediate examination of the absorption spectrum, peaks are visible at 290nm. (which corresponds to the tetrahydrofolate) and also at 282nm. (which corresponds to the dihydrofolate), so the tetrahydrofolate had already begun to oxidise. Over the next 15 minutes the peak at 290nm. had shifted entirely to 282nm. and a peak at 350nm. had appeared (which corresponded to the fully oxidised folate species.) Similar problems were observed with an aqueous solution of dihydrofolate which quickly oxidised to folate.

Reduction of Folate to Tetrahydrofolate.

Nitrogen gas was bubbled through deionised water for two hours. A 25mM solution of folate was made using this deoxygenated water. Solid sodium borohydride was added to the folate solution in a three times molar excess. The vigorous effervescence was allowed to subside (5 minutes only) before a sample was removed and diluted 100-fold into deoxygenated water. The oxidation of the tetrahydrofolate was monitored in a spectrophotometer. The tetrahydrofolate began to oxidise after 20 minutes as the peak at 290nm. began to shift to 282nm. The kinetic experiments were prepared in advance in deoxygenated buffer ready for the addition of tetrahydrofolate and reactions were incubated for only 15 minutes instead of the usual 30 minutes. Using this method the tetrahydrofolate remained reduced throughout the length of the experiment.

Preparation of Dihydrofolate.

A 25mM solution of commercially obtained dihydrofolate was made in deoxygenated water containing 50mM DTT. A sample was removed immediately and diluted 100-fold into deoxygenated water and its absorption spectrum monitored. After 50 minutes, a peak began to appear at 350nm., indicating the formation of the folate species. However for the purposes of a normal kinetic reaction prepared in advance in deoxygenated buffer the dihydrofolate would remain in a reduced state over a 30 minute incubation.

2.14 Development of an assay for DHPS.

DHPS was assayed in early investigations by determination of dihydropteroate produced microbiologically using *Streptococcus faecalis* according to the method of Brown *et al.* (1961). More recently researchers have favoured the measurement of DHPS activity using a radioactively-labelled substrate, [^{14}C]-pABA, to produce [^{14}C]-dihydropteroate. A method for the separation of unreacted pABA from dihydropteroate was developed by Okinaka & Iwai (1969) and Richey & Brown (1969) which utilised paper chromatography. During the chromatography, the dihydropteroate remains at the origin whereas the pABA migrates with an R_f value of 0.78.

The origin was cut from the chromatography paper, the radioactivity measured in a scintillation counter and DHPS activity calculated as a function of dihydropteroate formation. Although this method is accurate it is enormously time-consuming.
A simple and swift alternative to paper chromatography was required to separate the dihydropteroate formed from the unreacted pABA.

2.15 The diethyl ether extraction method.

This procedure was developed from a method published in 1973, [Thijssen, H.H.W. (1973)] and was successfully used for some inhibition studies. Unreacted pABA was separated from dihydropteroate by acidification and diethyl ether extractions. At an acidic pH of 3.8, pABA can be extracted preferentially into diethyl ether from aqueous solutions: the partition coefficient $P_{pH\ 3.8}$ diethyl ether/water = 1.4 leaving dihydropteroate in the aqueous layer. [Blanchard, K. C. (1941)] [^{3}H]-pABA was chosen because of its availability, its relative ease of handling and disposal compared with [^{14}C]-pABA.

2.16 Assay conditions for the diethyl ether extraction method.

The general assay buffer solution contained: 100mM Tris/HCl, pH 8.0
10mM $MgCl_2$
10mM DTT

This buffer was stable for up to one month if pre-sterilised and kept at 4°C. A general experiment contained radioactive pABA, non-radioactive pABA, pterin pyrophosphate, DHPS and the buffer described above. The concentrations of substrates and inhibitors were varied. A typical reaction mixture contained, in a total volume of 50µl:

10-50nM [^{3}H]-pABA, 41.9Ci/mmole
0-100µM pterin pyrophosphate
0.2-10µM pABA
50mM Tris/HCl, pH 8.0
5mM DTT
5mM magnesium chloride
0-10ng DHPS

Those components, which were present at fixed concentrations in an experiment, were made up together in a larger volume, mixed well then dispensed into individual eppendorf tubes. If a substrate or inhibitor was present in the reaction at differing concentrations, these were added to the reaction tubes individually. Finally, the reaction was initiated by the addition of DHPS. After incubation at 25°C for 30 minutes, the reactions were stopped by the addition of 150µl of ice-cold quenching buffer. [Figure 2.1]

The acidic quenching buffer contained:

21.01g citric acid

35.81g di-sodium hydrogen orthophosphate

in a final volume of 100ml. using deionised water. The solution was corrected to pH 3.8 using 5.0M NaOH. The high concentration and pH were important because the original reaction mixture was already buffered. [Meshnick, pers. comm., Thijssen, (1973)] The tubes were kept on ice until extraction. The solutions were extracted with 5x800µl aliquots of diethyl ether. The tubes were vortexed then centrifuged at 4300g for 60 seconds and the diethyl ether layer removed. Any residual diethyl ether was allowed to evaporate. 150µl of the extracted aqueous layer was added to 5ml. of scintillation fluid in a vial. Vials were vortexed well and counted in a RackBeta liquid Scintillation Counter. No correction was made for quenching of scintillation radiation.

2.17 Validation of the assay conditions for the diethyl ether extraction method.

Figure 2.2 shows that 4 extractions removed the majority of the pABA when no DHPS was present. Protein has a tendency to bind pABA in a non-specific manner. [Thijssen, H.H.W. (1969)]. Therefore, to ensure complete removal of all possible pABA when DHPS was present in a reaction, five extractions were necessary.

Figure 2.2 also shows that a background level of radioactivity remained in the aqueous layer and could not be removed by diethyl ether extractions. One possible explanation was that the [^{3}H]-pABA had exchanged the tritium atoms with protons in the aqueous layer. It was hypothesised that this exchange reaction could be acid-catalysed and occur when the quenching buffer at pH 3.8 was added.

Figure 2.1: DHPS Assay: The Diethyl Ether Extraction Method.

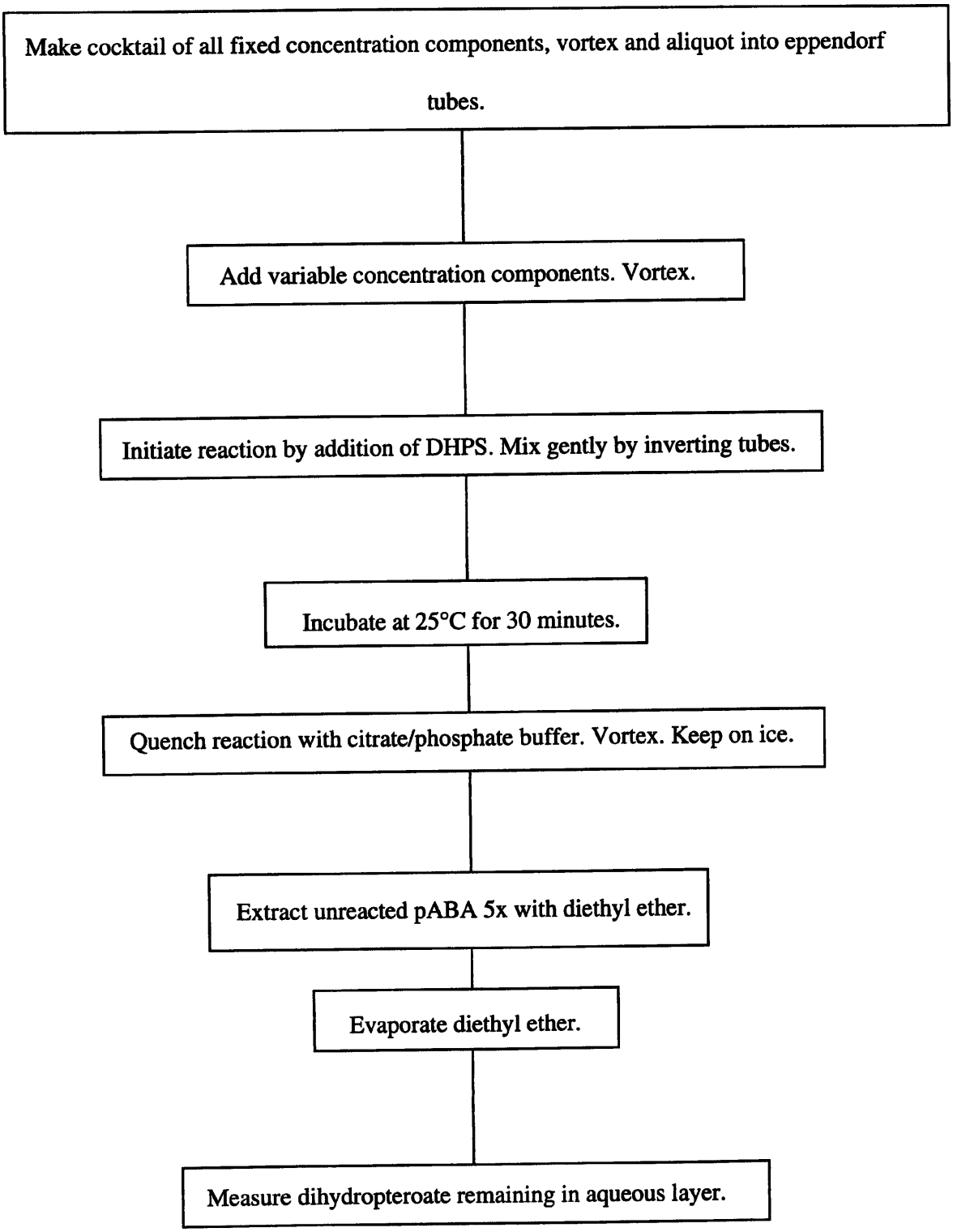

Figure 2.2: Extraction of [^{3}H]-pABA with diethyl ether.

The 50µl reaction volume contained:

10nM [^{3}H]-pABA, 41.9 Ci/mmole

50mM Tris/HCl, pH 8.0

5mM magnesium chloride

5mM DTT

The tubes were subjected to between 0 and 8 extractions with diethyl ether.

Each point is the mean value of three experiments.

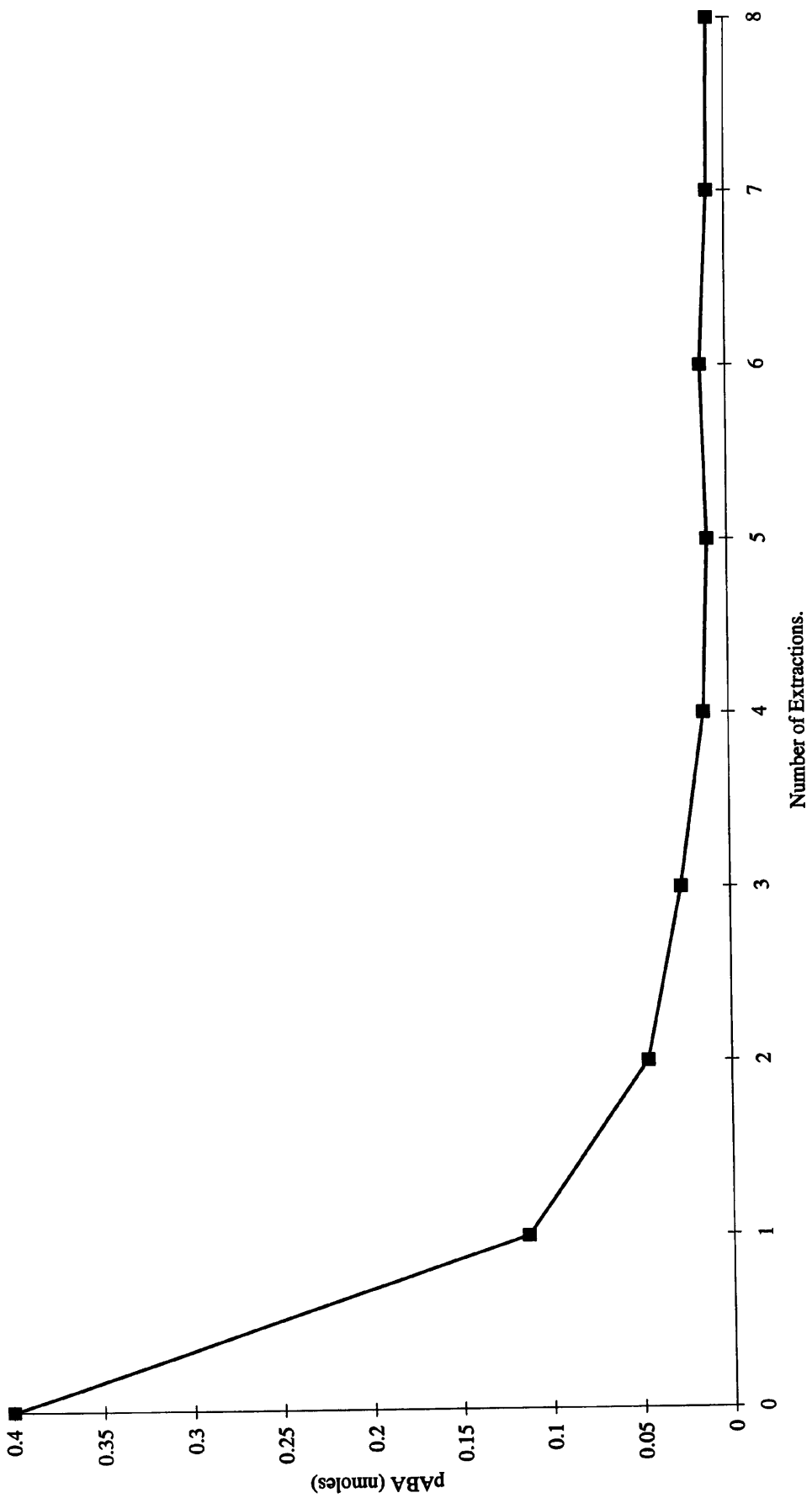

Figure 2.2: Diethyl Ether Extraction of radioactive pABA.

An experiment was designed to test this hypothesis by subjecting [^{3}H]-pABA to incubation under different conditions [Table 2.1] Tritium exchange did indeed occur and appeared to be acid catalysed.

80% more counts remained in the mixtures which had been subjected to the buffer at pH 3.8 for 30 minutes compared with those that had not. This was reduced to 35% on incubation at 0°C. Incubating the mixtures at 25°C for an extra 60 minutes increased the number of counts remaining in the aqueous layer by 44%. Therefore, to minimise this variable, all tubes were placed on ice immediately after the addition of cold, acidic, quenching buffer and were extracted as quickly as possible. The remaining counts were extracted as background.

2.18 Linearity of the assay.

It was necessary to verify that dihydropteroate production was linear with time and protein concentration to ensure that DHPS followed standard reaction kinetics. The incubation time was 30 minutes. A time-course experiment was performed to ensure the activity of DHPS was linear over the proposed incubation time. Figure 2.3 shows the relationship between dihydropteroate formed and time to be linear up to 30 minutes. The relationship between the amount of dihydropteroate formed and protein concentration was also shown to be linear up to 3.0ng/ml. DHPS [Figure 2.4]

Table 2.1: Tritium exchange of [^{3}H]-pABA with protons in the aqueous layer.

Conditions	Average CPM
Incubated at 25°C, 30mins, quenched & extracted	229 ± 8
Incubated at 0°C, 30mins, quenched & extracted.	233 ± 7
Quenched, incubated at 25°C for 30mins, extracted.	1193 ± 24
Quenched, incubated at 0°C for 30 mins, extracted.	359 ± 18
Quenched, incubated at 25°C for 90 mins, extracted.	2136 ± 53

The reaction tubes contained 10nM [^{3}H]-pABA (41.9Ci/mmole), 50mM Tris/HCl, pH 8.0, 5mM DTT and 5mM Magnesium chloride. The assay did not contain pterin pyrophosphate or DHPS. The results are a mean value ± S.E.M. (n=3)

Figure 2.3: Diethyl ether extraction method: Dihydropteroate production as a function of time.

The assay conditions were as described in Section 2.16. The concentrations of substrates were:

10nM [^{3}H]-pABA, 41.9 Ci/mmole

4.0μM pterin pyrophosphate

60ng/ml. DHPS was used and varying incubation times between 0 and 60 minutes.

Three experiments were used for each data point and the mean value plotted.

Figure 2.3: Diethyl ether extraction method: Dihydropteroate production as a function of time.

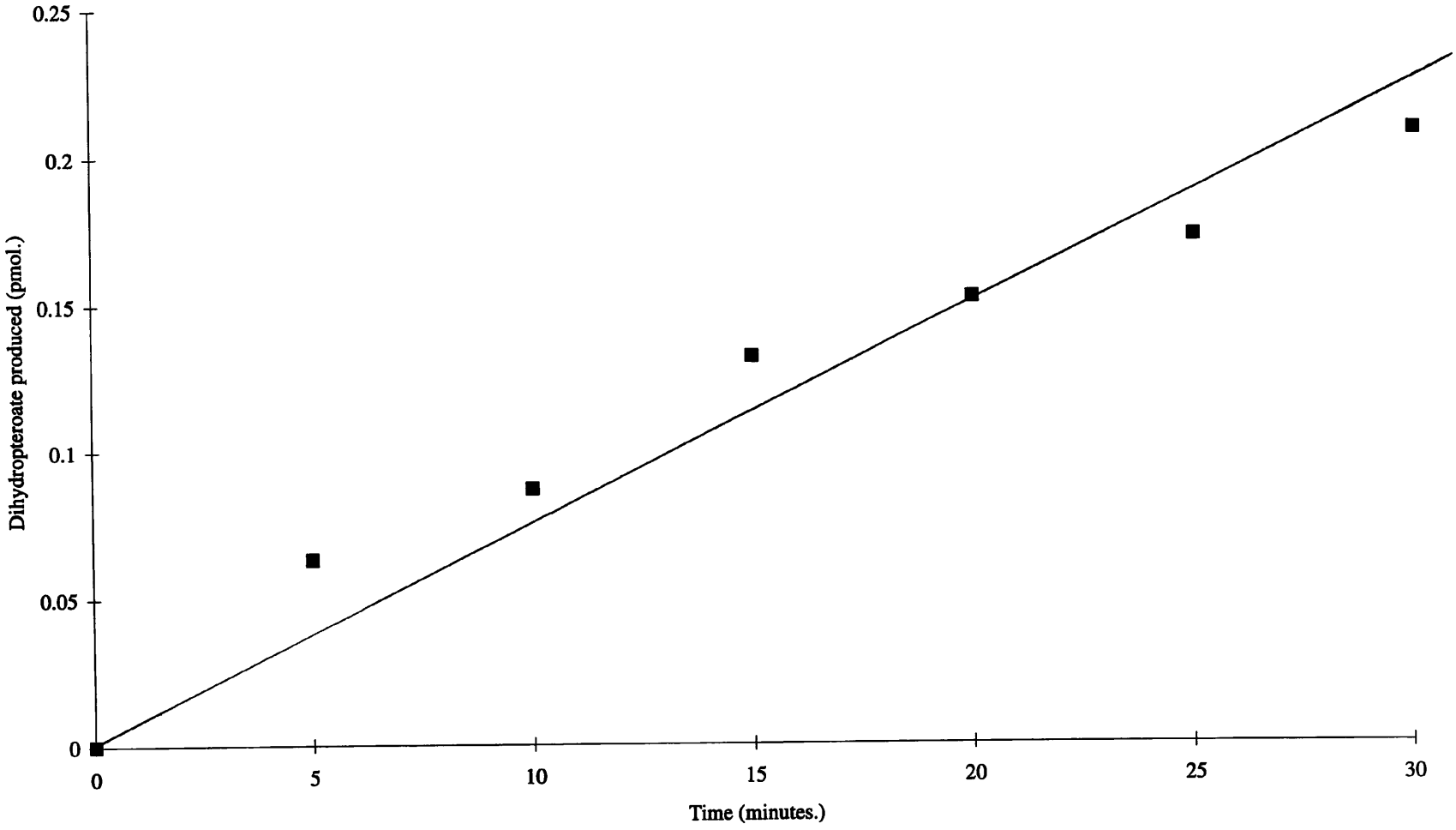

Figure 2.4: Diethyl ether extraction method: Dihydropteroate production as a function of protein concentration.

The assay conditions used for this experiment were as described in Section 2.16. The concentrations of substrates were:
10nM [^{3}H]-pABA, 41.9 Ci/mmole
4.0μM pterin pyrophosphate.
Non-radioactive pABA was not used.
Varying concentrations of DHPS were used between 0-3.0ng/ml. The rate of dihydropteroate production was linear over that range. Three experiments were performed for each data point and the mean values plotted.

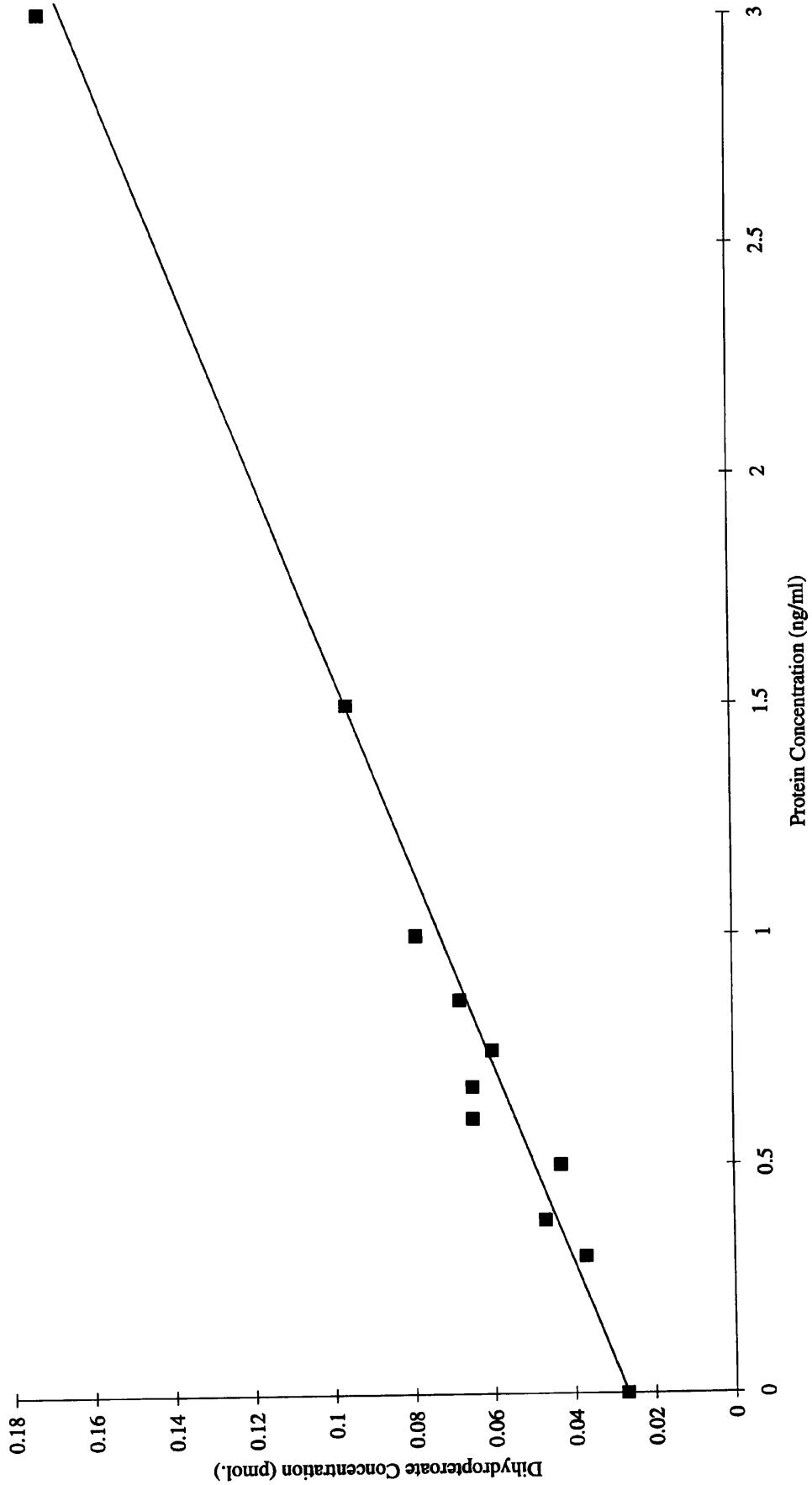

Figure 2.4: Diethyl ether extraction method: Dihydropteroate production as a function of protein concentration.

2.19 An alternative approach: Separation of pABA and dihydropteroate by reverse-phase chromatography.

The reverse phase method was developed for several reasons. The diethyl ether assay was found to be error prone: errors up to 13% were obtained (S.E.M. for n = 3 was 9%). Furthermore, the diethyl ether was difficult to pipette accurately. Work had to be carried out in a fume hood at all times and the procedure was lengthy due to centrifuging between each extraction. The exchange of tritium with protons in the buffer was a source of error which had been reduced as much as possible but could not be eliminated. Another source of error was in allowing the residual diethyl ether to evaporate after the final extraction.

This allowed an unknown and variable quantity of pABA to be reincorporated into the aqueous layer. These errors could be minimised using a different separation method based on the use of small 1.0ml. C18 reverse-phase chromatography columns.

2.20 Assay conditions for the reverse-phase extraction method.

Commercial [^{14}C]-pABA has a lower pABA concentration and lower specific activity compared to the [^{3}H]-pABA so larger reaction volumes were used.

A typical reaction mixture was prepared to contain, in a total volume of 1.0ml:

333.4nM [^{14}C]-pABA, 60mCi/mmole

0.5-10μM pterin pyrophosphate

0-10μM pABA

50mM Tris/HCl, pH 8.0

5mM DTT

5mM magnesium chloride

0-50ng DHPS

The components were made up together in a cocktail, mixed well and dispensed into individual eppendorf tubes. Variable concentrations of components, substrates and inhibitors, were added to the reaction tubes individually. Finally the reaction was initiated by the addition of DHPS. After incubation at 25°C for 30 minutes the reaction was stopped by the addition of 0.5ml of ice-cold 0.4mM pABA, 0.1M ammonium acetate/acetic acid buffer, pH 4.0. The tubes were kept on ice for 10 minutes.

The combination of low temperature and pH quenched the reaction and the high concentration of pABA ensured that any reaction which continued would utilise non-radioactive pABA and would not contribute significantly to the measured rate. Before use, the reverse-phase columns were washed with 10ml. of deionised water, followed by 10ml. of 0.1M ammonium acetate/acetic acid, pH 4.0. The reaction mixtures were applied to the columns and washed through with a further 10ml. of 0.1M ammonium acetate/acetic acid, pH 4.0. The columns were centrifuged at 4300g for 2 minutes and then washed with 2.5ml. of 100% methanol. The resulting eluents were placed into individual vials for scintillation counting. The columns were centrifuged again at 4300g for 2 minutes and the residual methanol added to the same vials. 2.5ml. of scintillation fluid was added, the vials sealed and vortexed well. The vials were counted in a RackBeta Liquid Scintillation counter. The columns were washed with a further 5.0ml. of methanol to remove any remaining contaminants and stored in a sealed vessel to prevent drying. [Figure 2.5]

2.21 Validation of the assay conditions for the reverse-phase extraction method.

As dihydropteroate is produced from the condensation of pABA with pterin pyrophosphate, the hydrophobicity of the pterin ring could be used to separate the pABA and dihydropteroate.

The purpose of the following experiments was to establish conditions under which unreacted pABA would elute from the columns in an aqueous fraction and dihydropteroate would elute in a methanol fraction. The results in Figure 2.6 show that pABA elutes from the columns in 10ml. of 0.1M ammonium acetate/acetic acid, pH 4.0. The results in Figure 2.7 show that dihydropteroate binds to the column in the ammonium acetate buffer, but can be eluted with 100% methanol. The results in Figure 2.8 show the separation of dihydropteroate from unreacted pABA: 95% of the [^{14}C]-dihydropteroate could be recovered in 2.5ml of methanol. Subsequent results were adjusted assuming a 95% recovery of dihydropteroate.

Figure 2.5: DHPS Assay: Reverse-Phase Separation Method.

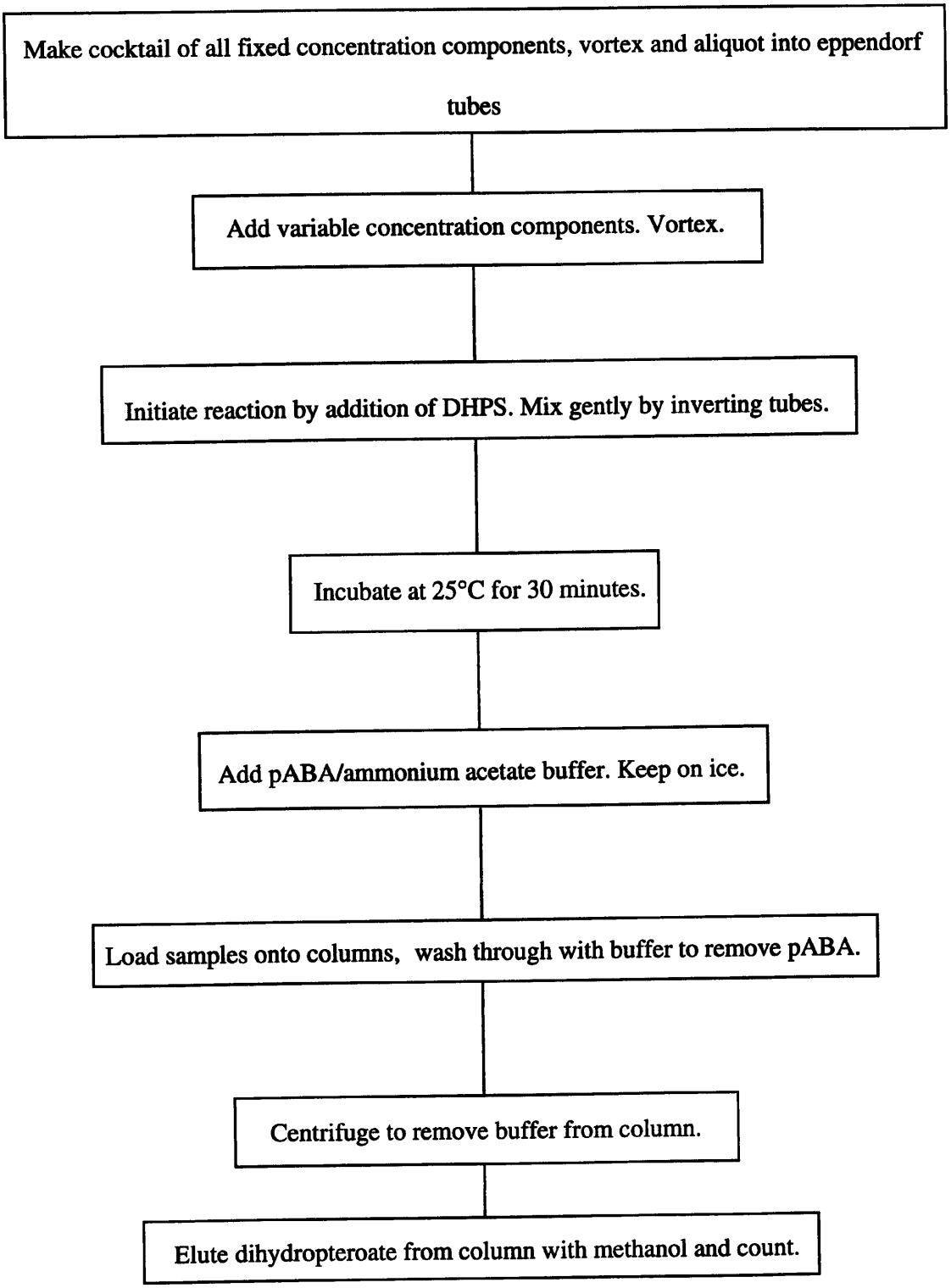

Figure 2.6: Elution of [^{14}C]-pABA from a C_{18} reverse-phase column.

A 1.0ml. solution was made up to contain:
333.4nM [^{14}C]-pABA, 60mCi/mmole
50mM Tris/HCl, pH 8.0
5mM magnesium chloride
5mM DTT.
The solution was washed through a column with 10ml. of 0.1M ammonium acetate/acetic acid, pH 4.0. 1.0ml. fractions were collected, dissolved into 4ml. of scintillation fluid in vials, vortexed well and counted.

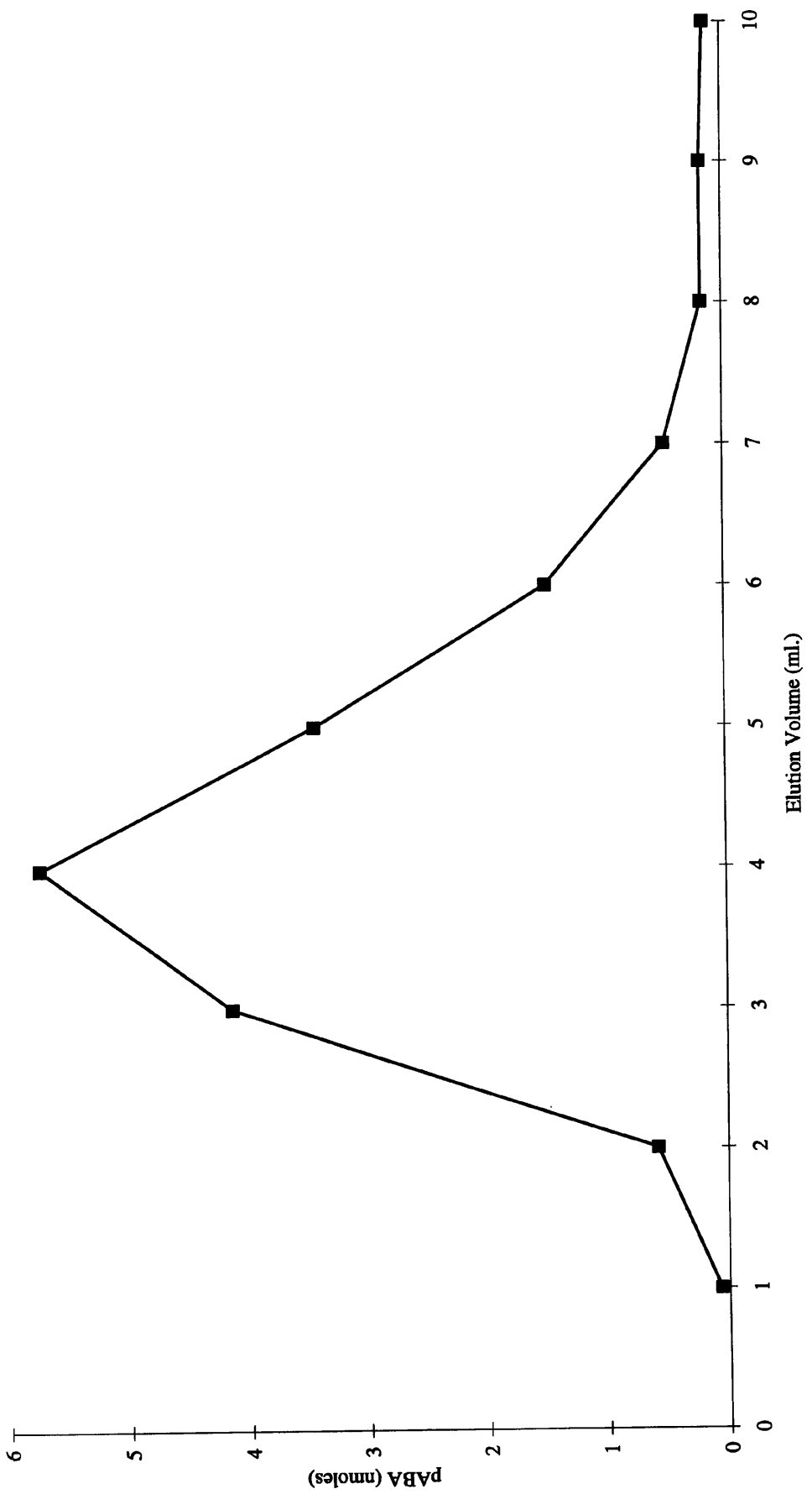

Figure 2.6: Elution of pABA from a C18 reverse-phase column.

Figure 2.7: Elution of [^{14}C]-Dihydropteroate from a C_{18} reverse-phase column.

Assay conditions were used as described in Section 2.21 The concentrations of substrates were:
333.4nM [^{14}C]-pABA, 60mCi/mmole
10μM pterin pyrophosphate
0.4mg/ml DHPS was added and the reaction incubated at 25°C for 2 hours to produce [^{14}C]-dihydropteroate and leave very little unreacted [^{14}C]-pABA in the mixture. The mixture was washed through a column with 10ml.of 0.1M ammonium acetate/acetic acid, pH 4.0 and centrifuged to remove all residual ammonium acetate. Dihydropteroate was eluted using 6ml of 100% methanol. 0.5ml. samples were collected in vials containing 4.0ml. scintillation fluid for counting.

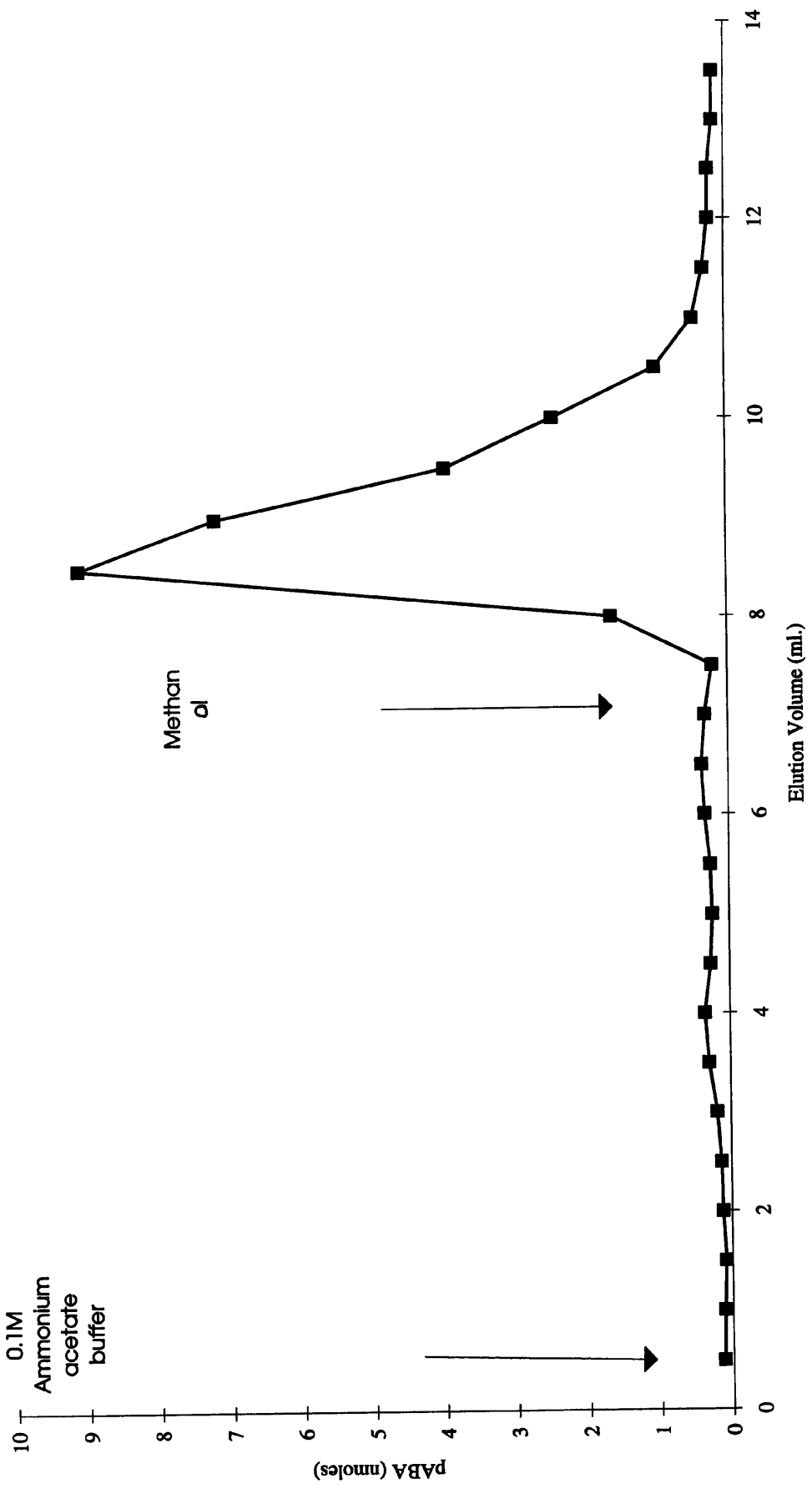

Figure 2.7: Elution of dihydropteroate from a C18 reverse-phase column.

Figure 2.8: Separation of Dihydropteroate from pABA by reverse-phase chromatography.

Assay conditions were used as described in Section 2.21. The concentrations of substrates were:
333.4nM [^{14}C]-pABA, 60mCi/mmole
4.0μM pterin pyrophosphate
50μg/ml. DHPS was added and the reaction incubated at 25°C for 30 minutes. Dihydropteroate was eluted with 2.5ml. methanol. 1.0ml. samples were collected.

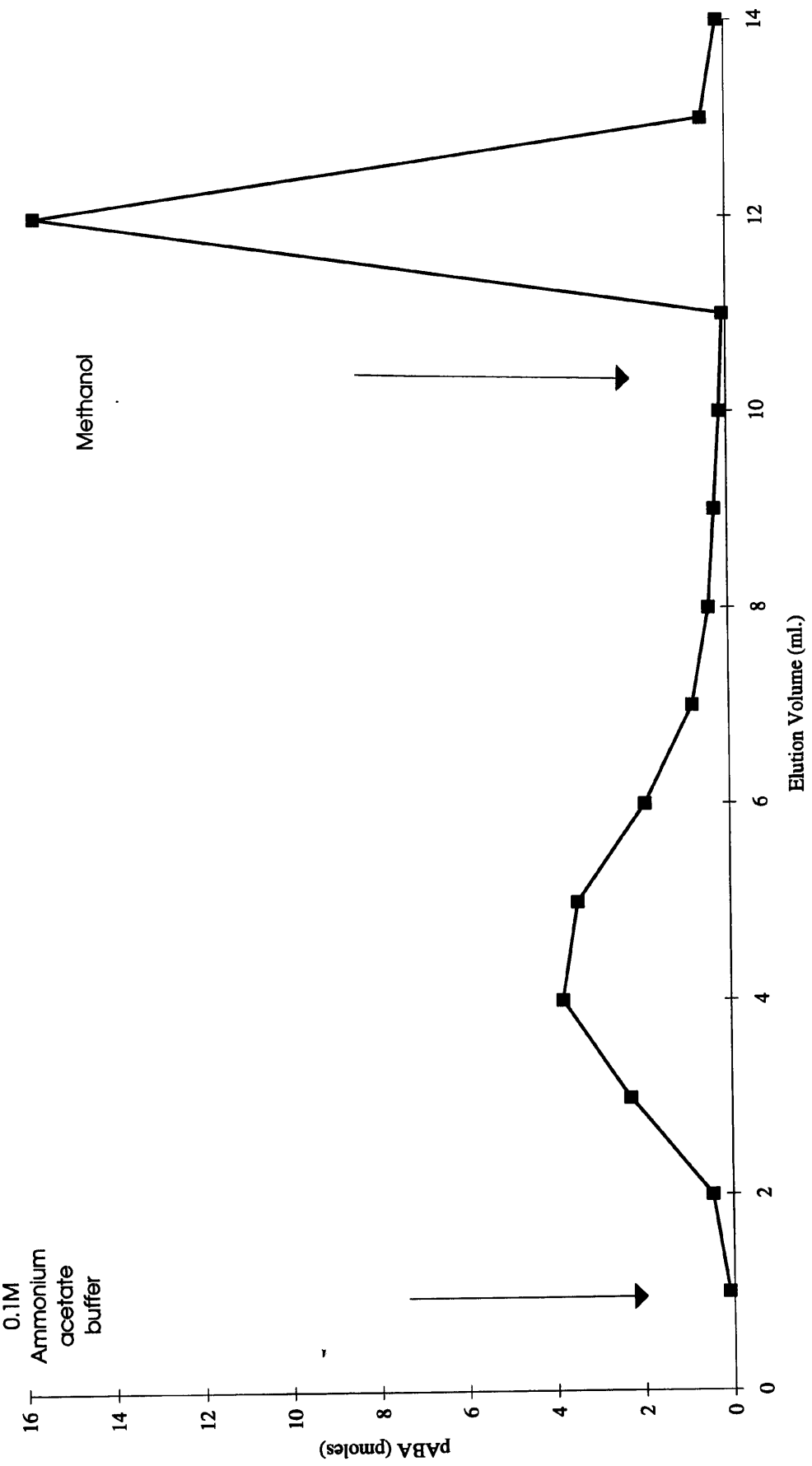

Figure 2.8: Separation of dihydropteroate from pABA by reverse-phase chromatography.

2.22 Linearity of the reverse-phase extraction method.

The results in Figure 2.9 show the relationship between dihydropteroate production and time to be linear up to 60 minutes. The results in Figure 2.10 show the relationship between dihydropteroate production and DHPS concentration to be linear up to 50ng/ml. of pure DHPS.

2.23 Hummel and Dreyer Experiments.

These experiments provide a valuable qualitative or quantitative method to study the binding of a ligand to a protein. [Hummel & Dreyer (1962)] By saturating a chromatography column with a detectable ligand (i.e A_{280} absorption or radiolabelled) and passing a protein sample through that column, any ligand which the protein is capable of binding can be observed as a change in absorbance or radioactivity of the eluate.

Non-absorbing or radioactive ligands can be added or removed from the column equilibrating buffer and the effect on the binding of the ligand to the protein can also be monitored.

A 25cm glass column of G-50 Sephadex was poured (1.5cm diameter) according to the manufacturer's instructions. The column was equilibrated with a buffer containing 50mM Tris/HCl, pH 8.0 and 5mM magnesium chloride. At least 3 column volumes of the buffer were applied to the column until a stable base line at A_{280} was detected on the UV monitor.

To investigate whether DHPS could bind a substrate (both absorb UV light at A_{280}) the column was equilibrated with the buffer described above containing a fixed concentration of substrate. Once the column was fully equilibrated and a stable base line observed on the UV detector, a continual flow of this buffer was maintained throughout the experiment.

For a control, 1ml of buffer which did not contain substrate was loaded onto the column before the usual flow of buffer containing substrate was restored. A trough was observed on the UV monitor corresponding to the 1ml of buffer minus substrate passing through the detector.

For the experiment, 1ml of DHPS in buffer containing no substrate was loaded onto the column. As with the control, the flow of buffer containing substrate was immediately restored to elute the sample. A peak was observed on the UV monitor corresponding to the DHPS eluting from the column and absorbing at A_{280}. If DHPS was capable of binding the substrate, it must have bound the substrate from the solution continually flowing through the column. The peak height may be due to both protein and substrate absorption. This hypothesis can be tested using protein in the controls but this method used too much protein to justify.

However if DHPS has bound substrate, the subsequent trough observed on the UV monitor following the protein peak will be larger than the control trough - in proportion to the amount of substrate bound by DHPS. The amount of a ligand bound by a protein can be quantitatively analysed by calibrating the size of the peaks and troughs with known quantities of ligand and protein, as originally envisaged by Hummel and Dreyer. [Hummel & Dreyer, (1962)]

In this piece of work, the experiments were used to obtain a rapid indication of whether DHPS could bind its substrates and *pseudo*-substrates in the presence or absence of different non-absorbing ligands.

2.24 Development of a Binding Assay.

The Hummel and Dreyer experiments provided qualitative information on the nature of the reaction mechanism of DHPS. However, to obtain accurate, quantitative information from these experiments would be more difficult and time-consuming. A binding assay was therefore developed to measure quantitatively the binding constants of substrates, products and inhibitors of DHPS. [See Figure legends for precise details of experiments.]

2.25 Coupling of DHPS to Sepharose Beads.

2 x 5.6g of CNBr-activated sepharose-4B were weighed into two sterile tubes and both were washed twice with 20ml. of 1mM HCl for 20 minutes, inverting the tubes to mix. The tubes were centrifuged at 200g for 5 minutes between washes and the supernatants removed.

Figure 2.9: Reverse-phase separation method: Dihydropteroate production as a function of time.

Assay conditions for this experiment were as described in Section 2.20.
The following concentrations of substrates were used:
333.4nM [^{14}C]-pABA, 60mCi/mmole
4.0μM pterin pyrophosphate.
Non-radioactive pABA was not used.
Varying incubation times were used. 10ng/ml. DHPS was used.
Three experiments were performed for each data point and the mean values were plotted.

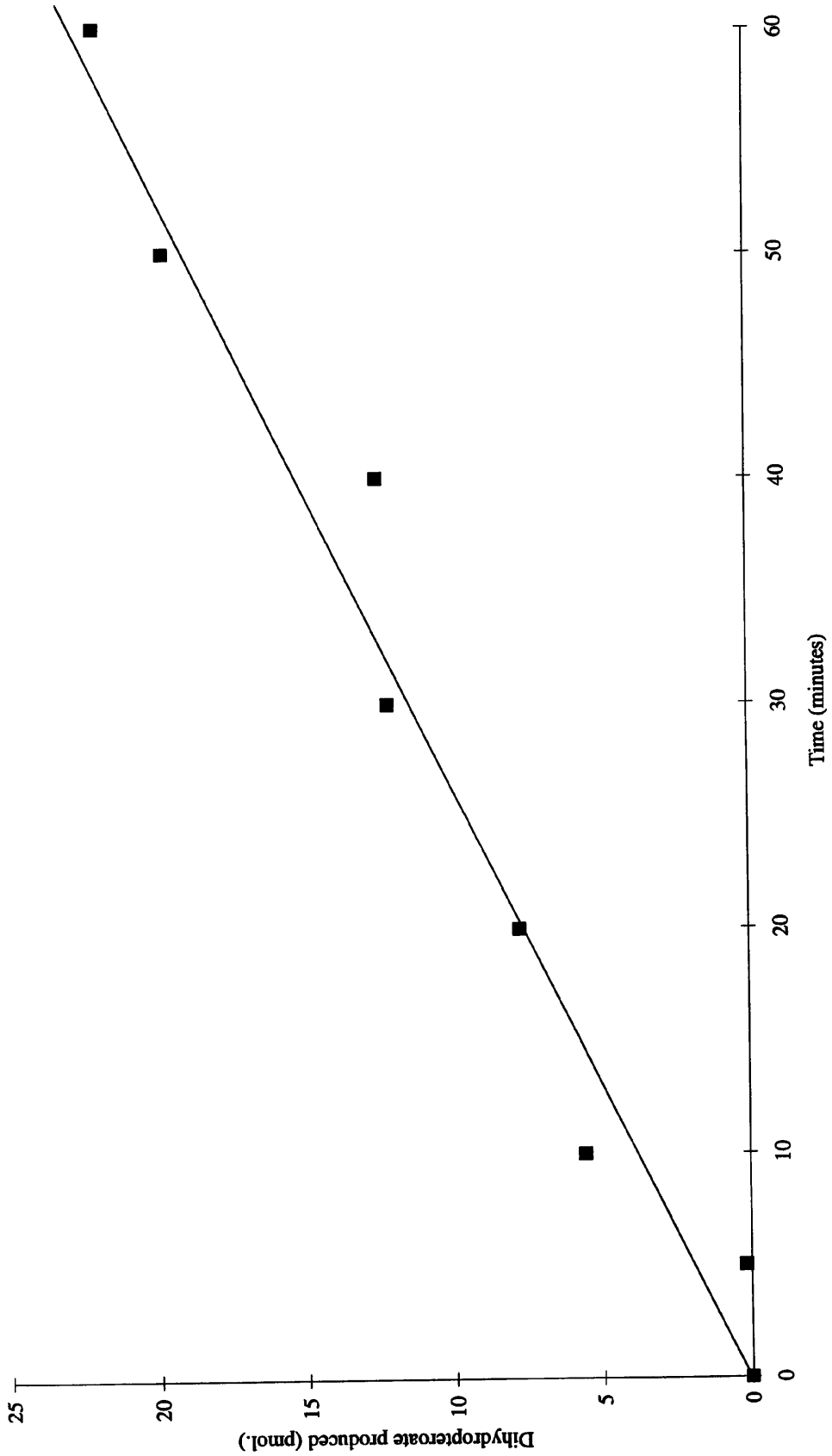

Figure 2.9: Reverse-phase separation method: Dihydropteroate production as a function of time.

Figure 2.10: Reverse-phase separation method: Dihydropteroate production as a function of protein concentration.

Assay conditions for this experiment were as described in Section 2.20 with no non-radioactive pABA. The following concentrations of substrates were used:
333.4nM [^{14}C]-pABA, 60mCi/mmole
4.0μM pterin pyrophosphate.
Varying concentrations of DHPS were used.
The dashed line shows that the rate of dihydropteroate production is linear with the DHPS concentration up to 40ng/ml. Three experiments were performed at each data point and the mean value plotted.

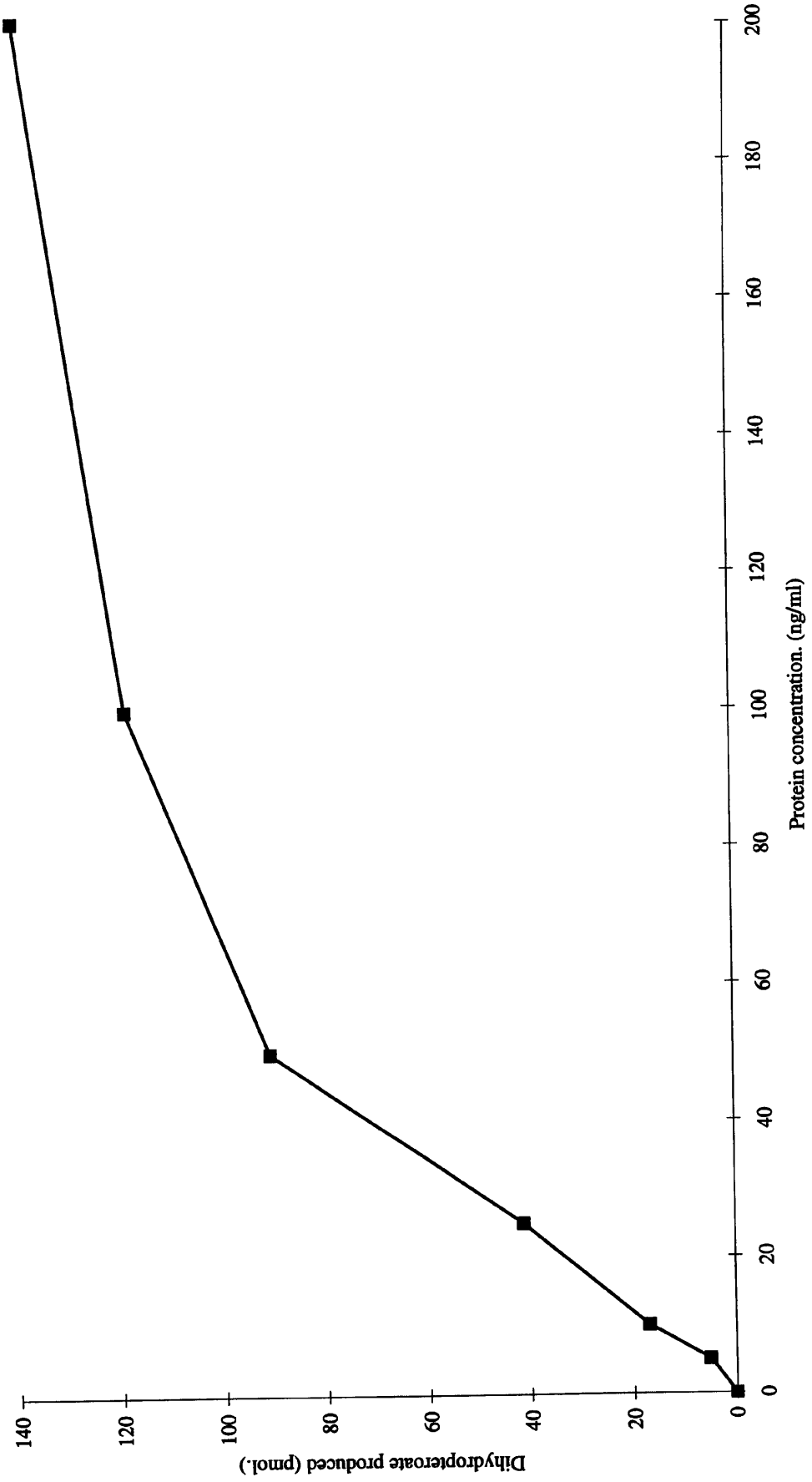

Figure 2.10: Reverse-phase separation method: Dihydropteroate production as a function of protein concentration.

The beads were washed with 20ml. of coupling buffer which contained 0.5M NaCl, 0.1M $NaHCO_3$/NaOH, pH 8.3, for 20 minutes before centrifuging as above and removing the supernatants. The DHPS solution had been dialysed against the coupling buffer and 30mg of DHPS (600µl) was added to 10ml. of coupling buffer and mixed. The absorbance at 280nm. of this solution was measured, before it was added to one of the tubes. The other control tube received 10.6ml. of coupling buffer alone. The tubes were continuously and gently inverted at 30°C for 1 hour while the protein bound to the Sepharose beads. The tubes were centrifuged as described above and the absorption at 280nm. of the supernatant was measured.
The proportion of DHPS which had bound to the column was calculated to be 95% from the decrease in absorbance, so the supernatant was removed from both the experimental and control tubes. The beads were washed with 20ml. of 0.1M Tris/HCl, pH 8.0 for 20 minutes to block any remaining binding sites. The supernatant was removed after centrifugation and 5ml. of 0.02M Tris/HCl, pH 8.0 was added to each tube. 0.05% sodium azide was also added to discourage bacterial growth and the beads were stored at 4°C.[Figure 2.11]. The total volume of experimental bead slurry was 25ml.

2.26 General protocol for the binding assay.

The reaction volume used in all experiments was 100µl. Experimental and control reactions were performed in triplicate for each data point. For this reason, a cocktail of all the reaction components (excluding the beads) was made up, vortexed and 80µl of this cocktail dispensed into each reaction tube. This method ensured that the concentration of components was identical between control and experimental tubes.

A standard cocktail contained:

0.5-5µM [^{14}C]-pABA or [^{14}C]-dihydropteroate, approximately 60mCi/mmole

50mM Tris/HCl, pH 8.0

5mM DTT

5mM magnesium chloride

plus other ligands depending upon the experiment:

0-500µM sodium pyrophosphate in 0.1M Citrate/NaOH, pH 6.0 (made immediately before use)

0-200µM sulphonamides

0-100µM dihydropterin.

Figure 2.11: Coupling DHPS to CNBr-activated Sepharose Beads.

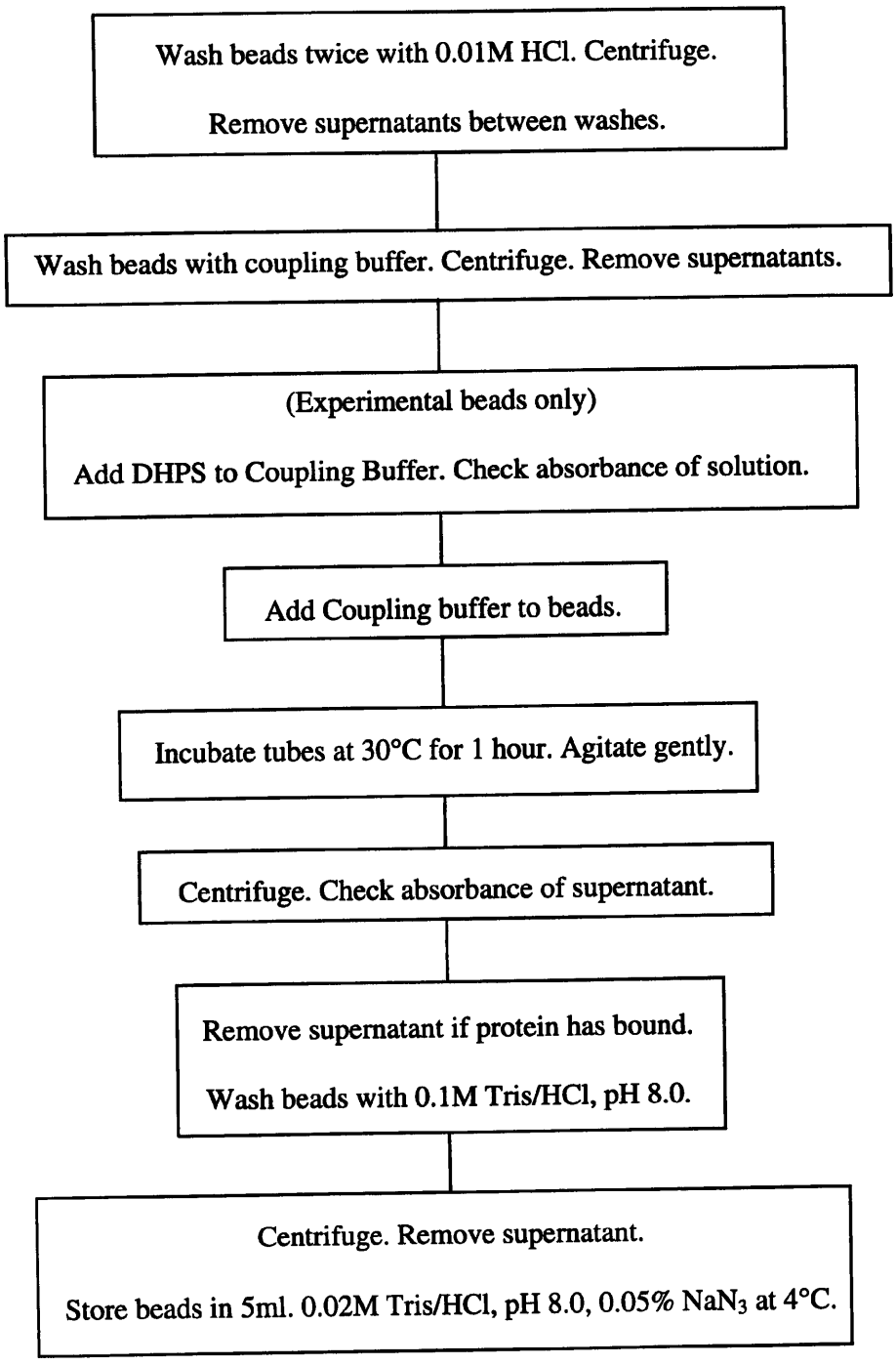

Deionised water was used to make up the volume of cocktails. 20µl. of control or experimental beads were added to the cocktail and the tubes flicked gently to mix. The tubes were left at 25°C for 20 minutes. Truncated pipette tips were used to dispense the bead slurry to improve the accuracy of pipetting. Each mixture was pipetted into a minicolumn [See Section 2.3] which had been fitted onto an eppendorf tube. The columns and tubes were centrifuged at 4300g for 2 minutes to recover unbound ligand and the columns were transferred onto fresh eppendorf tubes. The eluate was pipetted into a scintillation vial and 2.5ml. of scintillation fluid added, vortexed well and counted. The counts corresponded to unbound radioactive ligand. 100µl. of 0.1M glycine/HCl, pH 2.8 was added to the beads in the top of each minicolumn and left for 5 minutes to allow the beads to rehydrate. The buffer eluted bound ligand from the beads with 95% recovery. The columns were centrifuged as described above and the eluate counted as before. These counts corresponded to bound radioactive ligand. [Figure 2.12]. A second wash of the minicolumn with 100µl of glycine/HCl buffer gave a background level of radioactivity (less than 3%).

2.27 Validation of the Binding Assay.

The data in Table 2.2 shows that the binding of pABA to DHPS reaches equilibrium within 20 minutes of mixing the DHPS into the reaction. The results in Figure 2.13 show that the DHPS immobilised on the sepharose beads is catalytically active, although approximately 12 times reduced compared with a solution of DHPS of the same concentration.

2.28 The Hanging DropTechnique.

The hanging drop technique [McPherson, (1990)] was adopted to crystallise DHPS. Tissue culture plates with flat bottoms were used with a well capacity of approximately 3.5ml and an area/well of about 2.0ml. The plates contained 24 wells so 24 different sets of crystallisation conditions could be tested at any one time. 1.0ml of the reservoir solution was pipetted into the well and 1µl of this solution mixed with 1µl of protein solution on a cover slip.

Figure 2.12: The Binding Assay.

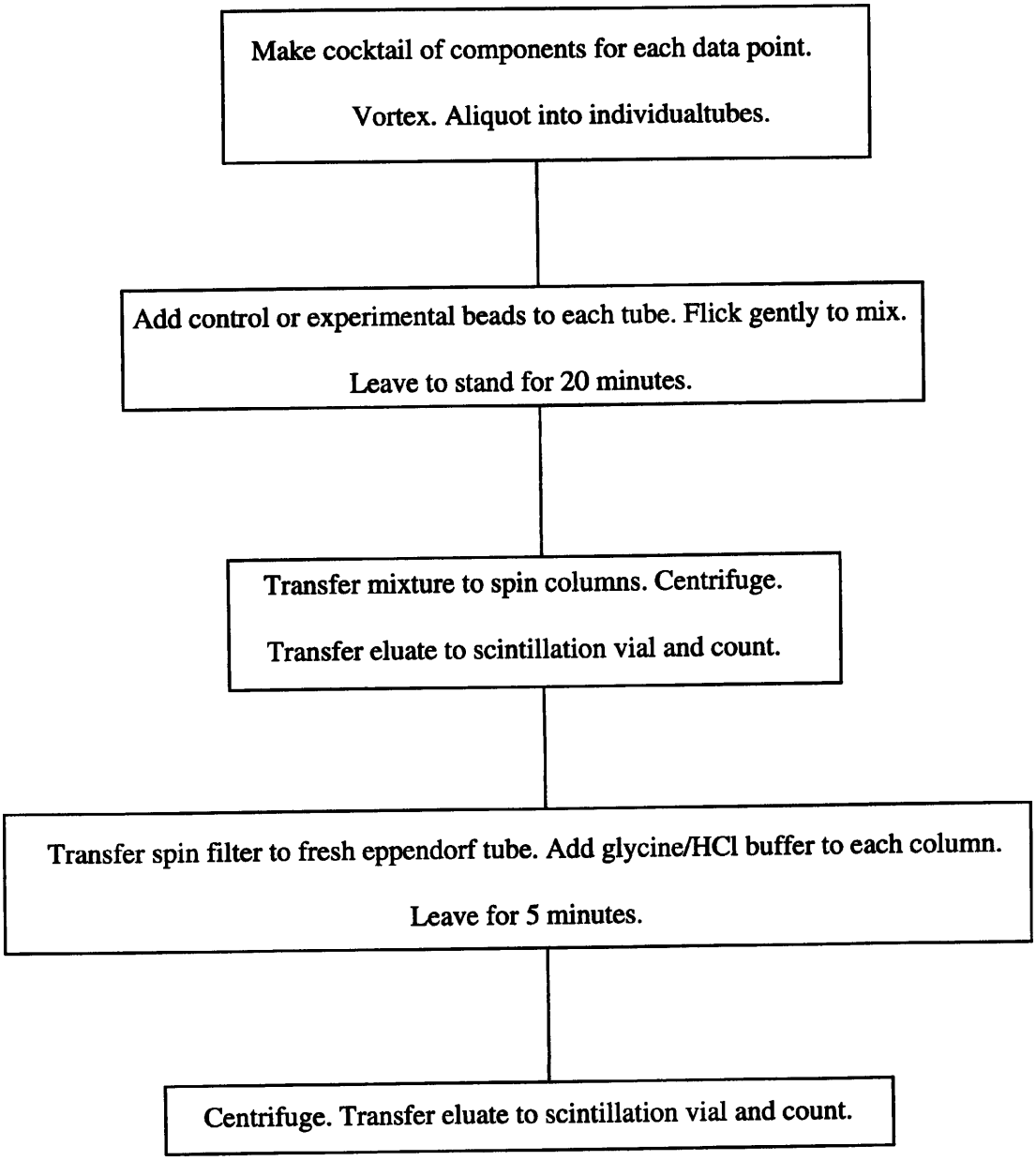

Table 2.2: Rate of formation of the binding equilibrium.

Incubation Time (min.)	Bound pABA (nM)
20	75.4 ± 2.2
60	69.1 ± 2.2
120	71.0 ± 0.7

Assay conditions were as described earlier. [Section 2.26]
The concentration of [^{14}C]-pABA was 500nM. (60mCi/mmole) and the concentration of sodium pyrophosphate was 0.5mM. Data are presented as the mean values of triplicate experiments ± standard deviation.

Figure 2.13: Enzymatic activity of DHPS immobilised on sepharose beads.

Assay conditions were as described in Section 2.26. The concentrations of substrates were:

500nM [^{14}C]-pABA, 60mCi/mmole

4.0μM pterin pyrophosphate

Varying concentrations of DHPS were used and the velocities of DHPS in solution and DHPS immobilised on sepharose beads were compared on a log. graph.

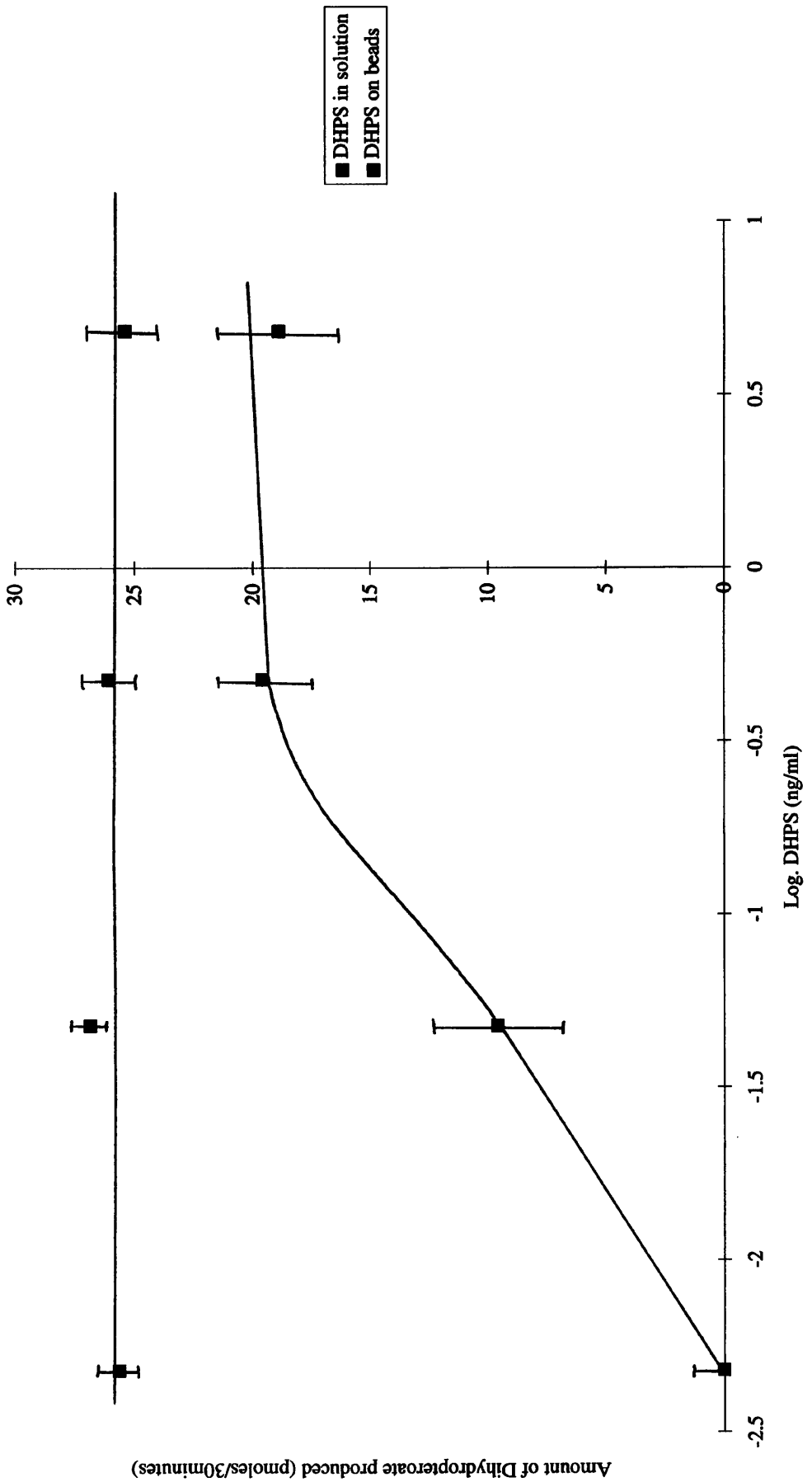

Figure 2.13: Enzymatic activity of DHPS immobilised on sepharose beads.

This 2µl droplet was suspended from the underside of the coverslip over the reservoir and the well chamber sealed with silicone grease. The plates were stored in a constant temperature of 20°C.

2.29 The extinction coefficient of *Streptococcus pneumoniae* DHPS.

DHPS concentrations were estimated using an extinction coefficient of $\varepsilon_{280} = 9650M^{-1}cm^{-1}$, calculated by the method of Gill and von Hippel (1989).

2.30 The Psi-Plot Program.

The Psi-Plot Program version 2, manufactured by PolySoftware International, US, is a non-linear least squares method used to fit the equilibrium binding and kinetic data in Chapters 5 & 6 where described.

Chapter 3. Purification of *S. pneumoniae* DHPS.

3.1 Introduction - Purification of recombinant *S. pneumoniae* DHPS from *E. coli.*

DHPS and the folate biosynthetic pathway was closely studied from the 1960s onwards because it is the target for inhibition by sulphonamide drugs. The work of Brown and others defined the folate pathway and the first kinetic studies on DHPS were published by Ortiz & Hotchkiss in 1966. Crude cell extracts or an ammonium sulphate fractionation were used in all cases as the source of DHPS. In 1979, *Escherichia coli* DHPS was partially purified by elution from a Sephadex G-100 column but the low levels of native expression limited further purification. [Roland, *et al* (1979)] In 1987, the first purification protocol appeared using a recombinant streptococcal *dhps* gene, for the preparation of μg quantities of recombinant DHPS expressed in *E. coli.*[Lopez, *et al* (1987)].The *E.coli* DHPS protein was purified; 2.7g from 110g wet weight of cells using three different chromatographic steps, rectangular-shaped crystals were grown and diffracted to 2.6 Angstroms.[Dallas, *et al* (1992)] More recently, the crystal structure of unliganded *E.coli* DHPS has been solved to 2.0 Angstrom resolution and revealed that DHPS adopts a 'TIM'-barrel structure. [Achari, *et al* (1997)] *Staphylococcus aureus* DHPS has also recently been reported as 'produced at high level in *E.coli* and was purified to more than 95% (data not shown)'. This work confirmed the DHPS enzyme belonged to the 'TIM'-barrel group of proteins. [Hampele, *et al.* (1997)] Finally DHPS has been purified from the mitochondria of pea leaves in microgram quantities. [Rebeille, *et al.* (1997)]

Milligram quantities of highly pure DHPS were required for this study, especially for the crystallisation trials. A novel purification strategy was therefore devised to permit the purification of mg. quantities of pure DHPS.

3.1.1 Over-expression and harvesting of DHPS.

Flasks of 2YT medium were inoculated with XL1-Blue/pKK/DHPS cells. They were agitated at 37°C overnight (12-16 hours). Flasks of fresh 2YT medium were inoculated with 0.025 vol. each of the overnight culture. These fresh cultures were grown to an optical density at 600nm. of 0.4-0.6, then induced with 0.5mM IPTG.

After a further 2.5-3 hours of growth, the cells were harvested by centrifugation at 11600g for 10 minutes. The cell pellet was washed once with 2 volumes of resuspension buffer containing:-

100mM Tris/HCl, pH 7.5
50mM sodium chloride
2mM PMSF
1mM DTT
1mM EDTA [Beynon & Oliver, (1995)]

The pellet was resuspended in an equal volume of the same buffer. The cells were cooled on ice then, keeping the cells cool, disrupted by probe sonication using a Soniprep-150. The cell debris was separated from the supernatant by centrifugation at 48 200g for 30 minutes and the supernatant was retained. SDS-PAGE of the supernatant revealed a protein band corresponding to a molecular weight of about 34kDa., indicating high levels of expression of DHPS. [Figure 3.1]

3.1.2 Polyethyleneimine (PEI) precipitation.

A PEI precipitation step was introduced to remove nucleic acid contamination. Removing the nucleic acids early in the purification simplified subsequent column chromatography steps by removing non-protein material which absorbed at 280nm. The working life of the chromatography columns used during later stages of the purification was also greatly extended.

In principle, RNase and DNase could be added to digest the nucleic acid but this was not an acceptable option because a considerable quantity of protein would be introduced, only to be removed during a later purification step. An alternative method employed polyethyleneimine which, in a high salt solution, would precipitate nucleic acids. [Burgess, (1991)]

The supernatant was made up to 1.0M sodium chloride by dropwise addition of a 5.0M sodium chloride solution. 0.2% PEI was added with stirring and the solution left on ice for 30 minutes. The thick, white precipitate of PEI and nucleic acids was removed by centrifugation at 9220g for 10 minutes and the supernatant retained.

After a further 2.5-3 hours of growth, the cells were harvested by centrifugation at 11600g for 10 minutes. The cell pellet was washed once with 2 volumes of resuspension buffer containing:- 100mM Tris/HCl, pH 7.5

50mM sodium chloride

2mM PMSF

1mM DTT

1mM EDTA [Beynon & Oliver, (1995)]

The pellet was resuspended in an equal volume of the same buffer. The cells were cooled on ice then, keeping the cells cool, disrupted by probe sonication using a Soniprep-150. The cell debris was separated from the supernatant by centrifugation at 48 200g for 30 minutes and the supernatant was retained. SDS-PAGE of the supernatant revealed a protein band corresponding to a molecular weight of about 34kDa., indicating high levels of expression of DHPS. [Figure 3.1]

3.1.2 Polyethyleneimine (PEI) precipitation.

A PEI precipitation step was introduced to remove nucleic acid contamination. Removing the nucleic acids early in the purification simplified subsequent column chromatography steps by removing non-protein material which absorbed at 280nm. The working life of the chromatography columns used during later stages of the purification was also greatly extended.

In principle, RNase and DNase could be added to digest the nucleic acid but this was not an acceptable option because a considerable quantity of protein would be introduced, only to be removed during a later purification step. An alternative method employed polyethyleneimine which, in a high salt solution, would precipitate nucleic acids. [Burgess, (1991)]

The supernatant was made up to 1.0M sodium chloride by dropwise addition of a 5.0M sodium chloride solution. 0.2% PEI was added with stirring and the solution left on ice for 30 minutes. The thick, white precipitate of PEI and nucleic acids was removed by centrifugation at 9220g for 10 minutes and the supernatant retained.

Figure 3.1: Gel showing the purification of streptococcal DHPS.

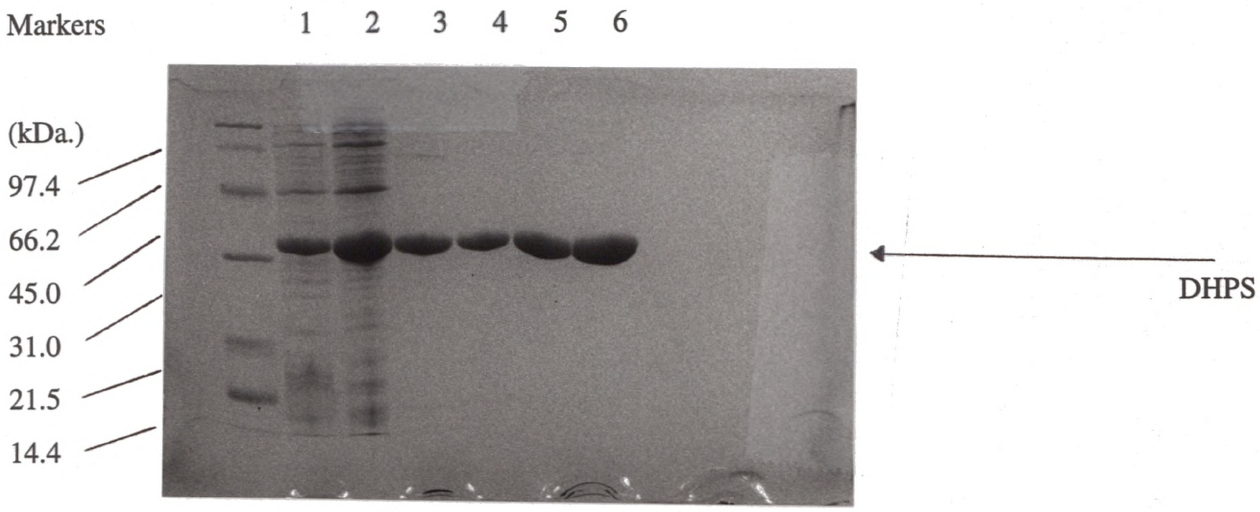

1. Sonication; 2. Ammonium sulphate ; 3. DEAE-Sephacel Column; 4. Mono-Q Column; 5. Chromatofocusing Column; 6. Size-Exclusion Column.

3.1.3 Ammonium sulphate precipitation.

Ammonium sulphate was added to the supernatant to give 50% saturation (29.5g / 100ml.). The solid was gradually added and dissolved to prevent local regions of high ammonium sulphate concentrations. The solution was kept on ice for one hour to encourage precipitation and it was occasionally inverted gently to mix. (The protein formed bubbles if stirred continuously.) A pellet of precipitated protein was obtained by centrifuging at 9220g for 10 minutes. It was dissolved in 10ml. of the resuspension buffer described in 3.1.1.

The solution was dialysed overnight at 4°C against 100 x vol. of 0.02M Tris/HCl, pH 7.5 to remove the salt. During dialysis the ionic strength of the solution gradually decreased and most of the remaining PEI and nucleic acids precipitated. After dialysis the solution was centrifuged at 9220 g for 10 minutes to remove this precipitate.

3.1.4 DEAE-sephacel column.

This DEAE-sephacel purification step was used to remove those proteins which did not bind to the column i.e. were positively charged, and those which had a strong negative charge and bound to the column more tightly than DHPS. This allowed many of the major contaminants to be removed from the preparation quickly without a loss of large quantities of DHPS.

A column of DEAE-sephacel, with chloride as the counter ion, was equilibrated with 0.02M Tris/HCl, pH 7.6 buffer. The dialysed protein solution was applied to the column. The column was washed with 4 column volumes of the above Tris buffer. The DHPS was eluted using 2 column volumes of 0.5M sodium chloride in the Tris buffer, as monitored by absorbance measurement at 280nm. [Figure 3.2] This eluate was dialysed overnight against 0.02M Tris/HCl, pH 7.5 buffer, and then centrifuged at 9 220g for 10 minutes to remove the PEI/nucleic acid which continued to precipitate during dialysis. The eluate was concentrated in an ultrafiltration cell over a PM30 membrane to a volume of approximately 5.0ml. The presence of DHPS was confirmed by SDS-PAGE [Figure 3.1]

Figure 3.2: Elution of streptococcal DHPS from the DEAE-sephacel column.

The column was equilibrated with 0.02M Tris/HCl, pH 7.5 and proteins eluted with the same buffer until the A_{280} decreased to less than 0.01 and DHPS was eluted by the application of the above buffer plus 0.5M NaCl. (as indicated by the arrow.) The flow rate used was 2.0ml/min.

Figure 3.2: Elution of streptococcal DHPS from the DEAE-Sephacel Column.

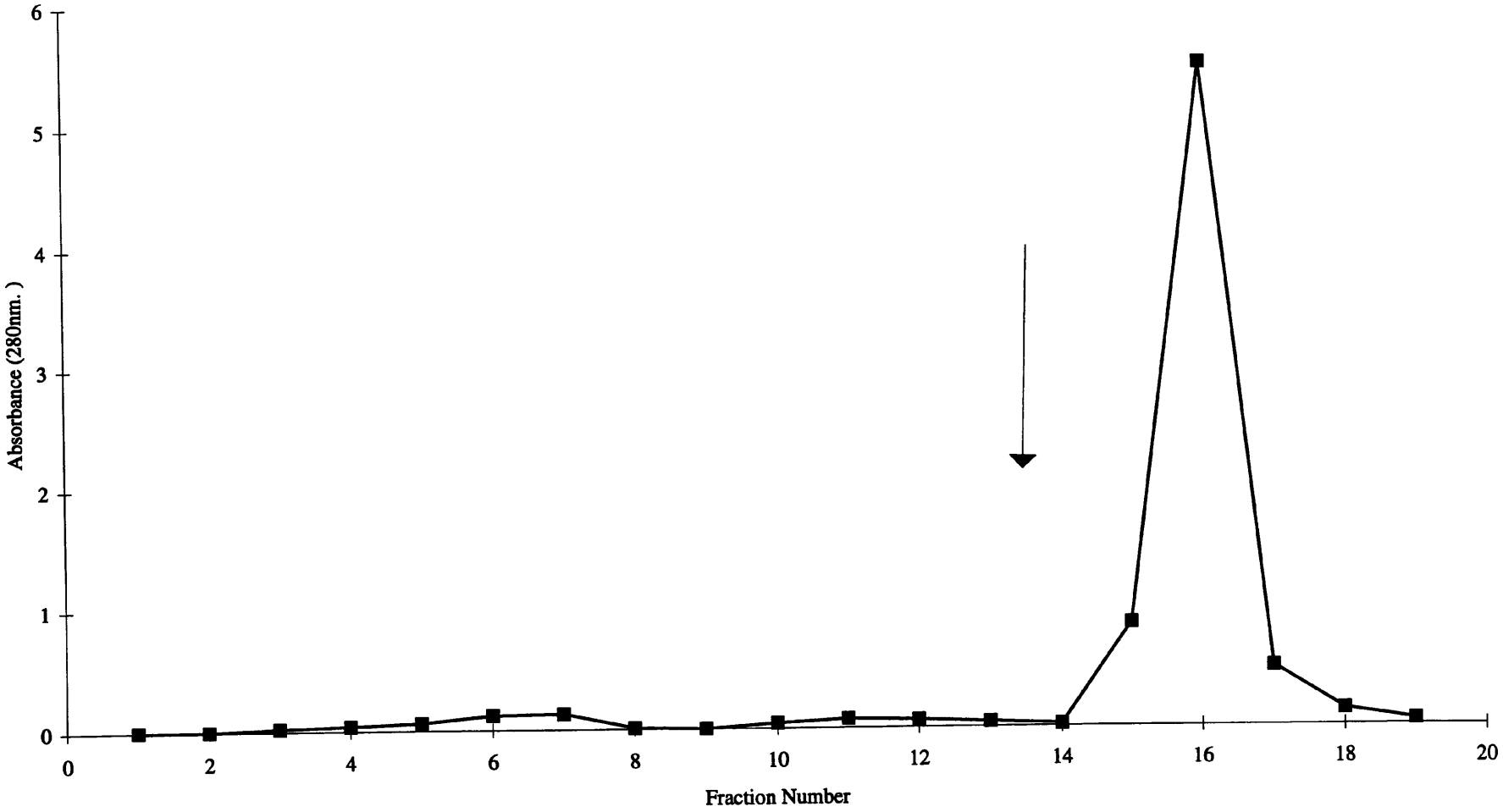

3.1.5 Mono-Q FPLC column.

Some high and low molecular weight components were still visible on the gel and so a higher resolution anionic exchange column was used to purify DHPS further.
A gradient was established using the above buffer and one containing 0.02M Tris/HCl, pH 7.5, 1.0M sodium chloride. DHPS was eluted from the column at 0.34-0.36M sodium chloride as monitored by absorbance at 280nm. [Figure 3.3] Fractions were pooled, dialysed overnight against the size-exclusion buffer described below and concentrated in an Amicon ultrafiltration cell over a PM30 membrane to a volume of approximately 2.0ml. A Centricon-30 concentrator was used to reduce the volume to less than 1.0ml. SDS-PAGE confirmed that the collected fraction contained DHPS and was well separated from the previous peak of nucleic acid. Application of more than 10mg. of DHPS to the column required a more shallow second gradient to continue to elute the nucleic acids separate from the DHPS.

3.1.6 Superdex-200 high resolution column.

Although the bands are not visible on the photograph, [Figure 3.1] some contaminants remained. In an attempt to remove those impurities which eluted at the same salt concentration as DHPS, a size exclusion column was employed. The contaminants were mainly of higher molecular weight than DHPS and so should be easily removed. 150-200µl samples containing up to 10mg of protein were injected onto the size exclusion column which had been pre-equilibrated with a buffer containing:

0.15M sodium chloride

0.05M di-sodium orthophosphate/ NaOH, pH 7.0

DHPS eluted as a peak 28 minutes after injection well separated from the high molecular weight contaminants. [Figure 3.4] The fractions containing DHPS were pooled, dialysed against 0.02M Tris/HCl, pH 7.5 to remove the phosphate buffer and concentrated in a Centricon-30 to a final protein concentration of 30mg/ml. This was estimated as described in 3.1. The DHPS was pure as judged by SDS-PAGE and Coomassie-Blue staining. [Figure 3.1]

Figure 3.3: Elution of DHPS from the Mono-Q column.

A Mono-Q 10/10 column was used, pre-equilibrated in 0.02M Tris/HCl, pH 7.5. DHPS was loaded in a sample volume of 1-2ml. at a flow rate of 2.0ml/min. DHPS was eluted using 0.5M NaCl where indicated by the salt gradient.

Figure 3.3: Elution of DHPS from the Mono-Q column.

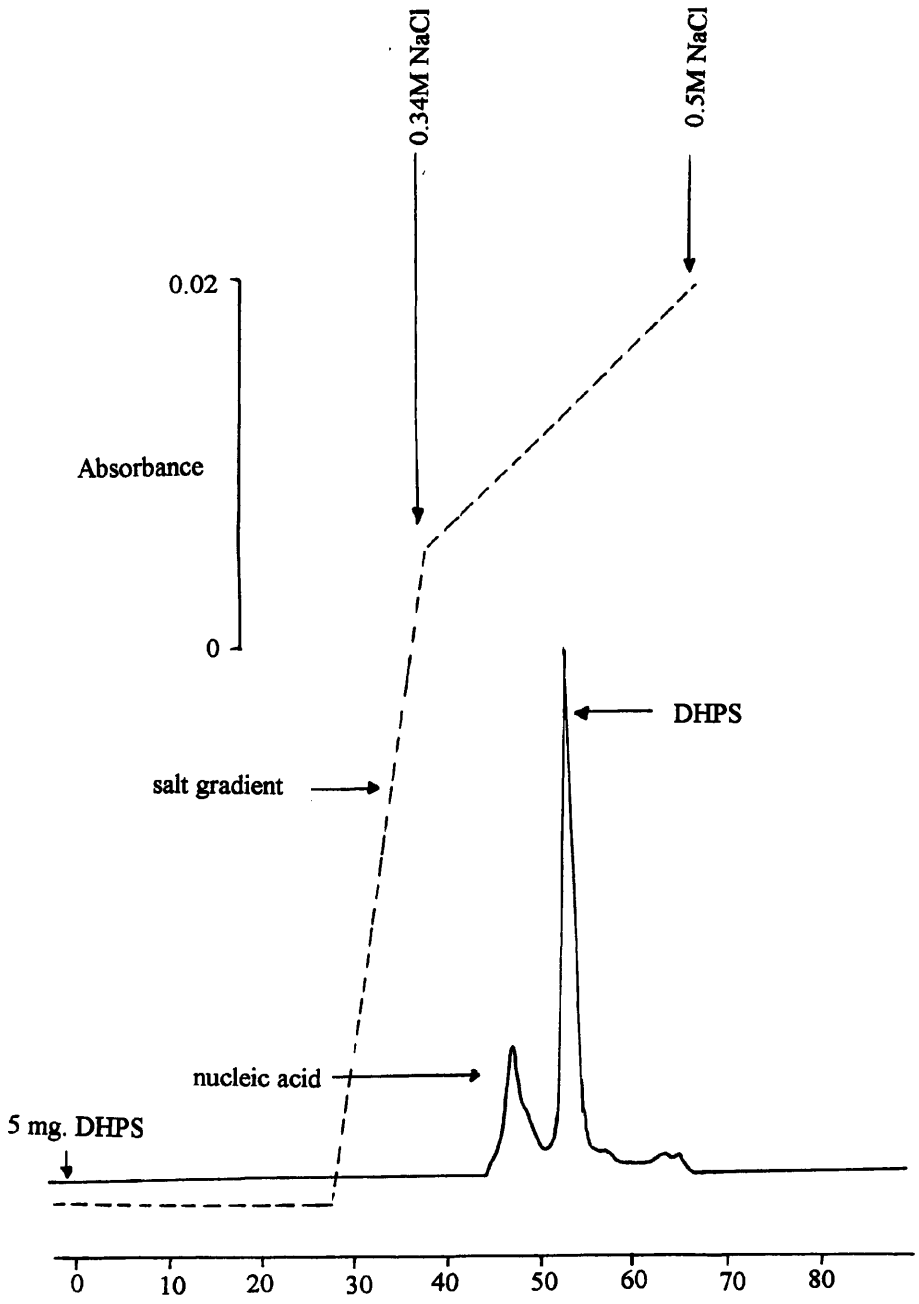

Figure 3.4 Elution of DHPS from the Superdex-200 HR Column.

The column was equilibrated with 0.15M NaCl, 0.05M NaH_2PO_4, pH 7.0. DHPS was applied to the column in a sample volume of 100-200µl. DHPS was eluted at a flow rate of 0.5ml/min.

Figure 3.4: Elution of DHPS from the Superdex-200 HR Column.

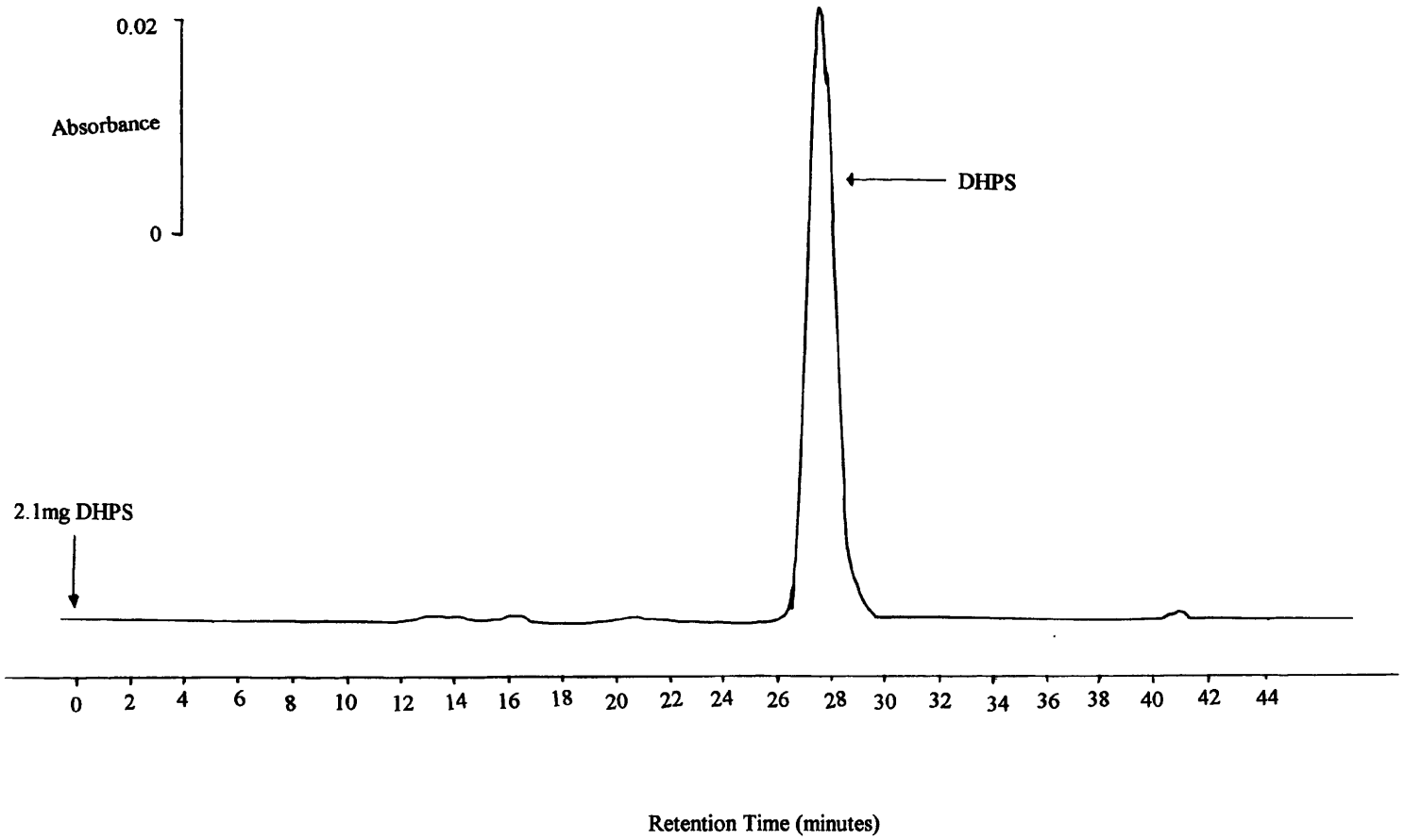

3.1.7 Calibration of the Superdex-200 HR column.

The streptococcal DHPS protein has been reported to elute from a gel filtration column with an apparent molecular weight of 78 kDa., consistent with it being a dimer of 34kDa. subunits. [Lopez, *et al* (1987)]

Retention times are an approximately linear function of the logarithm of the molecular weight of the protein. A calibration graph was constructed for the Superdex-200 column and in excellent agreement with the results of Lopez, *et al.*, the molecular weight of the DHPS protein was measured as 79.4kDa. [Figure 3.5] This confirmed that streptococcal DHPS is likely to be a homodimer of two 34 kDa monomers.

3.1.8 Purification table. [Table 3.1]

A purification table was constructed using the [^{3}H]-pABA radiochemical assay and an initial cell culture of 2.25 litres. The streptococcal DHPS protein was over-expressed to very high levels, and consequently required only a 2.4-fold increase in purity to obtain a homogeneous preparation. It can be seen from the SDS-PAGE [Figure 3.1] that the DEAE-sephacel column removed the majority of the contaminating protein and nucleic acid contamination before the DHPS was applied to the Mono-Q column on the FPLC system. Use of the high resolution FPLC columns ensured an absolutely homogeneous preparation of DHPS for the crystal trials and the likely removal of pyrophosphatase activity at the expense of the overall yield obtained at the end of the preparation.

3.1.9 Chromatofocusing chromatography.

This technique was employed to try to improve the purity of DHPS for crystallography. Crystals of DHPS had been grown using DHPS purified as described above, but were limited in size to a maximum of 30 x 30 x 300μm. They was not sufficiently large to obtain good X-ray data. [See Chapter 4]

The purity of DHPS had been determined by SDS-PAGE followed by Coomassie Brilliant Blue staining. Proteins present in quantities less than 0.5μg protein cm^{-2} of gel would be undetectable by this staining method. Silver-staining rather than Coomassie-staining is reportedly capable of detecting as little as 0.1ng protein mm^{-2} of native gel. [Chapter 1, Protein Purification Methods]

Figure 3.5: Calibration graph of the Superdex-200 HR column.

The elution buffer was 150mM NaCl, 0.05M NaH_2PO_4/HCl, pH 7.0. and a flow rate of 0.5ml/min. 10mg of protein was loaded onto the column in a volume of 200µl. (50mg/ml) The proteins used for the calibration graph are listed in the table below.

Protein	Molecular Weight (kDa.)
Goat IgG	160
Chloramphenicol Acetyl Transferase	75
Pepsin	35
Protein G	7

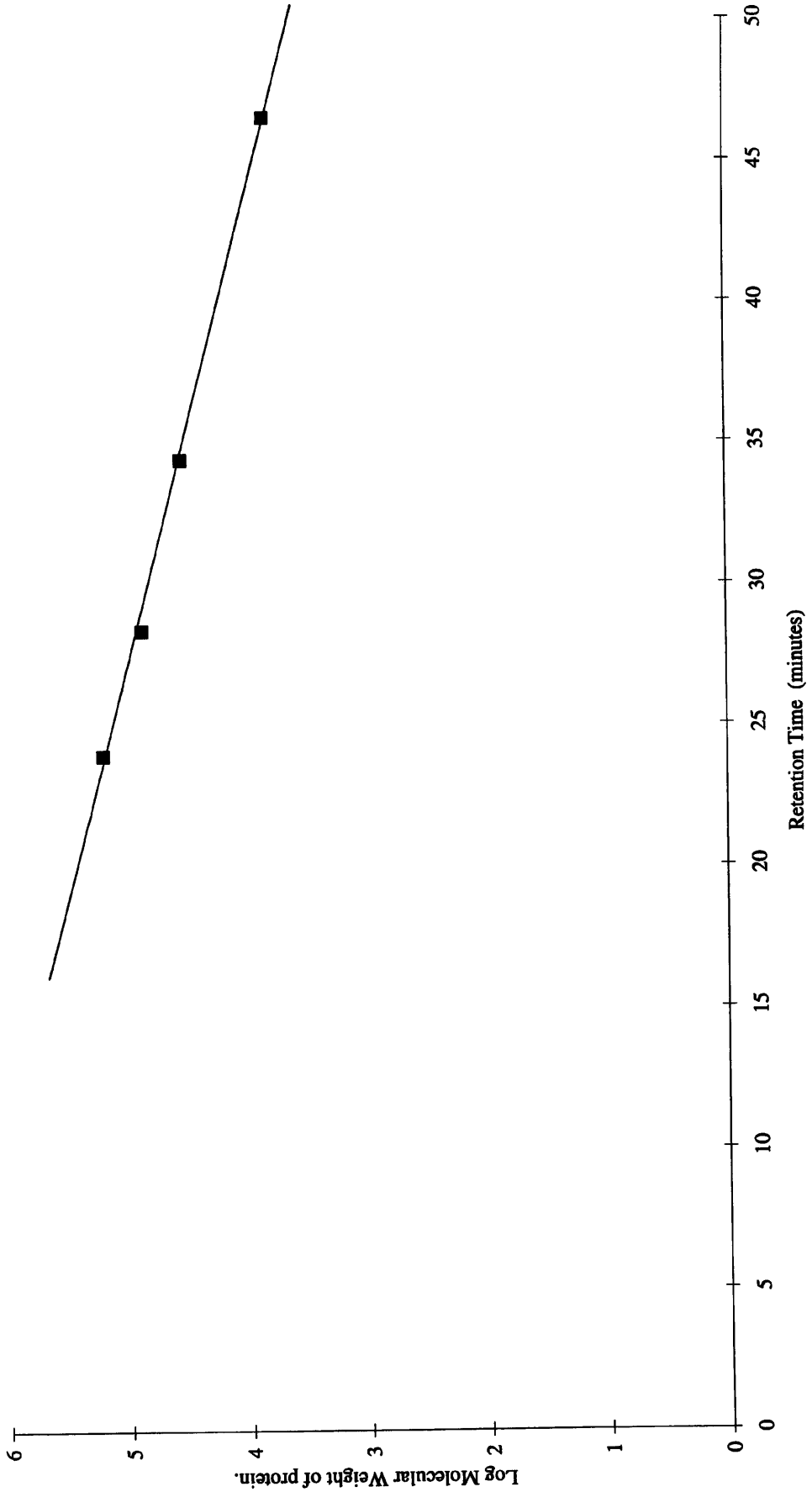

Figure 3.5: Calibration graph of the Superdex-200 column.

Table 3.1: Purification table of *S. pneumoniae* DHPS using the diethyl ether extraction method.

The activity of DHPS was measured using the following reaction mixture:
10nM [^{3}H]-pABA, 41.9Ci/mmole
990nM pABA
4μM pterin pyrophosphate
50mM Tris/HCl, pH 8.0
5mM DTT
5mM magnesium chloride
Successive dilutions of the DHPS solution were tested in the above reaction until a reading of approximately 50% conversion of pABA was obtained. The reaction volume was made up to 50μl. with distilled water. Each dilution was assayed in triplicate and a mean value calculated. The diethyl ether extraction method was used as described in Chapter 2.

Purification Step[#]	Volume (ml)	Protein (mg/ml)	Units[1]	Units/ml	Specific Activity (Units/mg)	Yield (%)	Purification
Sonication supernatant	62	19.9	145266	2343	122	100	1
Ammonium sulphate	31	18.0	67735	2185	121	47	0.99
DEAE-Sephacel chromatography	55	9.2	51855	941	102	36	0.84
Mono-Q chromatography	13	12.0	27463	2113	176	19	1.44
Size-exclusion chromatography	2.1	15.0	9274	4416	294	6.4	2.41

Table 3.1: Purification table of *S. pneumoniae* DHPS using the diethyl ether extraction method.

[#] From a 2.25litre initial cell culture.

[1] Units (U) are defined as nmoles of dihydropteroate produced per minute at 25°C.

A native gel of a 'pure' DHPS sample was run and stained with silver (Gel not shown as staining reaction is continuous and the background is unacceptable after 2 minutes). Small bands could be seen indicating the presence of other proteins. An attempt was made to further purify the DHPS by inserting a chromatofocusing step into the protocol after the Mono-Q column. The choice of buffer depended on the range of the pH gradient used in elution. This in turn is determined by the pI of the protein to be purified.

The pI of streptococcal DHPS was not known so initally a pH gradient from 7 to 4 was used. The protein solution from the Mono-Q column had been dialysed overnight in two litres of the imidazole buffer and concentrated to a volume of 1.0-2.0ml. Samples containing 10-20mg.of protein were applied and washed on to the column with 2 column volumes of the elution buffer.

Figure 3.6 shows that streptococcal DHPS eluted at the end of the pH gradient around pH 4.0. For maximal resolution ideally the pI of DHPS would have been about midway between the pH extremes of the gradient. The poor resolution is therefore partly due to the low elution point of streptococcal DHPS. As they eluted, the fractions were stored on ice and DHPS precipitated at its isoelectric point. The precipitate was centrifuged at 9220 x g for 10 minutes and redissolved in about 1.0ml. of size exclusion buffer. The activity of DHPS was unaffected by precipitation at pH 4.0; the precipitation step therefore greatly improved the purity of DHPS because other contaminants did not precipitate at this low pH. This was seen by trace obtained from the size exclusion column which showed fewer contaminants than before isoelectric precipitation. [Figure 3.7]

The purification table was repeated to include the chromatofocusing column step. [Table 3.2] It showed that a greater degree of purification was obtained by the chromatofocusing column (and subsequent isoelectric precipitation), although the yield was inevitably reduced. Using this pure homogeneous DHPS preparation, crystals were grown to 50 x 50 x 500 μm and as a result a set of X-ray diffraction data was obtained.

Figure 3.6 Elution of streptococcal DHPS from the chromatofocusing column.

The elution buffer was 0.025M imidazole/HCl, pH 7.4. The Polybuffer was diluted 1:8 in water and adjusted to pH 4.0 with HCl.1.0mg. of DHPS was loaded in 1.0ml imidazole buffer and washed onto the column in 12ml. of imidazole buffer. Polybuffer was pumped onto the column where indicated by the Start of pH gradient. The flow rate was 0.5ml/min and the chart speed was 0.5cm/ml.

Figure 3.6 Elution of streptococcal DHPS from the chromatofocusing column.

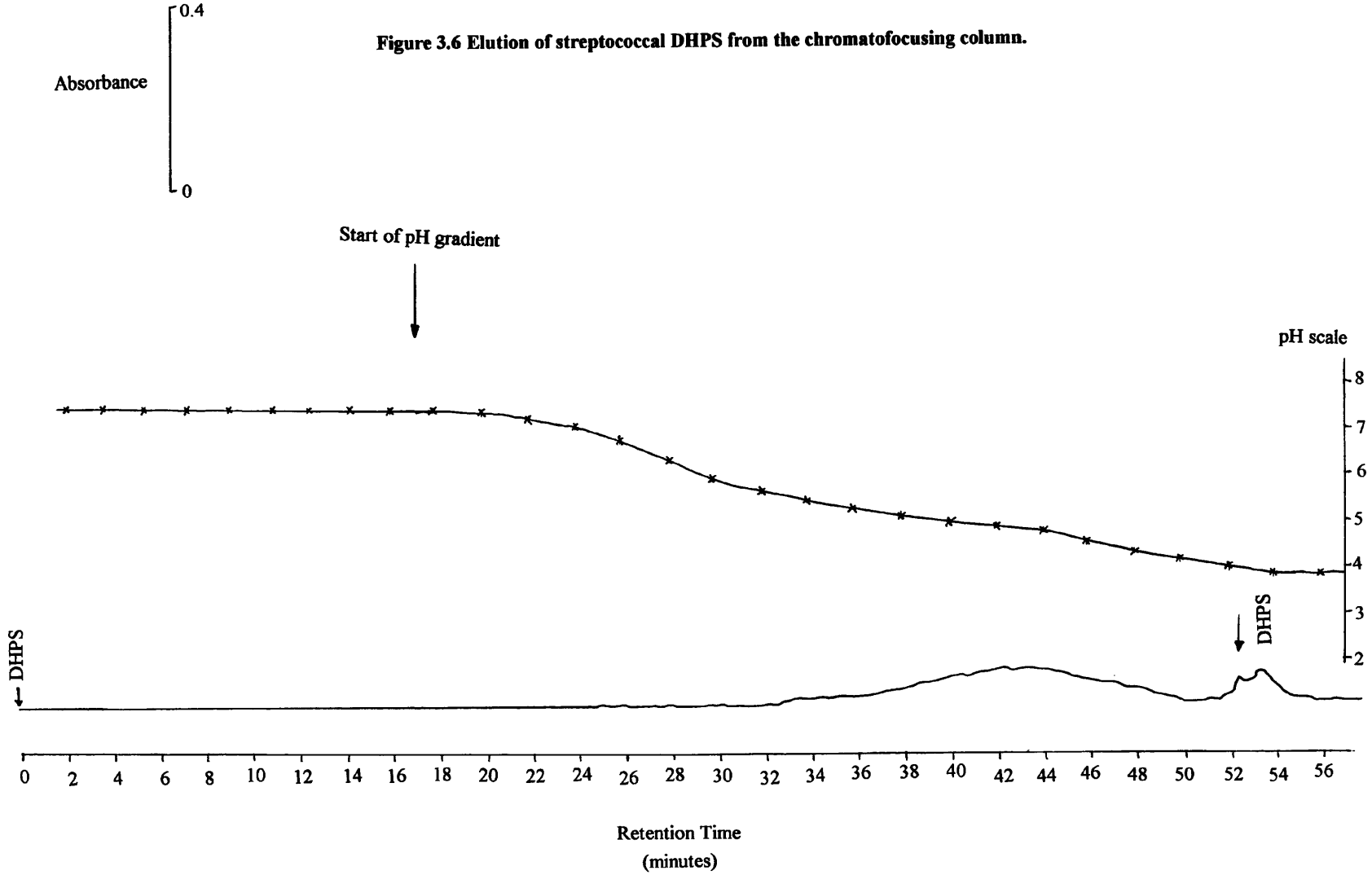

Figure 3.7: Elution of streptococcal DHPS from the Superdex-200 HR column after the chromatofocusing step.

The column was equilibrated with 0.15M NaCl, 0.05M NaH_2PO_4, pH 7.0. DHPS was applied to the column in a sample volume of 100-200µl. DHPS was eluted at a flow rate of 0.5ml/min.

Figure 3.7: Elution of streptococcal DHPS from the Superdex-200 HR column after the chromatofocusing step.

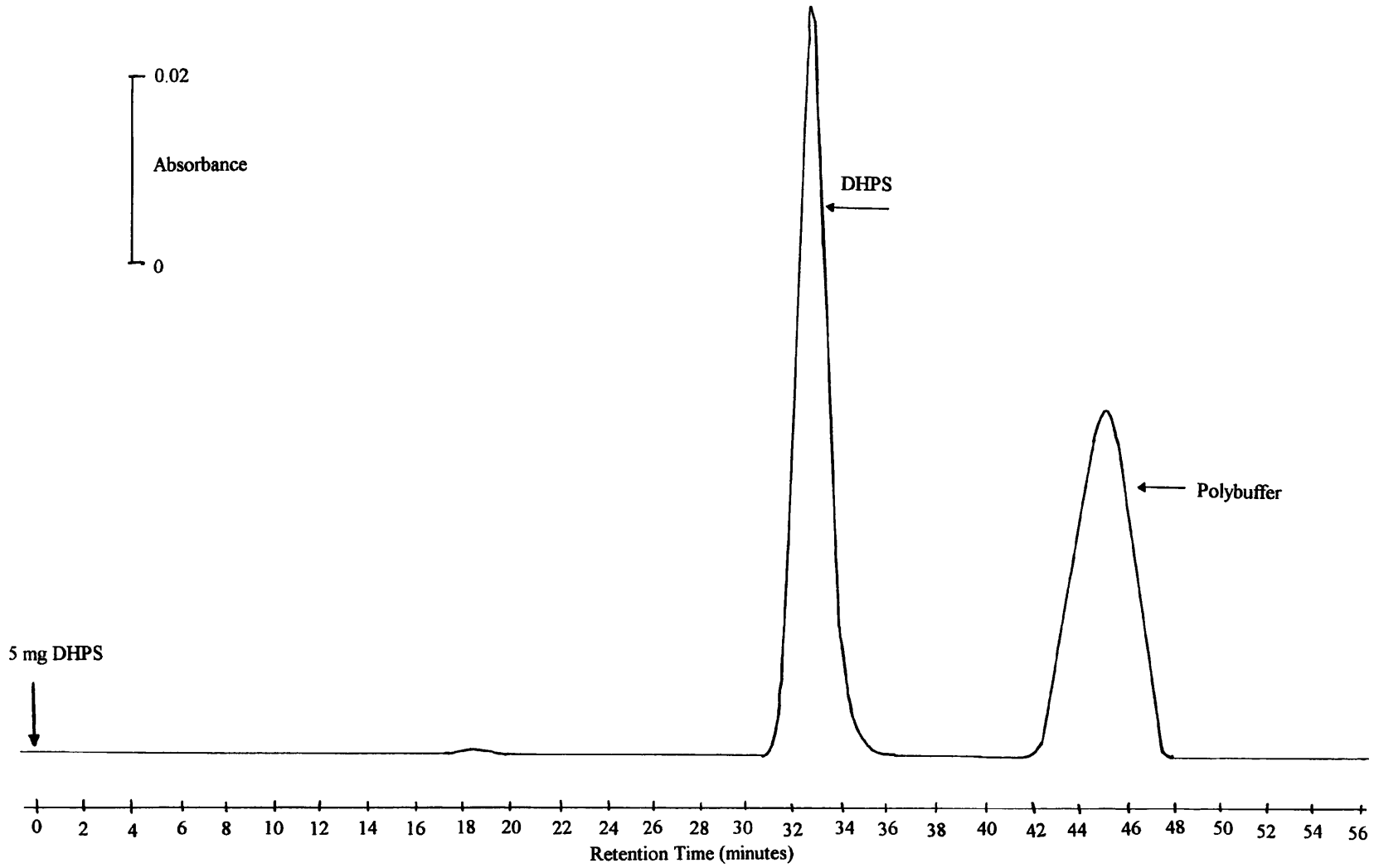

Table 3.2: Purification table of *S. pneumoniae* DHPS including chromatofocusing using the reverse-phase column separation method.

The activity of DHPS was measured using the following reaction mixture:
333.4nM [^{14}C]-pABA, 60mCi/mmole.
3.66μM pABA
4μM pterin pyrophosphate
50mM Tris/HCl, pH 8.0
5mM DTT
5mM magnesium chloride
Successive dilutions of DHPS were tested in the above reaction until readings of approximately 50% conversion of pABA were obtained. The reaction volume was made up to 100μl. with distilled water. Each dilution was assayed in triplicate and the mean value calculated. The reverse-phase column separation method was used.

Purification Step[#]	Volume (ml)	Protein (mg/ml)	Units[1]	Units/ml	Specific Activity (U/mg)	Yield (%)	Purification
Sonication supernatant	45	10.79	26760	595	55.1	100	1
Ammonium sulphate	9	19.2	11700	1300	67.8	44	1.23
DEAE-Sephacel chromatography	6.5	4.4	2979	458	104	11	1.88
Mono-Q chromatography	3	3.6	1689	563	159	6.3	2.88
Chromatofocusing.	1	4.8	1099	1099	231	4.1	4.20
Size-exclusion chromatography	0.4	6.2	621	1553	249	2.3	4.52

Table 3.2: Purification table of *S. pneumoniae* DHPS including Chromatofocusing using the reverse-phase column separation method.

[#] From a 2.25litre initial cell culture.
[1] Units (U) are defined as nmoles of dihydropteroate produced per minute at 25°C.

3.1.10 Summary.

By following this protocol, up to 60mg. of pure streptococcal DHPS (as seen on SDS-PAGE) could be obtained from 2.25 litres of liquid culture. Using the standard laboratory equipment as described, this DHPS can be obtained in about four days. The difference in the degree of purification achieved from Table 3.1 to Table 3.2 is largely due to the better assay technique and practice over time. DHPS was inevitably lost as the ammonium sulphate precipitation step was made at only 50%. However at 55% precipitation, the amount of DHPS which is recovered increases only marginally but a considerable increase the quantity of contaminating proteins can be visualised on an SDS-PAGE gel. (not shown) The chromatofocusing step demonstrated the huge increase in purity obtained on isoelectric precipitation and subsequent size exclusion chromatography. Although very little protein remained, these two step added to an overall increase in purity of over 4.5-fold.

3.2 The DHPS monomer-dimer equilibrium.

Streptococcal DHPS elutes from the size-exclusion column as a dimer of approximately 79kDa. [Figure 3.6] On a denaturing SDS-PAGE gel in the presence of 5mM DTT, DHPS migrates with a subunit molecular weight of 34kDa.[Figure 3.1]

It is possible that DHPS may naturally exist both as a monomer and a dimer under certain conditions. If the dimer dissociates into monomers at low concentrations, for example, this could have important implications for a possible regulatory mechanism for the enzyme. It would also be important in the context of this piece of work because the crystallographic studies require that DHPS is at a very high concentration of at least 5mg/ml., yet the kinetics require that DHPS is at very low concentrations of around 30ng/ml. or less. To examine whether DHPS dimers dissociate at low concentrations, a series of experiments were performed using the Superdex-200 HR column.

Figure 3.8 shows that 43μg of DHPS eluted at a molecular weight of 79kDa. from the size-exclusion column consistent with a dimer. However on decreasing the quantity of DHPS to 0.5μg, two peaks of equal height were seen. [Figure 3.9] One corresponded to the usual elution time for the dimer with a molecular weight of 79kDa. and the new peak corresponded to protein with a molecular weight of 19.5kDa. By decreasing the amount of DHPS further, any protein eluting from the column would be undetectable on the UV detector at 280nm. In order to be able to visualise any peaks, the UV detector was changed to a wavelength of 214nm. and the zinc lamp rather than the mercury lamp was used. The absorption coefficient for DHPS was much higher at this lower wavelength enabling any protein which eluted to be detected on the chart recorder. A series of small peaks and one major peak eluted from the column. [Figure 3.10]

There was no detectable peak eluting at 28 minutes corresponding to the DHPS dimer at 79kDa. The major peak corresponded to the protein with a molecular weight of 19.5kDa. This may seem to be too low a molecular weight for the monomer as we would expect a weight around 34kDa. from the gene sequence. Although both SDS-PAGE and size-exclusion chromatography separate proteins on the basis of their size, the shape of the dimer is likely to be different to the monomer.

Figure 3.8 Elution of DHPS as a dimer from the Superdex-200 HR column.

For the experiments described in Figures 3.8-3.10, the same set of markers on the same column were used, as in Figure 3.5 (p93), and the plot obtained was linear. The manufacturer's information indicated that the column was relatively insensitive to differences in volume and concentration of the sample loaded. The column was therefore used in the same manner for these analytical experiments as the preparative method described previously.

The elution profile was measured at 280nm. in a buffer comprising 0.15M NaCl, 0.05M NaH_2PO_4, pH 7.0. 43ng DHPS was loaded onto the column in a volume of 50µl. (86ng/ml) A flow rate of 0.5ml/min. and a chart speed of 1.0cm/ml. was used.

Figure 3.8 Elution of DHPS as a dimer from the Superdex-200 HR column.

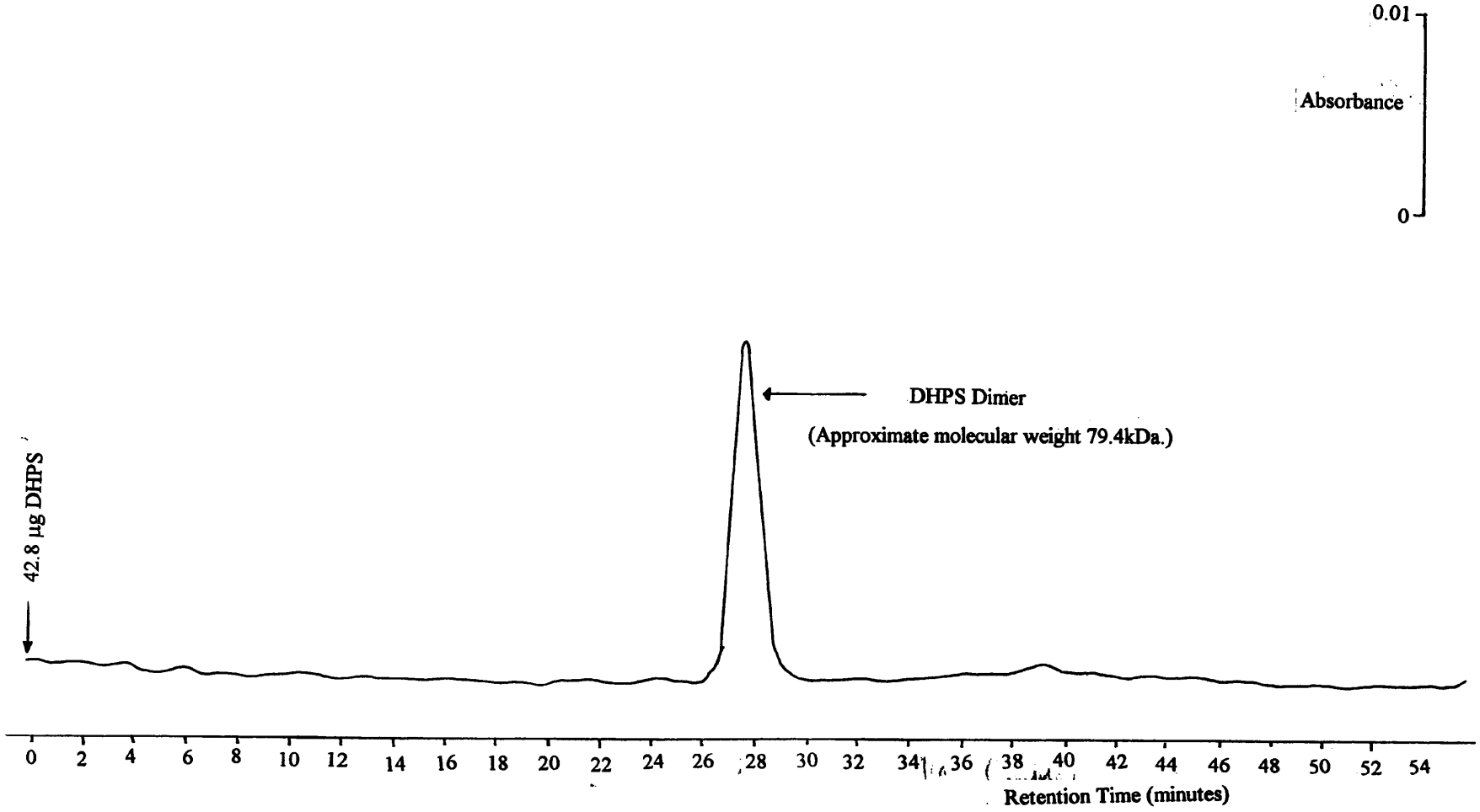

Figure 3.9 Elution of DHPS as both a monomer and a dimer from the Superdex-200 HR column.

The elution profile was measured at 280nm. in a buffer comprising 0.15M NaCl, 0.05M NaH_2PO_4, pH 7.0. DHPS was loaded onto the column in a volume of 50µl. A flow rate of 0.5ml/min. and a chart speed of 1.0cm/ml. was used.

Figure 3.9 Elution of DHPS as both a monomer and a dimer from the Superdex-200 HR column.

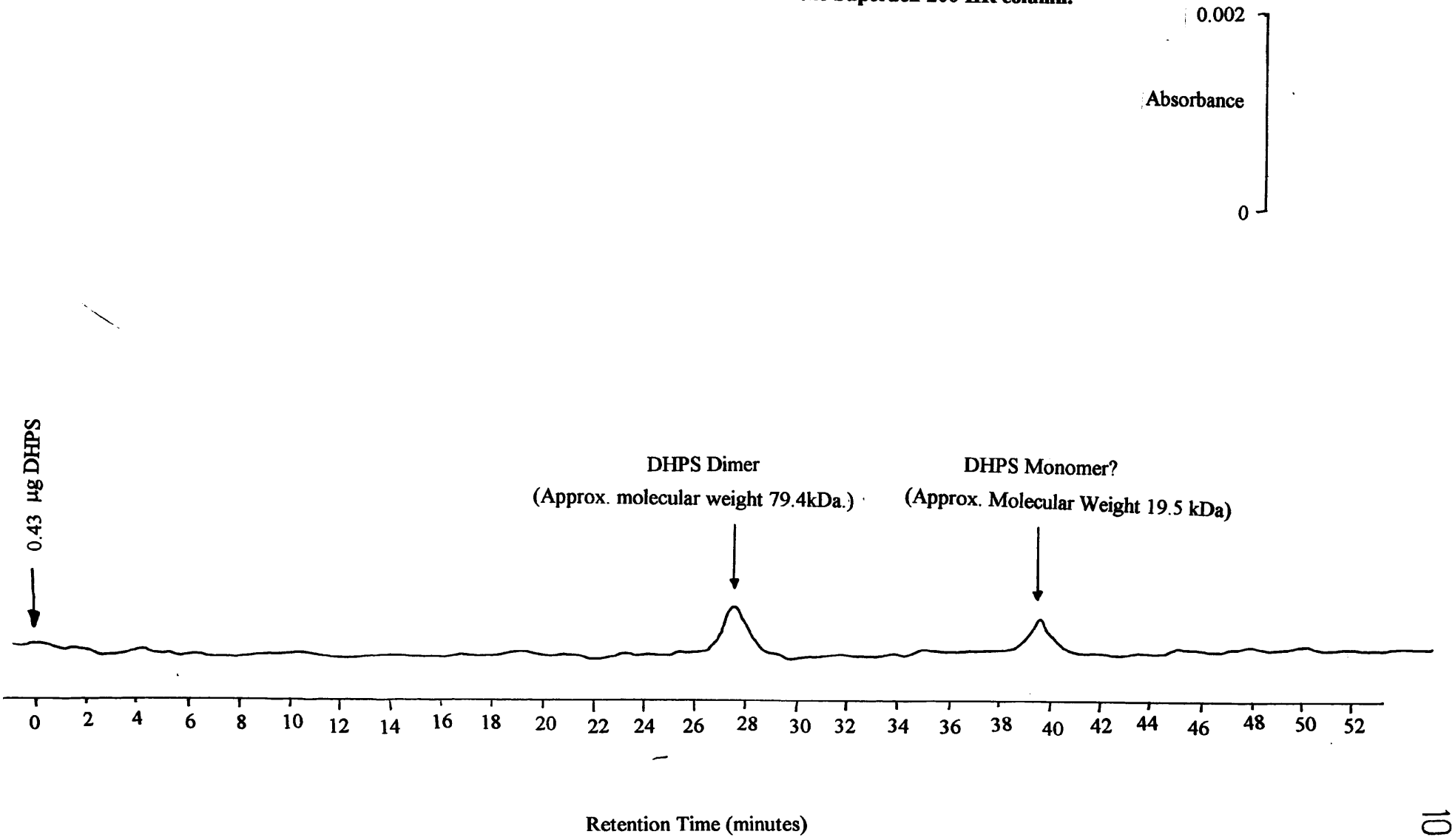

Figure 3.10 Elution of DHPS as a monomer from the Superdex-200 HR column.

The elution profile was measured at 214nm. in a buffer comprising 0.15M NaCl, 0.05M NaH_2PO_4, pH 7.0. DHPS was loaded onto the column in a volume of 50µl. A flow rate of 0.5ml/min. and a chart speed of 1.0cm/ml. was used.

Figure 3.10 Elution of DHPS as a monomer from the Superdex-200 HR column.

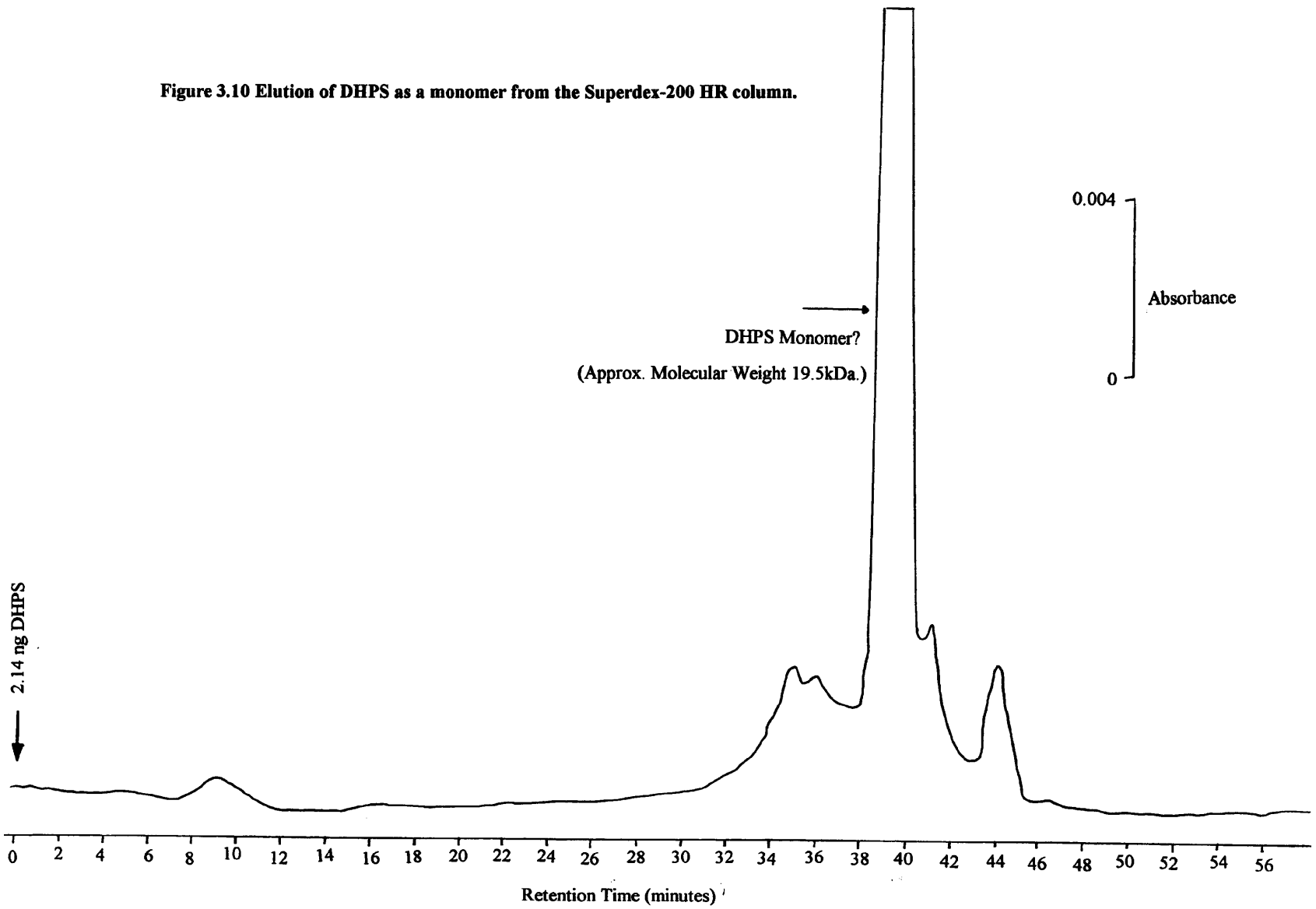

Some proteins show anomalous behaviour on size-exclusion chromatography, particularly proteins which are not spherical in shape. This will cause non-linear elution from the column and so this protein of apparent molecular weight 19.5kDa. is most probably the monomer as no other proteins were injected onto the column, and the protein cannot exist in a form any smaller than a monomer. There is some evidence to support this work from the crystal structures of the *E.coli* and *Staphylococcus aureus* DHPS proteins; they have been shown to crystallise as dimers.
To conclude, there is a DHPS monomer:dimer equilibrium which may have a regulatory effect on the enzyme.

3.3 Circular dichroism spectroscopy.

A rapid, simple method to examine the secondary structure of proteins in solution is circular dichroism or CD spectroscopy. Many secondary structure motifs have characteristic CD spectra. [Greenfield, (1996)] A CD spectrum was obtained for a sample of streptococcal DHPS purified as decribed earlier in the chapter. [Figure 3.11] A comparison of the spectrum obtained with those seen from reference spectra from predominantly α-helix or β-sheet structures suggest that DHPS is folded in solution with some α-helix and some β-sheet structure due to the negative ellipticity between 240nm and 200nm, then positive ellipticity below 200nm. [Kyte, (1995a)]
The spectrum of DHPS is not sufficiently accurate to determine the relative quantitites of each structure. Confirmation of the presence of these structures must be obtained from crystallographic studies.

Figure 3.11: Circular dicroism spectrum.

CD measurements were made using a Jobin Yvon CD6 spectropolarimeter at Zeneca Pharmaceuticals, Alderley Park, U. K.

Measurements were made in a 10mm quartz cell at 7°C in 0.15M sodium chloride, 0.05M sodium hydrogen orthophosphate, pH 7.0.

The concentration of DHPS in the cell was 50μM.

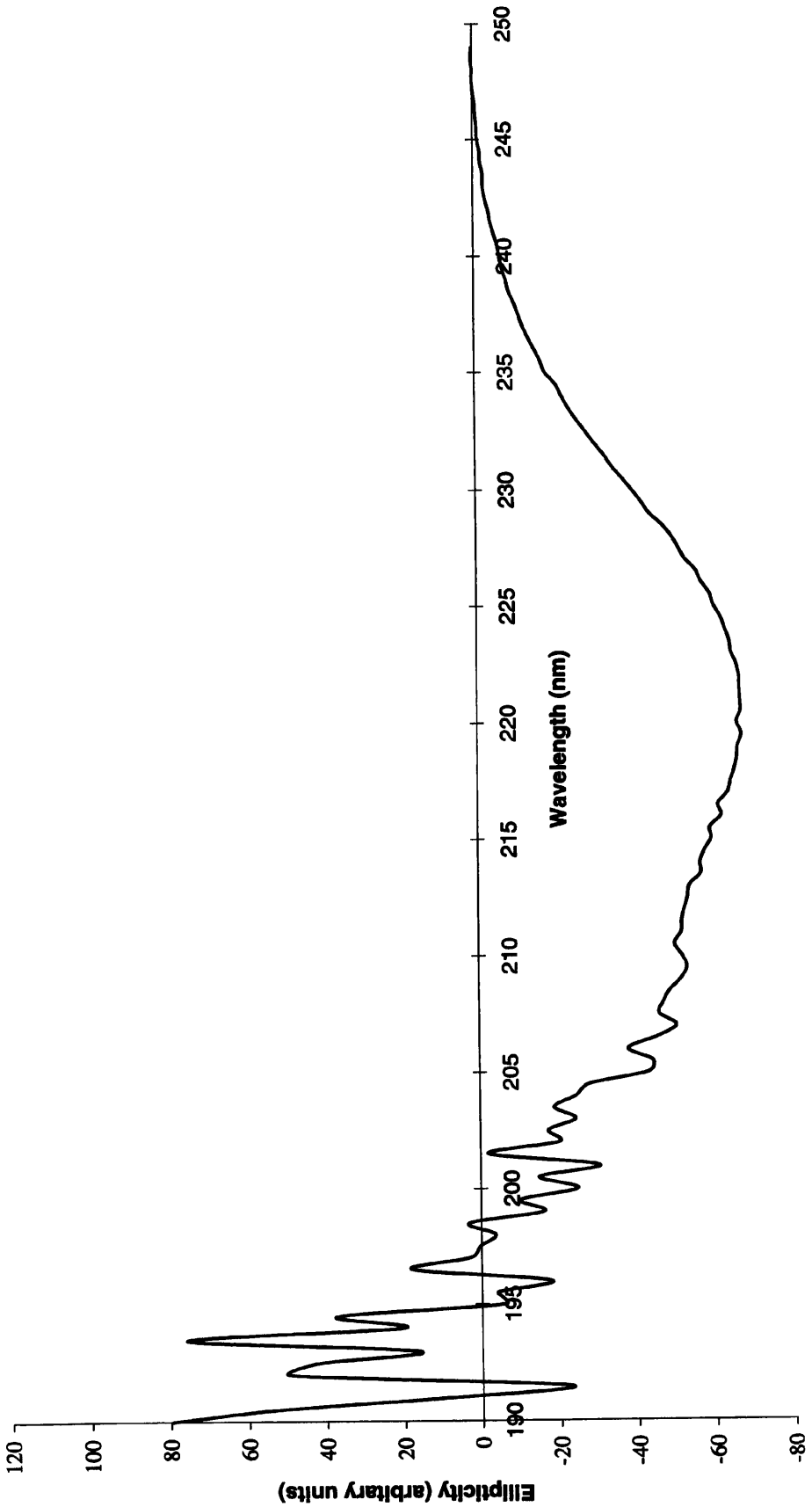

Figure 3.11: Circular dicroism spectrum.

3.4 Introduction - Purification of *Neisseria meningitidis* DHPS.

Very little work had been undertaken on DHPS from *N.meningitidis*, although both *S. pneumoniae* and *N. meningitidis* can cause bacterial meningitis. *dhps* gene sequences of several sulphonamide-resistant and sensitive strains of *N. meningitidis* have been published and a molecular weight of 30kDa. for the DHPS polypeptide has been determined from the gene sequence. [Radstrom, *et al* (1992)]. In this report the *dhps* gene was expressed in maxicells but no attempt had been made to purify the protein.

Two clones, pNMBT101 and pNMBT1912, of the *N. meningitidis* gene from a sulfonamide resistant strain MO 035 (B:15, Su^r) were obtained from C. Fermer, Uppsala University, Sweden. An *Ssp*I fragment which contained the entire *dhps* gene had been inserted into the *Sma*I site of the pUC13 vector to produce pNMBT1912. The coding region of the *dhps* gene, amplified by PCR, was inserted into the *Kpn*I and *Sal*I sites of pUC19 to produce pNMBT101. The nucleotide sequence pNMBT101 had been determined and was identical to the *dhps* gene in pNMBT1912. [Fermer, *et al* (1995), Kristiansen, *et al* (1995)].

The pUC family of plasmids contain an ampicillin resistance gene. To maintain selection of the pUC plasmids hosting the *dhps* gene and the XL1-Blue episome, all plates and cultures contained 100µg/ml. ampicillin and 10µg/ml. tetracycline. Where controls consisted of XL1-Blue cells with no pUC vector, only 10µg/ml. tetracycline was present. The pUC family of plasmids contain a polylinker site in the *lac Z* gene so the *lac* promoter should be inducible with IPTG. All cultures were grown at 37°C with agitation.

3.4.1 Testing the clones for expression of DHPS.

In two separate experiments, the clones pNMBT1912 and pNMBT101 were transformed into *E.coli* XL1-Blue cells according to the protocol described in Chapter 2. Control cells were XL1-Blue with no pUC vector. Flasks of 2YT were used to grow transformant and control cells. The control cells, as expected, grew more quickly than the transformed cells.

For this reason a smaller volume of inoculant was used for the controls flasks. Growth rates were monitored. [Figure 3.12] All cultures were induced with 0.5mM IPTG when their optical density at 600nm. reached 0.4-0.6. The cultures were allowed to grow for a further 2.5 hours. The cells were harvested by centrifugation at 11 600g for 10 minutes. The cell pellet was treated in the same manner as the streptococcal preparation up to and including the sonication step. The cell debris was removed by centrifuging at 48 200g for 30 minutes. The supernatants were removed and made up to 50% ammonium sulphate. The protein was allowed to precipitate on ice for 30 minutes. The solutions were centrifuged at 11 600g for 10 minutes and the supernatants removed.

The protein pellets were redissolved in 0.02M Tris/HCl, pH 7.5 and dialysed overnight against 1 litre of the same Tris buffer to remove the salt. A 12.5% acrylamide gel was used to analyse the samples.[Figure 3.13] The gel showed clearly that the control and pNMBT101 had produced very little DHPS whereas pNMBT1912 had over-expressed DHPS. The DHPS activity of each sample was also tested. pNMBT101 had produced approximately twice as much DHPS than the control whereas pNMBT1912 had produced over 100 x more DHPS than the control. [Table 3.3] pNMBT101 produced very little DHPS and its growth rate was comparable with the control. There may be a problem with the correct open reading frame or the ribosome binding site, as inspection of the sequence shows there to be a non-optimal Shine-Dalgano sequence.

The pNMBT1912 construct restricted the growth of the XL1-Blue cells compared with pNMBT101 and the control cells. The polylinker site of pUC plasmids is situated between the promoter and operator in the *lac* operon, so IPTG would be expected to induce expression of the *dhps* genes in both pNMBT101 and pNMBT1912. The poor rate of growth coupled with expression of the *dhps* gene in pNMBT1912 suggests that the production of large quantities of neisserial DHPS protein places a burden upon the cell and as a consequence slows the growth rate. This is in marked contrast to the behaviour of the streptococcal protein. To examine this theory, a comparison of the growth rates of pNMBT1912 and control cells in the presence and absence of IPTG was made.

Figure 3.12: Comparison of the growth rates of clones compared with control.

A 1:400 dilution was used to inoculate the control cultures.

A 5:400 dilution was used to inoculate the pNMBT1912 and pNMBT101 cultures.

All three cultures were induced with 0.5mM IPTG where indicated by the arrow.

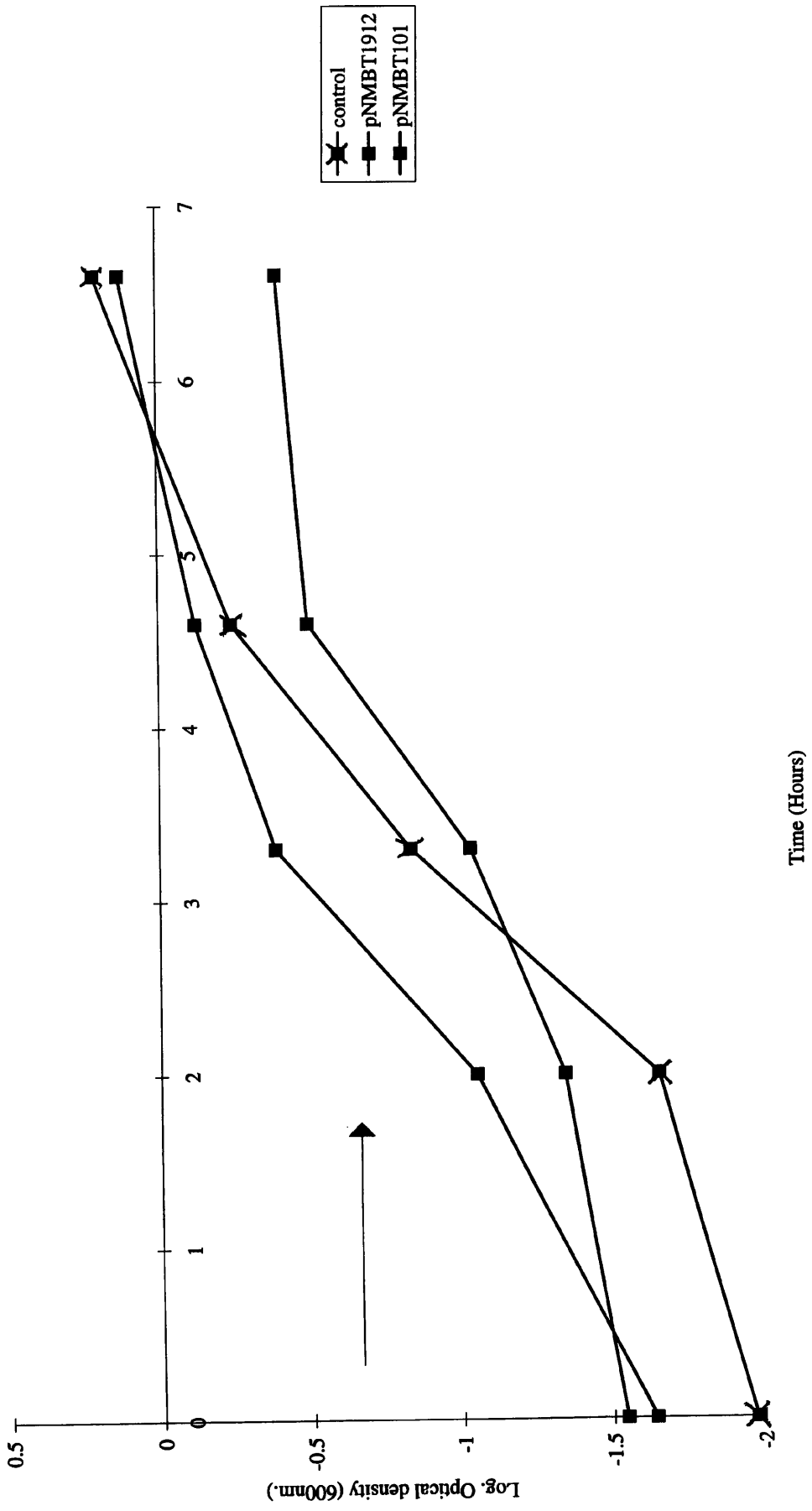

Figure 3.12: Comparison of the growth rates of clones compared with control.

Figure 3.13: Gel showing the over-expression of DHPS from pNMBT1912.

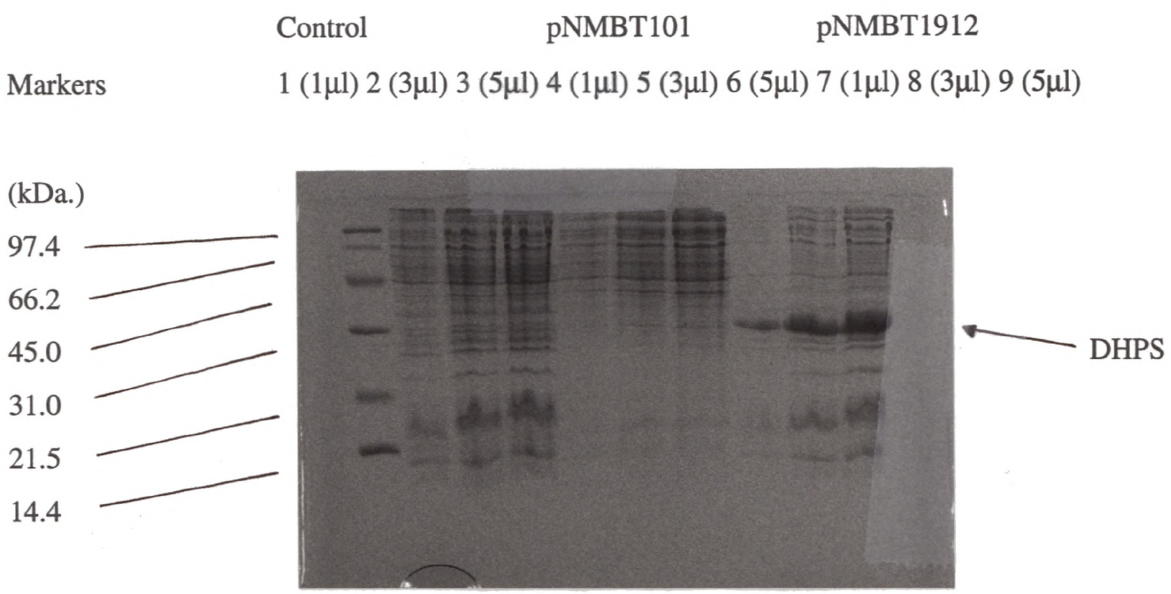

Table 3.3: Comparison of DHPS expression in clones compared with the control.

Culture	Units[1] /ml
pNMBT1912	186.6
pNMBT101	3.7
Control	1.6

100ml cultures were grown and harvested as described in 3.4.1.

[1] Units are nmoles of dihydropteroate produced per minute at 25°C.

3.4.2 Induction of pNMBT1912.

Two control flasks and two experimental flasks were set up. The inoculant used for the 4 flasks was added in a 1:50 dilution. The growth of the cultures was monitored each hour by measuring the optical density at 600nm [Figure 3.14]. One control and one experimental culture was induced at an optical density of 0.4. The cultures were individually harvested after a further 2 hours of growth and sonicated as previously described. A 0.2% PEI precipitation step was followed by protein precipitation at 55% ammonium sulphate to maximise the yield of DHPS.

A 12.5% acrylamide gel was run [Figure 3.15]. This showed that DHPS was produced in significant quantities when IPTG was added to the experimental culture.

Table 3.4 shows the activity of the DHPS harvested from pNMBT1912 and that a 10-fold increase in the amount of DHPS was seen when IPTG was present in the medium. These results indicate that the expression of DHPS protein was under the partial control of a functional *lac* operon controlled by IPTG, but is somewhat 'leaky' because 0.393 Units of activity/ml. in the absence of IPTG is much higher than endogenous levels of DHPS in *E. coli*. The expression of this protein appears to slow the growth of XL1-Blue cells for some unknown reason.

3.4.3 Production and partial purification of DHPS.

Due to the long incubation time of these cells, flasks of 2YT medium were inoculated with separate XLI-Blue/pNMBT1912 colonies direct from a 2YT agar plate. The optical densities of the cultures was approximately 1.4 after 16 hours of growth. The cultures were induced with 0.5mM IPTG and the cells harvested after a further 2.5 hours of growth. The cell pellet was treated in the same manner as the streptococcal cell pellet through the sonication and PEI precipitation steps. A 55% ammonium sulphate precipitation was performed to maximise the yield of DHPS. The protein pellet was redissolved in 4.0ml. of 0.02M Tris/HCl,pH 7.5 and dialysed overnight at 4°C against 500x vol. of the above Tris buffer. The dialysed protein was centrifuged at 9 200g for 10 minutes to remove the PEI/nucleic acid precipitate.

The protein solution was applied to a DEAE-Sephacel column which had been pre-equilibrated with 3 column volumes of the Tris buffer described above.

Figure 3.14: Effect of IPTG on growth rates of control and pNMBT1912.

A 1:50 dilution was used to inoculate all four cultures. The cultures marked with + were induced with 0.5mM IPTG where indicated by the arrows.

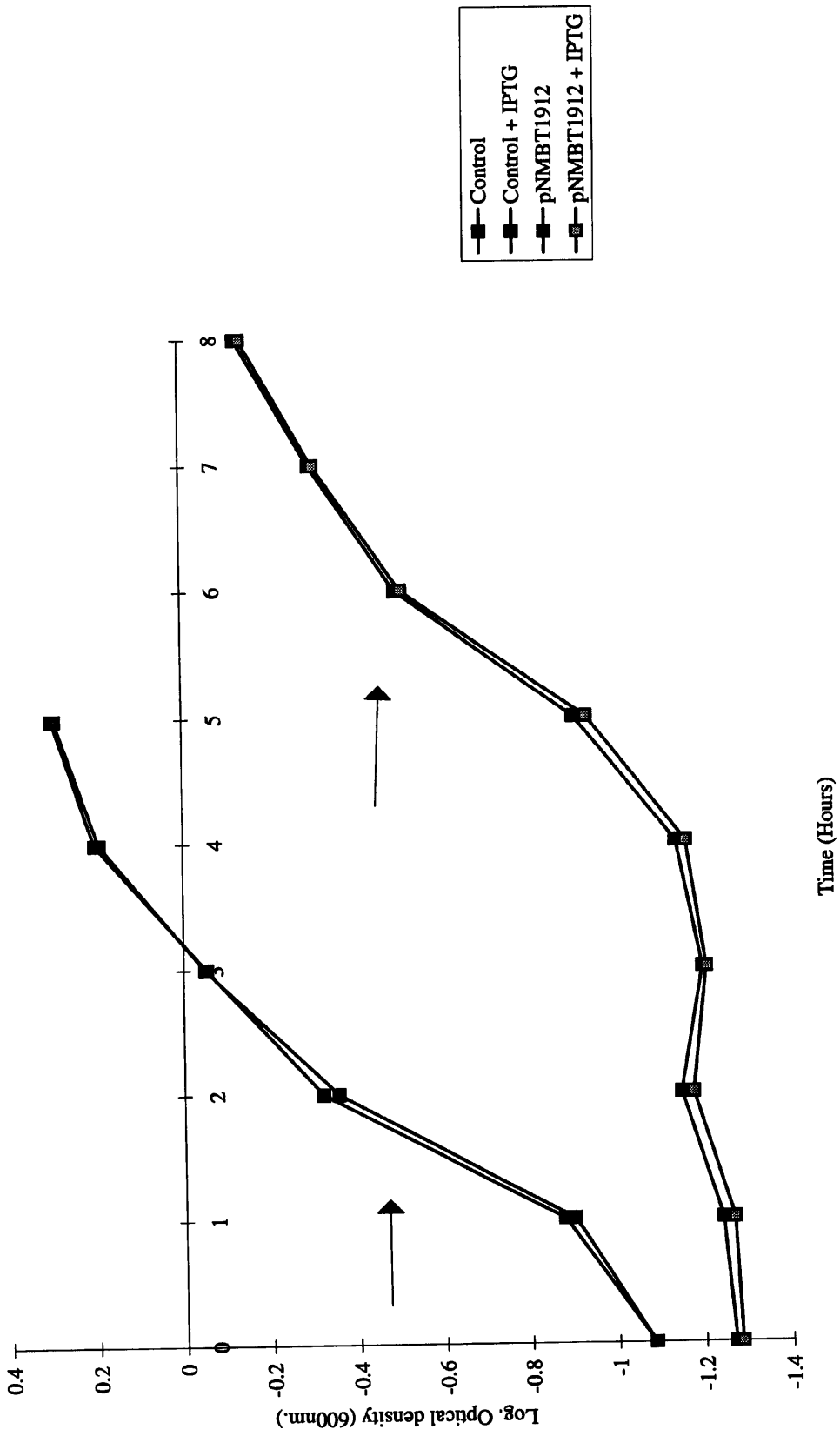

Figure 3.14: Effect of IPTG on growth rates of control and pNMBT1912.

Figure 3.15: Gel showing induction and over-expression of DHPS.

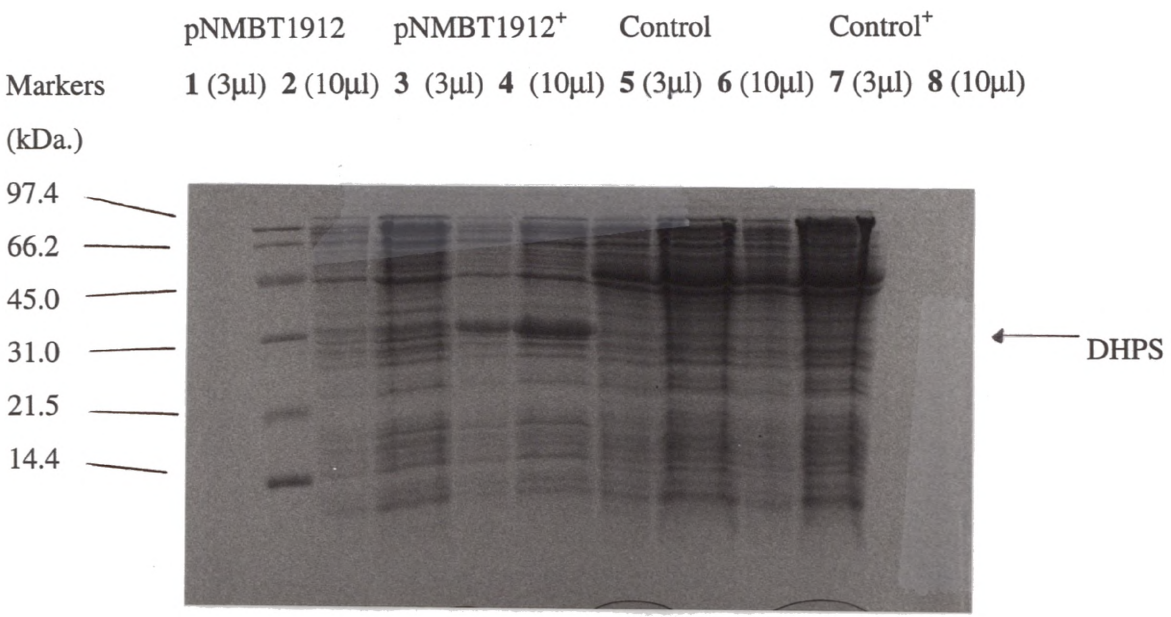

+ Culture induced with 0.5mM IPTG.

+ Culture induced with 0.5mM IPTG.

Table 3.4: Induction of pNMBT1912.

Inoculant	Units[1] /ml.
XL1-Blue/pNMBT1912	0.393
XL1-Blue/pNMBT1912 (induced)	3.719

100ml cultures were grown and harvested as described in 3.4.2.

[1] Units (U) are defined as nmoles of dihydropteroate produced per minute at 25°C.

DHPS was not retained by the column, as confirmed by SDS-PAGE analysis of column fractions. (gel not shown) [Figure 3.16] The DHPS was recovered from the column and concentrated to approximately 2.0ml.

3.4.4 Chromatofocusing chromatography.

The remaining neisserial DHPS was applied to a chromatofocusing column to further purify the protein. This knowledge would help to determine the elution conditions for the DEAE-sephacel column for any later purification attempts. The chromatofocusing column was equilibrated as described in Figure 3.6 and the protein solution was dialysed overnight against the imidazole elution buffer. The entire sample at this stage was only 1mg. so the absorbance detector was adjusted to a very sensitive setting to ensure a peak would be detectable. A problem with this approach was the increasing background caused by the Polybuffer as the pH gradient began. The Polybuffer absorbs UV light at 280nm. A clear peak was obtained and the pI of *N. meningitidis* DHPS was 5.58. [Figure 3.17] The protein may have been too weakly charged to adhere to the DEAE-sephacel column.

3.4.5 Summary.

N. meningitidis DHPS was partially purified using a DEAE-sephacel column and a chromatofocusing column. Further improvements have to be made before milligram quantities of pure neisserial DHPS protein can be produced. These may include the use of a cation exchange column to purify neisserial DHPS rather than an anion exchange column.

Figure 3.16: Elution of neisserial DHPS from the DEAE-sephacel column.

The elution buffer used was 0.02M Tris/HCl, pH 7.5 plus NaCl where described below and the flow rate was 2ml/min.

The peak in fraction 8 was eluted with 0.1M NaCl.

Fraction 14 was eluted in 0.2M NaCl.

Fraction 23 was eluted in 0.3M NaCl.

Fraction 30 was eluted in 0.4M NaCl.

Fraction 35 was eluted in 0.5M NaCl.

Fraction 38 was eluted in 1.0M NaCl.

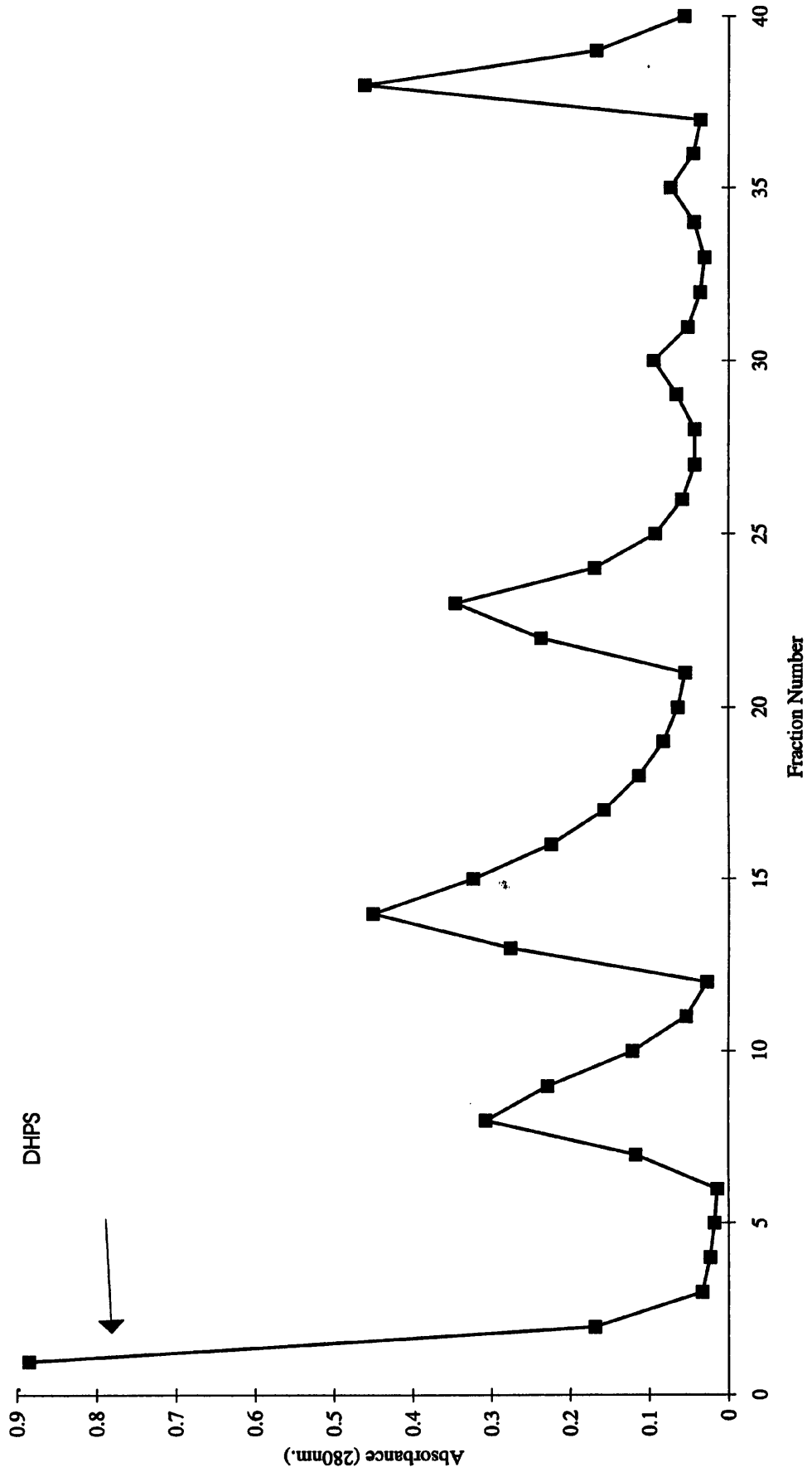

Figure 3.16: Elution of neisserial DHPS from the DEAE-sephacel column.

Figure 3.17 Elution of neisserial DHPS from the chromatofocusing column.

The elution buffer was 0.025M imidazole/HCl, pH 7.4. The Polybuffer was diluted 1:8 in water and adjusted to pH 4.0 using HCl. 1.0mg. of DHPS was loaded in 1.0ml imidazole buffer and washed onto the column in 12ml. of imidazole buffer. Polybuffer was pumped onto the column where indicated by the Start of pH gradient. The flow rate was 0.5ml/min and the chart speed was 0.5cm/ml.

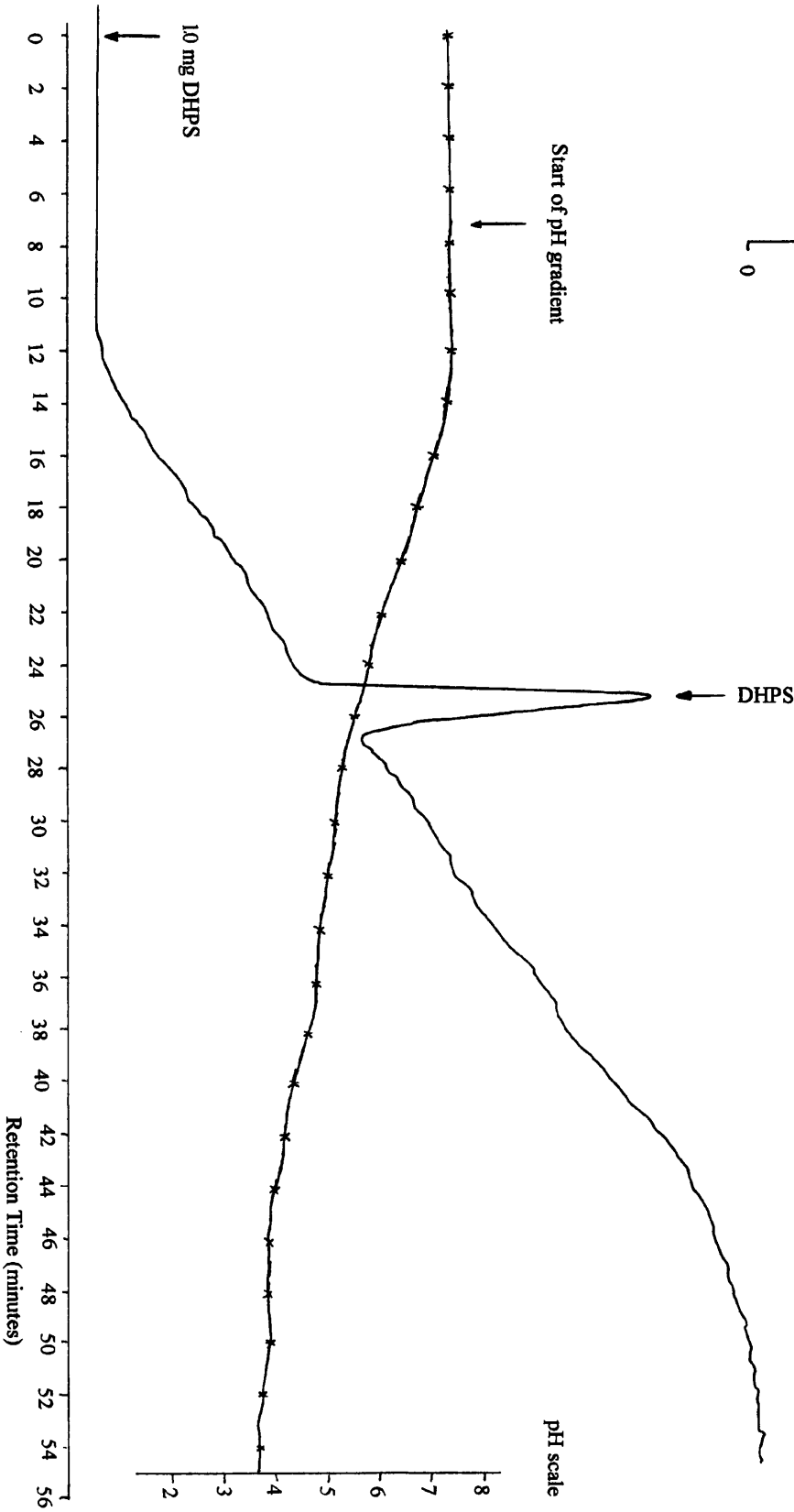

Figure 3.17 Elution of neisserial DHPS from the chromatofocusing column.

Chapter 4: Crystallisation and preliminary X-ray diffraction analysis of *S. pneumoniae* DHPS.

4.1 Introduction.

X-ray crystallography is the only method by which the relative positions of almost all the atoms of a protein can be measured. [Perutz, (1992) and McRee, (1993)]

Solving the crystal structure of streptococcal DHPS would provide important information about the residues which recognise and stabilise the binding of substrates at the active site and which residues facilitate the condensation reaction between those substrates. The basis for recognition of the sulphonamides is very important and would be revealed by a binary complex or pseudo-ternary complex with a sulphonamide bound at the active site. Once the structure is known a comparison of primary sequence information of those proteins displaying resistance to sulphonamides can be made. The effects of those mutations can then be mapped to specific areas of the polypeptide chain.

The *Staphylococcus aureus* DHPS structure has been solved with pterin pyrophosphate bound at the active site. [Hampele, *et al.* (1997)] Most of the conserved residues were found to contribute to the receptor interface with this substrate. Although there was no experimental evidence for the position of the pABA-binding site, the remaining conserved residues were clustered together so this area was assumed to be the pABA binding site. The residues implicated in sulphonamide resistance however were not confined to a discrete area but spread over the surface of the protein, with the exception of the 6 bp insertion common to *S. pneumoniae* and *E. coli* which mapped to the dimer interface. There was also some evidence to support a different and more complex mechanism involved in determining sulphamethoxazole resistance in *S. aureus* than that observed for TMP resistance where a single amino acid substitution in DHFR was sufficient. [Dale, *et al.* (1997)]

Correlation of the molecular structure of proteins with their mechanism and function is important, especially in the design of new drugs and pharmacological agents. Without a clear picture of the binding site of the drug on its target enzyme, a rational approach to novel drug design is impossible.

4.2 DHPS: Current Crystallographic Information.

At the present time there is no published crystallographic data concerning the structure of DHPS from *Streptococcus pneumoniae*.

In 1992, Dallas and coworkers reported a successful attempt to crystallise DHPS from *Escherichia coli* using the hanging drop technique. [See Section 2.28] Crystals were grown at 4°C in PEG 8000 and took over 1 month to grow. [Dallas, *et al.* (1992)] The structure of the *E.coli* DHPS has now been solved to 2.0 Angstroms [Achari, *et al.* (1997)] Crystals were grown in conditions of high salt by macroseeding. They revealed that the DHPS polypeptide folds as an eight-stranded α/β 'TIM'-barrel structure. The structure of DHPS from *Staphylococcus aureus* has also been solved recently. [Hampele, *et al.* (1997)]. From the crystallographic data, DHPS from *Staphylococcus aureus* has the same fold as the *E. coli* enzyme and crystallises as a non-crystallographic dimer with only one molecule of pterin pyrophosphate bound/dimer in the crystal.

4.3 Crystallising DHPS from *Streptococcus pneumoniae*.

The most difficult and time-consuming step in crystallography is obtaining single crystals, large enough for X-ray analysis. In order to crystallise a protein, the properties of the solvent in which it is dissolved must be gradually changed. The concentration of the precipitating agents can be increased, or a physical property such as temperature or pH changed to a point where the system is forced towards supersaturation. The most commonly used method to achieve supersaturation, and the one used in this study, is vapour diffusion.

The optimal crystallisation conditions for a particular protein are extremely difficult to predict due to the vast numbers of variables involved. Each set of conditions contains a buffer, a salt and/or precipitating agents and additives. The concentrations of these components, in addition to the temperature, ionic strength of the solution, and the type of precipitant present will all influence the tendency of the protein in solution to crystallise. This array of variables is not only large but also combinatorial.

Therefore in this study a limited set of cystallisation conditions was used for an initial screen to identify the principal factors that determine DHPS crystallisation.

A crystallisation matrix was adopted after Jancarik & Kim (1991) All solutions of DHPS contained 0.05% sodium azide to prevent bacterial growth and were made using Milli-Q water or an equivalent.

Microcrystals grew in one of the initial conditions of the screen - 0.2M sodium acetate, 0.1M MES/NaOH, pH 6.5 and 28% PEG 6000. This condition was compared with others where no crystal growth had been observed to enable the conditions to be expanded i.e. higher and lower PEG concentrations or molecular weights, salt and buffer types or concentrations.

4.4 Formation of Apoenzyme Crystals at 20°C.

Initial crystallisation matrix screens were set up using a 11.1mg/ml. DHPS solution (final concentration in the droplet) and 1µl droplets in a ratio 1:1 with the reservoir buffer on microscope slides. The slides were inverted over 1ml. of reservoir buffer [See Section 2.28] Figure 4.1 describes the procedure used to obtain the largest set of DHPS apoenzyme crystals. Within the range of conditions in which crystal growth was observed, several wells grew thousands of tiny crystals. The optimum condition grew only three needle-shaped crystals in about 1 week which were much larger than previously obtained, at 30µm. wide and 300µm. long. [Figure 4.2]

Using DHPS purified by isoelectric focusing and then gel filtration, similar size crystals were grown using 2µl and 5µl drops of DHPS in a ratio 1:1 with reservoir buffer over a wider range of conditions - 0.2M sodium acetate, 0.1M MES, pH 6.5 and 22-33% PEG 6000.

4.5 Formation of Apoenzyme Crystals at 7°C.

Initial crystallisation matrix screens were set up using a solution of DHPS at 20mg/ml. (final concentration in the droplet) in a reservoir buffer in a ratio 1:1. The screens were stored at 7°C in an incubator. One condition gave needle-shaped crystals, but they took one month to grow to approximately 200µm x 10µm x 10µm. [Figure 4.3]

Another condition grew large flat crystals (approximately 1mm x 200µm x 50µm) after about one week which disappeared after two weeks.

Figure 4.1: Formation of DHPS apoenzyme crystals at 20°C.

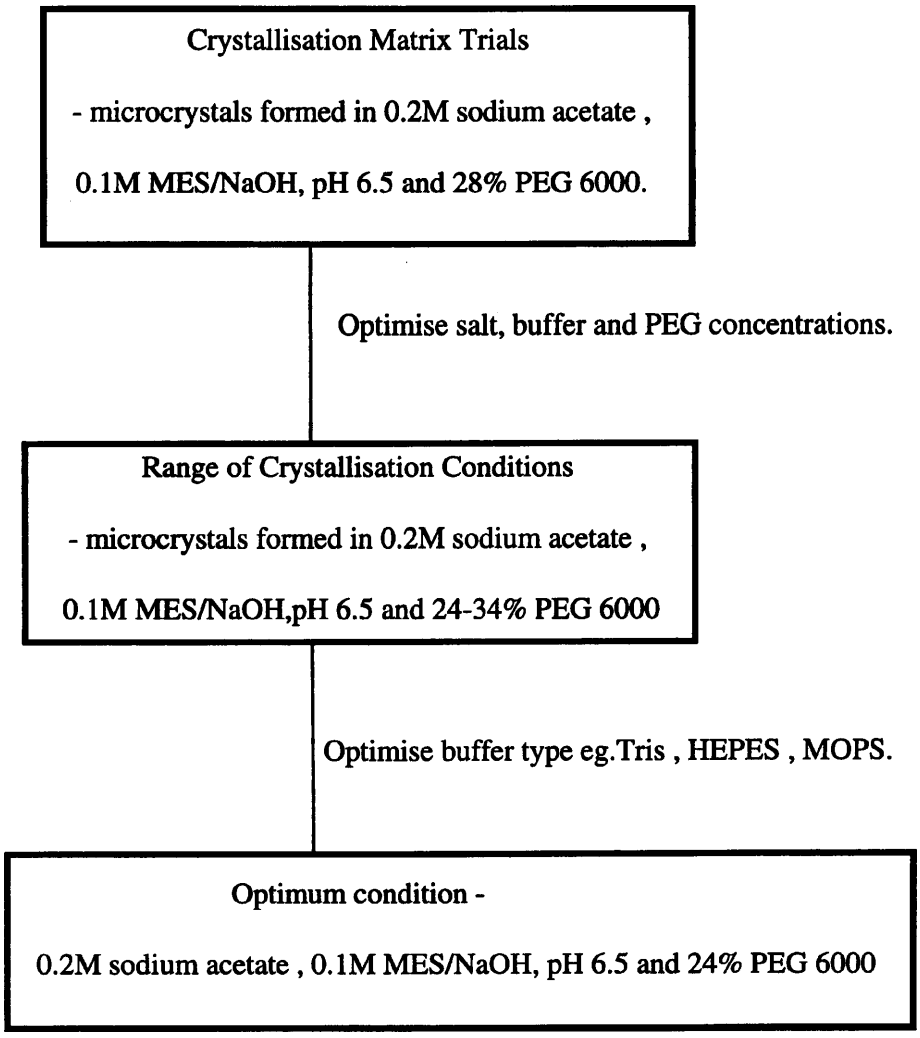

Figure 4.2 Apoenzyme crystals grown at 20°C.

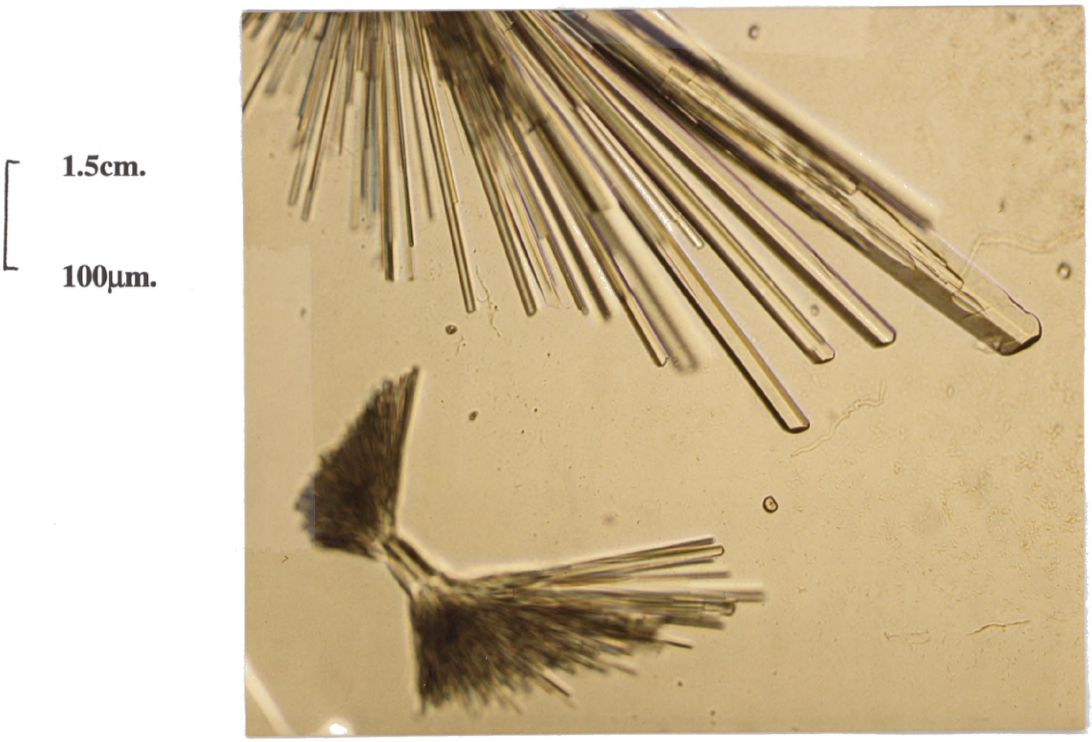

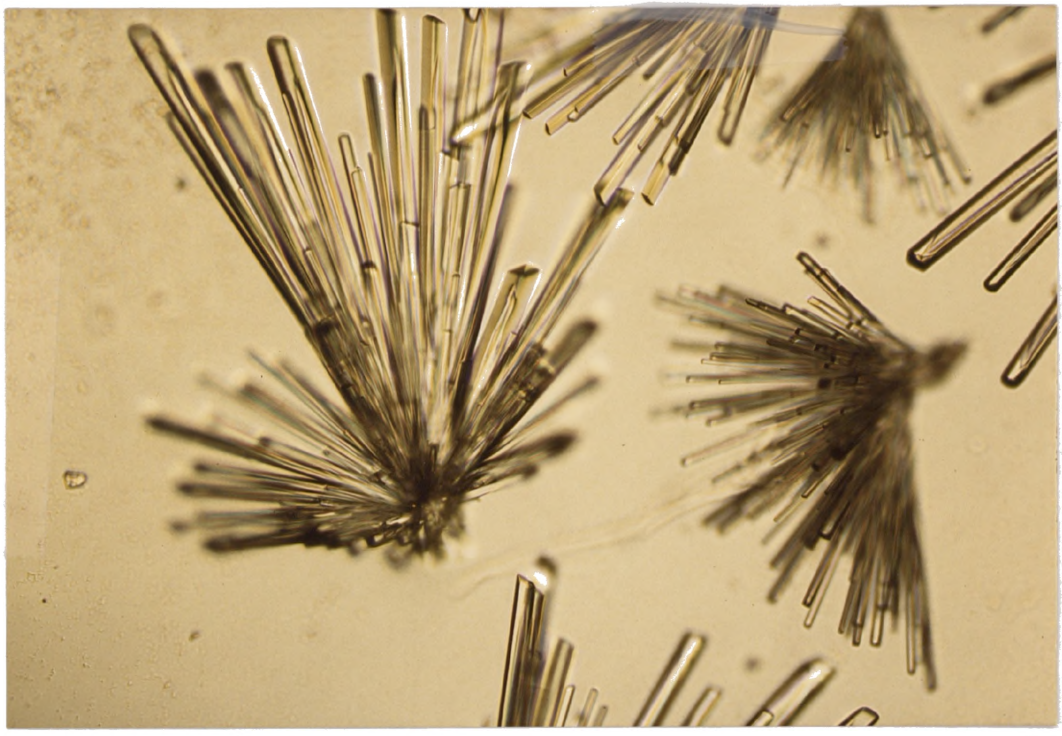

Figure 4.3 Formation of apoenzyme crystals at 7°C.

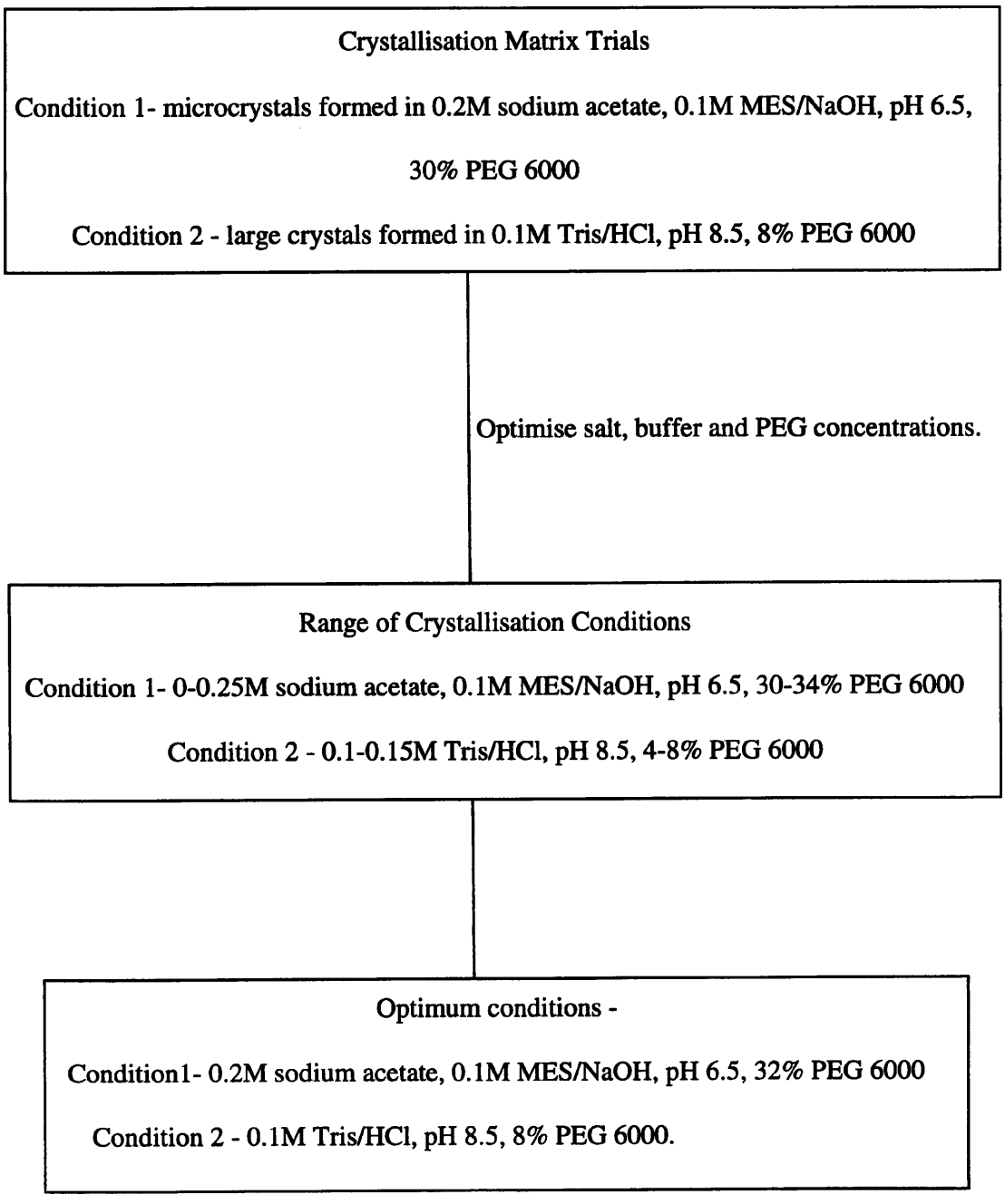

These conditions were expanded and the crystals again grew after one week but all had redissolved by the end of the second week. In principle, these crystals could be regrown and quickly removed from the reservoir solutions at higher PEG concentrations and suspended over lower PEG concentrations of 2-3% PEG 6000. Initial formation of nucleation sites probably occurred at 1-2% PEG and crystals grew quickly through to 3% PEG but then redissolved at concentrations greater than 4% PEG 6000. The optimum conditions for growth of these crystals could be found with a little more work and may provide excellent crystals for data collection. They were shown to be crystals of protein by absorbing Coomassie Brilliant Blue dye.

4.6 Formation of DHPS/pABA Binary Complex Crystals.

The three-dimensional structure of DHPS complexed with a substrate, substrate analogue or an inhibitor is more useful than the apoenzyme alone, as it can reveal the active site and contribute to knowledge of the catalytic mechanism

The same initial crystallisation screens were set up using a solution of DHPS at 11.1mg/ml. (final concentration in the drop) containing 1mM pABA at 20°C. Growth of needle-shaped microcrystals was observed after three days in a single condition.[Figure 4.4] The conditions in this set were varied to try to improve the size and quality of the crystals. From the original matrix of crystallisation conditions, it was clear that the type of salt was important as well as its concentration because no growth was observed in 0.2M ammonium sulphate, 0.1M MES, pH 6.5 and 30% PEG 6000. Crystals of a similar size to the apoprotein were obtained.

4.7 Formation of DHPS / SMX Binary Complex Crystals.

Initial crystallisation matrix screens were set up using a solution of DHPS at 19.1mg/ml. (final concentration in the droplet) containing 3mM SMX at 20°C. Growth of needle-shaped crystals was observed after three days under similar conditions to those observed with DHPS/pABA. [Figure 4.5] The type of buffer required for optimal growth was investigated but MES continued to produce the largest crystals.

Figure 4.4: Formation of DHPS / pABA binary complex crystals.

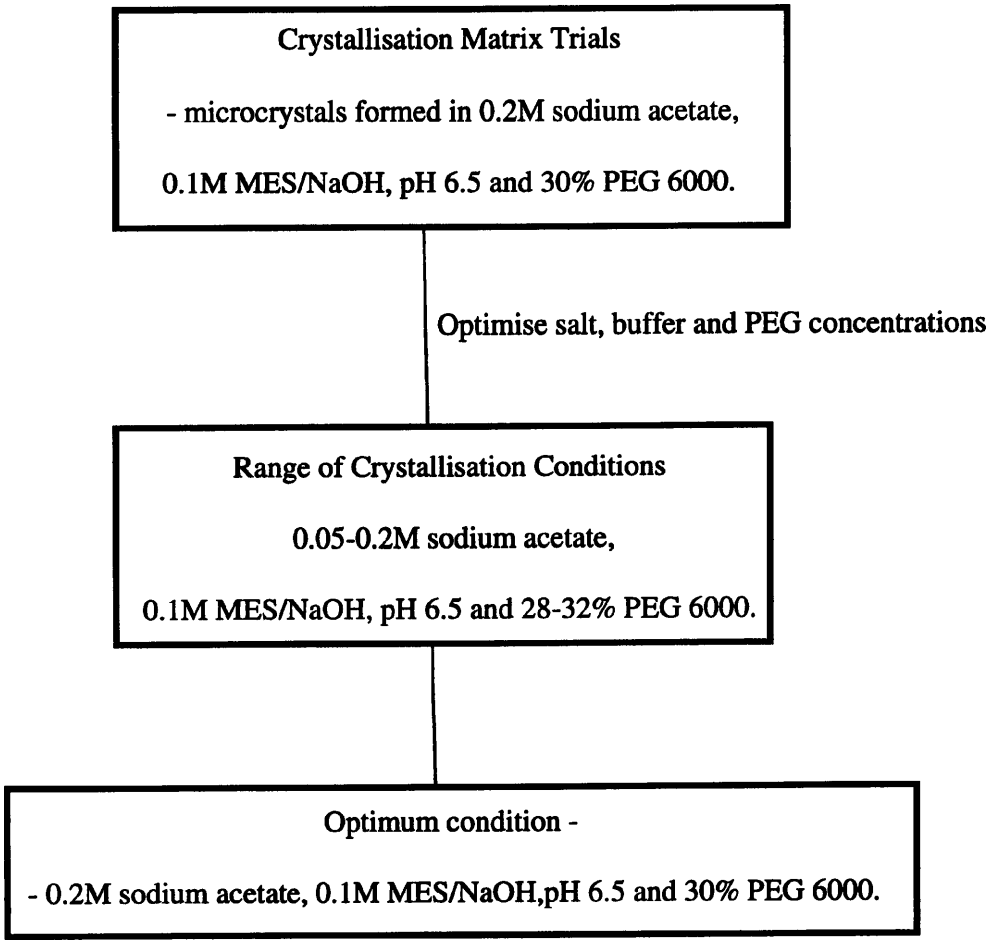

Figure 4.5 Formation of DHPS / SMX binary complex crystals.

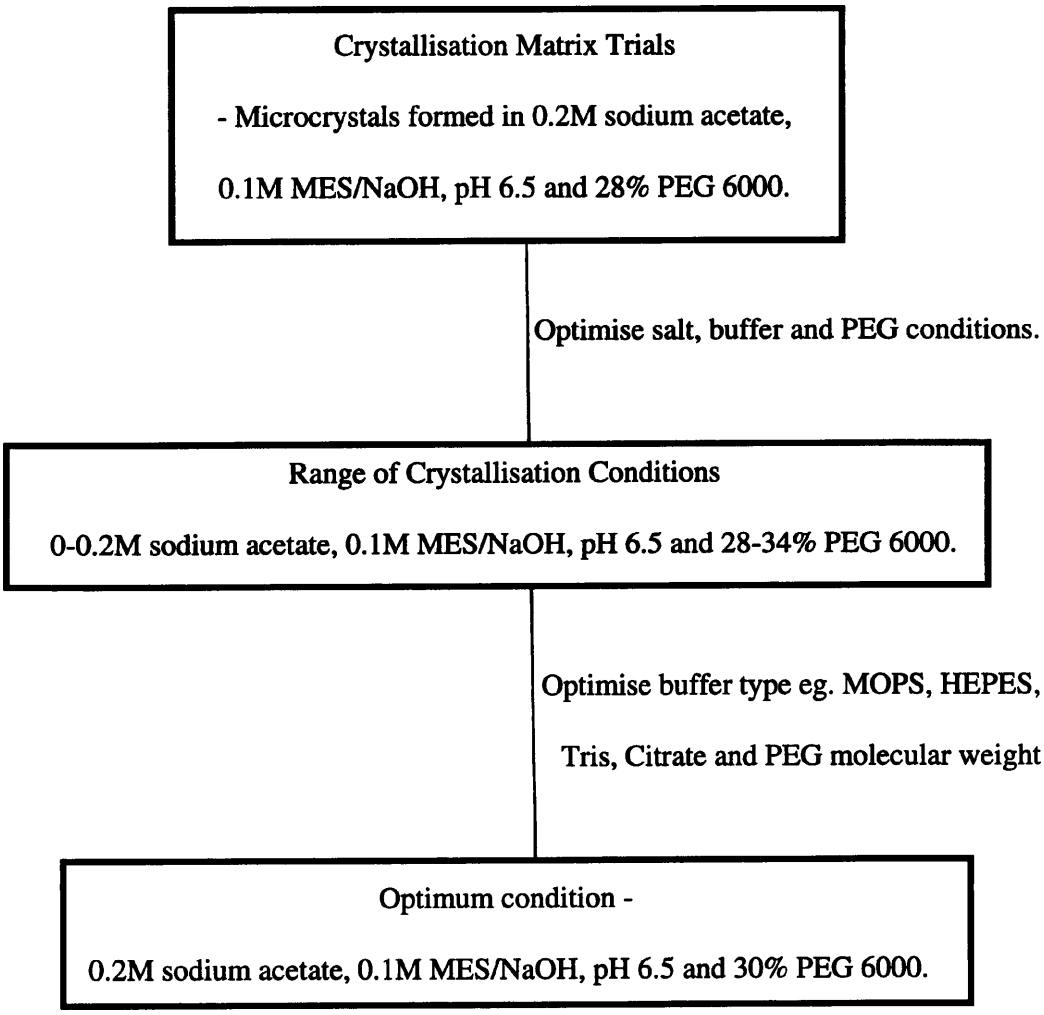

Microcrystals were also obtained with two conditions after two weeks incubation at 20°C - 30% PEG 4000, 0.1M sodium acetate and 0.1M MES, pH 6.5, and also 28% PEG 6000, 0.1M sodium acetate, 0.1M MES, pH 6.5 and 1% isopropanol. These conditions produced smaller crystals than all those mentioned earlier - approximately 10μm x 15μm x 60μm.

To conclude, at 20°C native DHPS crystals, DHPS/pABA and DHPS/SMX crystals grew in similar sets of conditions related by the initial screen condition of 0.2M sodium acetate, 0.1M MES/NaOH, pH 6.5 and 30% PEG 6000.

At 7°C, native DHPS crystals grew both in the above condition and a different set of conditions - 0.1M Tris/HCl, pH8.5, 8% PEG 6000. As mentioned in Section 4.5 this second condition is worth further investigation.

When attempting to crystallise an enzyme in the presence of a substrate or inhibitor, it is impossible to be certain that the enzyme has bound the ligand until the crystal structure has been solved and a comparison with the apoenzyme structure made. In this work therefore it is not known whether pABA and SMX are bound to DHPS until larger crystals can be grown and their structures solved to a resolution of less than three Angstroms.

4.8 Formation of DHPS/Pterin pyrophosphate and DHPS/sodium pyrophosphate Binary Complex Crystals.

For the reasons given above, a study of the crystallisation behaviour of DHPS in complex with its other substrate/ligand was undertaken. Initial crystallisation matrix screens were set up using a solution of DHPS at 24mg/ml. (final concentration in the droplet) containing 10μM pterin pyrophosphate or 10μM sodium pyrophosphate at 20°C. In both cases growth of a fine microcrystalline precipitate occurred after 3-5 days in one single condition. [Figure 4.6] This precipitate developed into tiny (less than 30μm in length) diamond-shaped crystals over the following two weeks.

Although the conditions were manipulated to try to improve the size of the crystals and reduce the numbers formed in each droplet, crystals sufficiently large for X-ray analysis could not be grown.

Figure 4.6 Formation of DHPS/pterin pyrophosphate and DHPS/sodium pyrophosphate crystals.

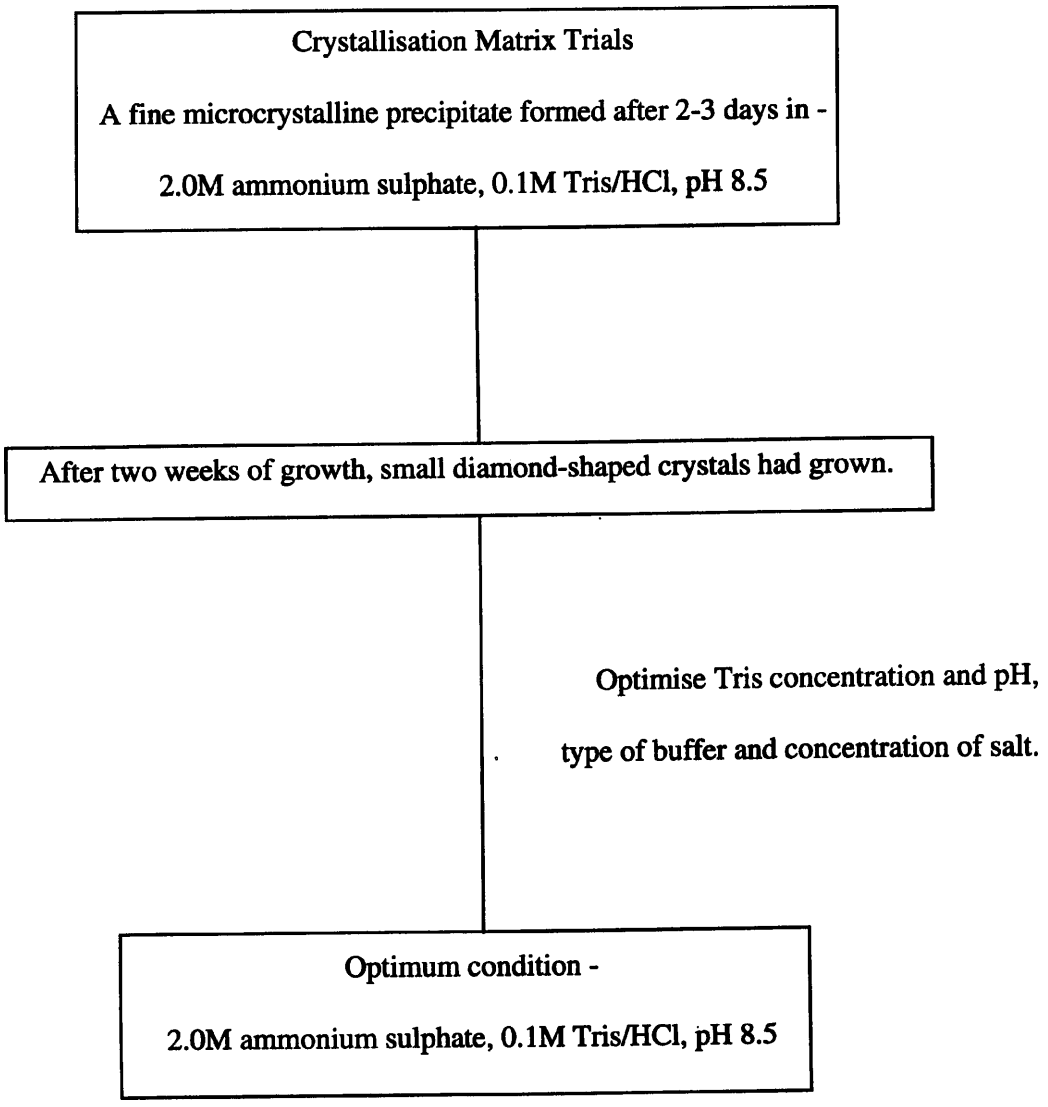

4.9 Formation of Crystals of a DHPS / Pseudo-Ternary Complex.

Matrix screens were set up using DHPS at 22mg/ml. (final concentration in the droplet) with one substrate and an analogue of the other substrate, with both at either 30μM or 300μM at 20°C. In the first instance, DHPS with pterin pyrophosphate and benzoic acid as an analogue of pABA were used.

Diamond-shaped crystals were observed growing at the 300μM concentration of substrates but no crystals were seen with the substrates at 30μM. [Figure 4.7] The size of these small (less than 30μm in length) crystals could not be increased by altering the buffer type, concentration or pH or changing the salt concentration.

Secondly, DHPS with pABA and sodium pyrophosphate as an analogue of pterin pyrophosphate were used. No crystals grew at either 30μM or 300μM.

4.10 Seeding Crystals.

Often vast numbers of small crystals quickly grow in droplets. Crystallisation conditions can be manipulated as described to try to increase the size of crystals and limit the number of nucleation sites for crystal formation. If the crystals are still not of a sufficient size or quality for X-ray analysis, another approach commonly used is seeding. Certain conditions may support the growth of crystals but are incapable of producing nucleation sites for initial crystal formation. Seeding involves transferring pre-formed crystals into these conditions so they can increase in size more perfectly by slower controlled growth. [Fitzgerald, (1987)]

4.10.1 Macroseeding.

Macroseeding involves removing pre-formed crystals from one well, adding protein to the droplet to enable further growth, then resealing this droplet over a fresh well of different conditions. All seeding experiments were performed at 20°C. The protein concentration in the resuspended droplets was approximately 20mg/ml at a final concentration. Crystals of native DHPS grown in 0.1M MES/NaOH, pH 6.5, 28% PEG 6000 and sodium acetate concentrations between 0.1-0.25M were used for macroseeding into reservoir solutions containing 0.2M sodium acetate, 0.1M MES/NaOH, pH 6.5 and 22-26% PEG 6000.

Figure 4.7 Formation of DHPS / pseudo-ternary complex crystals.

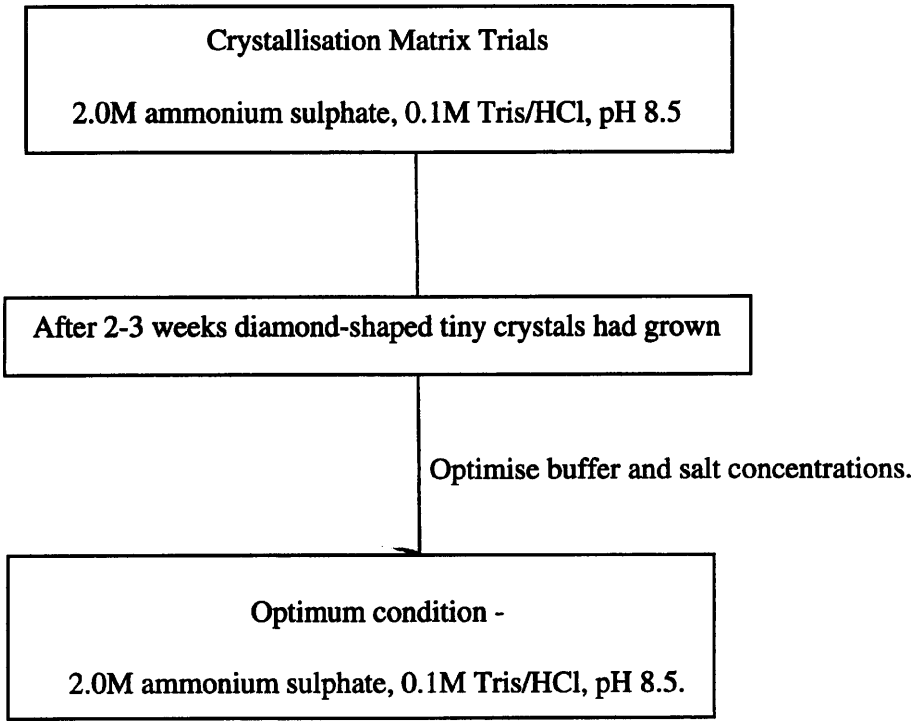

Crystals grown in 0.2M sodium acetate, 0.1M Mes/NaOH, pH 6.5 and 32% PEG 6000 were resuspended over the reservoir solution containing 0.2M sodium acetate, 0.1M MES/NaOH, pH 6.5 and 18% PEG 6000. Crystals grown in 0.2M sodium acetate, 0.1M MES/NaOH, pH 6.5 and 30% PEG 6000 were resuspended over the reservoir solution containing 0.2M sodium acetate, 0.1M MES/NaOH, pH 6.5 and 16% PEG 6000. The transferred crystals in the droplets continued to grow in 26, 24, 22 and 16% PEG 6000, 0.1M MES/NaOH, pH 6.5 and 0.2M sodium acetate. These conditions were capable of supporting crystal growth but were not found to initiate crystal formation. These crystals did not grow to a sufficient size for X-ray analysis.

4.10.2 Microseeding.

One method of microseeding involves transferring crystals from one droplet into an entirely new droplet containing a fresh supply of protein. The droplet is resealed over new conditions which support crystal growth but cannot initiate new crystal formation. A cat whisker has barbs along its length. By drawing a whisker through a droplet of crystals and then through the new droplet, crystals are deposited. [Wilson, (1991).] The crystals act as pre-formed nucleation sites and can continue to grow if conditions are suitable.

Microcrystals of apoenzyme, grown in 0.2M sodium acetate, 0.1M MES/NaOH, pH 6.5 and 32% PEG 6000 were transferred using a cat whisker into fresh droplets containing 0.2M sodium acetate, 0.1M MES/NaOH, pH 6.5, 16-27% PEG 6000 and 10mg/ml. DHPS. The concentration of PEG was lowered to try to prevent formation of nucleation sites but allow the crystals to continue to grow. Formation of new nucleation sites still occurred in 27%-24% PEG 6000 but in wells containing 23-18% PEG 6000 the crystals continued to grow slowly. However because the crystals were very small initially, they did not reach a size sufficient for X-ray analysis. The crystals in droplets containing less than 18% PEG 6000 redissolved and did not recrystallise.

If crystals are sufficiently large to allow handling (200μm x 20μm x 20μm), they can be individually removed using a fine pipette, gently washed in a solution in which the crystal will not dissolve (usually a higher PEG concentration) then placed into the fresh droplet of protein to continue to grow. [Thaller, *et al.* (1981)]

This procedure can be repeated as often as required providing the crystal can withstand the stress involved in pipetting. The washing step removes the outer layer of crystals forming on the core crystal, allowing more prefect crystal growth in the fresh solution.
Crystals grown in 0.2M sodium acetate, 0.1M MES/NaOH, pH 6.5 and 28% PEG 6000 were washed in a solution containing 0.2M sodium acetate, 0.1M MES/NaOH, pH 6.5 and 38% PEG 6000, (to prevent the crystal redissolving) then transferred into a droplets containing different concentrations of DHPS, 0.2M sodium acetate, 0.1M MES/NaOH, pH 6.5 and 18% PEG 6000. The results are summarised in Table 4.1. 1mg/ml DHPS was not sufficient for growth of the crystal and 15mg/ml. was too high and caused ragged, uncontrolled crystal growth. The crystals formed in 5 and 10mg/ml. DHPS were of a sufficient size for X-ray analysis, at approximately 500μm x 50μm x 50μm.

4.11 Results of X-ray Diffraction of Apoenzyme Crystals.

The largest crystals grown as described above in section 4.10.2 were taken to the Synchrotron Radiation Source at Daresbury and X-ray diffraction studied. Bragg diffraction was obtained to beyond 3 Angstrom resolution. [Figure 4.8] Reflections can be clearly seen outside the solvent ring which is about 3-4.5 Angstroms.
Auto-indexing of the reflections using the Denzo Program [Otwinoski, (1986)] established that the space group was P_{212121} or an enantiomorph. The cell dimensions were calculated as a = 47.56, b = 90.34 and c = 138.47 Angstroms. [Table 4.2] Diffraction data were collected and processed for three images: the overall R_{merge} is 92% for data between 30 and 2.8 Angstroms. Weak diffraction spots can be seen to a resolution well beyond 2.8 Angstroms indicating that larger crystals could well diffract to an even higher resolution.
From the calculated cell dimensions given in Table 4.2, assuming a dimer in the asymmetric unit (2 x 34000 Daltons) and four dimers per unit cell, a packing density of 2.2 cubic Angstroms/Da. would be predicted. This therefore predicts a dimer in the assymetric unit.

Table 4.1 Results of microseeding .

DHPS Concentration in droplet.	Crystal growth observations.
1mg/ml.	Crystal did not grow.
5mg/ml.	Crystal grew very slowly over a month then stopped.
10mg/ml.	Crystal grew slowly over several weeks then stopped.
15mg/ml.	Crystal grew very quickly over 1 week then stopped, seemed ragged around the edges.

Figure 4.8 Oscillation X-ray diffraction image of an *S. pneumoniae* DHPS crystal.

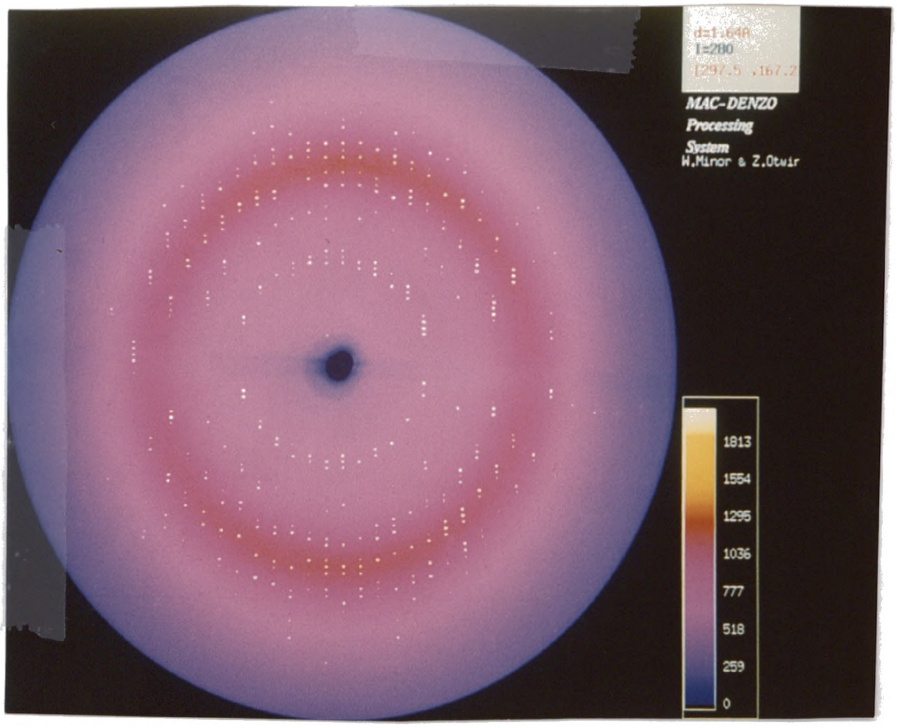

A native DHPS crystal (50µm x 50µm x 500µm) was grown by macroseeding as described in 4.11.2, harvested into mother liquor (0.2M sodium acetate, 0.1M MES/NaOH, pH 6.5, 18% PEG 6000) and mounted into a quartz capillary tube. The diffraction image was recorded on a 30cm. mar detector at a crystal to film distance of 228.5mm on station 7.2 at the SRS, Daresbury, U.K., using a wavelength of 1.488 Angstrom X-ray radiation. The oscillation range was 1.5° and the exposure time was 200 seconds. The crystal was mounted with the longer dimension along the spindle axis.

Table 4.2 Table of X-ray diffraction data.

Shell limit (Angstroms)					
Lower	Upper	Average Intensity	Average error	Normal Chi Square	Linear R-factor
30.00	5.59	11219.6	896.2	1.551	0.069
5.59	4.44	8109.6	601.0	1.842	0.100
4.44	3.88	8444.5	652.4	1.884	0.107
3.88	3.53	5404.2	481.6	1.683	0.090
3.53	3.27	4270.3	473.7	0.639	0.073
3.27	3.08	3556.0	444.1	1.182	0.104
3.08	2.93	2252.6	381.8	1.171	0.117
2.93	2.80	1670.9	355.8	1.065	0.150
All reflections		5776.3	543.7	1.400	0.092

A total of 998 reflections (6.5% of the total for all data between 30 and 2.8 Angstroms) Data was processed for three images ($\varphi = 0°$, 45° and 90°) from the crystal shown in Figure 4.9 using the software package Denzo. Refined cell dimensions are a = 47.58, b = 90.30 and c = 138.42.

4.12 Conclusions.

Table 4.3 summarises the optimum crystallisation conditions for DHPS.

There are two distinct crystal morphologies. Crystals of the apoenzyme and DHPS grown in the presence of pABA or SMX are needle-shaped. Crystals of DHPS grown in the presence of pterin pyrophosphate, pyrophosphate and pterin pyrophosphate/benzoic acid are diamond-shaped. There are several possible explanations for these observations. Assuming DHPS has bound pABA or SMX when present in the droplet, the structure of the native DHPS is not perturbed by the binding and the binary complex forms needle-shaped crystals similar to the apoenzyme. However on binding pterin pyrophosphate or pyrophosphate, the conformation of the binary complex must alter sufficiently to cause the protein to crystallise into a different morphology. This explanation would suggest that DHPS can bind both its substrates pABA and pterin pyrophosphate, possibly in a random binding order. [See Chapter 5]

If apoprotein DHPS does not bind the ligands pABA and SMX, the needle-shaped crystals observed would be unliganded DHPS and not the binary complexes - DHPS/pABA or DHPS/SMX. When DHPS was crystallised in the presence of pterin pyrophosphate or pyrophosphate however a different crystal morphology was observed; indicating that DHPS had bound these ligands. This explanation would suggest that DHPS can bind pterin pyrophosphate and pyrophosphate but not pABA or SMX to any significant extent.

A fixed-order reaction pattern with pterin pyrophosphate binding to the native DHPS first which alters its conformation to facilitate the binding of pABA would support this explanation. [See Chapter 5]

Table 4.3 Summary of optimum crystallisation conditions for DHPS.

Ligand	Condition
None	0.2M sodium acetate, 0.1M MES/NaOH, pH 6.5, 24% PEG 6000 at 20°C. 0.2M sodium acetate, 0.1M MES/NaOH, pH 6.5, 32% PEG 6000 at 7°C. 0.1M Tris/HCl, pH 8.5, 8% PEG 6000 at 7°C.
pABA or SMX	0.2M sodium acetate, 0.1M MES/NaOH, pH 6.5, 30% PEG 6000 at 20°C.
pterin pyrophosphate, sodium pyrophosphate, pterin pyrophosphate/ benzoic acid.	2.0M ammonium acetate, 0.1M Tris/HCl, pH 8.5 at 20°C.

Chapter 5: An investigation into the mechanism of the DHPS reaction.

5.1 Introduction.

The aim of the work presented in this chapter was to try to determine the order of addition and departure of the substrates and products from *S. pneumoniae* DHPS during the reaction cycle. This information is important for several reasons. As discussed in Chapter 4, the interpretation of crystallographic data depends upon a knowledge of which substrate(s) bind to the apoenzyme. The order of addition of substrates also has a direct bearing on the effect of inhibitors on the enzyme activity. This will be examined in more detail in Chapter 6.

For a two substrate, two product reaction, DHPS could adopt one of several different mechanisms. (Some of the possibilities are summarised in Chapter 1.) The order of substrate addition to an enzyme can be determined by either the direct measurement of substrate binding at equilibrium, as shown with glucose-6-phosphate isomerase from rabbit muscle [Koike, (1969)], or by analysis of the steady state kinetics of the enzyme. (for example, hexokinase from rat brain and phosphogluconate dehydrogenase from sheep liver [Kyte,(1995)]) For this study both approaches were adopted.

5.2. Current knowledge of the DHPS mechanism.

There is currently no published information concerning the mechanism of DHPS from *S. pneumoniae* or any other streptococcal species. Also, the only information regarding the mechanism of DHPS from any other organisms has been confined to steady-state kinetic studies.

A kinetic analysis of the mechanism of *Staphylococcus aureus* DHPS has recently been reported and a random order of addition of substrates to the enzyme was proposed. [Hampele, *et al.* (1997)] The calculated equilibrium binding constants for pterin pyrophosphate and pABA were 9.3μM and 5.4μM respectively. It was also suggested that the dimeric enzyme normally operates with only half-site reactivity. In the mitochondria of pea leaves, DHPS catalyses the formation of 7,8-dihydropteroate as a bifunctional hexameric enzyme with HPPK.

Reported K_m values for pterin pyrophosphate and pABA were 30μM and 0.6μM respectively. [Rebeille, *et al.* (1997)] By kinetic analysis, DHPS was proposed to adopt a random order of addition of substrates. The presence of magnesium was also shown to be essential for maximum activity.

Apparent K_m values for pterin pyrophosphate and pABA for *E. coli* DHPS were reported as 1.9μM and 0.5μM respectively, although no conclusions were reported about the mechanism of the enzyme. [Talarico, *et al.* (1992)] Similar values for *E. coli* DHPS were also reported by Dallas, *et al.* (1992) Apparent K_m values of 2.5μM and 0.34μM have been reported for pterin pyrophosphate and pABA with *P. carinii* DHPS, but again, no inferences were made about possible mechanism. [Hong, *et al.* (1995)] This chapter presents both binding and kinetic data in an attempt to discern a reaction mechanism for DHPS from *S. pneumoniae.*

5.3. Hummel and Dreyer experiments.

Hummel and Dreyer experiments, based on the original theory of Hummel & Dreyer in 1962, provide a simple and rapid method to observe the binding of substrates to the enzyme. This method relies upon the substrates absorbing UV light at 280nm and fortunately, in the case of DHPS, both substrates can be tested to see whether they are bound by the apoenzyme.

The experiments were performed as described in Chapter 2. For each experiment, the column was saturated with buffer containing substrate. For the experimental run, a solution of buffer containing DHPS but no substrate was applied to the column and eluted using the original equilibration buffer containing substrate. The absorbance of the eluate at 280nm was monitored continuously. DHPS eluted from the column as a peak in absorbance, followed by a trough, caused by the lack of substrate in the buffer at that point. For the control, a solution of buffer containing no DHPS or substrate was applied to the column. Under these circumstances, a trough was formed by the solution which had been applied to the column eluting through the UV detector, because the solution contained no absorbing substrate.

If DHPS had bound substrate from the column, a larger trough relative to control, would be created because of a larger reduction in absorbing substrate at that point in the buffer. No attempt was made to quantify the amount of substrate bound by DHPS in these experiments.

5.3.1 Summary of results.

Figure 5.1 shows the elution profile of DHPS in the presence of pterin pyrophosphate/magnesium. The size of the experimental troughs are marginally larger than the control troughs. Given that the difference is only small, it is not possible to conclude from these results that DHPS definitely binds pterin pyrophosphate. A small difference between control and experimental troughs would perhaps be expected because a low concentration of substrate was used. It was prohibitive both in terms of cost and problems with high absorbance of the ligand at 280nm to try to use a 10-fold higher concentration, which may have shown more conclusively whether DHPS binds pterin pyrophosphate.

When DHPS was applied to a column pre-equilibrated with pABA and magnesium, there was no observable difference between the experimental and control troughs. [Figure 5.2] This indicates that DHPS cannot bind pABA in the presence of magnesium alone.

In these experiments, other non-absorbing ligands can be added or removed from the equilibrating buffer to see whether they affect the binding of the absorbing substrate by DHPS. Sodium pyrophosphate is a cheap, readily available chemicalwhich was used in these experiments, together with magnesium to generate a *pseudo*-ternary complex with DHPS and pABA, by acting as an analogue of pterin pyrophosphate. (It must be borne in mind however that this can also be considered as a *pseudo*-ternary complex for the products as pyrophosphate is a product of the reaction and pABA similar in structure to one portion of the dihydropteroate molecule.)

Figure 5.1: Absorption elution profile of DHPS in the presence of 2.5μM pterin pyrophosphate.

The equilibration buffer contained 50mM Tris/ HCl, pH 8.0, 5mM magnesium chloride and 2.5μM pterin pyrophosphate. Experiment 1 involved the application and elution of a 1ml solution containing 3.4mg DHPS in the above equilibration buffer minus pterin pyrophosphate. Experiment 2 involved the application and elution of a 1ml solution containing 6.8mg DHPS in the above equilibration buffer minus pterin pyrophosphate. The control involved the application and elution of a 1ml solution of equilibration buffer minus pterin pyrophosphate. The elution profile was measured at 25°C, at a chart speed of 2mm/min and a flow rate of 5ml/min.

Figure 5.1: Absorption elution profile of DHPS in the presence of 2.5μM pterin pyrophosphate.

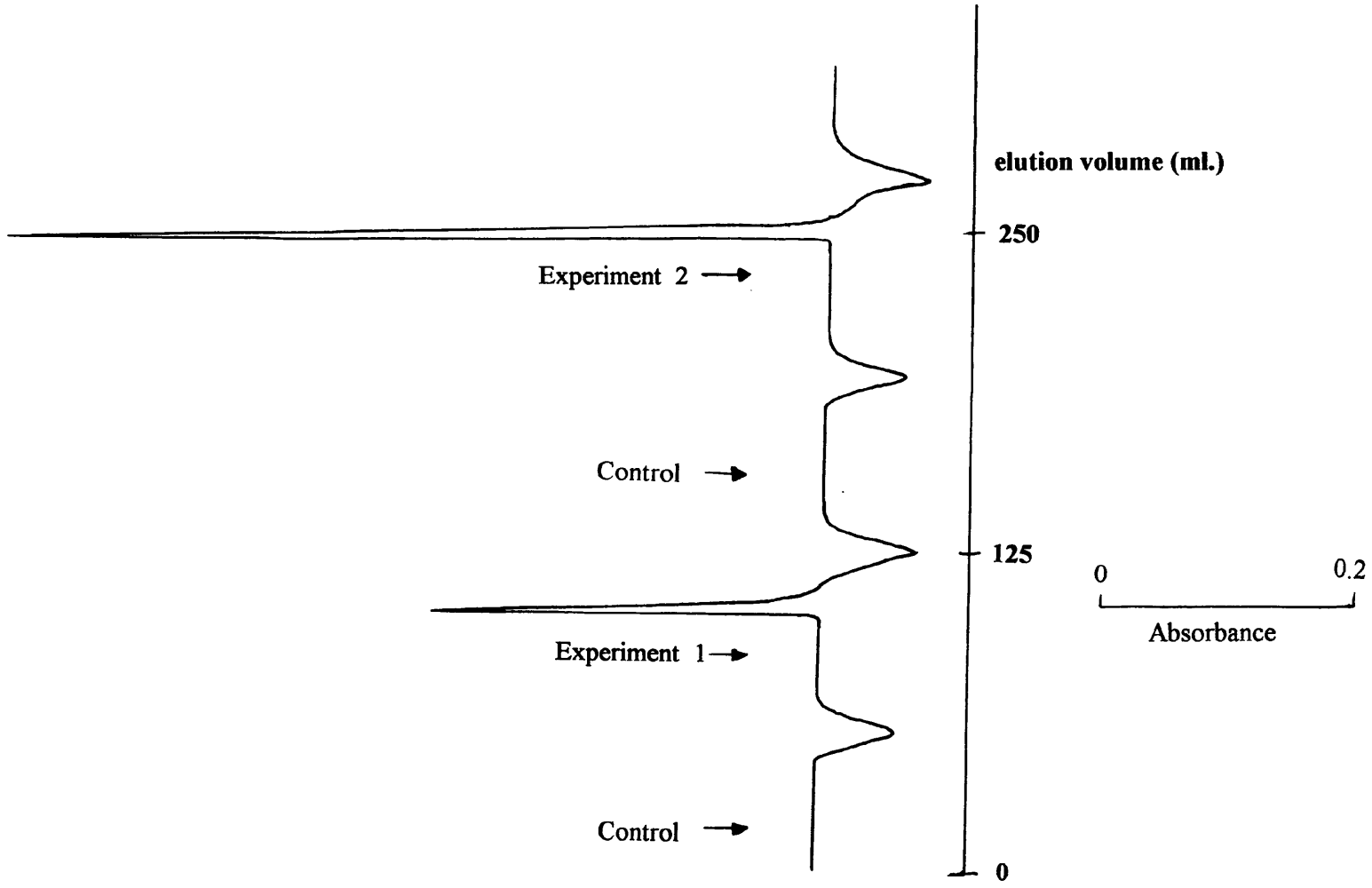

Figure 5.2: Absorption elution profile of DHPS in the presence of 10μM pABA.

The equilibration buffer contained 50mM Tris/ HCl, pH 8.0, 5mM magnesium chloride and 10μM pABA. The experiment involved the application and elution of a 1ml solution containing 3.4mg DHPS in the above equilibration buffer minus pABA. The control involved the application and elution of a 1ml solution of equilibration buffer minus pABA. The elution profile was measured at 25°C, at a chart speed of 5mm/min and a flow rate of 5ml/min.

Figure 5.2: Absorption elution profile of DHPS in the presence of 10μM pABA.

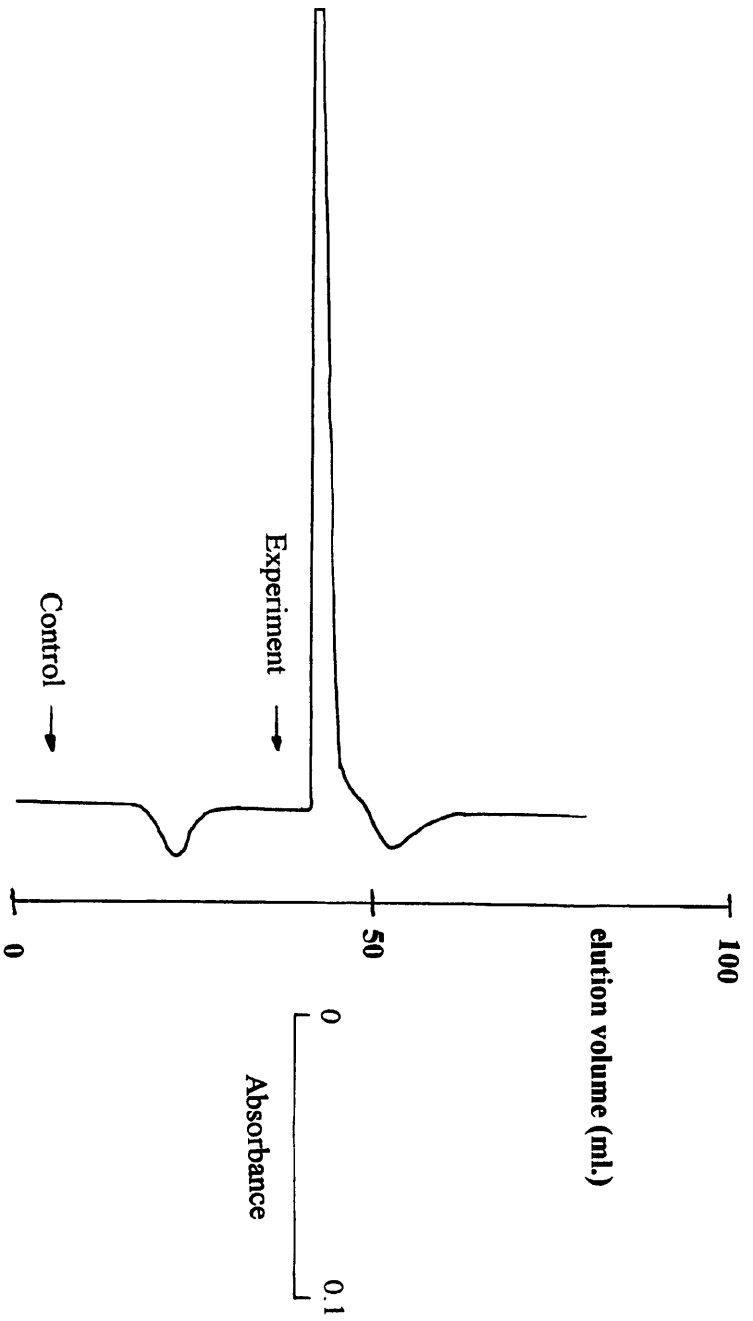

When a low concentration of sodium pyrophosphate was included in the same experiment, there was no observable difference between the sizes of the experimental and control troughs [Figure 5.3], indicating that DHPS cannot bind pABA in the presence of 10μM pyrophosphate and magnesium. However when the concentration of sodium pyrophosphate was increased to100μM, the size of the experimental trough was greatly increased compared to that of the control. [Figure 5.4] It therefore appears that DHPS can bind pABA in the presence of 100μM pyrophosphate and magnesium.
When magnesium chloride was omitted from the equilibration buffer, DHPS was no longer able to bind pABA in the presence of 100μM pyrophosphate. [Figure 5.5]
To examine whether orthophosphate could facilitate the binding of pABA by DHPS in a similar manner to pyrophosphate, sodium dihydrogen orthophosphate was substituted at the same concentrations - 10μM and 100μM.
There was no difference in the sizes of the experimental and control troughs when 10μM orthophosphate [Figure 5.6] or 100μM orthophosphate was present. [Figure 5.7]
It is clear, therefore, that orthophosphate is unable to substitute for pyrophosphate as a ligand for DHPS.

5.3.2 Conclusions.

From these experiments, DHPS may be capable of binding pterin pyrophosphate in the presence of magnesium chloride but is unlikely to bind pABA in the presence of magnesium alone. However DHPS can bind pABA in the presence of a sufficiently high concentration of pyrophosphate and magnesium. The pyrophosphate and magnesium probably forms a pyrophosphate/magnesium complex which can act as an analogue of pterin pyrophosphate/magnesium in a *pseudo*-ternary complex with pABA.
This information suggests that pterin pyrophosphate/magnesium is the first substrate bound by DHPS and can be mimicked by a pyrophosphate/magnesium complex, at least as far as the induction of pABA binding. pABA can then bind to the DHPS/pyrophosphate or DHPS/pterin pyrophosphate binary complex, possibly as a result of a conformational change in the protein. This evidence therefore tends to support a compulsory order of binding of the substrates.

Figure 5.3: Absorption elution profile of DHPS in the presence of 10μM pABA and 10μM sodium pyrophosphate.

The equilibration buffer contained 50mM Citrate/ HCl, pH 6.0, 5mM magnesium chloride, 10μM pABA and 10μM sodium pyrophosphate. The identical experiments involved the application and elution of 1ml solutions containing 3.4mg DHPS in the above equilibration buffer minus pABA and sodium pyrophosphate. The controls involved the application and elution of 1ml solutions of equilibration buffer minus pABA and sodium pyrophosphate. The elution profile was measured at 25°C, at a chart speed of 2mm/min and a flow rate of 5ml/min.

Figure 5.3: Absorption elution profile of DHPS in the presence of 10μM pABA and 10μM sodium pyrophosphate.

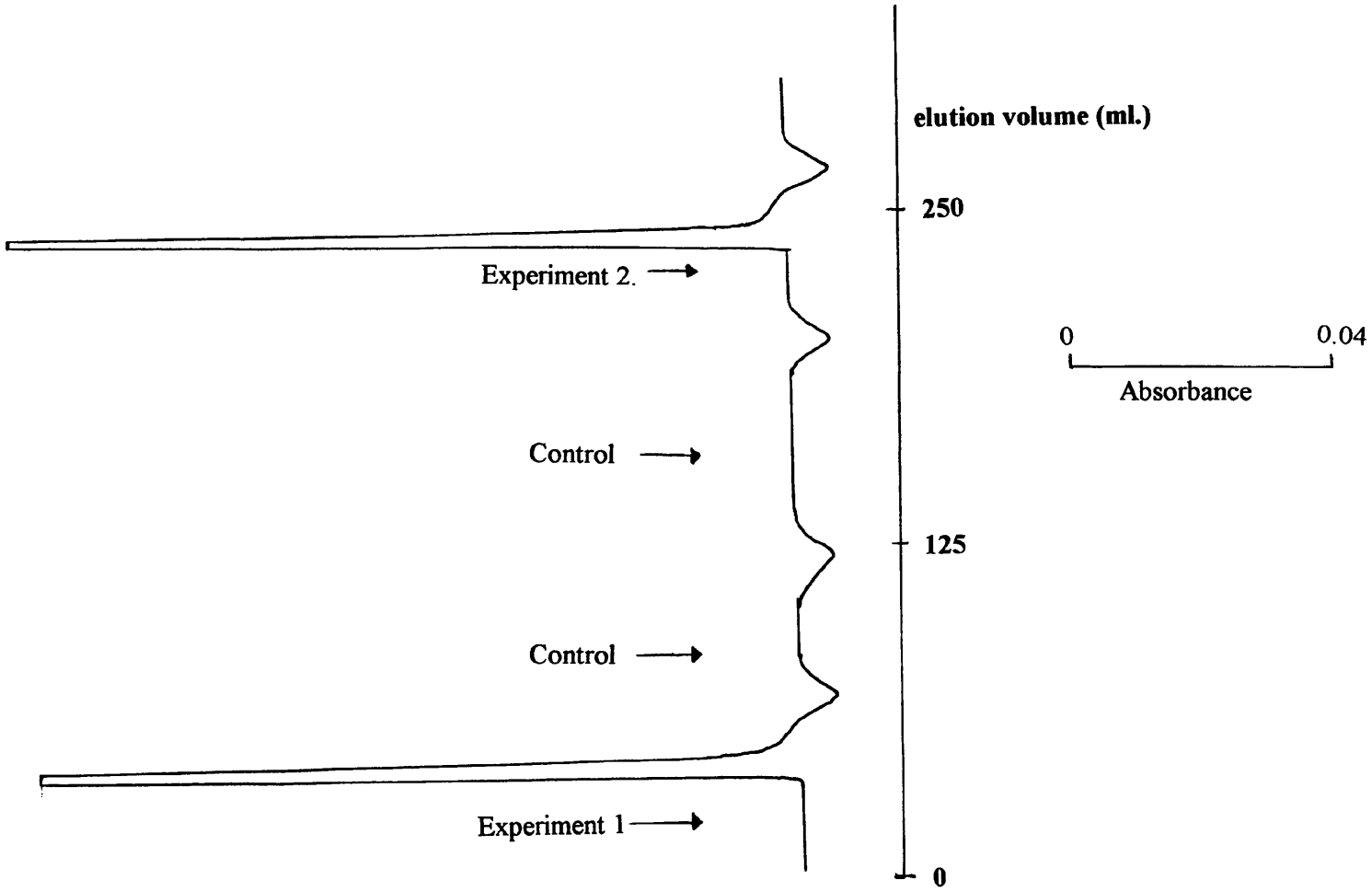

Figure 5.4: Absorption elution profile of DHPS in the presence of 10μM pABA and 100μM sodium pyrophosphate.

The equilibration buffer contained 50mM Citrate/ HCl, pH 6.0, 5mM magnesium chloride, 10μM pABA and 100μM sodium pyrophosphate. The identical experiments involved the application and elution of 1ml solutions containing 3.4mg DHPS in the above equilibration buffer minus pABA and sodium pyrophosphate. The controls involved the application and elution of 1ml solutions of equilibration buffer minus pABA and sodium pyrophosphate. The elution profile was measured at 25°C, at a chart speed of 2mm/min and a flow rate of 5ml/min.

Figure 5.4: Absorption elution profile of DHPS in the presence of 10μM pABA and 100μM sodium pyrophosphate.

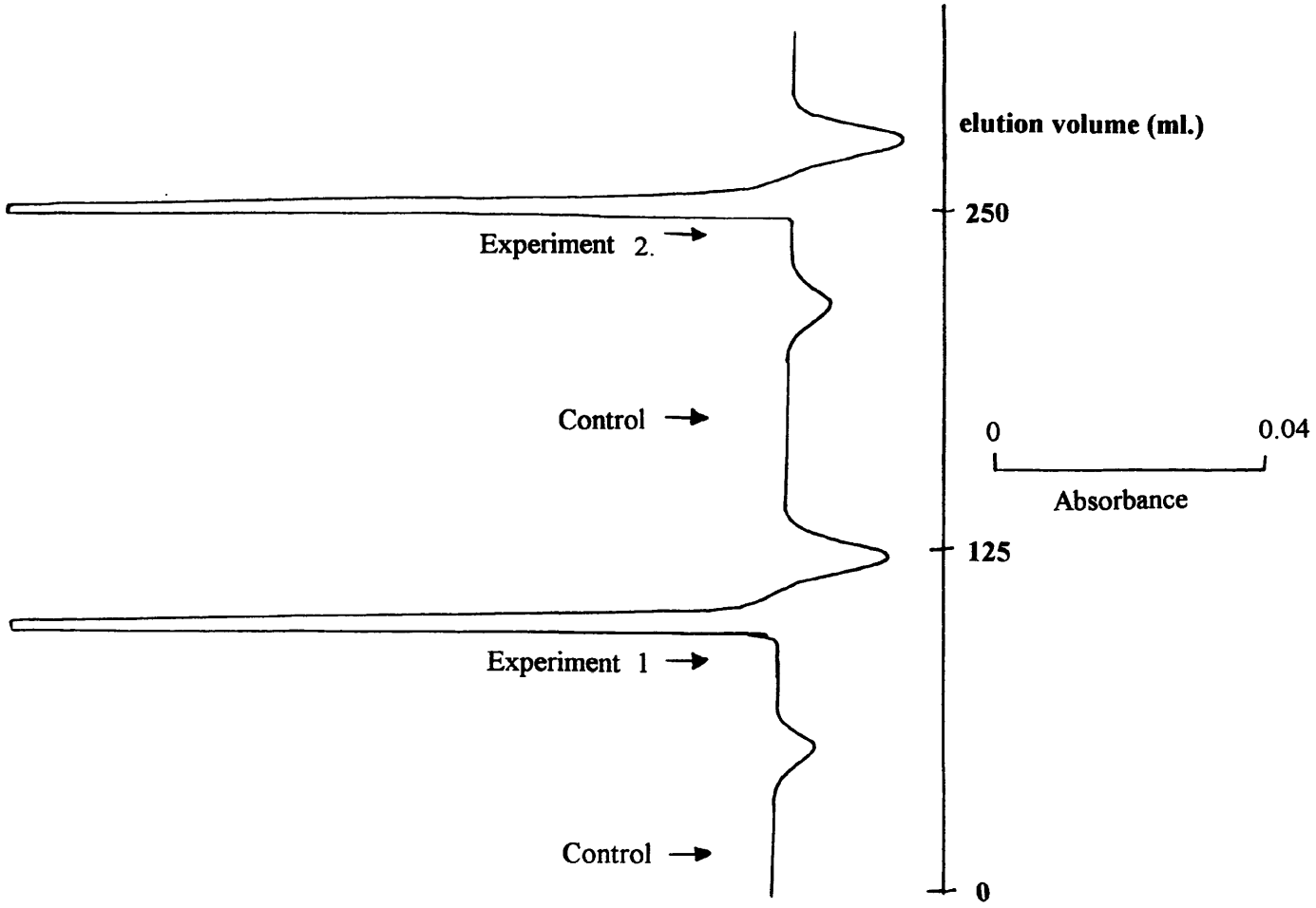

Figure 5.5: Absorption elution profile of DHPS in the presence of 10μM pABA and 100μM sodium pyrophosphate. (no magnesium)

The equilibration buffer contained 50mM Citrate/ HCl, pH 6.0, 10μM pABA and 100μM sodium pyrophosphate. The experiment involved the application and elution of a 1ml solution containing 3.4mg DHPS in the above equilibration buffer minus pABA and sodium pyrophosphate. The control involved the application and elution of a 1ml solution of equilibration buffer minus pABA and sodium pyrophosphate. The elution profile was measured at 25°C, at a chart speed of 2mm/min and a flow rate of 5ml/min.

Figure 5.5: Absorption elution profile of DHPS in the presence of 10μM pABA and 100μM sodium pyrophosphate. (no magnesium)

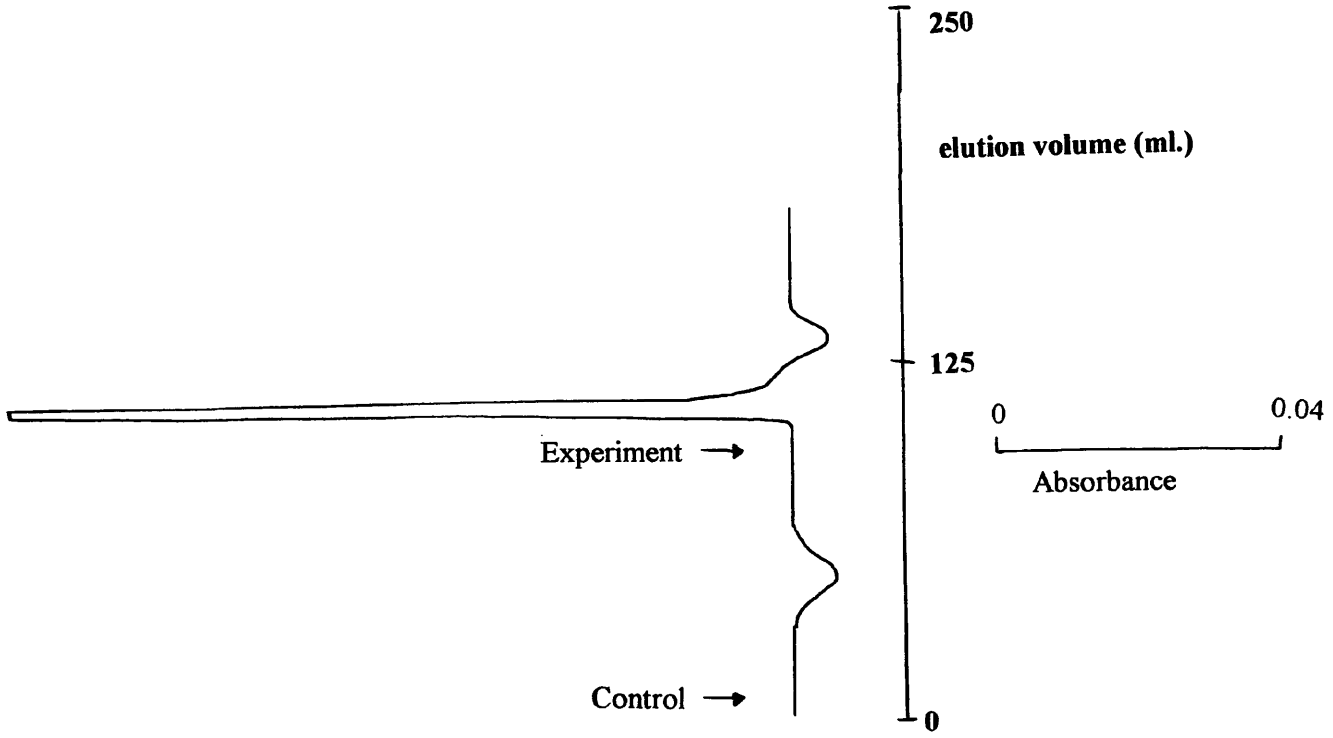

Figure 5.6: Absorption elution profile of DHPS in the presence of 10μM pABA and 10μM sodium dihydrogen orthophosphate.

The equilibration buffer contained 50mM Citrate/ HCl, pH 6.0, 5mM magnesium chloride, 10μM pABA and 10μM sodium dihydrogen orthophosphate. The identical experiments involved the application and elution of 1ml solutions containing 3.4mg DHPS in the above equilibration buffer minus pABA and orthophosphate. The control involved the application and elution of a 1ml solution of equilibration buffer minus pABA and sodium orthophosphate. The elution profile was measured at 25°C, at a chart speed of 2mm/min and a flow rate of 5ml/min.

Figure 5.6: Absorption elution profile of DHPS in the presence of 10μM pABA and 10μM sodium dihydrogen orthophosphate.

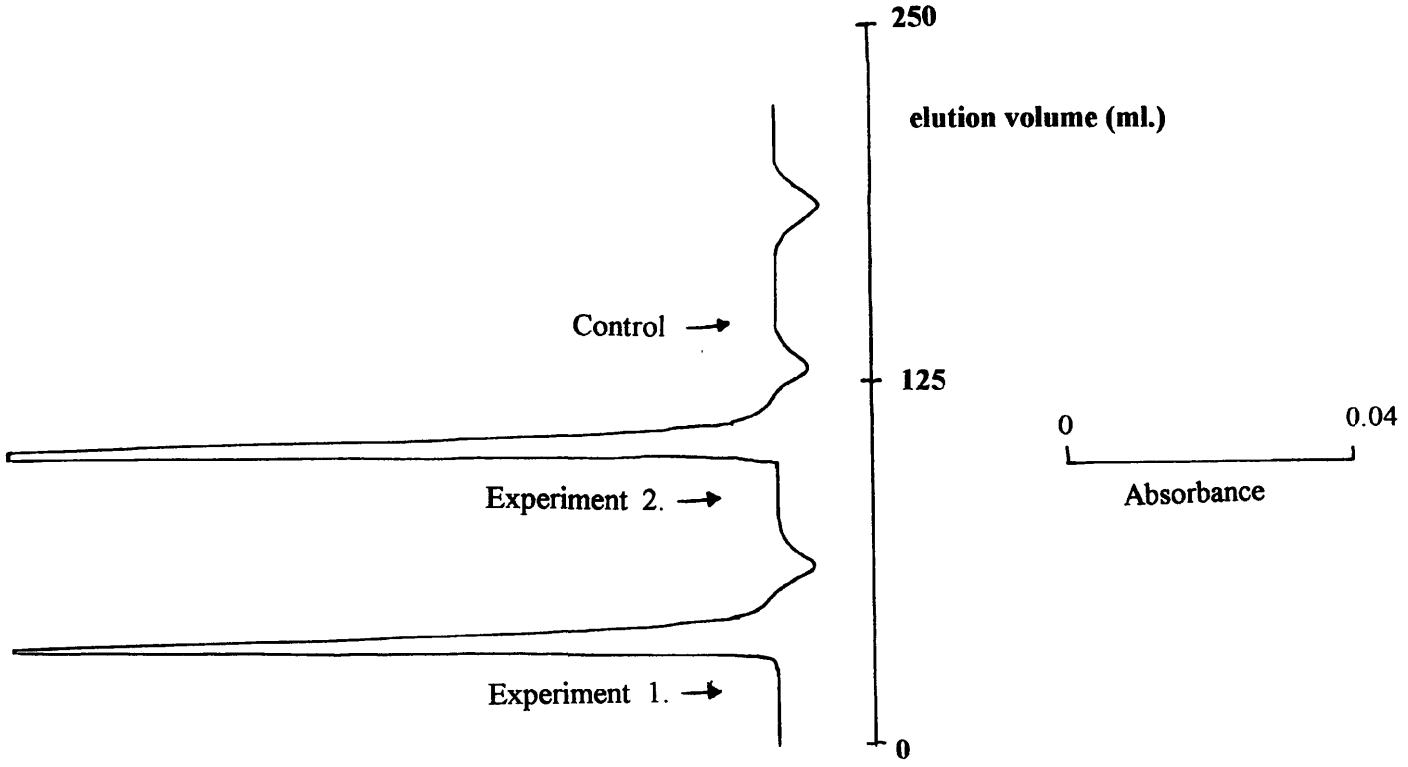

Figure 5.7: Absorption elution profile of DHPS in the presence of 10μM pABA and 100μM sodium dihydrogen orthophosphate.

The equilibration buffer contained 50mM Citrate/ HCl, pH 6.0, 5mM magnesium chloride, 10μM pABA and 100μM sodium orthophosphate. The experiment involved the application and elution of a 1ml solution containing 3.4mg DHPS in the above equilibration buffer minus pABA and sodium orthophosphate. The control involved the application and elution of a 1ml solution of equilibration buffer minus pABA and sodium orthophosphate. The elution profile was measured at 25°C, at a chart speed of 2mm/min and a flow rate of 5ml/min.

Figure 5.7: Absorption elution profile of DHPS in the presence of 10μM pABA and 100μM sodium dihydrogen orthophosphate.

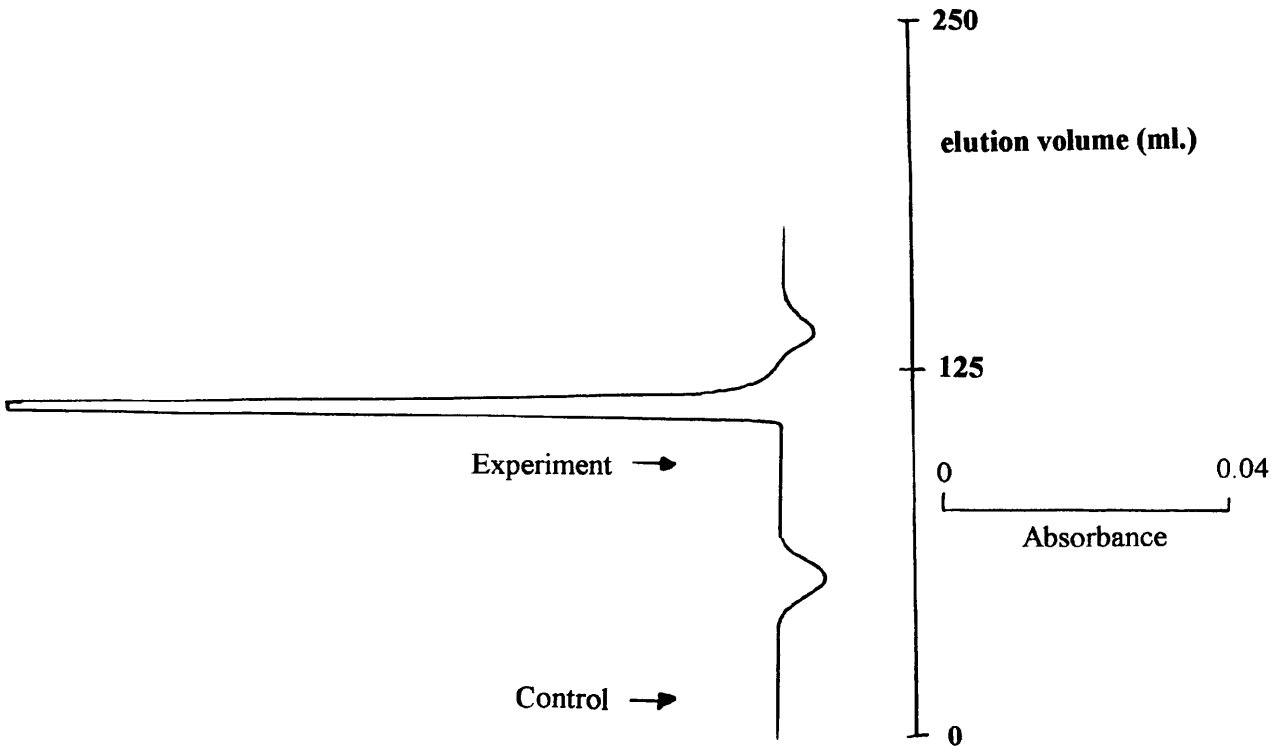

In principle, orthophosphate may bind at either the α- or β-phosphate pockets of the pterin pyrophosphate binding site, or be unable to bind to either site. The results suggest that a single phosphate group does not interact with the correct residues or sufficient residues within the binding pocket to cause the structural change necessary to facilitate the binding of pABA by DHPS. In the crystal structure of *Staphylococcus aureus* DHPS, the pyrophosphate moiety of pterin pyrophosphate interacts with side chain atoms of four different residues. The β-phosphate group interacts with Arg239, Asn11 and His241 but the α-phosphate group interacts with only Arg52. [Hampele, *et al.* (1997)] This pattern is confirmed from the *E. coli* crystal structure which indicates that the β-phosphate group is surrounded by positively-charged residues. These form hydrogen bonds to the β-phosphate group by the NH1 of Arg63, both NH groups of Arg255, the Nε2 of His257 and the ND2 of Asn22. [Achari, *et al.* (1997)] The α-phosphate group in contrast makes interactions with the main chain NH-groups of Thr62 and Arg63 and the hydroxyl-group of Thr62. All these residues are conserved in the *S. pneumoniae* DHPS sequence. [See Chapter 1 for sequence alignments] Pyrophosphate would appear to be capable of making a sufficient number or all of these interactions to allow the binding of pABA, whereas orthophosphate cannot.

A major limitation of these experiments is the large amount of enzyme required for each experimental run. Although DHPS could be purified in milligram quantities, only a limited amount of qualitative information could be obtained from each experiment. For this reason, an equilibrium binding experiment was developed to obtain quantitative equilibrium binding information to substantiate these results.

5.4 Quantification of substrate equilibrium binding to DHPS using immobilised enzyme.

The Hummel and Dreyer experiments were limited in their use due to the problems mentioned in Section 5.5 and difficulties faced in trying to quantify the results. Equilibrium dialysis was an alternative method to both detect and quantify the binding of substrates and products to DHPS. However, numerous technical difficulties prevented the collection of useful equilibrium dialysis data.

Another approach, which allowed easy separation of enzyme-bound and unbound substrate, was the immobilisation of enzyme on Sephadex beads. Rapid filtration could be used to remove and collect the unbound ligand. The bound ligand could also be removed in a second step by elution at low pH, effectively stripping the ligand from the protein. This type of binding assay proved to be extremely valuable in generating reliable and reproducible data. The assay was developed and validated. [See Sections 2.24-2.27]

5.4.1 Determination of the equilibrium binding constant for pABA.

The availability of [^{14}C]-pABA allowed equilibrium binding constants for the binding of pABA to DHPS in the presence of different ligands to be measured. No binding of pABA alone to DHPS could be detected in the Hummel and Dreyer experiments so a wider range of pABA concentrations were used in the binding assay to determine an equilibrium binding constant for pABA/magnesium alone.

Experiments were performed using concentrations of 1-100μM pABA in a buffer containing 50mM Tris/HCl, pH 8.0, 5mM DTT and 5mM magnesium chloride. There was no detectable binding of pABA by DHPS under any conditions, (data not shown) indicating that the equilibrium binding constant (K_d), for pABA binding to DHPS must be considerably greater than 100μM.

An experiment to determine the equilibrium binding constant for pABA in the presence of an excess of sodium pyrophosphate and magnesium was also performed. The data in Figure 5.8 show an increase in the amount of pABA bound by DHPS as the total concentration of pABA increases. A non-linear least squares fitting procedure was used to fit the binding data, assuming a single, saturable binding site. The data are consistent with a single binding site for pABA on the DHPS/pyrophosphate binary complex. The K_d for pABA was determined to be 830nM, with a total binding capacity of 1400nM. From the Hummel and Dreyer experiments, the binding of pABA to DHPS was absolutely dependent on the presence of magnesium. Equilibrium binding experiments were performed over a wide range (0-1mM) of sodium pyrophosphate concentrations and a fixed (500nM) pABA concentration but magnesium chloride was omitted from the buffer.

Figure 5.8: Determination of the equilibrium binding constant for pABA.

The experiment was conducted as described in Chapter 2. The 100µl reaction volume contained: 0-5µM [^{14}C]-pABA
300µM sodium pyrophosphate (stock made in 100mMCitrate/HCl, pH 6.0 and used immediately)
50mM Tris/HCl, pH 8.0
5mM DTT
5mM magnesium chloride and
6µM DHPS immobilised on sepharose beads

The volume was made up to 100µl with distilled water. Data were fitted using a non-linear least-squares procedure as described in Chapter 2. For the derivation of the equation used for fitting see Section 9.6. The model assumed a single saturable binding site for pABA on DHPS and predicted a K_d value for pABA of 830nM and a binding capacity for pABA of 1400nM. This binding capacity can be expressed as 0.14nmoles of pABA bound to 0.6nmoles of DHPS. Since the same amount of DHPS was used in all equilibrium binding experiments this expression can be used as a calibration of 'binding capacity' in all the subsequent experiments.

Figure 5.8: Determination of the binding constant for pABA.

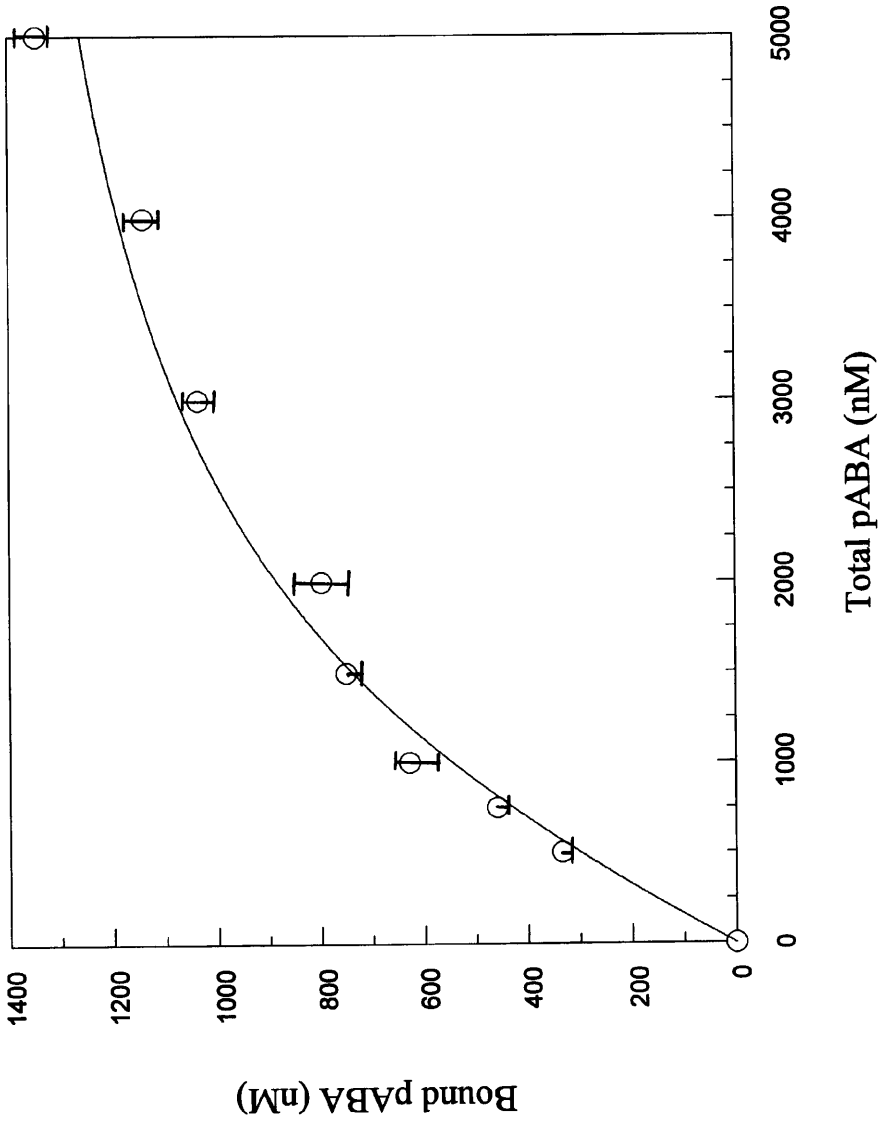

No binding of pABA by DHPS was detectable, (data not shown) demonstrating that pABA is capable of binding only to a DHPS/pyrophosphate/magnesium complex and not to a DHPS/pyrophosphate complex.

5.4.2 Determination of the equilibrium binding constant for dihydropteroate.

Dihydropteroate is a product of the DHPS reaction and as such its binding behaviour to DHPS could reveal important information concerning the enzyme mechanism. An examination of the equilibrium binding constant for dihydropteroate will reveal whether it can bind to the DHPS apoprotein and the dependence of binding on the presence of other ligands may also provide information about the order of release of products from DHPS.

Radiolabelled dihydropteroate is not commercially available, so [^{14}C]-dihydropteroate was made using DHPS, by incubating equimolar concentrations of [^{14}C]-pABA with pterin pyrophosphate. The stock of dihydropteroate therefore contained an equimolar amount of pyrophosphate.

Exogenous pyrophosphate was also added to an excess concentration of 300μM and held constant throughout the experiment. Although theoretically these two compounds can react by the reverse DHPS reaction, no detectable back reaction was ever measured. [See Section 5.5.1]

The data in Figure 5.9 show an increase in the amount of dihydropteroate bound as the total dihydropteroate concentration increases. The data are consistent with a single, saturable binding site for dihydropteroate on DHPS,giving an equilibrium binding constant for dihydropteroate of 510nM. Examination of total ligand bound in Figures 5.8 and 5.9 reveals that less than half the number of sites on DHPS are occupied by dihydropteroate (400nM) compared to pABA (1400nM) suggesting that dihydropteroate binds to 1/3 fewer sites. This phenomenon suggests that pABA and dihydropteroate induce different conformational responses in DHPS. It was also clear that only 1400nM pABA had bound to the 6000nM DHPS used in the experiments. The immobilisation of DHPS on Sepharose beads may have prevented the binding of ligands in some way.

Figure 5.9: Determination of the binding constant for dihydropteroate.

The experiment was conducted as described in Chapter 2. The 100µl. reaction volume contained: 25, 50, 75, 100, 250, 500, 750 or 1000nM [^{14}C]-dihydropteroate
300µM sodium pyrophosphate (stock made up in 100mM Citrate/HCl, pH 6.0 and used immediately)
50mM Tris/HCl, pH 8.0
5mM DTT
5mM magnesium chloride and
6µM DHPS immobilised on sepharose beads.

The volume was made up to 100µl with distilled water. Data were fitted using a non-linear least-squares procedure as described in Chapter 2. For the derivation of the equation used to fit the data see Section 9.7. The model assumed a single saturable binding site for dihydropteroate on DHPS and predicted a K_d value of 510nM and a binding capacity for dihydropteroate of 400nM.

Figure 5.9: Determination of the binding constant for dihydropteroate

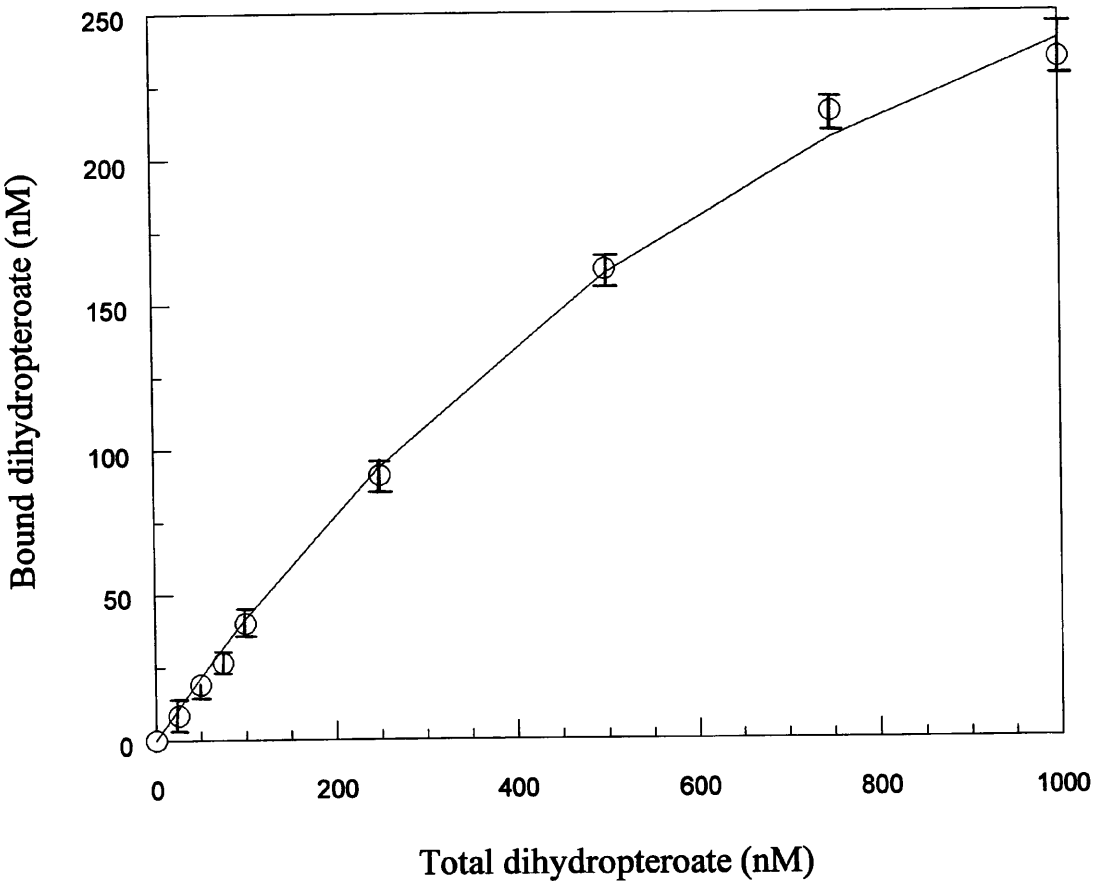

5.4.3 Determination of the equilibrium binding constant for sodium pyrophosphate.

It has already been shown that the binding of pABA by DHPS is dependent on the prior binding of pyrophosphate and magnesium. The affinity of DHPS for pyrophosphate is unknown but can be measured indirectly from its effect on binding of pABA by DHPS.

$$E + PPi\text{-}Mg^{2+} \rightleftharpoons \underset{1}{E.PPi\text{-}Mg^{2+}} + pABA \rightleftharpoons \underset{2}{E.PPi\text{-}Mg^{2+}.pABA}$$

By fixing the concentrations of pABA, DHPS and magnesium and then adding sodium pyrophosphate at increasing concentrations, an increase in the amount of bound pABA can be measured. In this indirect manner, an equilibrium binding constant for pyrophosphate binding to DHPS could be deduced. The data in Figure 5.10 shows that the binding of pABA to DHPS is indeed dependent on the concentration of pyrophosphate: as the concentration of pyrophosphate increased the amount of bound pABA also increased. The data were fitted to the model above, assuming that DHPS must bind pyrophosphate before pABA is able to bind, and a single, saturable binding site for pyrophosphate - a K_d of 115μM was obtained,.

The preparation of [^{14}C]-dihydropteroate contained an equimolar quantity of pyrophosphate. It was possible, however, to show that the binding of dihydropteroate was partially dependent upon the concentration of pyrophosphate by adding incremental amounts of exogenous pyrophosphate. The data in Figure 5.11 shows that the amount of bound dihydropteroate measured increases by about 50% as the concentration of pyrophosphate increased.

To conclude, pyrophosphate has a single, saturable binding site on DHPS and binding of pABA to DHPS is absolutely dependent on pyrophosphate. This contrasts with the behaviour of dihydropteroate where the binding was dependent on pyrophosphate, but to a more limited extent.

177

Figure 5.10: Determination of the binding constant for sodium pyrophosphate.

The experiment was conducted as described in Chapter 2. The 100µl reaction contained:

2-100µM sodium pyrophosphate (stock made up in 100mM Citrate/HCl, pH 6.0 and used immediately)

500nM [^{14}C]-pABA

50mM Tris/HCl, pH 8.0

5mM DTT

5mM magnesium chloride and

6µM DHPS immobilised on sepharose beads.

The reaction volume was made up to 100µl. with distilled water. Data were fitted using the non-linear least-squares procedure as described in Chapter 2. For the derivation of the equation see Section 9.5. The model assumed a single saturable binding site for pyrophosphate on DHPS and predicted a K_d value for pyrophosphate of 115µM and a binding capacity for pABA of 1800nM.

Figure 5.10: Determination of the binding constant for sodiumPPi.

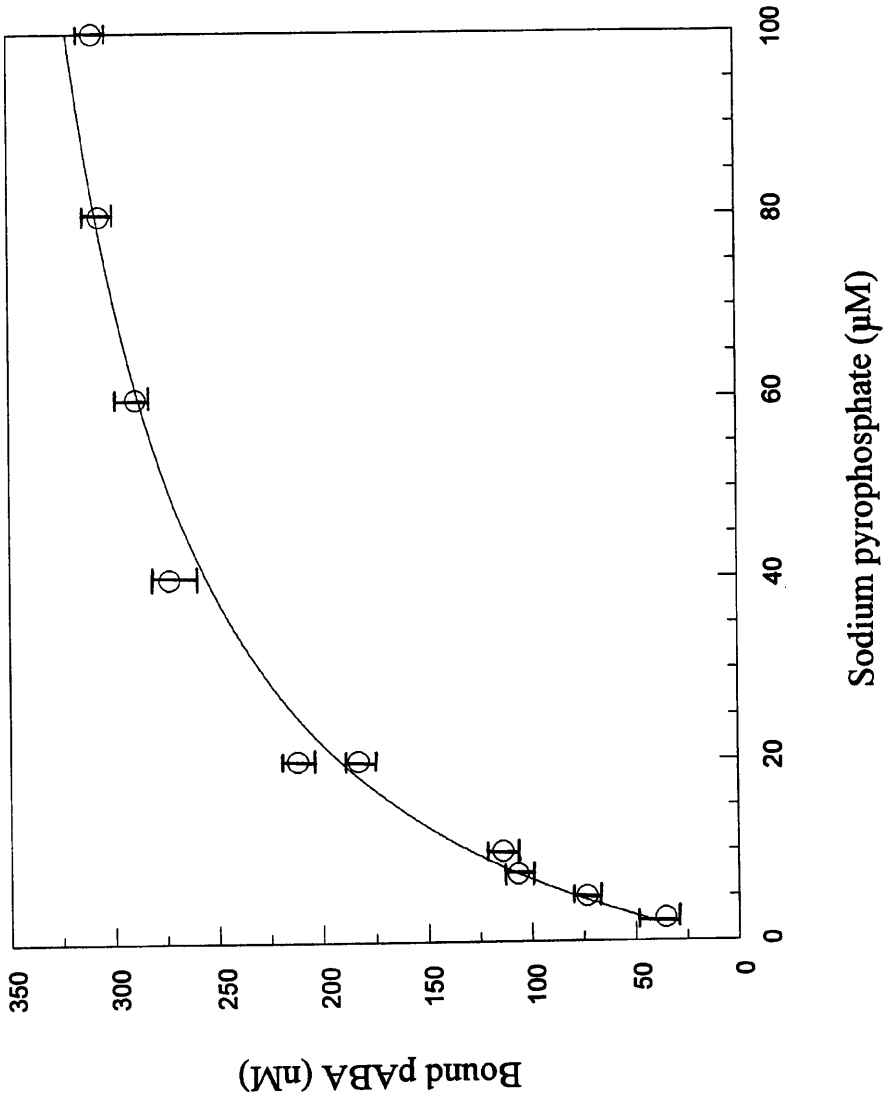

Figure 5.11: Effect of sodium pyrophosphate on the binding of dihydropteroate by DHPS.

Binding assays were carried out as described in Chapter 2. The 100µl reaction contained:

500nM [^{14}C]-dihydropteroate

0-1000µM sodium pyrophosphate (stock made up in 100mM Citrate/HCl, pH 6.0 and used immediately)

50mM Tris/HCl, pH 8.0

5mM DTT

5mM magnesium chloride and

6µM DHPS immobilised on sepharose beads

The reaction volume was made up to 100µl. with distilled water.

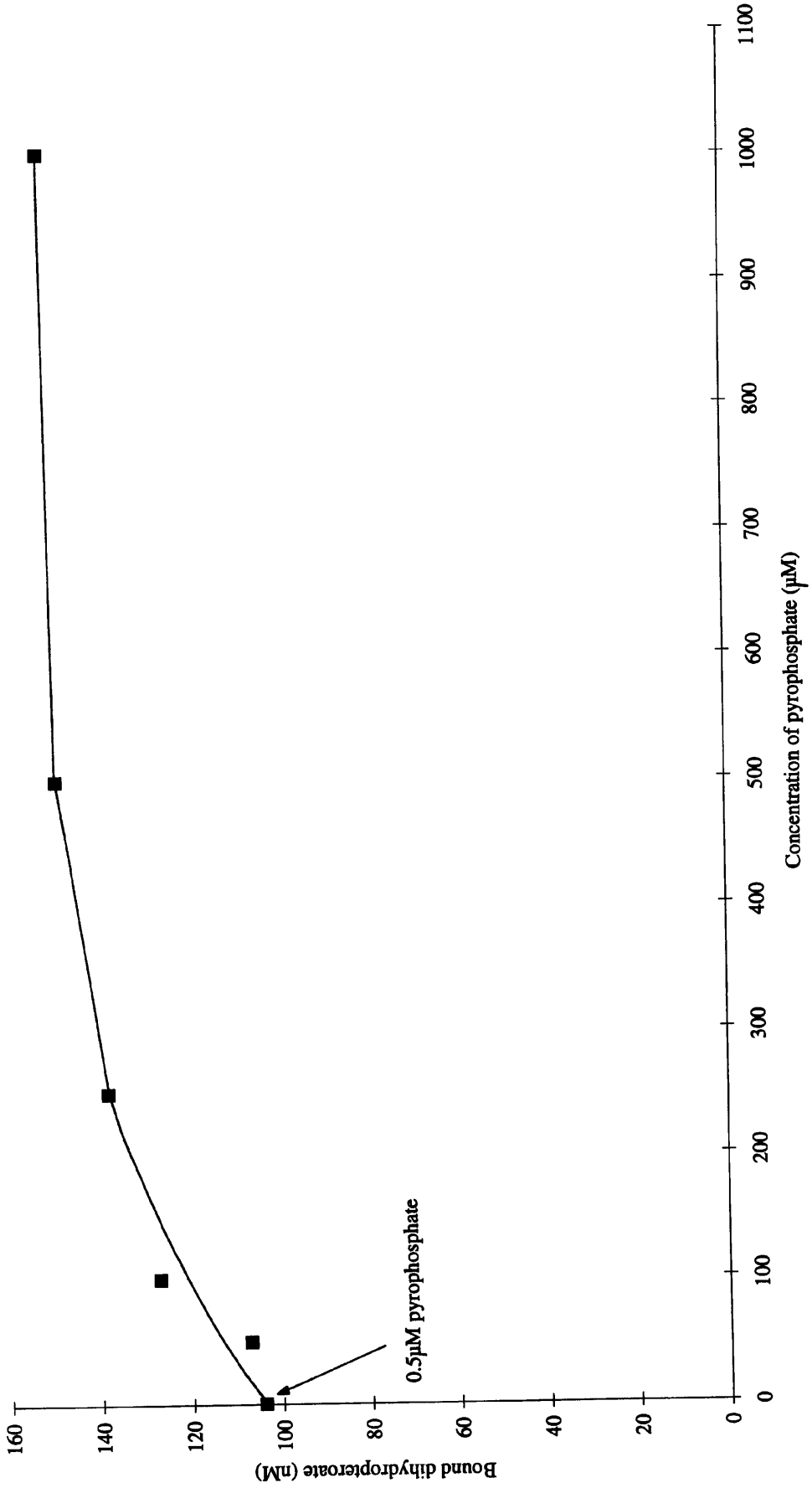

Figure 5.11: Effect of sodium pyrophosphate on the binding of dihydropteroate by DHPS.

5.4.4 Examination of the effect of orthophosphate on pABA binding.

The physiological concentration of pyrophosphate in a cell is low due to the presence of pyrophosphatases. [Upson, (1996)] The concentration of phosphate *in vivo* is normally much higher at around 1-10mM. The Hummel and Dreyer experiments showed that although pyrophosphate is capable of facilitating the binding of pABA, orthophosphate is not. The normal concentration of orthophosphate *in vivo* is not 100μM but closer to 10mM, so it is possible that higher concentrations of orthophosphate could play a role in DHPS activity.

An experiment was conducted to study pABA-binding over a range of orthophosphate concentrations from 0-20mM in a 50mM Tris/HCl, pH 8.0, 5mM DTT, 5mM magnesium chloride buffer containing 500nM [^{14}C]-pABA. There was no detectable binding of pABA by DHPS at any concentration of orthophosphate indicating that the equilibrium binding constant for orthophosphate is greater than 20mM and thus would not affect the DHPS reaction *in vivo*. It is clearly important for DHPS to be capable of distinguishing orthophosphate from pyrophosphate when the former is present at much higher concentrations *in vivo*.

5.4.5 The effect of pterin on the equilibrium binding constant of pABA.

It can be hypothesised that DHPS could bind pyrophosphate/magnesium within the pyrophosphate pocket of the pterin pyrophosphate binding site, whilst pABA occupies an adjacent binding site. This could only be directly confirmed by the solution of the crystal structure of the relevant ternary complex. If this assumption is true, we might expect that DHPS could also bind pterin - the two ring heterocyclic compound without the -CH_2OH adduct of the substrate. If the pterin and pyrophosphate/magnesium can all bind at the pterin pyrophosphate binding site, DHPS would form a *pseudo*-ternary complex on binding of pABA to its binding site, which would be very close to the true ternary complex for the substrates. There were problems in trying to detect the binding of pterin as it could not be easily radiolabelled, so an equilibrium binding constant for pterin binding could not be measured directly. However the effect of pterin binding to DHPS could be measured indirectly via its effects on pABA binding.

Equilibrium binding constants of pABA at four different concentrations of pterin were measured. [Figure 5.12] At each concentration, pABA binding was characteristic of a single, saturable binding site, and the data were fitted in the same way as described in Section 9.7. Table 5.1 shows that the equilibrium binding constant for pABA declined as the concentration of pterin increased, i.e. the binding of pterin together with pyrophosphate and magnesium has the effect of increasing the affinity of DHPS for pABA.

5.4.6 Summary of the equilibrium binding experiments.

Ligand	**K_d**	**Other Ligand(s)**
pABA	>100μM	Mg^{2+}
pABA	830nM	pyrophosphate, Mg^{2+}
dihydropteroate	510nM	pyrophosphate, Mg^{2+}
pyrophosphate	115μM	pABA, Mg^{2+}
orthophosphate	>20mM	pABA, Mg^{2+}
Ligand	**K_d**	**Other Ligand(s)**
pABA (0μM pterin)	570nM	pyrophosphate, Mg^{2+}
pABA (1μM pterin)	500nM	pyrophosphate, Mg^{2+}
pABA (10μM pterin)	440nM	pyrophosphate, Mg^{2+}
pABA (50μM pterin)	230nM	pyrophosphate, Mg^{2+}
pABA (100μM pterin)	190nM	pyrophosphate, Mg^{2+}

These results confirm the conclusions from the Hummel and Dreyer Experiments. pABA is only bound by DHPS in the presence of pyrophosphate and magnesium, which indicates a compulsory binding order of substrates. In the forward reaction, pterin pyrophosphate/magnesium probably binds to DHPS first, followed by pABA. The DHPS apoprotein has also been shown to bind dihydropteroate with high affinity in the presence of magnesium and pyrophosphate.

Figure 5.12: The effect of pterin on the equilibrium binding constant for pABA.

The binding of pABA was measured as described in Chapter 2. The 100µl reaction contained: 0-100µM Pterin
500nM [^{14}C]-pABA
300µM sodium pyrophosphate (stock made up in 100mM Citrate/HCl, pH 6.0 and used immediately)
50mM Tris/HCl, pH 8.0
5mM DTT
5mM magnesium chloride and
6µM DHPS immobilised on sepharose beads

The reaction volume was made up to 100µl using distilled water. The results are the mean values of triplicate experiments. Data were fitted using the non-linear least-squares procedure described in Chapter 2. For the equation used to fit the data see Section 9.6.

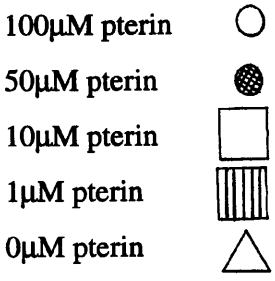

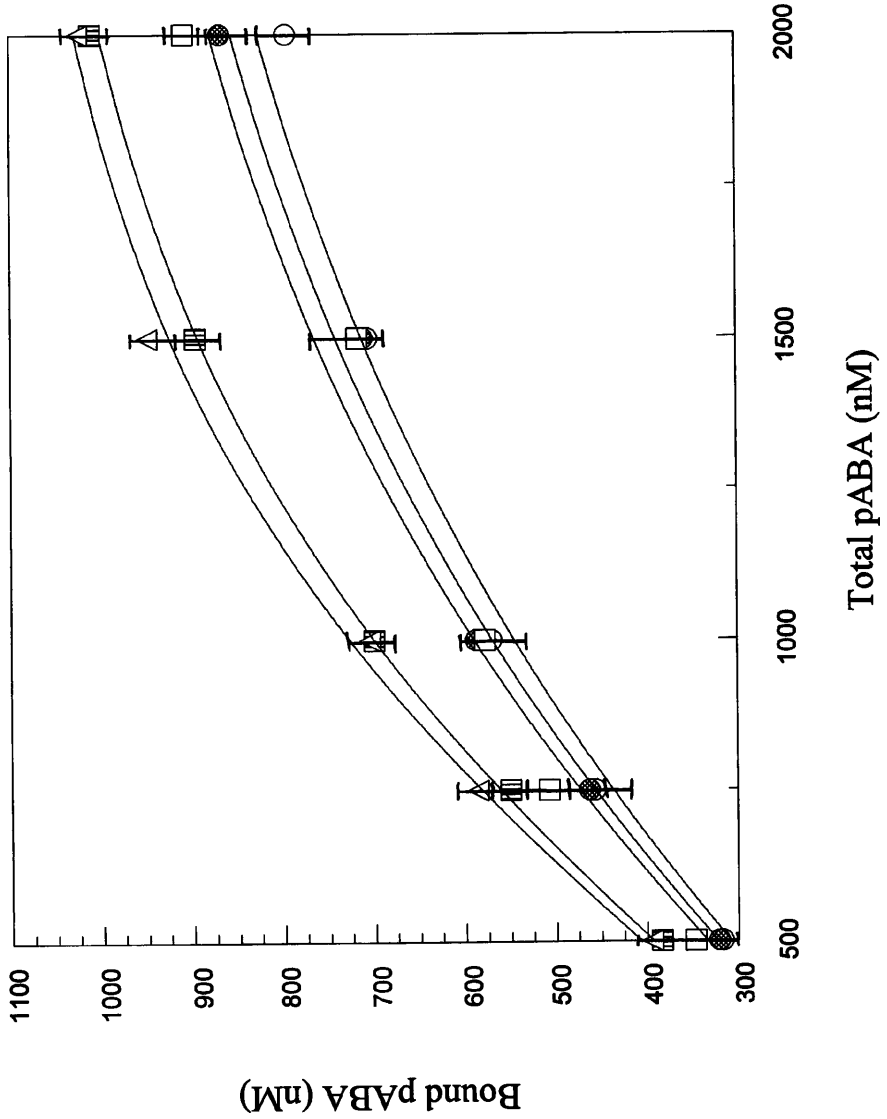

Figure 5.12: The effect of pterin on the binding constant for pABA.

Table 5.1: Dissociation equilibrium binding constants for pABA at different concentrations of pterin in the presence of pyrophosphate and magnesium.

Concentration of Pterin (μM)	K_d for pABA (nM)
0	567
1	495
10	442
50	226
100	188

5.4.7 Conclusions.

Extrapolation of Figure 5.11 suggests that DHPS can probably bind some dihydropteroate without pyrophosphate/magnesium present, although DHPS has a greater capacity for the ligand in the presence of pyrophosphate. The only firm conclusion that can be drawn about the mechanism of release of the two products is that it is unlikely that dihydropteroate leaves first, followed by pyrophosphate, in a compulsory order mechanism. The converse however may occur i.e. that pyrophosphate leaves first followed by dihydropteroate in a compulsory order mechanism, or a random order of departure may be adopted by the products. The reduced capacity of dihydropteroate binding compared with pABA requires a more complex explanation. Each monomer apparently possesses a single, saturable binding site on DHPS and yet only one of the two monomers appears to be capable of binding dihydropteroate. One explanation could be that each monomeric binding site is equally capable of binding a dihydropteroate molecule or a pABA molecule, but on the binding of one molecule of dihydropteroate a conformational change occurs within the dimer to prevent the binding of a second molecule. This conformational change in the dimer may also effectively prevent any reverse reaction between dihydropteroate and pyrophosphate by altering the position of key residues at the active site. This rationale would presume that two molecules of pABA can bind to the DHPS dimer in the presence of pyrophosphate and magnesium, one at each monomeric binding site. pABA and dihydropteroate thus appear to effect different conformational responses in DHPS. This conclusion is supported by the pyrophosphate-dependence of pABA and dihydropteroate binding. The work presented here has indicated that in the forward reaction, pterin pyrophosphate/magnesium is likely to be the first substrate to be bound by DHPS, followed by pABA. The *Staphylococcus aureus* work demonstrated that oxidised pterin pyrophosphate was bound by only one of the monomers. [Hampele, *et al.* (1997)] Therefore even if pABA were capable of binding to both sites on the dimer, a reaction is only likely to occur at one site. A molecule of pterin pyrophosphate/magnesium, on binding to DHPS, may effect a similar conformational change to that postulated for dihydropteroate, causing the second pterin pyrophosphate binding site to become inaccessible or inactive.

It is interesting to note that this effect is not emulated by pterin, which does not displace pABA, as can be seen from Figure 5.12 where the binding capacity of pABA remains at 1400nM.

There were limitations to the binding experiments because a radioactive substrate or product must be available. Although radiolabelled pABA was available commercially, radiolabelled pterin pyrophosphate was not available and it would have been time-consuming and expensive to try to label and purify a sample. This excluded experiments involving the direct use of pterin pyrophosphate or pyrophosphate as ligands. Unfortunately this prevented an investigation into the possibility of half-of-sites reactivity by pterin pyrophosphate or pyrophosphate.

The effect of using immobilised enzyme rather than free enzyme for the binding experiments is not clear. From the accurate data collected and the agreement between results obtained from the Hummel and Dreyer and the equilibrium binding experiments it seems unlikely that the coupling of DHPS to Sephadex beads has had a seriously detrimental effect on the behaviour of DHPS. Indeed, the enzyme is still catalytically active in this form although not all sites appear to be capable of binding ligand. [See Chapter 2]

5.8 Steady-state kinetic experiments.

A kinetic study of the reaction is one method to obtain information about the order of binding of substrates and products to the enzyme. To date this has been the only method used to study the mechanism of DHPS from other organisms. [On subsequent graphs, when velocity appears plotted on the y-axis it is always measured per 30 minutes.] Initial velocity measurements were made at five concentrations of pABA and pterin pyrophosphate. The data were analysed according to a compulsory or random order mechanism of substrate addition using the non-linear least squares fitting procedure described in Chapter 2. The same data are presented in Figures 5.13-5.16, compared against predicted velocities for both reaction mechanisms and plotted with either pABA or pterin pyrophosphate as substrate concentration on the x-axis. For a compulsory order of addition of substrates, an equation relating the velocity of the reaction to substrate concentration was derived [Section 9.1] and the data fitted. For a reaction mechanism where pterin pyrophosphate binds first, the predicted kinetic parameters K_A and K_B were 3.62μM for pterin pyrophosphate and 30nM for pABA. [See Table 5.2] The results show that the agreement is poor between predicted and actual measurements, even bearing in mind the errors at each point. An examination of the data in figure 5.14 shows that the predicted values are not followed by the experimental data, especially at low concentrations of pterin pyrophosphate, and the same comments apply to the data in Figure 5.13. Generally, the compulsory order model underestimates the velocity at low concentrations of substrate and overestimates the velocity at high concentrations.

For a random order mechanism the predicted kinetic parameters K_A and K_B were 330nM for pterin pyrophosphate and 90nM for pABA. [See Section 9.8] Figures 5.15 and 5.16 show that the agreement with the data is better than for a compulsory order of addition of substrates although there is still some deviation from the results at low concentrations of pterin pyrophosphate compared with low concentrations of pABA. The conditions imposed on the data for fitting to a random order of binding have more variables than a fixed order of addition of substrates, so it is perhaps not surprising that the agreement is better for the random binding order mechanism.

Figures 5.13-5.16: Determination of kinetic parameters.

The kinetic experiments were performed as described in Chapter 2 using the reverse-phase column separation method.

A 1ml. reaction contained:

33.34nM [^{14}C]-pABA

Total pABA concentrations 33.34, 100, 200, 500, & 1000nM

Total pterin pyrophosphate concentrations 100, 500, 1000, 2000, 5000nM

50mM Tris/HCl, pH 8.0

5mM DTT

5mM magnesium chloride

3.12ng. DHPS to initiate the reaction.

The reaction volume was made up to 1ml. using distilled water.

Figure 5.13

5000nM pterin pyrophosphate

2000nM pterin pyrophosphate

1000nM pterin pyrophosphate

500nM pterin pyrophosphate

100nM pterin pyrophosphate

Figure 5.14

1000nM pABA

500nM pABA

200nM pABA

100nM pABA

33.34nM pABA

Figure 5.15

5000nM pterin pyrophosphate

2000nM pterin pyrophosphate

1000nM pterin pyrophosphate

500nM pterin pyrophosphate

100nM pterin pyrophosphate

Figure 5.15

1000nM pABA

500nM pABA

200nM pABA

100nM pABA

33.34nM pABA

Figure 5.13: Determination of kinetic parameters. (compulsory order)

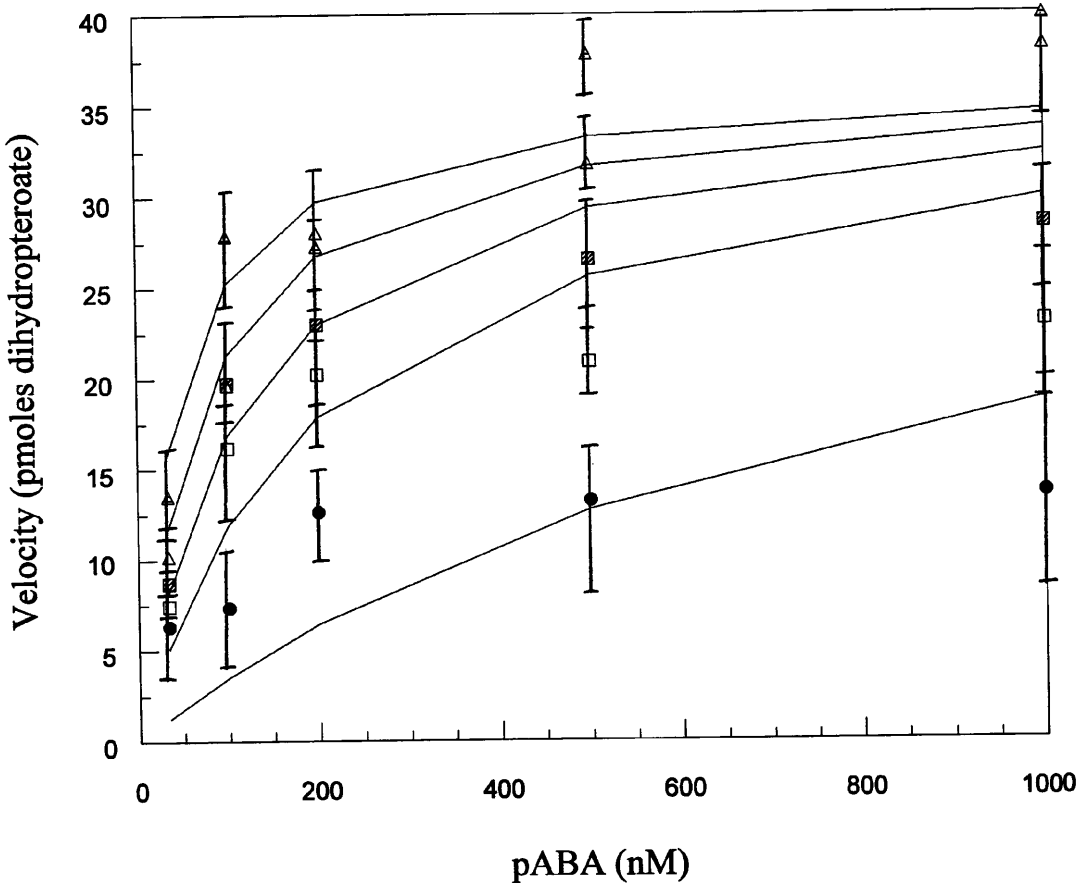

Figure 5.14: Determination of kinetic parameters. (compulsory order)

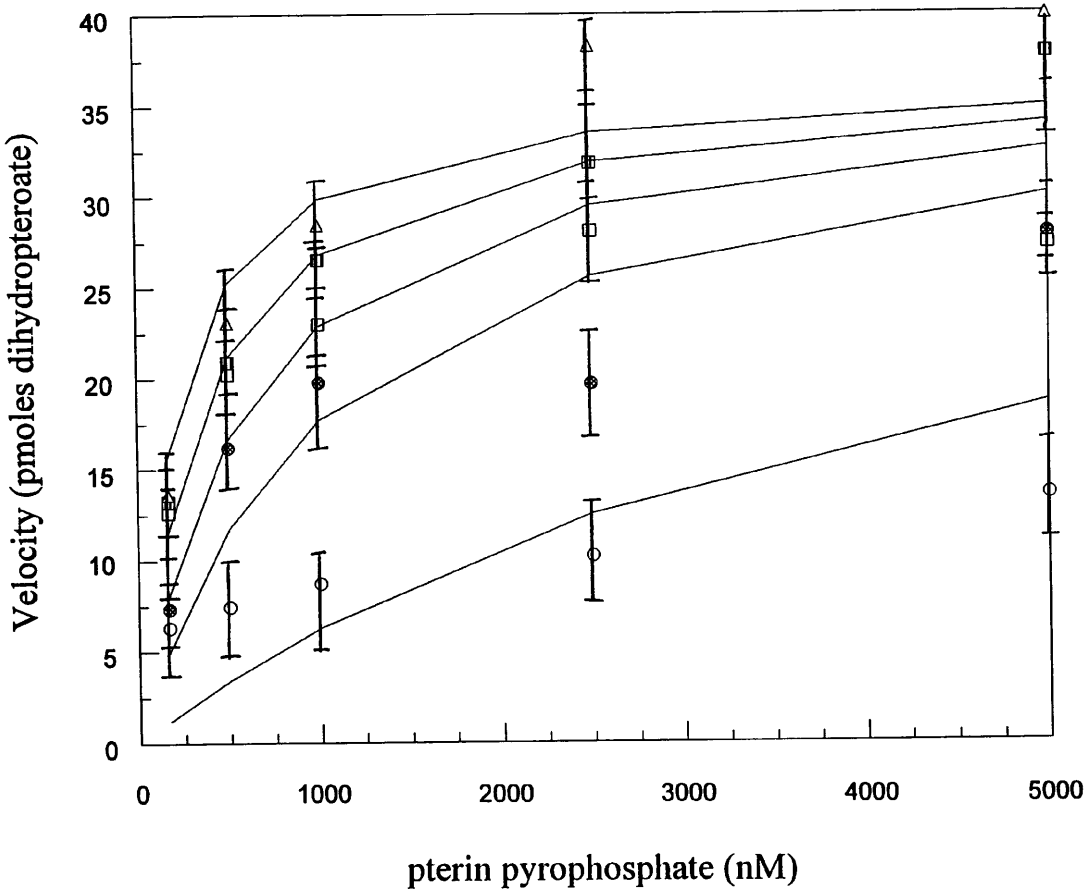

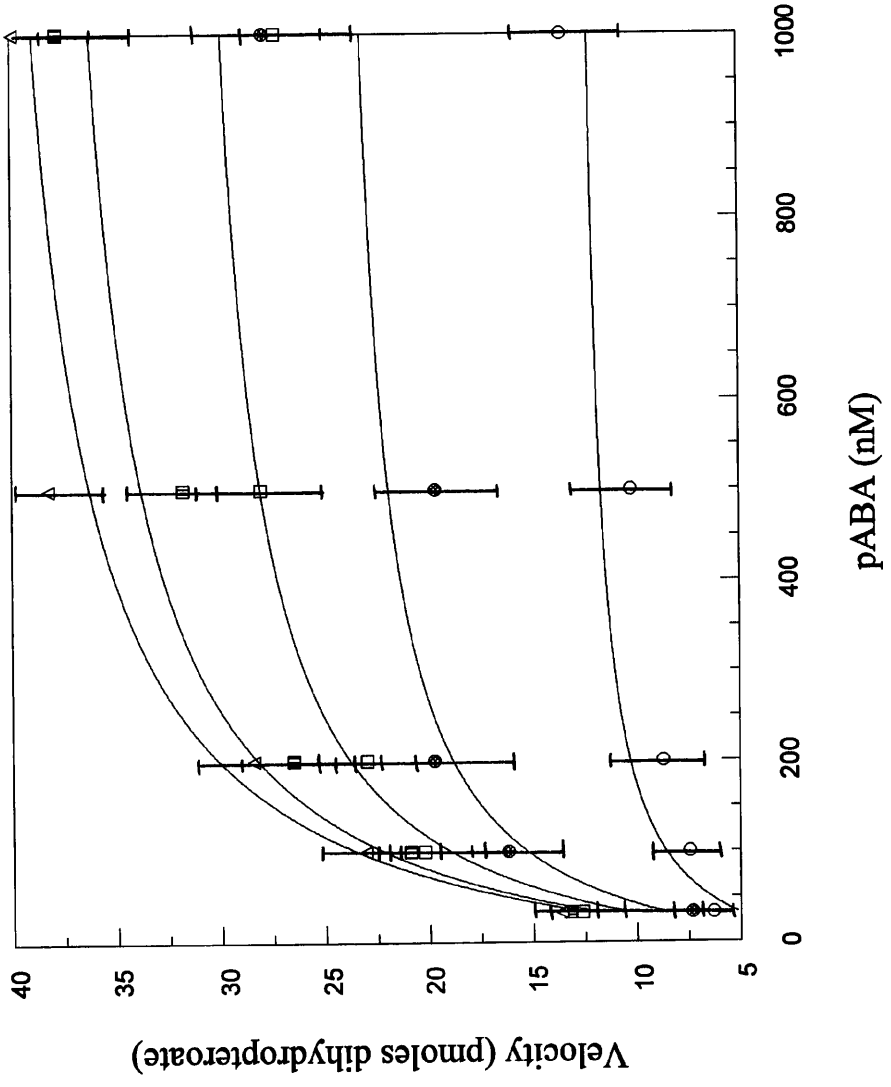

Figure 5.15: Determination of kinetic parameters. (random order)

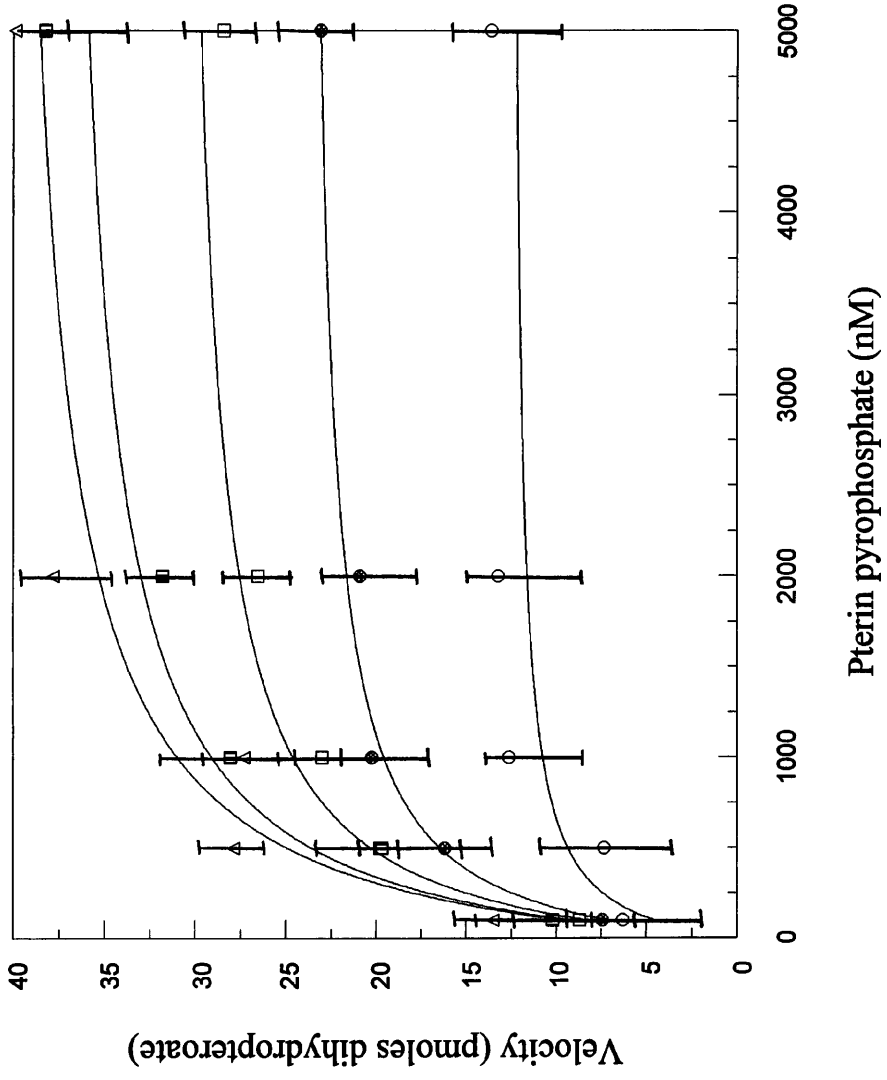

Figure 5.16: Determination of kinetic parameters. (random order)

Table 5.2: Steady state kinetic parameters.

(The kinetic parameters K_A, K_B, $K_A K_B^-$ and $K_B K_A^-$ were all measured in nanomolar concentrations.)

Pterin pyrophosphate (nM)	**Apparent $K_{m(pABA)}$(nM)**	**V_{max} (nmol/ 30min/3.12ng DHPS)**
100	60	15
500	60	25
1000	65	30
2000	100	40
5000	65	40

pABA (nM)	**Apparent $K_{m(Pterin\ PPi)}$(nM)**	**V_{max}(nmol/ 30min/3.12ng DHPS**
33.34	200	15
100	225	25
200	250	30
500	450	40
1000	245	40

Global parameters:	**Compulsory order model**	**Random order model**
$K_{B(pABA)}$ (nM)	30	90
$K_{A(Pterin\ pryophosphate)}$ (nM)	3620	330
$k_{cat}(s^{-1})$	0.22	0.26
$K_A K_B^-$ (nM)	-	100
$K_B K_A^-$ (nM)	-	30

However, it would appear from this analysis that the reaction is more likely to proceed via a random order of addition of substrates than a compulsory order of addition, which is an apparent contradiction of the results of the equilibrium binding experiments. Apparent K_m and V_{max} values were obtained at fixed concentrations of the two substrates and these data are summarised in Table 5.2. In a compulsory order reaction mechanism, the apparent K_m of one substrate is dependent of the concentration of the second substrate. By this definition, the data do not support a compulsory order of addition of substrates as the apparent K_m values for pABA do not increase as the concentration of pterin pyrophosphate increases, and the apparent K_m values for pterin pyrophosphate are similarly independent of the concentration of pABA. In a random order of addition of substrates the apparent K_m of one substrate can be independent of the concentration of the other substrate, which is demonstrated by the data summarised in Table 5.2. This data therefore supports the graphical conclusions that a random order of addition of substrates by DHPS is more likely.

5.5.1 Investigation into the reverse DHPS reaction.

In theory an enzyme-catalysed reaction is always reversible i.e. there is a rate of appearance of substrates when the products are added to the enzyme. However some enzymes, on thermodynamic grounds, are essentially irreversible.

To examine whether any significant reverse DHPS reaction occurred, [^{14}C]-dihydropteroate and pyrophosphate were incubated together in the presence of DHPS, and then passed through a C_{18} reverse-phase chromatography column. The results in Table 5.3 show there was no significant radioactivity in the ammonium acetate fraction which would suggest that formation of pABA by the reverse reaction is negligible.

5.5.2 Effect of pH on the DHPS reaction.

This experiment was a quick and approximate examination of the effect of pH on the *S. pneumoniae* DHPS reaction. There have been no reported attempts to examine the pH dependence of the DHPS reaction in this way. Most enzymes are sensitive to pH and their activity is reduced at either side of an intermediate range where the enzyme has its maximal activity.

Table 5.3: Investigation into the reverse DHPS reaction.

	Experiment (nmoles)	Control (nmoles)
Ammonium acetate fraction (containing pABA)	0.07 ± 0.005	0.07 ± 0.003
Methanol fraction (containing dihydropteroate)	1.43 ± 0.017	1.43 ± 0.03

A solution of 300μM [^{14}C]-dihydropteroate was made by reacting 1000nM [^{14}C]-pABA with 5000nM pterin pyrophosphate and DHPS, then purified by elution through a reverse-phase column. 1ml of 10mM sodium carbonate was added to the methanol fraction to dissolve the dihydropteroate into the aqueous phase and the methanol was allowed to evaporate. For the experiment, 15μM [^{14}C]-dihydropteroate was incubated with 50mM Tris/HCl, pH 8.0, 5mM magnesium chloride, 5mM DTT and 50μM sodium pyrophosphate (stock made up in 100mM Citrate/HCl, pH 6.0 and used immediately). 6μg DHPS was added and the mixture incubated at 25°C for 2 hours, cooled on ice and the radioactive species separated on a reverse-phase column. Control tubes contained no DHPS. Both experiment and control were performed in triplicate and results are given as mean ± standard error of the mean.

Extremes of pH can affect both the structure of a protein and its capacity to bind cofactors or metal activators. It can also affect the ionisation state of substrates, their capacity to bind to the enzyme and their reactivity in catalysis.

The reaction catalysed by DHPS, the formation of a C-N bond between the amine nitrogen of pABA and the methylene carbon of pterin pyrophosphate, might be expected to proceed via an S_N2 type reaction with a base catalyst, which may be pH sensitive. From the results of the isoelectric focusing column used in the purification procedure [Chapter 3], *S. pneumoniae* DHPS was found to precipitate at pH 4.0. On redissolving DHPS at pH 8.0 full activity was recovered, demonstrating that the activity of the protein is fully recoverable from pH 4.0. A kinetic experiment to measure maximal velocities of the DHPS reaction was performed over a range of pH values from 3.9 to 8.0 using different buffers and high concentrations of both substrates. Figure 5.17 shows that the activity declines sharply below pH 6.0, indicating the possible titration of an ionisable group at a pK_a of between 4.5-5.5. This value suggests the involvement of a histidine (imidazolium) group or a carboxylic acid group. [Dixon & Webb, (1964) Mahler & Cordes, (1966)] A histidine residue with a pKa reduced by about 1.0 pH unit would be the more plausible explanation of these results.

5.5.3 Summary of the kinetic experiments.

Kinetic analysis of the DHPS reaction and subsequent fitting of the data seem to suggest that DHPS is more likely to adopt a random order of binding of its two substrates than a compulsory order predicted by the equilibrium binding experiments.

There was no measurable reverse reaction, but there appears to be an ionisable group or groups with pK_a(s) in the 4.5-5.5 region involved in the DHPS reaction.

5.6 Conclusions.

The work presented in this chapter has combined novel ligand binding experiments with kinetic studies of *S. pneumoniae* DHPS to produce a complex picture of the enzyme mechanism. On the basis of binding experiments alone, Figure 5.18 proposes an ordered mechanism for binding of the two substrates and random order of release of the products by *S. pneumoniae* DHPS.

Figure 5.17: Investigation into the effect of pH on the DHPS reaction.

The kinetic experiments were performed as described in Chapter 2 using the reverse-phase column separation method. The 1ml. reaction contained:

0.3μM [^{14}C]-pABA

9.7μM pABA

10μM pterin pyrophosphate

50mM Citrate/Citric Acid (pH 3.94 - 6.0) ●

50mM Bis/Tris/HCl (pH 6.0-7.0) ▲

50mM Tris/HCl (pH 7.0-8.0) ■

5mM DTT

5mM magnesium chloride and

156ng. DHPS. The reaction volume was made up to 1ml. with distilled water.

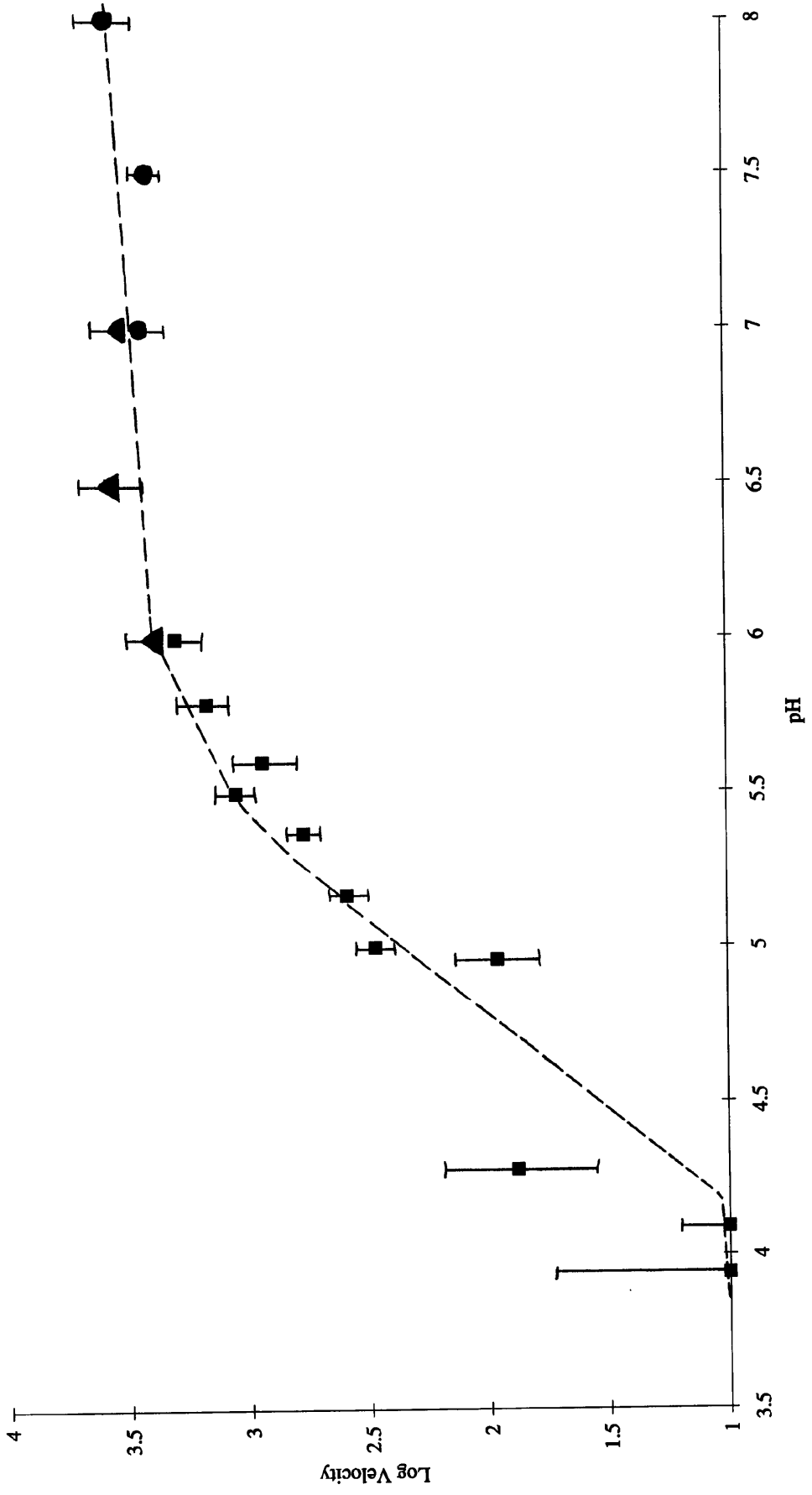

Figure 5.17: Investigation into the effect of pH on the DHPS reaction.

Figure 5.18: Proposed order of binding and release of substrates and products of the *S. pneumoniae* DHPS reaction.

(E represents DHPS, pterinPPi represents pterin pyrophosphate and PPi represents pyrophosphate.)

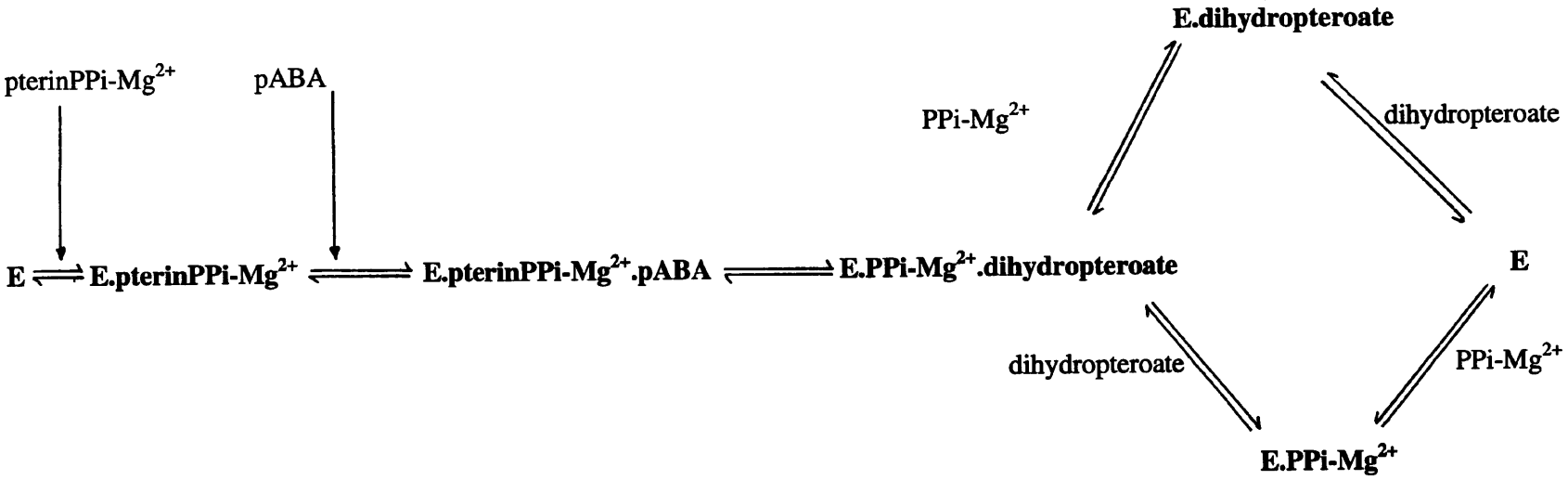

DHPS apoprotein has been shown by the equilibrium binding studies to be unable to bind pABA, so a random order of binding for the substrates under these conditions is not realistic. When an analogue of pterin pyrophosphate (pyrophosphate) is present, DHPS can readily bind pABA. This suggests that pterin pyrophosphate is normally bound first by DHPS, perhaps facilitating some sort of conformational change in the DHPS dimer which pyrophosphate is also able to generate, allowing pABA to be bound by DHPS.

In *E. coli* DHPS the pterin moiety is bound at the active site by four hydrophilic residues which contribute six hydrogen bonds - Asp96, Asn115, Asp185 and Lys221. Hydrophobic contributions are also made by Met139, Phe188 & 190, Gly217 and Ile117. [Achari, *et al.*(1997)] The pterin ring is recognised in a similar fashion by *S. aureus* DHPS. [Hampele, *et al.* (1997)] The hydrophilic residues involved in pterin binding are Asp84, Asn103, Asp167 and Lys203 and hydrophobic residues are Met128, Phe172 and Arg239. [Hampele, *et al.* (1997)] The strength of the molecular interactions for the pterin and pyrophosphate portions of the substrate indicate that each moiety can be bound as independent ligands.

The order of release of the products by DHPS is not as clear as its order of binding of substrates. Dihydropteroate is bound by DHPS with a similarly high affinity as pABA in the presence of pyrophosphate, but DHPS also appears capable of binding dihydropteroate in the absence of pyrophosphate, contrary to the behaviour with pABA. DHPS has an increased capacity for dihydropteroate in the presence of pyrophosphate. A compulsory order mechanism, in which dihydropteroate must be released first, appears unlikely because it has measurable affinity for the apoenzyme. If pyrophosphate is released first, the reduced affinity of DHPS for dihydropteroate might facilitate the loss of this second product in a compulsory order mechanism. DHPS may also release the two products in a random order mechanism.

Two other experimental observations suggest that the scheme in Figure 5.18 is not yet complete. Dihydropteroate occupies a third of the binding sites of DHPS compared to pABA. The possible explanation of limited-sites reactivity was discussed in Section 5.7 in connection with the *S. aureus* DHPS which has been shown to demonstrate similar behaviour with the oxidised form of pterin pyrophosphate and Mn^{2+}.

In the dimeric *S. aureus* DHPS protein, it was proposed that pterin pyrophosphate is bound by only one of the monomers. [Hampele, *et al.* (1997)] This binding may cause a conformational change in the protein structure to prevent the binding of another molecule at the other monomeric active site. This behaviour may be mimicked by dihydropteroate, perhaps because it contains the same pterin moiety as pterin pyrophosphate.

Both *S. aureus* and *E. coli* DHPS crystals have a single DHPS dimer in the asymetric unit which confirms that the enzyme forms a dimer in high concentrations. *E. coli* DHPS showed no evidence of half-of-sites reactivity or any differences between the two monomers in their ligand binding characteristics. There were no reported differences between the main-chain atomic structures of the two monomers from *E. coli* DHPS on the binding of pterin pyrophosphate. In *S. aureus* DHPS there is both kinetic and structural evidence for half-of sites reactivity. The two monomers are linked in a very similar manner to the *E. coli* DHPS, but there were some differences between the two monomeric structures when an analogue of pterin pyrophosphate was bound. In monomer A the two C-terminal amino acids (residues Phe266 and Ser267) are disordered compared with monomer B. In monomer B electron density, corresponding to two flexible loop regions connecting $\beta1\alpha1$(Asp15-Asn24) and $\beta2\alpha2$ (Arg52-Glu56), is poorly defined compared with monomer A. The pterin pyrophosphate analogue had bound to monomer A. This suggests that there may be a conformational change in the other monomer on the binding of pterin pyrophosphate, or differences in the crystal packing between two non-identical monomers. It is possible that *S. pneumoniae* DHPS operates in a different manner to DHPS from *E. coli* and more akin to *S. aureus* DHPS in demonstrating half-of-site reactivity.

The model proposed in Figure 5.18 does not satisfactorily account for the results of the kinetic experiments. When an attempt was made to fit the kinetic data obtained to a compulsory order of binding, the predicted velocities did not agree well with the experimental data. It is clear from an examination of the data that the apparent Michaelis' constant of one substrate is unaltered by changing the concentration of the second substrate, a phenomenon which is not predicted by a fixed order of binding.

Fitting the data to a kinetic model of random order binding gave a better correlation between the predicted and experimental velocities. However a random order of binding of substrates has been shown to be unlikely as the DHPS apoprotein cannot bind pABA. It is interesting in this respect that the kinetic results from the mitochondrial DHPS from peas also show a good fit to the random model. [Rebeille, *et al.* (1997)]

Interestingly the pea enzyme demonstrated strong product inhibition by dihydropteroate with a low inhibitor constant, (K_i) value determined with respect to both substrates. The *S. aureus* DHPS however, demonstrated substrate inhibition on addition of increasing concentrations of pABA. The situation appears to be more complex with the *S. pneumoniae* DHPS. Whilst it is clear that the enzyme can bind dihydropteroate with approximately the same affinity as pABA, there is no evidence of inhibition of the DHPS reaction by the products - as demonstrated by the linearity of the assays with time, up to a point where over half of the pABA present at the beginning of the reaction has been converted into dihydropteroate. [See Chapter 2]

A reasonable explanation for the discrepancy between the equilibrium binding data and the kinetics may involve the monomer-dimer equilibrium which was demonstrated in Chapter 3. This showed that as the concentration of DHPS decreased *in vitro*, the proportion of protein in a dimeric form decreased with a subsequent increase in a lower molecular weight protein, presumed to be the monomer. The relatively high concentrations of protein used in the crystallography and equilibrium binding experiments would involve DHPS predominantly in the dimeric form. The kinetic experiments, however, were performed using nanogram quantities of protein and would therefore involve DHPS predominantly in the monomeric form. Steady state kinetics has been the sole method used to analyse the DHPS reaction mechanism by other investigators. If the monomer-dimer phenomenon observed with *S. pneumoniae* DHPS was not restricted to this species but also occurred in *S. aureus* and *P. sativum*, the predictions made for random order mechanisms would agree with the results of this work. Unfortunately the precise quantities of enzyme used in the assays for *S. aureus* and *P.sativum* DHPS activities were not given.

However the velocities are given in picomoles of dihydropteroate produced, in a similar manner to the assay described in Chapter 2, for a similar specific activity of enzyme. If the monomer-dimer equilibrium did exist for these two species of DHPS, it is likely that the kinetics on these other proteins was also carried out on ng quantities of enzyme, which may be a monomeric form of the enzyme. If this hypothesis is correct, the scheme in Figure 5.18 only applies to the dimeric form and the monomer would exhibit a random order of substrate addition.

An investigation into the effect of pH on the *S. pneumoniae* DHPS reaction revealed the presence of a titratable, ionisable group or groups with pK_a value(s) between 4.5-5.5. There is a single conserved histidine residue in the *S. pneumoniae* DHPS sequence when compared with other DHPS sequences. [See Chapter 1] His284 in *S. pneumoniae* corresponds with His257 in *E. coli* and His241 in *S. aureus* which have been shown to interact with the β-phosphate group of pterin pyrophosphate. In the *E. coli* DHPS crystal structure, the His257 side-chain is also within Van der Waals contact distance of the aniline NH_2 group of the sulphanilamide and presumably the aniline NH_2 group of pABA, if it bound in the same way. For the reaction between the amine nitrogen and the methylene carbon to occur in *E. coli* DHPS, a small rearrangement is required at the active site to bring these two atoms closer together. Any movement of this nature would appear from the electron density maps to also bring the histidine residue closer to the aniline amine group.

To summarise, a fixed order mechanism for the addition of substrates and release of products is predicted from the equilibrium binding data performed on the dimeric form of *S. pneumoniae* DHPS. From the kinetic analysis performed on the monomeric form of the enzyme, a random order mechanism for the addition of the substrates is more likely. Previous work performed on DHPS from different species has consistently indicated a random order of addition of substrates, possibly also performed on a monomeric form of the enzyme. It is not clear whether DHPS exists as a monomer or a dimer *in vivo*, so either mechanism must be considered until further data can be acquired.

It is clear, however, that the *S. pneumoniae* DHPS is regulated in a different manner to other DHPS molecules because no evidence was found for substrate or product inhibition, unlike *S. aureus* or *P. sativum* DHPS. The monomer-dimer equilibrium may be a phenomenon which occurs solely in *S. pneumoniae* DHPS, and could be a means of regulation of DHPS activity ***in vivo***.

Chapter 6: Investigation into the Inhibition of DHPS by sulphonamides and other inhibitors.

6.1. Introduction.

In the late 1930s prevention of bacterial growth by sulphanilamide was known. By 1940, it had been discovered that pABA had `high anti-sulphanilamide activity` in *Streptococcus haemolyticus*. [Woods, (1940), Fildes, (1940)] On this basis a suggestion was made that sulphanilamide was a competitive inhibitor with respect to pABA because of its similarity in chemical structure. In 1962 Brown concluded that sulphonamides inhibit the synthesis of `folic acid compounds` by inhibiting the reaction between a compound believed to be hydroxymethyldihydropteridine and pABA in the presence of Mg^{++} and ATP to produce dihydropteroate. At this time the folate pathway had not been fully elucidated and it took several more years to discover the presence of DHPS. Bacterial cell-free extracts were used as the source of enzyme activity from *E.coli* B. Brown postulated that inhibition involved `competition of pABA and sulphonamide for the active region of the enzyme`. [Brown, (1962)] In kinetic studies, sulphonamides tested against *E. coli* DHPS were shown to be competitive inhibitors with respect to pABA or p-aminobenzoylglutamic acid. Three K_i values were presented for sulphathiazole (0.035μM), sulphamethoxazole (0.13μM) and sulphanilamide (5.7μM). [Roland, *et al.* (1979)] Measurements were made at only two inhibitor concentrations, indicating that these values may be inaccurate. Work has been performed more recently on the inhibition of *Pneumocystis carinii* DHPS by the sulphonamides but no claims have been made concerning the mode of inhibition. [Hong, *et al.* (1995, 1996)] Chio, *et al.* (1996) suggested that K_i values obtained for *Toxoplasma gondii, P. carinii* and *Mycobacterium avium* showed competitive inhibition of DHPS, but the velocity measurements were not given and only two concentrations of pABA and three concentrations of inhibitor were used in the study. There have not been any comprehensive sulphonamide inhibition studies performed on purified DHPS from *S. pneumoniae* or any other species reported in the mainstream literature.

From the evidence presented above it appears that the basis for the competitive model rests predominantly on the structural similarity between pABA and the sulphonamide class of drugs and that definitive evidence for this hypothesis is somewhat limited. There is very little information about the inhibition of the enzyme generally, despite the knowledge and widespread usage of sulphonamide drugs. (A consideration of the possible modes of inhibition adopted by the sulphonamides is given in Chapter 1.) Although a simple competitive model is easy to envisage it is by no means the only option or the sole possible mode of inhibition used. Using a combination of equilibrium binding experiments and kinetic experiments, a thorough investigation into the effect of the sulphonamides and certain other compounds on the activity of DHPS was undertaken. These are the first reported equilibrium binding studies of DHPS with sulphonamides. It is clear from the work presented in Chapter 5, that if sulphonamides do compete with pABA for its binding site on DHPS, their true target may not be the DHPS apoenzyme but the DHPS/pterin pyrophosphate/magnesium complex. The ultimate goal of this work is to understand the DHPS mechanism and structure sufficiently well to begin to rationally design new and more effective drugs. A more precise definition of the true target of the drugs is an important beginning.

6.2 Hummel and Dreyer Experiments

In a similar manner to chapter 5 these experiments provided a simple way to determine conditions for sulphonamide-binding by DHPS and to see whether the conditions are similar to those required for pABA-binding.

Sulphamethoxazole (SMX) is still used therapeutically and was chosen as a typical example of this class of drugs. Figure 6.1 shows the size of the experimental and control troughs were very similar when SMX was present on the column. Therefore DHPS cannot bind SMX when magnesium is present in the buffer at the concentrations used.

The size of the experimental trough was significantly larger than the control trough when sodium pyrophoshate was present together with SMX on the column. [Figure 6.2] In a similar manner to pABA, DHPS can bind SMX in the presence of pyrophosphate and magnesium. These results are consistent with those described in Chapter 5 for the binding of pABA by DHPS, with the enzyme unable to bind pABA or SMX without both pyrophosphate and magnesium being present.

6.3 Equilibrium binding experiments - Displacement of equilibrium binding of pABA by sulphonamides.

These experiments were performed to confirm the results of the Hummel and Dreyer experiments and to quantify the results by measuring equilibrium binding constants to DHPS of a range of sulphonamides, including SMX. The equilibrium binding constants were calculated indirectly by measuring their effect on the binding of a fixed concentration of [^{14}C]-pABA by a fixed concentration of DHPS. The experiments are valuable because they determine the relative affinity of DHPS for a variety of different sulphonamide ligands. If the sulphonamides are shown to be capable of displacing pABA from DHPS, this is evidence that these drugs can compete with pABA for its binding site on DHPS by a simple, competitive mode of inhibition. Five sulphonamides were chosen - sulphaquinoxaline (SQ), sulphamethoxazole (SMX), sulphanilamide (SA), sulphaphenazole (SP) and sulphanilic acid (SAA). SQ is used in veterinary medicine, SMX in widely used for treating human infections and SA was a drug commonly used before the development of extensive resistance to sulphonamides.

Figure 6.1: Absorption elution profile of DHPS in the presence of 10μM SMX.
(Experiments were conducted as described in Chapter 2.)

The equilibration buffer contained 50mM Tris/HCl, pH 8.0, 5mM magnesium chloride and 10μM SMX. The experiment involved the application and elution of a 1ml solution containing 3.4mg DHPS in equilibration buffer minus SMX. The control involved the application and elution of a 1ml solution of equilibration buffer minus SMX. The elution profile was measured at a chart speed of 5mm/min and a flow rate of 5ml/min.

Figure 6.1: Absorption elution profile of DHPS in the presence of 10μM SMX.

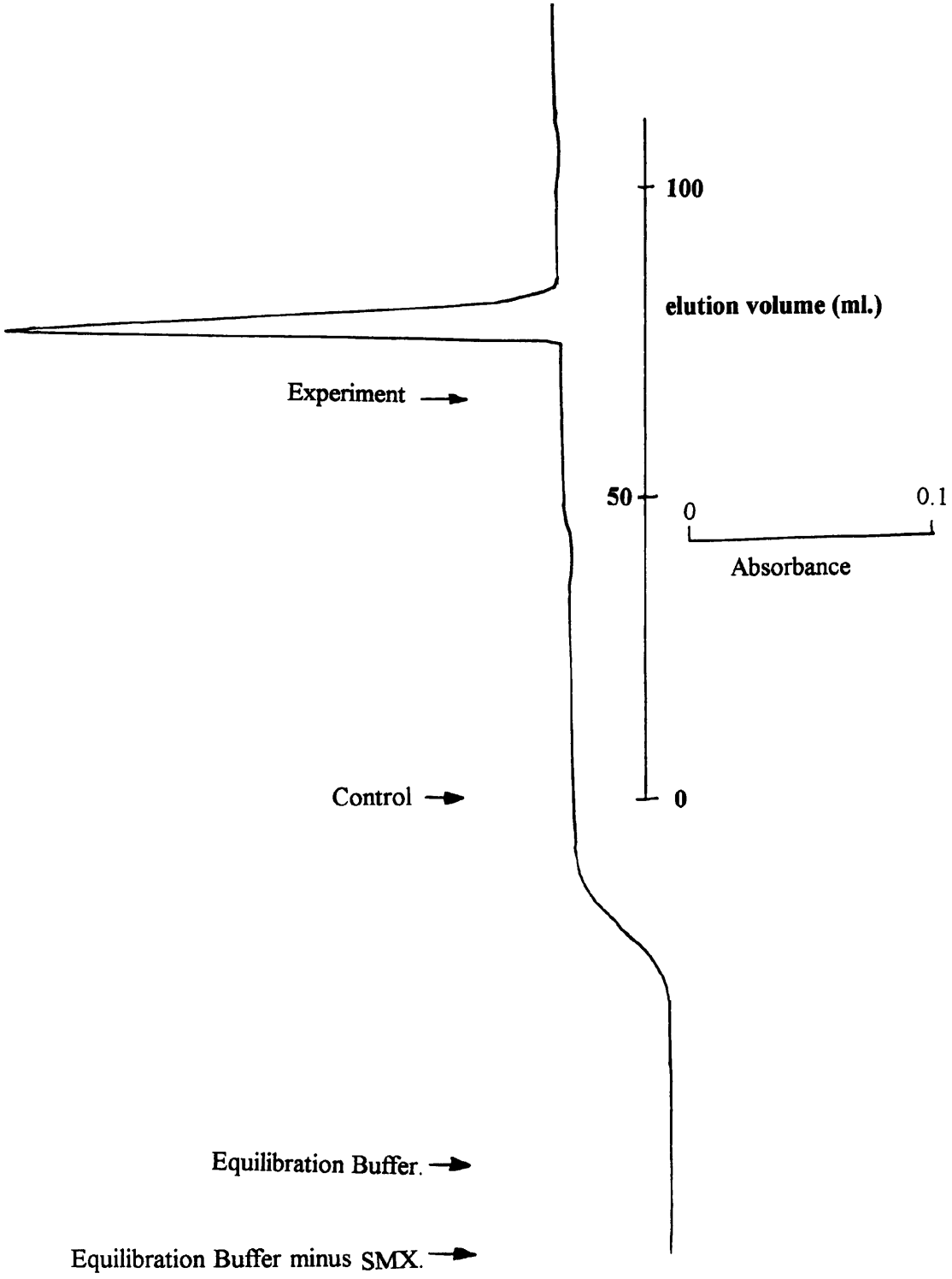

Figure 6.2: Absorption elution profile of DHPS in the presence of 10μM SMX and sodium pyrophosphate.

The equilibration buffer contained 50mM Tris/HCl, pH 8.0, 5mM magnesium chloride, 10μM SMX and 100μM sodium pyrophosphate. The experiment involved the application and elution of a 1ml solution containing 3.4mg DHPS in equilibration buffer minus SMX and pyrophosphate. The control involved the application and elution of a 1ml solution of equilibration buffer minus SMX and pyrophosphate. The elution profile was measured at a chart speed of 2mm/min and a flow rate of 5ml/min

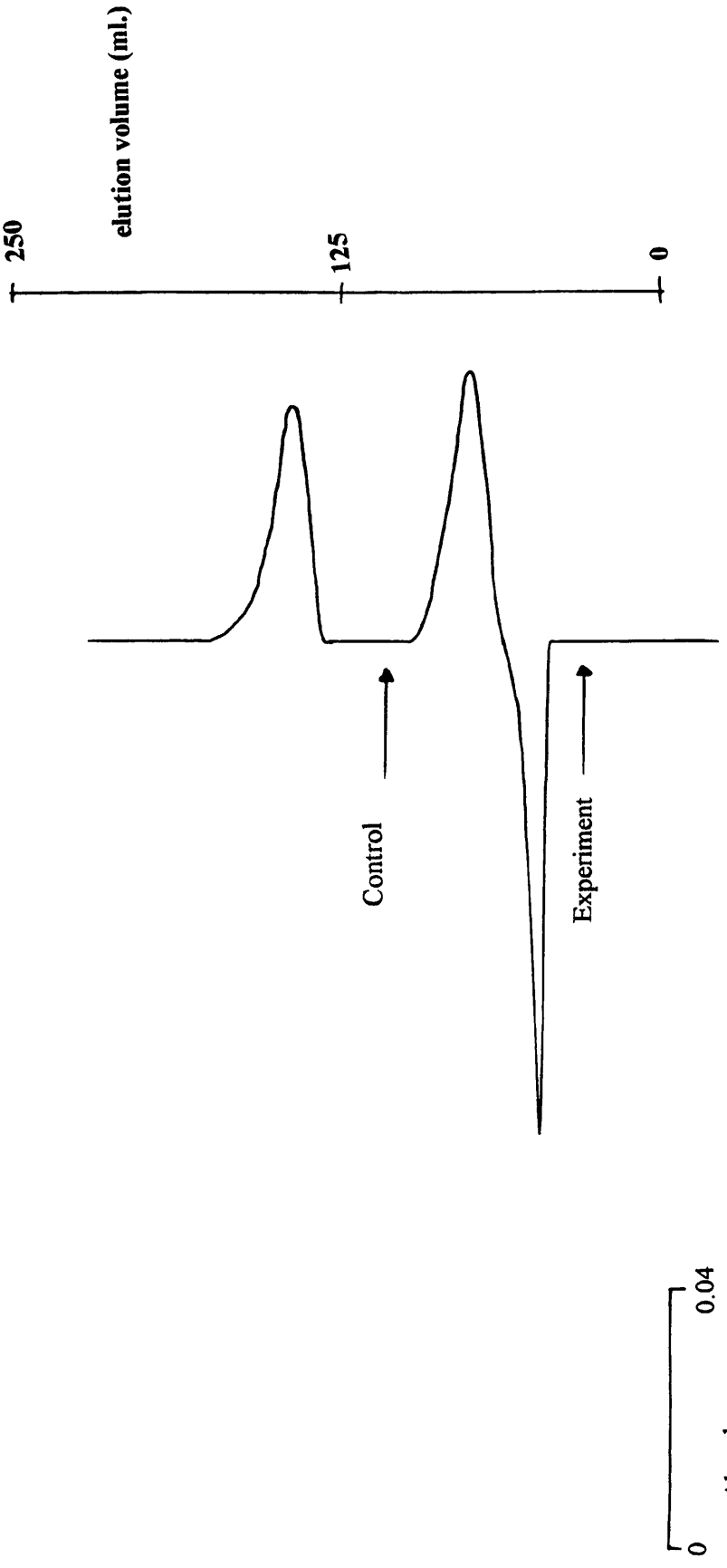

Figure 6.2: Absorption elution profile of DHPS in the presence of 10μM SMX and sodium pyrophosphate.

SP was chosen because it has a particularly bulky, hydrophobic R-group and SAA because it is the simplest in structure of all the sulphonamides. A comparison of inhibition shown by these five very different drugs may help to elucidate what governs the effectiveness of a drug and its recognition and binding at the active site of *S. pneumoniae* DHPS.

6.3.1 Determination of the equilibrium binding constants of the sulphonamides.

Figure 6.3 shows the effect of increasing concentrations of SQ on the amount of pABA bound by DHPS. Data were fitted to a simple competitive model shown below.
(E represent DHPS, PPi represents pyrophosphate)

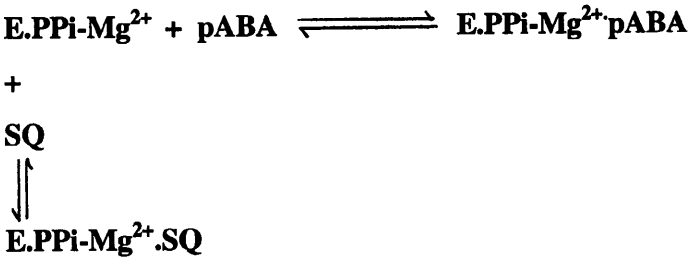

The results agree with a simple competitive model within experimental error and the corresponding equilibrium binding constant for SQ is predicted to be 630nM. It is interesting to note that SQ can effectively displace all pABA from its binding site(s) on DHPS.

The effect of an increasing concentration of SMX on the binding of pABA by DHPS is shown in Figure 6.4. This data also fitted well to a simple competitive model and the predicted equilibrium binding constant for SMX is 9.5μM. These two experiments represent a rigorous test of the competitive model because they cover a wide range of pABA and sulphonamide concentrations. The other three sulphonamides probably behave in the same manner and so less extensive experiments were performed to determine the values for their equilibrium binding constants.Data for the displacement of pABA by SA, SP and SAA are given in Figures 6.5-6.7. The K_d values cover two orders of magnitude from SA (38.9μM) to SP (490nM).

Figure 6.3: Determination of the binding constant for SQ.

The binding experiments were performed as described in Chapter 2. The 100µl. reaction contained:

500, 750, 1000, 1500 and 2000nM [^{14}C]-pABA
0, 2.5, 7.5, 20 and 100µM SQ
300µM sodium pyrophosphate (stock made immediately before use in 100mM Citrate/HCl, pH 6.0)
50mM Tris/HCl, pH 8.0
5mM DTT
5mM magnesium chloride and
6µM DHPS immobilised on Sepharose beads

The reaction volume was made up to 100µl with distilled water.

The results were fitted to a model using the software package 'Excel' and assuming simple, competitive inhibition. [For an explanation of the procedure and the derivation of the equation used see Section 9.4] Results were the mean of experiments performed in triplicate. The final values for the fitted parameters were:

$K_{d(SQ)}$ = 630nM, Capacity = 1580nM and $K_{d(pABA)}$ = 1050nM.

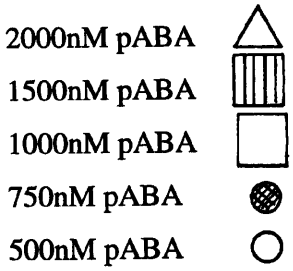

Figure 6.3: Determination of the binding constant for SQ.

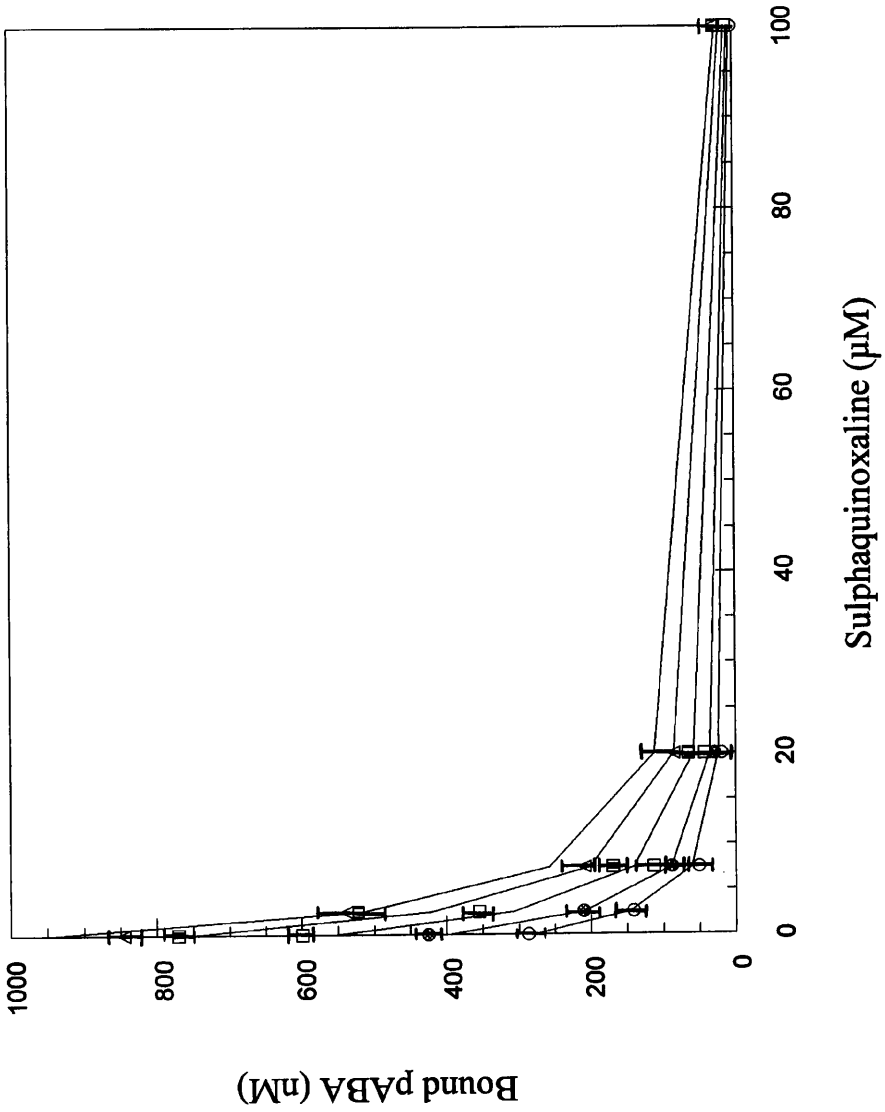

Figure 6.4: Determination of the binding constant for SMX.

The binding experiments were performed as described in Chapter 2. The 100µl. reaction contained: 600, 900, 1200, 1800 and 2400nM [^{14}C]-pABA
0, 5, 20, 50 and 150µM SMX
300µM sodium pyrophosphate (stock made immediately before use in 100mM Citrate/HCl, pH 6.0)
50mM Tris/HCl, pH 8.0
5mM DTT
5mM magnesium chloride and
6µM DHPS immobilised on sepharose beads

The reaction volume was made up to 100µl with distilled water.
The results were fitted to a mathematical model using the software package 'Excel' and assuming simple competitive inhibition. [For an explanation of the procedure and the derivation of the equation used, see Section 9.4.] Results were the mean of experiments performed in triplicate. The final values for the fitted parameters were: K_d(SMX) = 9.5µM, Capacity = 1500nM and $K_{d(pABA)}$ = 750nM.

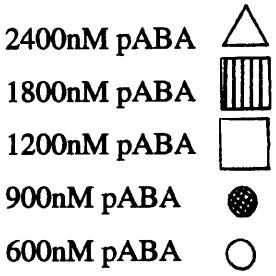

Figure 6.4: Determination of the binding constant for SMX.

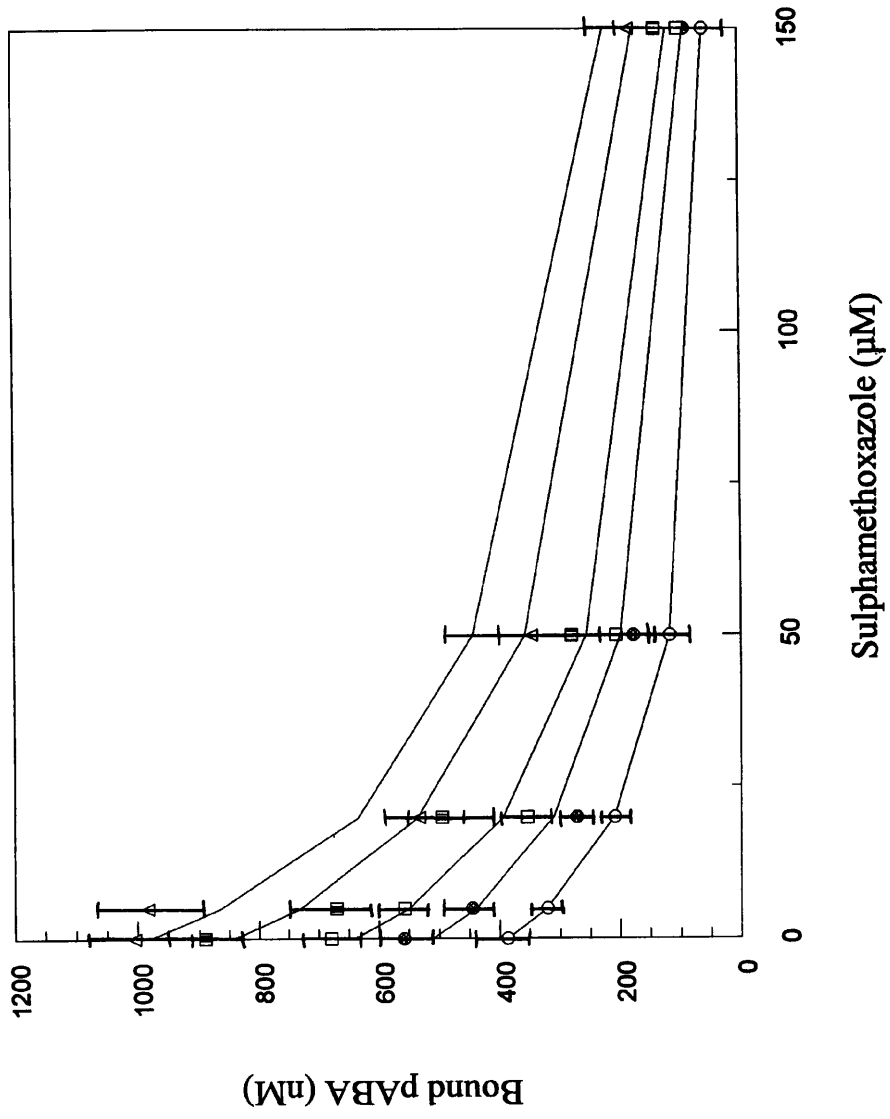

Figure 6.5: Determination of the binding constant for SA.

The binding experiment was performed as described in Chapter 2. A 100µl. reaction contained: 500nM [^{14}C]-pABA

0-200µM SA

300µM sodium pyrophosphate (stock made immediately before use in 100mM Citrate/HCl, pH 6.0)

50mM Tris/HCl, pH 8.0

5mM DTT

5mM magnesium chloride and

6µM DHPS immobilised on sepharose beads

The reaction volume was made up to 100µl using distilled water.

The results were fitted to a mathematical model assuming simple competitive inhibition. For the derivation of the equation used, see Section 9.3. Results were the mean of experiments performed in triplicate. The final values for the fitted parameters were: $K_{d(SA)}$ = 38.9µM and the binding capacity = 1µM.

Figure 6.5: Determination of the binding constant for SA.

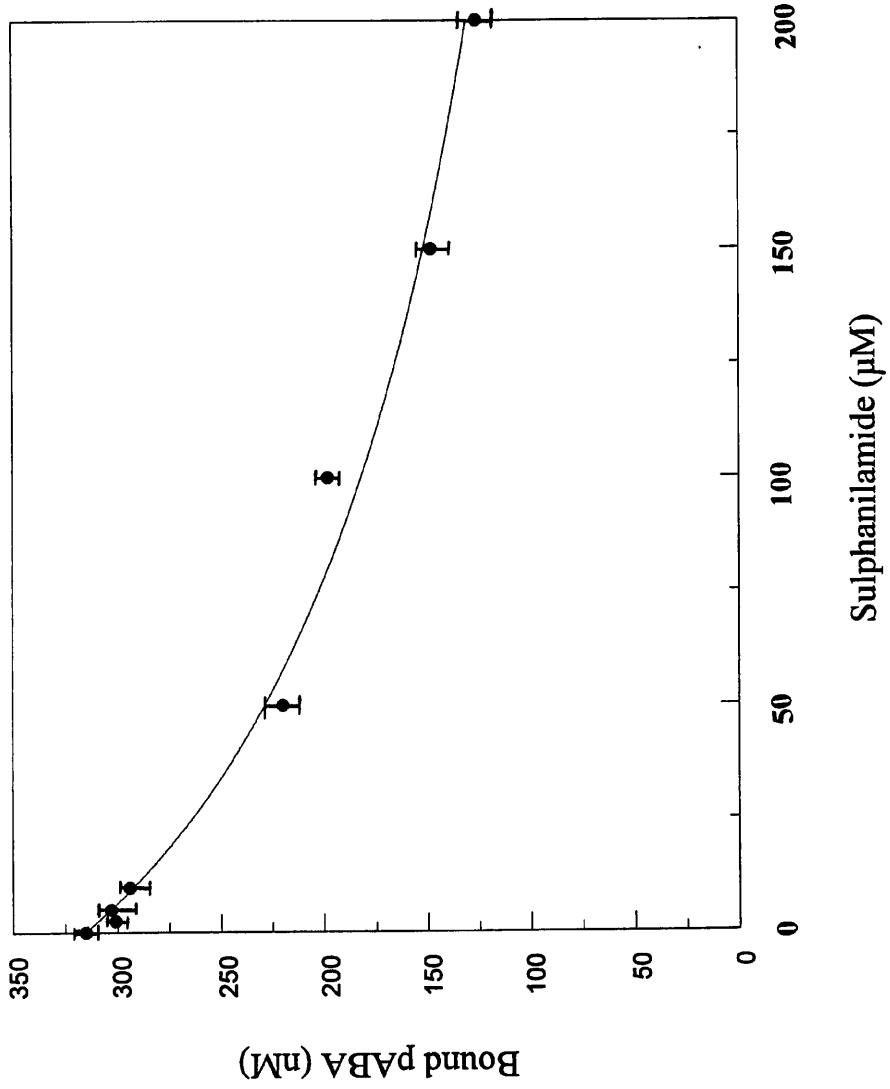

Figure 6.6: Determination of the binding constant for SP.

The binding experiments were performed as described in Chapter 2. The 100µl. reaction contained: 500nM [^{14}C]-pABA

0-200µM SP

300µM sodium pyrophosphate - an excess (stock made immediately before used in 100mM Citrate/HCl, pH 6.0)

50mM Tris/HCl, pH 8.0

5mM DTT

5mM magnesium chloride and

6µM DHPS immobilised on sepharose beads

The reaction volume was made up to 100µl with distilled water.

The results were fitted to a mathematical model using the software package 'Excel' and assuming simple competitive inhibition. [For an explanation of the procedure and the derivation of the equation used, see Section 9.4.] Results were the mean of experiments performed in triplicate. The final values for the fitted parameters were: $K_{d(SP)}$ = 490nM, Capacity = 1500nM and the $K_{d(pABA)}$ = 450nM.

Figure 6.6: Determination of the binding constant for SP.

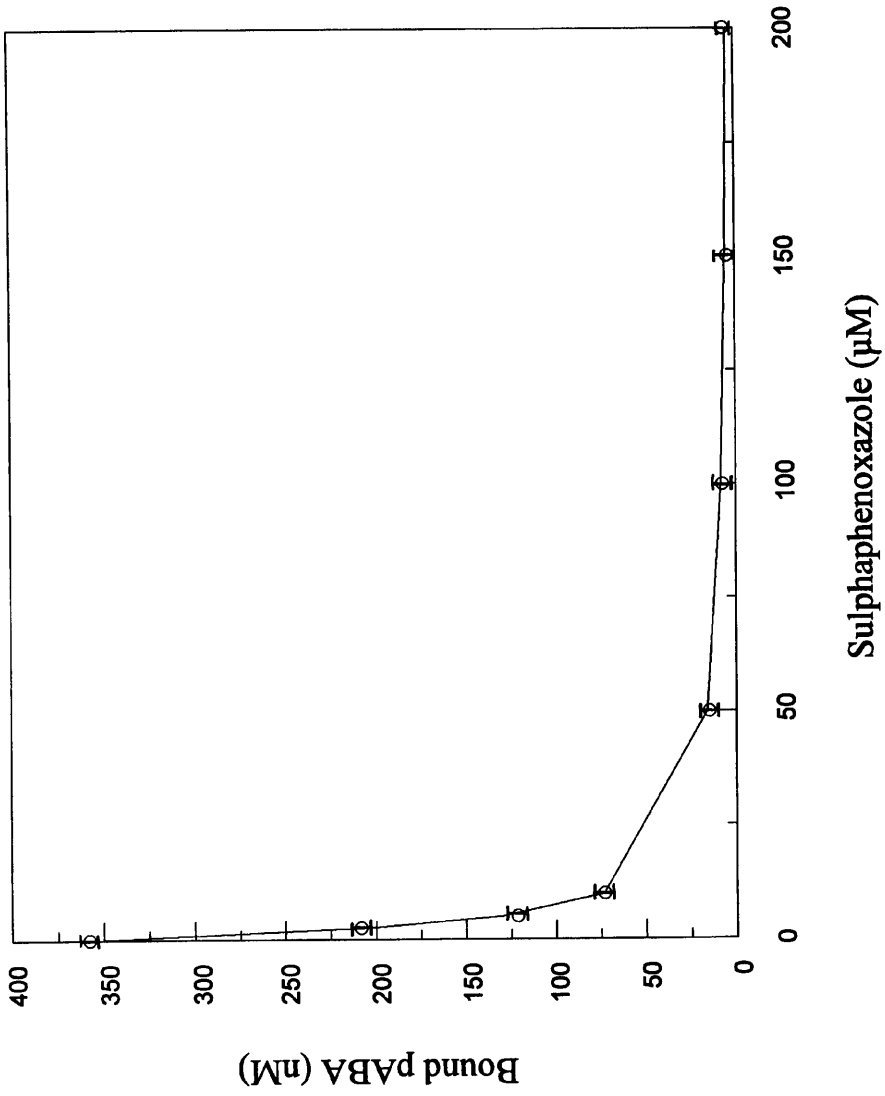

Figure 6.7: Determination of the binding constant for SAA.

The binding experiment was performed as described in Chapter 2. A 100µl. reaction contained: 500nM [^{14}C]-pABA

0-200µM SAA

300µM sodium pyrophosphate (stock made immediately before use in 100mM Citrate/HCl, pH 6.0)

50mM Tris/HCl, pH 8.0

5mM DTT

5mM magnesium chloride and

6µM DHPS immobilised on sepharose beads

The reaction volume was made up to 100µl using distilled water.

The results were fitted to a mathematical model assuming simple competitive inhibition. For the derivation of the equation used, see Section 9.3. Results were the mean of experiments performed in triplicate. The final values for the fitted parameters were: $K_{d(SAA)}$ = 10.6µM and the binding capacity = 1.15µM.

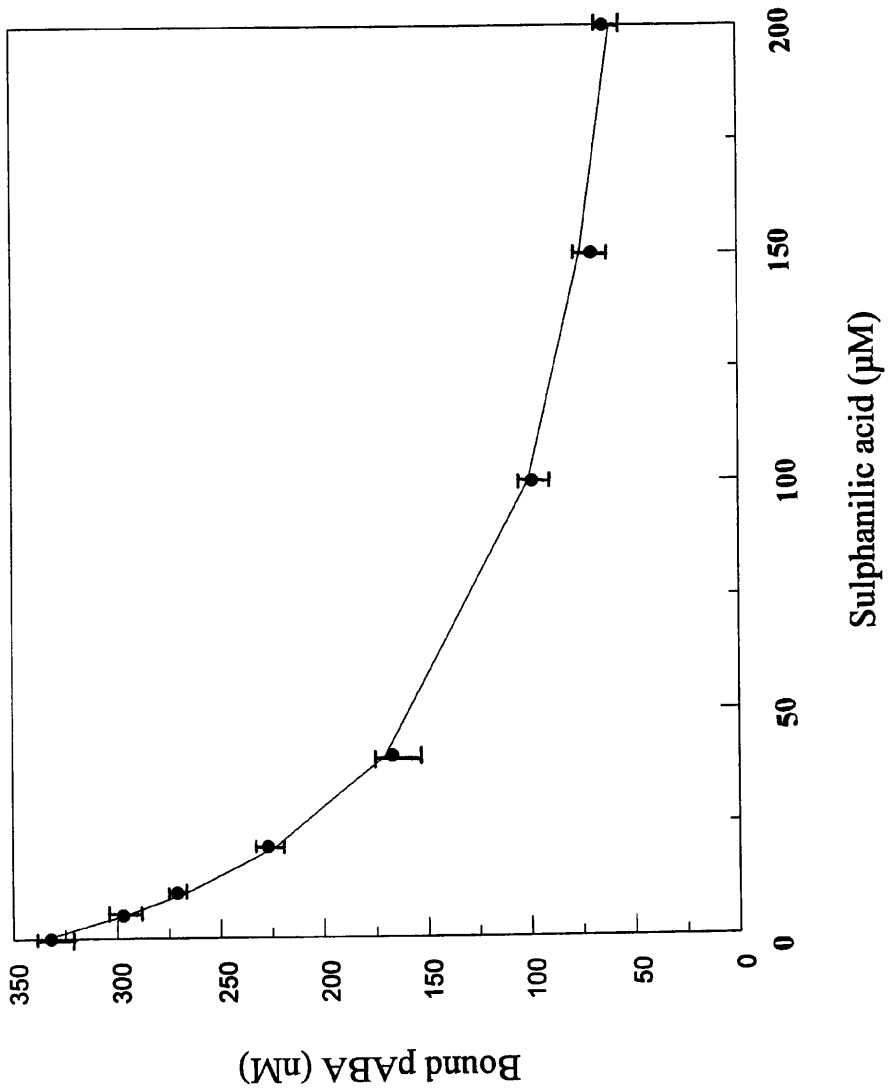

Figure 6.7: Determination of the binding constant for SAA.

6.4 Summary of results of the equilibrium binding experiments.

Sulphonamide	K_d (nM)	Capacity (nM)	$K_{d\ (pABA)}$(nM)
SA	**38900**	1000	-
SAA	**10600**	1150	-
SMX	**9500**	1500	750
SQ	**630**	1580	1050
SP	**490**	1500	450

The results summarised in the table above demonstrate that although all five sulphonamides displace pABA from its binding site on DHPS, they do so by two orders of magnitude difference in equilibrium binding constants. The structural similarity of SAA to pABA is very high but the simplest and smallest sulphonamides were actually amongst the least effective at displacing pABA bound by DHPS. The sulphonamides with very large hydrophobic substituents, SQ and SP, had the greatest capacity to displace bound pABA from DHPS. This is important information because simple, competitive inhibition by the sulphonamides must be occurring alongside another effect governed by the nature of the R-group. This will be considered in more detail later. The K_d values of SA, SMX and SAA are high compared with the K_d of pABA at 830nM, measured under the same conditions. The K_d values of SQ and SP, however, are lower than the K_d for pABA and this explains why relatively low concentrations of these drugs were required to displace virtually all the pABA from DHPS. [Determination of K_ds of SMX, SQ and SP were performed using 5 concentrations of pABA whereas $K_d$sof SA and SAA were determined using a single concentration of pABA and so confidence limits are different.]

6.5 Analysis of the inhibition of DHPS by steady state kinetics.

Kinetic measurements were used to test the inhibition of the DHPS reaction by a range of compounds. Three sulphonamides - sulphaquinoxaline SQ, sulphamethoxazole SMX and sulphanilamide SA were examined together with benzoic acid and aniline. Modified pABA compounds including benzoic acid have been tested as potential inhibitors of cell growth by Woods ,(1940). He found that both carboxylic acid and amino groups in *para*-positions to one another appear to be necessary to antagonise the action of sulphonamides.

0.12-0.58μM pABA was necessary to counter the inhibitory effect of 303μM sulphanilamide and allow cell growth. Acetylation of the NH_2- group of pABA led to a 10 000-fold decrease in antisulphanilamide activity compared with pABA (180μM of acetaminobenzoic acid was required to counter the inhibitory effect of 303μM sulphanilamide). Esterification of the carboxylic group led to a 1000-fold decrease in antisulphanilamide activity (36μM Novocaine was required to counter 303μM sulphanilamide). The effect of aniline was not measured.

An estimation of the K_is for several different sulphonamides may reveal more information about the strength of the stabilising bonds from DHPS for the pABA molecule at the active site.

Although there was no intention at the outset of this work to study the regulation of DHPS in detail within the folate pathway, K_is for a number of folate compounds were measured. If their K_i values were similar or below their concentrations *in vivo*, they could be regulators of the DHPS reaction. These compounds bear a more limited structural resemblance to pABA than the sulphonamides, benzoic acid and aniline; however these folate compounds have hydrophobic and hydrophilic moieties so may be capable of occupying the pABA-binding site. The pterin ring is still present, so these compounds could compete for the pterin pyrophosphate-binding site on DHPS or even bind at an allosteric site away from the active site.

Drug therapy often involves the use of two drugs in combination which act on different enzymes of the same pathway. Two drugs working synergistically can have a greater effect, e.g. Co-trimoxazole is five parts SMX in combination with one part Trimethoprim and this is the agent of choice in treating *Pneumocystis carinii* pneumonia. [Hong, *et al.* (1995)] K_i values for three inhibitors of the DHFR reaction - MTX, PMM and TMP were measured. They inhibit DHFR by mimicking the structure of DHF, so if DHF is capable of inhibiting the DHPS reaction to any extent, these DHFR inhibitors may also have an effect on the DHPS reaction.

6.5.1 Determination of inhibitor constants for the sulphonamides SQ, SMX and SA.

The initial velocity data collected for SQ and SMX inhibition of the DHPS reaction are presented in Figures 6.8 and 6.9, fitted to a simple, competitive inhibition model. The predicted K_i for SQ is 25nM and the K_i for SMX is 590nM. Both sets of data fit well to the predicted velocities suggesting that the assumptions made in the derivation of the simple competitive model were correct. The result obtained for the K_i for SMX must be treated with caution because the data were not obtained over a sufficiently large range of concentrations of SMX. As with the equilibrium binding experiments, these two results represent a more rigorous test of the competitive model and the other sulphonamides can be assumed to behave in a similar manner. For this reason, a single set of data at fixed pABA and pterinpyrophosphate concentrations was collected for SA, and a maximum K_i of 850nM is predicted for SA. [Figure 6.10]

6.5.2. Determination of the inhibitor constants of benzoic acid and aniline.

Table 6.1 shows the initial velocity measurements collected for the inhibition of the DHPS reaction by benzoic acid with respect to pABA-binding. The results show little inhibition of the reaction by benzoic acid, even at very low concentrations of pABA, suggesting that the K_i for benzoic acid is greater than 1mM.

The inhibition of the DHPS reaction by aniline, Table 6.2, also shows that no inhibition is observed until concentrations above 1mM are present. However the decrease in reaction velocity may not be due to aniline acting as a non-specific inhibitor at these concentrations. Aniline is a base and an organic solvent and may be altering the pH significantly or even denaturing the protein in some way. The experiment provided the necessary information - that aniline was not a potent inhibitor of the DHPS reaction and its K_i is greater than 1mM.

6.5.3 Determination of the inhibitor constants of folate, DHF and THF.

The folate compounds might be expected to competitively inhibit the DHPS reaction with respect to pterin pyrophosphate as the pterin ring is present in all three compounds, but in a different oxidation state in the case of folate and tetrahydrofolate. The inhibition of the DHPS reaction by folate, with respect to pterin pyrophosphate, is presented graphically in Figure 6.11.

227

Figure 6.8: Determination of the K_i for SQ.

Initial reaction velocities were measured at five concentrations 100, 200, 400, 1000 and 4000nM of [^{3}H]-pABA and five concentrations 0, 100, 200, 300 and 400nM of SQ. Excess pterin pyrophosphate and magnesium were present in the buffer listed below. The diethyl ether extraction method was used. Each point is a mean value of duplicate experiments. The data were fitted to a competitive inhibition model. For the equation used see Section 9.2, using the non-linear least squares method described in Chapter 2. The final values for the fitted parameters were: $appK_{i(SQ)}$ = 25nM and $appV_{max}$ = 4.1pmoles dihydropteroate/30minutes/3ng DHPS.

Each 50µl reaction contained:

pABA and SQ in one combination of the concentrations given above

40µM pterin pyrophosphate

50mM Tris/HCl, pH 8.0

5mM DTT

5mM magnesium chloride and

3ng DHPS

The reaction volume was made up to 50µl using distilled water.

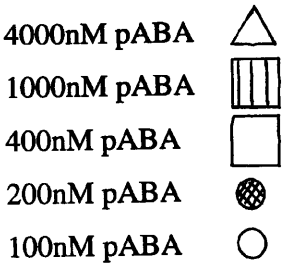

Figure 6.8: Determination of the Ki for SQ.

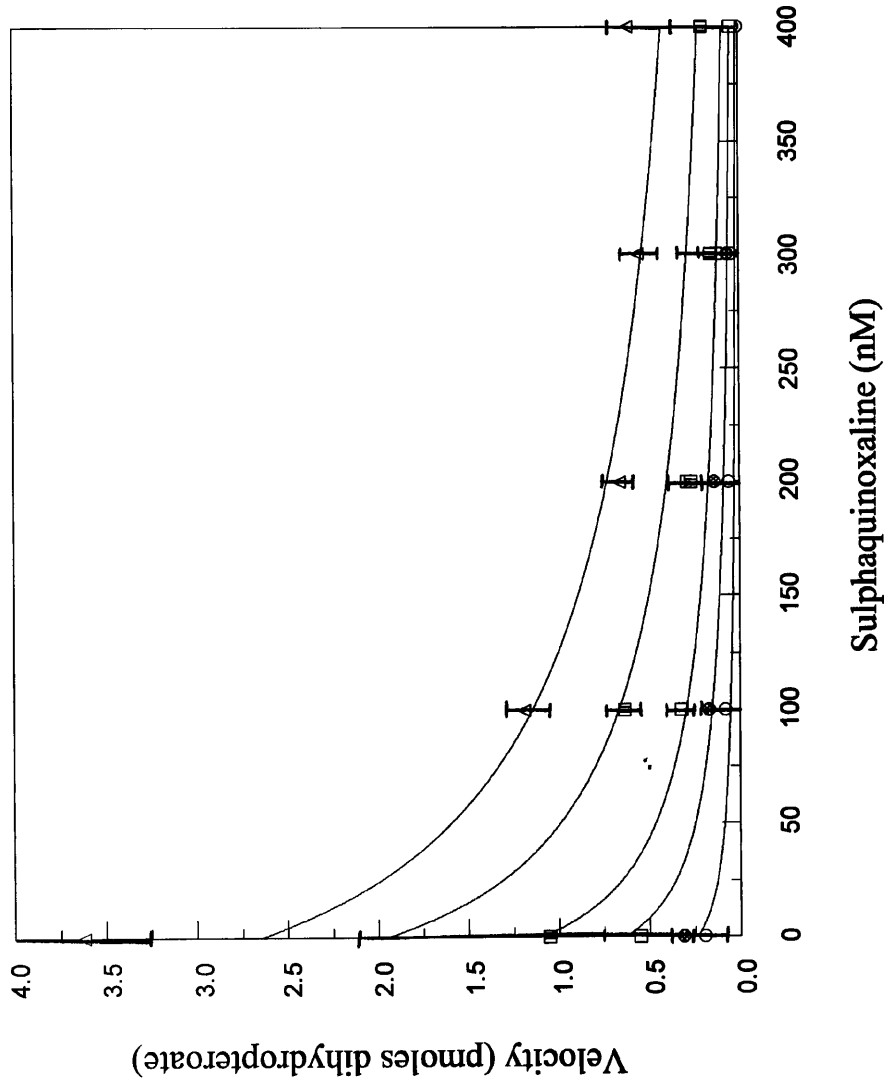

Figure 6.9: Determination of the K_i for SMX.

Initial reaction velocities were measured at five concentrations 33.34, 100, 200, 500 and 1000nM of [^{14}C]-pABA and five concentrations 0, 100, 200, 300 and 400nM of SMX. Excess pterin pyrophosphate and magnesium were present in the buffer at the concentration given below. The reverse-phase column separation method was used. Each point is the mean value of duplicate experiments. The data was fitted to a competitive inhibition model [For the equation used see Chapter 9.] using the non-linear least squares method described in Chapter 2. The final values for the fitted parameters were: app$K_{i(SMX)}$ = 590nM and appV_{max} = 70pmoles dihydropteroate/30minutes/3.12ng DHPS.

Each 1ml reaction contained:

pABA and SMX in one combination of the above concentrations

5µM pterin pyrophosphate

50mM Tris/HCl, pH 8.0

5mM DTT

5mM magnesium chloride and

3.12ng DHPS

The reaction volume was made up to 1ml using distilled water.

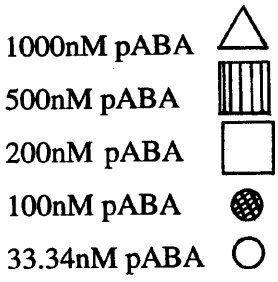

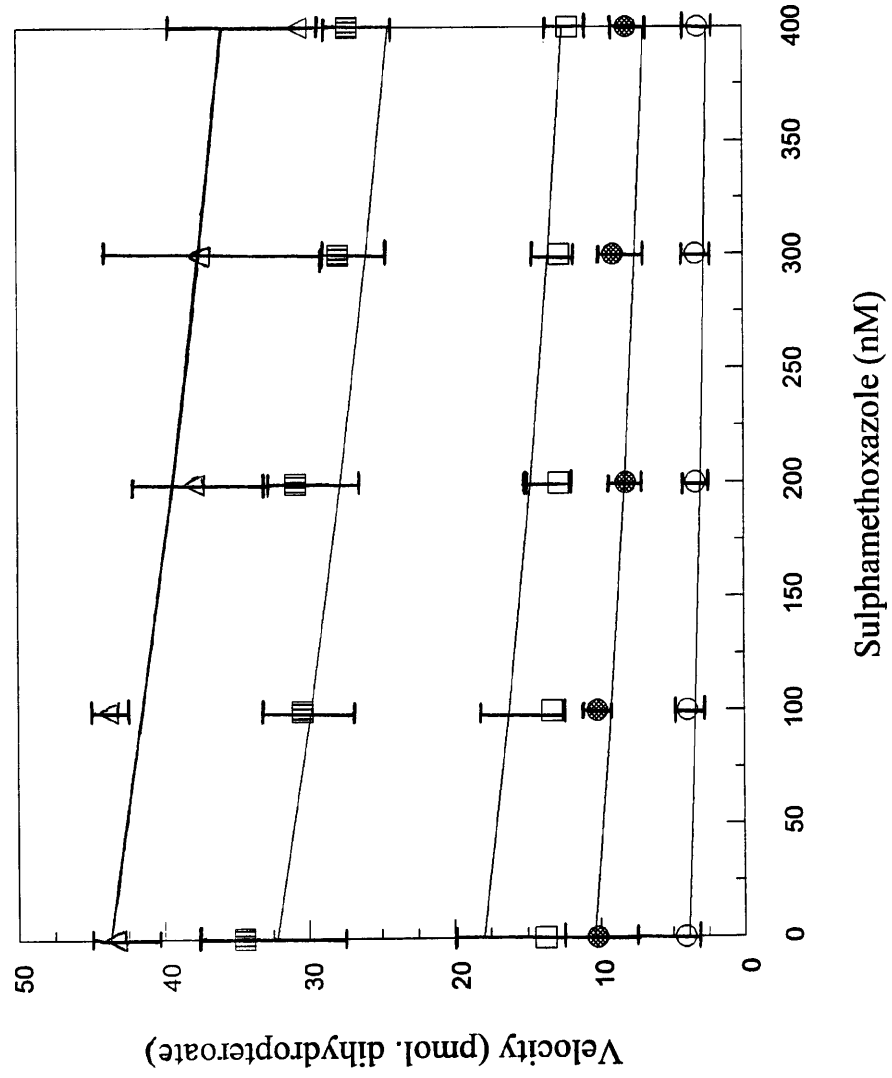

Figure 6.9: Determination of the Ki for SMX.

231

Figure 6.10: Determination of the K_i for SA.

Initial velocity measurements were made over a range of concentrations, 0-20μM of SA and a fixed concentration of 10nM [^{3}H]-pABA and 490nM pABA. Excess pterin pyrophosphate and magnesium was present in the buffer described below. The diethyl ether extraction method was used. Each point is the mean of triplicate experiments. The data was fitted to a competitive inhibition model as described for SMX. The final values for the fitted parameters were: app$K_{i(SA)}$ = 850nM and appV_{max} = 7.9pmoles dihydropteroate/30minutes/10ng DHPS.

The 50μl. reactions contained:

pABA and SA in one combination of the concentrations given above

17.5μM pterin pyrophosphate

50mM Tris/HCl, pH 8.0

5mM DTT

5mM magnesium chloride and finally

10ng DHPS

The reaction volume was made up to 50μl using distilled water.

Figure 6.10: Determination of the Ki for SA.

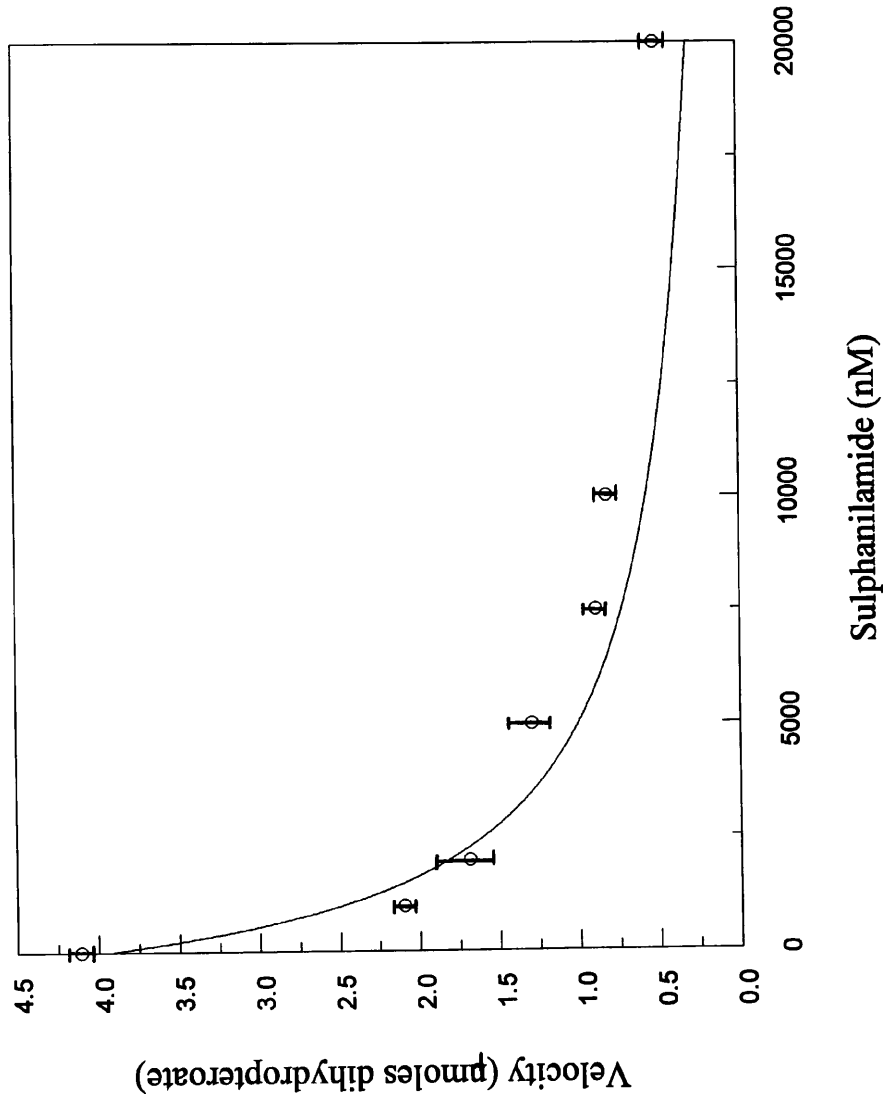

Table 6.1: Inhibition of DHPS by benzoic acid.

	Velocity (nmoles dihydropteroate)	
pABA (μM)	**No inhibitor**	**1mM benzoic acid**
0.25	0.17 ± 0.01	0.14 ± 0.01
0.5	0.16 ± 0.02	0.13 ± 0.01
1.0	0.18 ± 0.01	0.12 ± 0.01
2.0	0.16 ± 0.01	0.10 ± 0.01

Initial velocities were measured at four [^{3}H]-pABA concentrations 250, 500, 1000 and 2000nM and either no inhibitor or 1mM benzoic acid. Excess pterin pyrophosphate and magnesium were present in the buffer described below. The diethyl ether separation method was used. Each point is the mean of experiments performed in triplicate with the standard deviations. Together with the pABA and benzoic acid mentioned above, each reaction contained:

40μM pterin pyrophosphate
50mM Tris/HCl, pH 8.0
5mM DTT
5mM magnesium chloride and
3ng. DHPS

The reaction volume was made up to 50μl. with distilled water.

Table 6.2: Inhibition of DHPS by aniline.

Aniline (mM)	Velocity (pmoles dihydropteroate)
0	15 ± 0.3
0.01	14 ± 1.0
0.1	15 ± 0.8
1.0	17 ± 2.5
10.0	10 ± 0.9

Initial velocity measurements were made over a range of concentrations 0-10mM of aniline and a fixed concentration of 10nM [^{3}H]-pABA and 490nM pABA after a 30 minute incubation with enzyme. Excess pterin pyrophosphate and magnesium were present in the buffer described below. Each value is the mean of experiments performed in triplicate together with their standard deviations. Together with the pABA and aniline mentioned above, each reaction contained:

17.5μM pterin pyrophosphate
50mM Tris/HCl, pH 8.0
5mM DTT
5mM magnesium chloride and
12ng. DHPS

The reaction volume was made up to 50μl. using distilled water.

235

Figure 6.11: Determination of the K_i for folate.

Initial velocity measurements were made at two concentrations 0.5 and 5.0μM of pterin pyrophosphate and five concentrations 0, 50, 100, 150 and 200μM of folate over a 15 minute incubation period at 25°C. The counts were corrected to pmoles dihydropteroate produced over 30 minutes. The results were mean values of experiments performed in triplicate. In addition to pterin pyrophosphate and folate mentioned above, each experiment contained:

500nM [^{14}C]-pABA
4.5μM pABA
50mM Tris/HCl, pH 8.0
5mM DTT
5mM magnesium chloride
200ng DHPS

The reaction volume was made up to 1ml using distilled water. The results were fitted to a mathematical model using a non-linear least-squares procedure and assuming simple, competitive inhibition. [See Section 9.2.] The final values for the fitted parameters were $K_{i(folate)}$ = 25μM, app$K_{m\ (pterin\ pyrophosphate)}$ = 0.24μM and the appV_{max} = 0.34nmoles dihydropteroate/30mins/200ng DHPS.

2.5μM pterin pyrophosphate ●
0.5μM pterin pyrophosphate ○

Figure 6.11: Determination of the Ki for Folate.

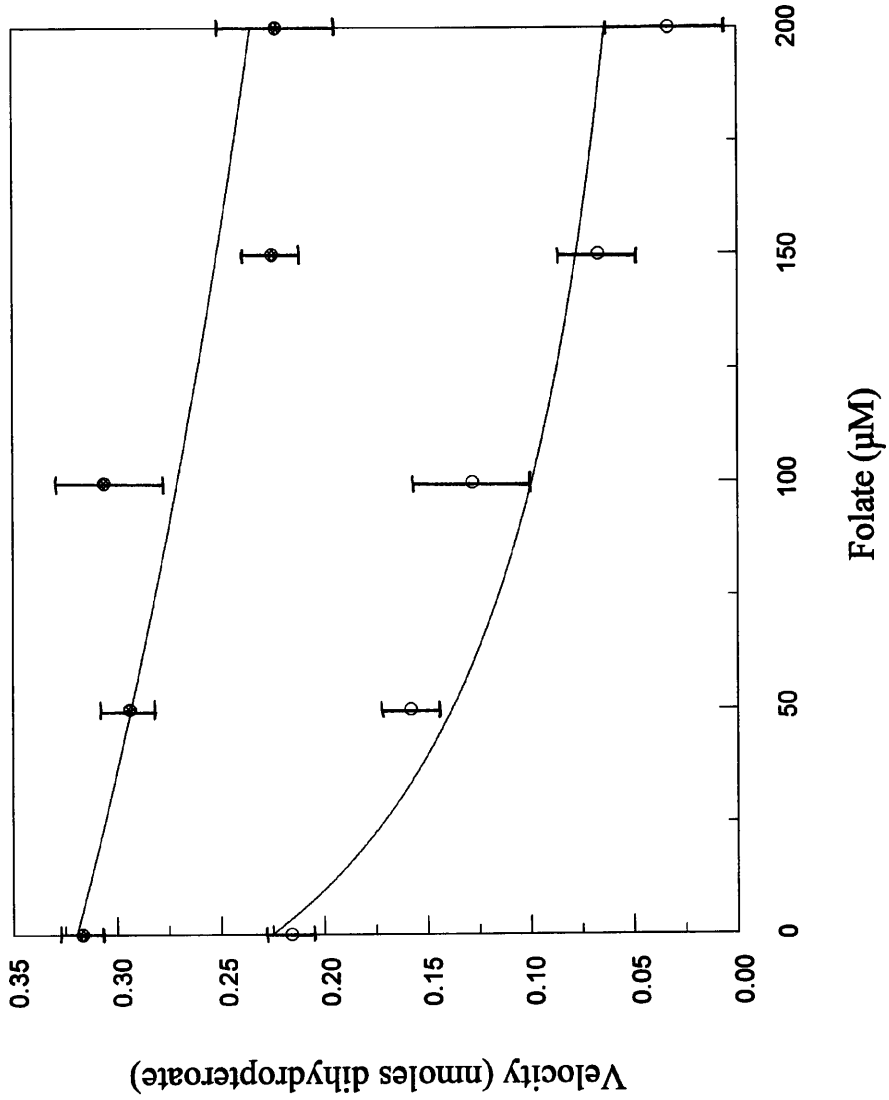

The data were recorded at two different concentrations of pterin pyrophosphate and fitted to a simple, competitive model of inhibition. The predicted value for the K_i for folate is 25μM and the K_m for pterin pyrophosphate is 0.24μM. The inhibition of the DHPS reaction by folate, with respect to pABA-binding, was also measured and the results are shown in Figure 6.12. The data was fitted in the same manner and a K_i value of 15μM is predicted together with a K_m for pABA of 0.9μM. The K_i values for dihydrofolate and tetrahydrofolate with respect to pterin pyrophosphate, were also determined to be 24μM [Figure 6.13] and 8μM [Figure 6.14] respectively, with the two predicted K_m values for pterin pyrophosphate 0.11μM and 0.09μM. These results demonstrate that the folate compounds can probably inhibit the reaction with respect to both substrates to similar extents.

6.5.4 Determination of the inhibitor constants of methotrexate (MTX), pyrimethamine (PMM) & trimethoprim (TMP).

These compounds, normally used as effective inhibitors of the DHFR reaction, are analogues of DHF and for this reason may have an effect on the DHPS reaction through their similarity to pterin pyrophosphate. By attempting to measure their inhibitor constants for inhibition of the DHPS reaction with respect to pterin pyrophosphate, any such effect can be evaluated.

Figure 6.15 shows the inhibition of the DHPS reaction by MTX. Although a single set of data was collected at a fixed concentration of pterin pyrophosphate, the agreement with a simple, competitive model of inhibition is good and the K_i for MTX is predicted to be at least 0.4mM and the apparent K_m for pterin pyrophosphate was 1000nM. The results of the inhibition of the DHPS reaction with PMM and TMP are tabulated. [Tables 6.3 and 6.4] The velocity of the reaction was halved on addition of approximately 1mM PMM, so the K_i for PMM is likely to be in this range. Significant inhibition occurred between 3-4mM TMP suggesting the K_i for TMP to be around that concentration.

Figure 6.12: Determination of the K_i for folate with respect to pABA.

Initial velocity measurements were made at two concentrations 250 and 500nM of [^{14}C]-pABA and five concentrations 0, 50, 100, 150 and 200μM of folate recorded over a 15 minute incubation period then corrected to pmoles dihydropteroate produced over 30 minutes. The results are mean values of experiments performed in triplicate. In addition to pABA and folate, each reaction contained:

5μM pterin pyrophosphate
50mM Tris/HCl, pH 8.0
5mM DTT
5mM magnesium chloride and
200ng DHPS

The reaction volume was made up to 1ml using distilled water. The data were fitted to a mathematical model using a non-linear least-squares procedure and assuming simple competitive inhibition. [See Section 9.2.] The final values for the fitted parameters were $K_{i(folate)}$ = 15μM, app$K_{m(pABA)}$ = 0.94μM and the appV_{max} = 0.6nmoles dihydropteroate/30mins/200ng DHPS.

500nM pABA ●
250nM pABA ○

Figure 6.12: Determination of the Ki for Folate with respect to pABA.

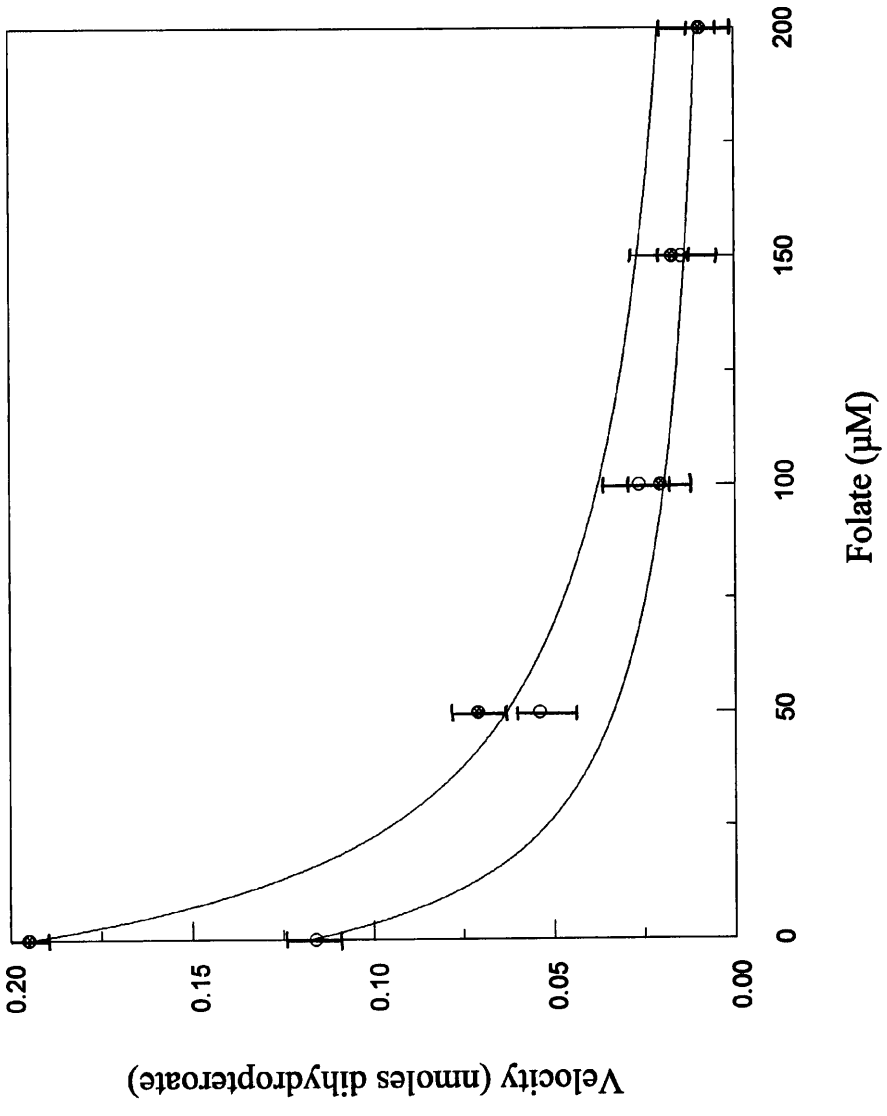

240

Figure 6.13: Determination of the K_i for Dihydrofolate.

Initial velocity measurements were made at two concentrations 0.5 and 2.5μM of pterin pyrophosphate and five concentrations 0, 50, 100, 150 and 200μM of DHF over a 15 minute incubation period and corrected to pmoles of dihydropteroate produced in 30 minutes. The results are mean values of experiments performed in duplicate. In addition to pterin pyrophosphate and DHF, each experiment contained:

500nM [^{14}C]-pABA

4.5μM pABA

50mM Tris/HCl, pH 8.0

5mM DTT

5mM magnesium chloride and

200ng DHPS

The reaction volume was made up to 1ml using distilled water. The results were fitted to a mathematical model using a non-linear least squares procedure and assuming simple, competitive inhibition. [See Section 9.2] The final values for the fitted parameters were $K_{i(dihydrofolate)}$ = 24μM, appK_m = 0.11μM and appV_{max} = 0.8nmoles dihydropteroate/30mins/200ng DHPS.

2.5μM pterin pyrophosphate ●

0.5μM pterin pyrophosphate ○

Figure 6.13: Determination of the Ki for Dihydrofolate.

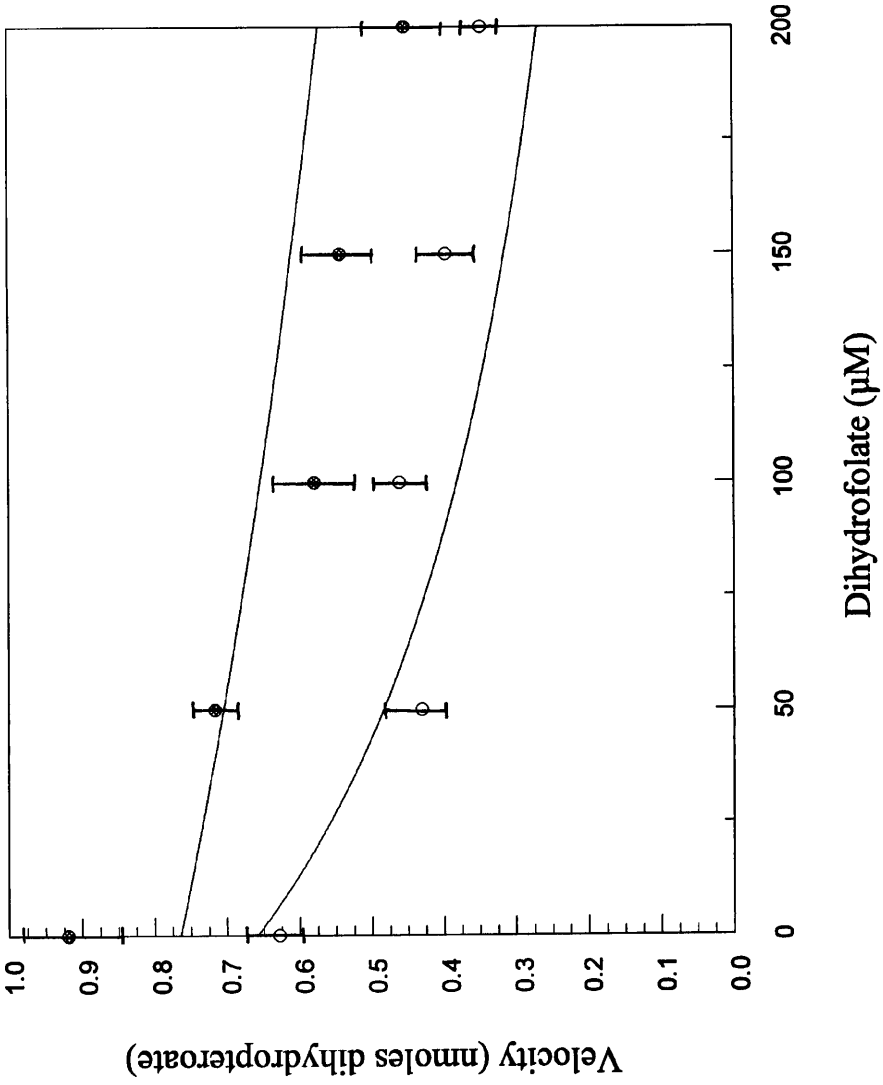

Figure 6.14: Determination of the K_i for Tetrahydrofolate.

Initial velocity measurements were made at two concentrations 0.5 and 2.5μM of pterin pyrophosphate and five concentraions 0, 50, 100, 150 and 200μM of THF over a 15 minute incubation period and corrected to pmoles of dihydropteroate produced in 30 minutes. The results are mean values of duplicate experiments. In addition to pterin pyrophosphate and THF mentioned above, each experiment contained:

500nM [^{14}C]-pABA
4.5μM pABA
50mM Tris/HCl, pH 8.0
5mM DTT
5mM magnesium chloride and
400ng DHPS

The reaction volume was made up to 1ml using distilled water. The results were fitted to a mathematical model using a non-linear least squares procedure and assuming simple competitive inhibition. [See Section 9.2] The final values for the fitted parameters were $K_{i(\text{tetrahydrofolate})}$ = 4.7μM, $\text{app}K_{m(\text{pterin pyrophosphate})}$ = 0.09μM and $\text{app}V_{max}$ = 0.6nmoles dihydropteroate/30mins/400ng DHPS.

2.5μM pterin pyrophosphate ●
0.5μM pterin pyrophosphate ○

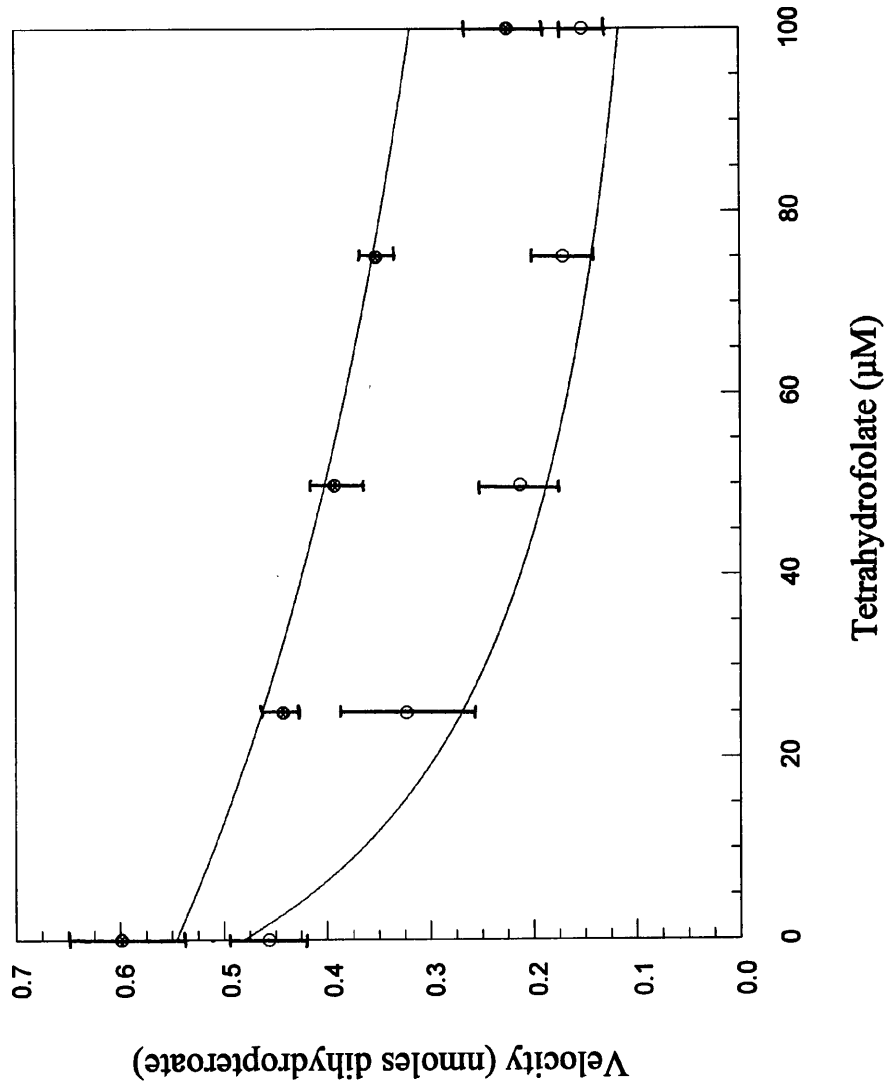

Figure 6.14: Determination of the Ki for Tetrahydrofolate.

Figure 6.15: Determination of the K_i for MTX.

Initial velocity measurements were made at a fixed concentration of 5μM pterin pyrophosphate and five concentrations 0, 0.5, 1.0, 1.5 and 2.0mM of MTX. The highest concentration of MTX available in the reaction was 2mM (dissolved in 50% water: ethanol with 1 drop of 1M Tris base) due to solubility problems. Results were mean values of experiments performed in triplicate. In addition to pterin pyrophosphate and MTX, each experiment contained:

500nM [^{14}C]-pABA

4.5μM pABA

50mM Tris/HCl, pH 8.0

5mM DTT

5mM magnesium chloride and

100ng DHPS

The reaction volume was made up to 1ml using distilled water. The results were fitted to a mathematical model using a non-linear least squares procedure and assuming simple competitive inhibition. [See Section 9.2] The final values of the fitted parameters were $K_{i(MTX)}$ = 0.4mM, app$K_{m(\text{pterin pyrophosphate})}$ = 1000nM, and appV_{max} = 0.12nmoles dihydropteroate/30minutes/100ng DHPS.

Figure 6.15: Determination of the Ki for MTX.

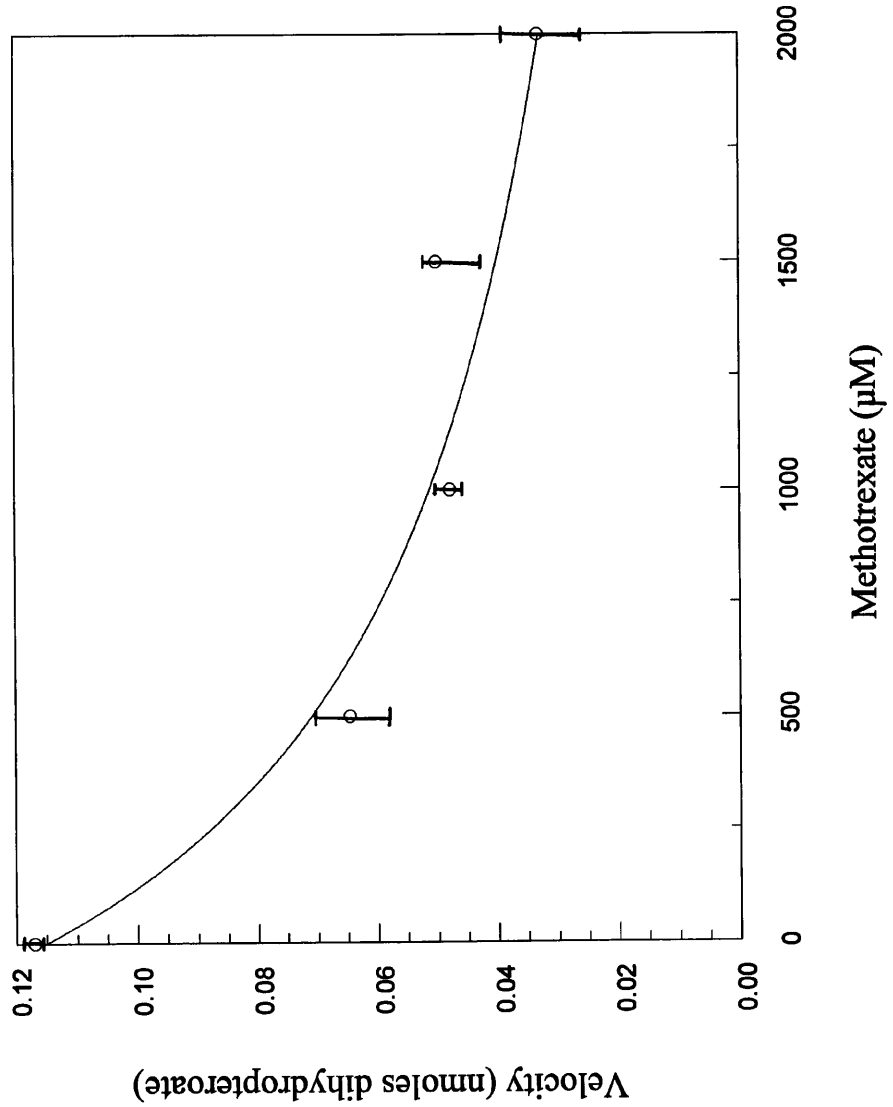

Table 6.3: Inhibition of DHPS by PMM.

PMM (μM)	Velocity (pmoles/30mins/10ng DHPS)
0	8.5
1	9.0
10	8.4
100	7.6
400	5.0
1000	4.7
4000	5.0

The PMM was dissolved in 50% water: ethanol at 60°C to a maximum concentration of 4mM in the reaction. Initial velocity measurements were made at a fixed concentration of 5μM pterin pyrophosphate and a wide range of PMM concentrations. The data given are mean values of duplicate experiments. In addition to pterin pyrophosphate and PMM, each reaction contained:

500nM [^{14}C]-pABA
4.5μM pABA
50mM Tris/HCl, pH 8.0
5mM DTT
5mM magnesium chloride and
10ng DHPS

The reaction volume was made up to 1ml. using distilled water.

Table 6.4: Inhibition of DHPS by TMP.

TMP (mM)	Velocity (pmoles dihydropteroate/30mins/100ng)
0	1127 ± 12
1	1089 ± 64
2	1084 ± 97
3	958 ± 10
4	275 ± 39

TMP was dissolved in 50% water:ethanol to a concentration allowing 4mM in the reaction. Initial velocity measurements were made at five concentrations 0, 1, 2, 3 and 4mM of TMP and a fixed concentration, 5μM pterin pyrophosphate. Each point was measured in triplicate and mean values are given in the table together with their standard deviations. In addition to the pterin pyrophosphate and TMP, each reaction contained:

500nM [^{14}C]-pABA
4.5μM pABA
50mM Tris/HCl, pH 8.0
5mM DTT
5mM magnesium chloride and
100ng DHPS

The reaction volume was made up to 1ml using distilled water.

6.6 Summary of the results of the kinetic experiments.

Inhibitor.	K_i	App.K_m	App.V_{max} (nmoles/30min/xngDHPS
SQ	25nM	-	0.004/3ng
SMX	590nM	-	0.007/3.12ng
SA	850nM	-	0.008/10ng
benzoic acid	1mM	-	-
aniline	>1mM	-	-
folate (with respect to pterinPPi)	25µM	0.24µM	0.3/200ng
folate (with respect to pABA)	15µM	0.94µM	0.6/200ng
DHF	24µM	0.11µM	0.8/200ng
THF	8µM	0.09µM	0.6/400ng
MTX	>0.4mM	1.0µM	0.12/100ng
PMM	1-2mM	(Pt-PP)-	-
TMP	3-4mM	-	-

The sulphonamides clearly inhibit DHPS more potently than the other compounds. SQ was a very potent inhibitor of the DHPS reaction, SMX was not as strong as SQ but a better inhibitor than SA.

Benzoic acid did not inhibit the DHPS reaction to any significant extent and this confirmed the original results of Woods (1940). Likewise aniline was a poor inhibitor of the DHPS reaction. The carboxylic acid group and the amine groups of pABA are likely to be key points of recognition within the active site of DHPS. This point is discussed in more detail in Section 6.7.

The DHFR inhibitors were poor inhibitors of the DHPS reaction with millimolar concentrations of these compounds necessarily present before significant inhibition was observed. At such high concentrations of these chemicals, the decrease in initial velocity measured may have been due to changes in pH or solvent conditions rather than inhibition of pABA-binding to DHPS.

The folate compounds, although not potent inhibitors like the sulphonamides, did inhibit the DHPS reaction at micromolar concentrations, apparently as either competitive inhibitors of pterin pyrophosphate binding or pABA-binding to DHPS. The degree of inhibition did not vary greatly with the reduction state of the pterin ring.

6.7 Conclusions.

The work presented in this chapter is the first attempt to comprehensively study the inhibition of DHPS activity by sulphonamides *in vitro* and to correlate this inhibition with equilibrium binding measurements.

The displacement of pABA by all five of the sulphonamides tested fits a single-site, simple competitive model for inhibition of DHPS (shown below).

(E represents DHPS, pterinPPi represents pterin pyrophoshate/magnesium and Sul presents the sulphonamides)

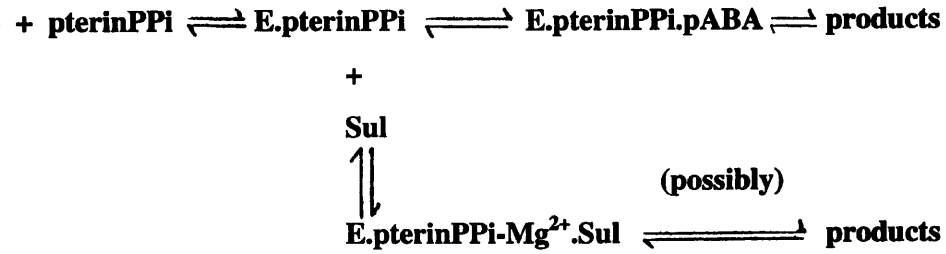

It might be argued that larger and more hydrophobic sulphonamides like SP and SQ behave in a more complex manner given their closer structural similarity to the product dihydropteroate, rather than pABA. For example, in Chapter 5 it was shown that dihydropteroate bound less than half the number of sites on DHPS compared with pABA. However it has been shown here that both SP and SQ are capable of displacing *all* the pABA bound by DHPS, so they must bind at both pABA sites. This conclusion is supported by the kinetics where it has been demonstrated that all five sulphonamides studied exhibit competitive inhibition with respect to pABA. Therefore, despite the wide structural diversity of the sulphonamide drugs, they show a remarkable degree of similarity in their inhibition characteristics.

The study of folate, DHF and THF compounds demonstrated that the oxidation state of the pterin ring was not an important factor in their inhibition of the DHPS reaction. This is a very interesting observation because it is known that DHPS will not use oxidised pterin pyrophosphate as a substrate. [Hampele, *et al.* (1997), own observations] This suggests that the folate compounds are bound by DHPS in a different manner to the pterin pyrophosphate substrate, perhaps with the ring in a different orientation so that residue(s) which normally recognise the pterin ring in its reduced state do so in a different way. It is clear that there is no support for the hypothesis that DHF and THF can be feedback regulators of DHPS and folate biosynthesis.

The DHFR inhibitors were not found to inhibit the DHPS reaction to any significant extent. Sulphonamides have been tested in the past as inhibitors of DHFR activity, [Dieckmann & Jung, (1986), Huovinen, *et al.* (1995)] but this is the first information concerning the action of DHFR inhibitors on DHPS.

Aniline and benzoic acid were not effective inhibitors and provided important information concerning the recognition and binding of pABA by DHPS. DHPS is capable of binding pABA from solution at nanomolar concentrations but required millimolar concentrations of aniline and benzoic acid before any significant inhibition was observed. Several orders of magnitude difference in binding suggest that at least one stabilising hydrogen bond is normally present at the pABA-binding site to stabilise the -COOH and the $-NH_2$ groups. Initial crystallographic studies of the *E. coli* pABA binding site suggest the molecule binds between the main chain residue Arg220 and the side chain of Lys221 on one side, and the side chain of Arg63 on the other side. Arg220 and Lys221 lie within a particularly conserved region of the protein, but Arg63 is only partially conserved with *Plasmodium falciparum* and *Toxoplasma gondii* having different amino acids at that locus. The $-NH_2$ of the sulphonamide $-SO_2NH_2$ group donates a hydrogen bond to the carbonyl of Ser219 whilst one of the sulphate oxygen atoms accepts a hydrogen bond from the guanidinium group of Arg63. These important residues are conserved between *E. coli* and *S. pneumoniae* and are Arg236, Lys237, Arg58 and Ser235 in the *S. pneumoniae* enzyme.

It is anticipated that the aniline -NH_2 group is in close proximity to the carbonyl of Thr62 in *E. coli* and this hydrogen bond may be absent from the complex with benzoic acid. This residue is again highly conserved and corresponds to Thr57 in *S. pneumoniae*.

Sulphanilic acid is structurally very similar to pABA and has an equilibrium binding constant of about 10μM compared with pABA at about 0.8μM. There is an order of magnitude difference in the dissociation constant corresponding to a ligand containing a sulphate group instead of a carboxylic acid at the pABA binding site. The most effective sulphonamide at displacing pABA from its binding site was SP. The difference between the most effective and the least effective sulphonamide is 100-fold, 350nM compared to 38.9μM, indicating that the R-group is an important factor in determining the ability of the sulphonamides to inhibit the DHPS reaction and displace to pABA from its binding site. This suggests that substituents on the sulphate group of the sulphonamides make interactions with residues in DHPS that are somewhat outside the catalytic site of the enzyme. These residues may be much less conserved at the sequence level than residues within the catalytic site.

In the *E. coli* DHPS, sulphanilamide binds in a fairly open region described above with residues Phe190 and Pro61, in addition to the residues interacting directly with the sulphanilamide molecule, appearing to form the pABA/sulphonamide-binding pocket. [Achari, *et al.* (1997)] These residues are again highly conserved in *S.pneumoniae* - Phe206 and Pro59. The sulphonamide resistant *suld* mutant described earlier in Chapter 1, an insertion of Ile-Glu into the sequence after Glu67, occurs after this important conserved region containing Thr57, Arg58 and Pro59. This mutation will inevitably disrupt the main chain conformation in this region, perhaps causing a structural change in the sulphonamide binding site or making unavailable those residues outside the catalytic site of the enzyme that are involved in sulphonamide binding.

It is clear that, although the sulphonamides examined here behave as simple, competitive inhibitors, a range of more subtle and complex factors affect their relative efficacy, and these remain to be determined at the molecular level.

Chapter 7 Discussion.

The work presented in chapters three to six has been concerned with the structure and mechanism of *S. pneumoniae* DHPS and its inhibition by the sulphonamide drugs. In chapter three, a concentration-dependent equilibrium was observed between monomeric and dimeric forms of the enzyme. *S. pneumoniae* DHPS was shown to be monomeric at ng/ml concentrations used in the kinetic assays, but dimeric at μg/ml concentrations used in the Hummel & Dreyer and Sepharose bead binding experiments. Consequently the crystallographic and equilibrium binding studies were performed using predominantly a dimeric form of DHPS and the kinetic studies were performed using a monomeric form of DHPS. Two schemes in Figures 7.1 and 7.2 have been proposed to try to account for results and observations from the previous chapters.

7.1 Ligand binding to DHPS studied by crystallography.

In chapter 4, two different crystal morphologies were reported for *S. pneumoniae* DHPS and two possible hypotheses were advanced to explain this. The apoenzyme may have bound all the ligands to which it was exposed, with DHPS/pABA and DHPS/SMX binary complexes growing as needle-shaped crystals, and the DHPS/pterin pyrophosphate, DHPS/pyrophosphate and DHPS/pterin pyrophosphate/benzoic acid complexes growing as diamond-shaped crystals. The other possibility, in light of the fact that the apoenzyme crystals were also needle-shaped, is that the apoenzyme had not bound pABA or SMX and the crystals which formed were actually those of apoenzyme only. The binding of pterin pyrophosphate may have caused a conformational change within the DHPS dimer allowing it to crystallise in a different morphology. This conformational change could be mimicked by pyrophosphate and was also observed in crystals of the *pseudo*-ternary complex of pterin pyrophosphate and benzoic acid. [Figure 7.1] The results of the equilibrium binding experiments support the second hypothesis because DHPS was not observed bound with pABA or SMX alone at the higher protein concentrations used for the equilibrium binding experiments and the crystal trials. The presence of pyrophosphate facilitated the binding of pABA and SMX by DHPS, and pterin pyrophosphate also appeared to be bound by DHPS, suggesting a change in the conformation of the DHPS protein.

Figure 7.1: Proposed model for the mechanism of *S. pneumoniae* DHPS as a dimer.

(○ pterin pyrophosphate, ▲ pABA, ○▲ dihydropteroate)

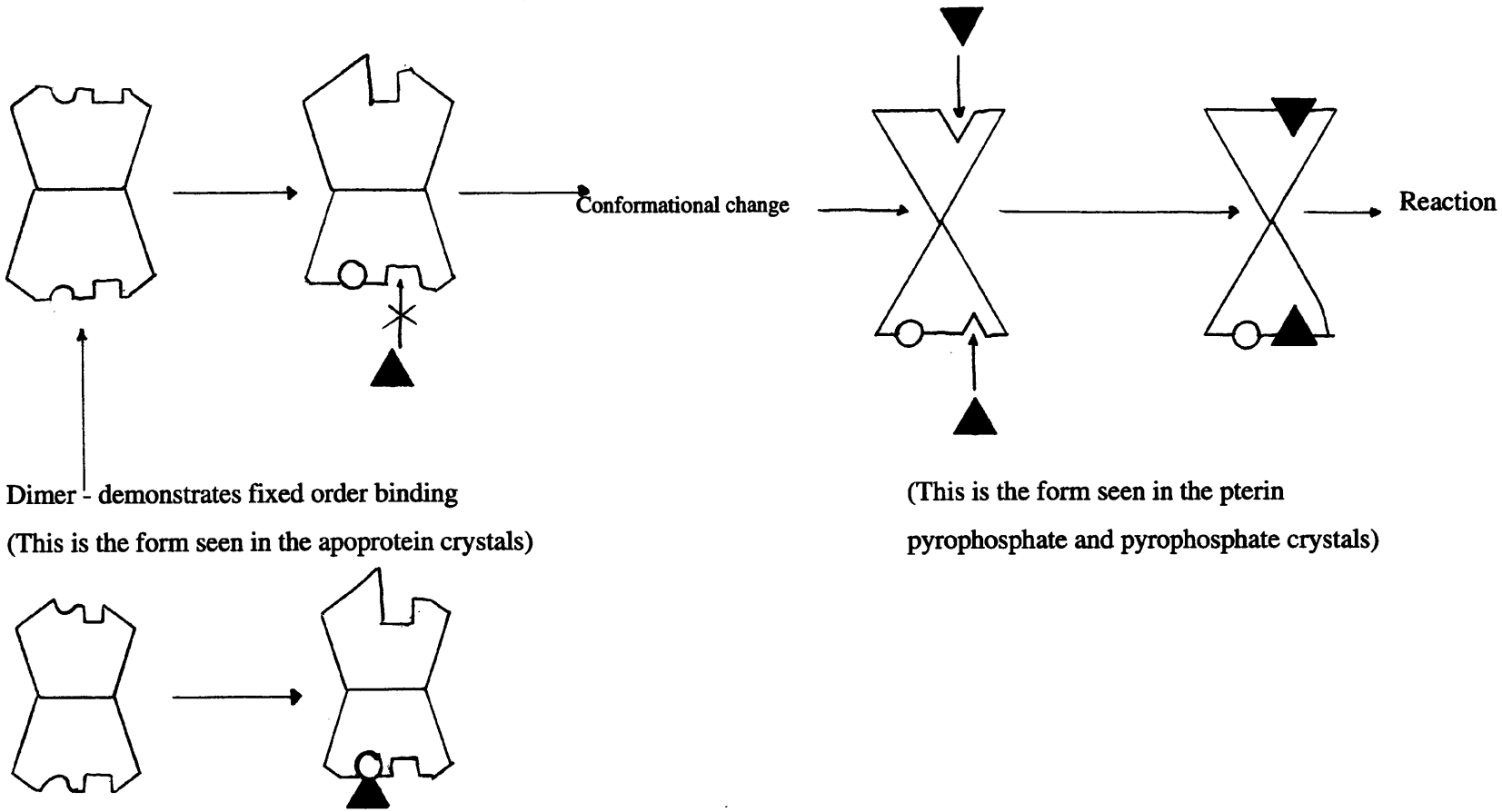

Figure 7.2: Proposed model for the mechanism of *S. pneumoniae* DHPS in the monomeric form.

(○ pterin pyrophosphate, ▲ pABA)

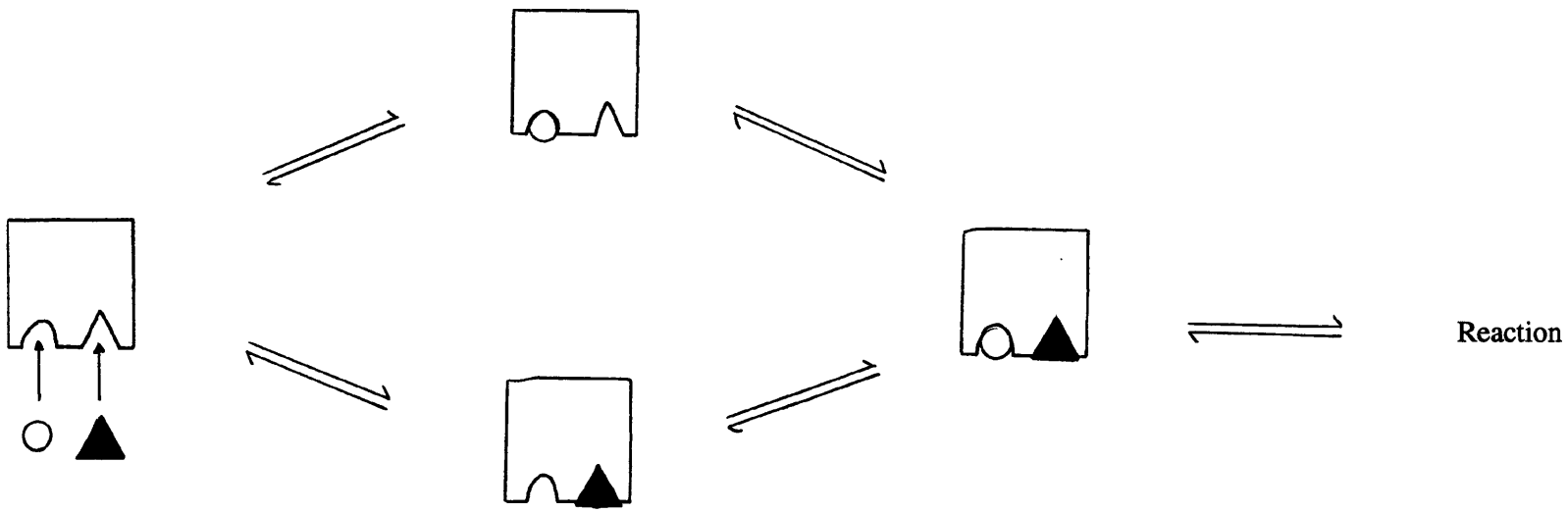

Monomer - demonstrates random order binding.

In the *E. coli* DHPS work, attempts to form a binary complex between a sulphonamide and DHPS showed no evidence of binding. [Achari, *et al.* (1997)] In order to bind sulphanilamide to *E. coli* DHPS, these workers made a *pseudo*-ternary complex with 6-hydroxymethyl-7,8-dihydropterin, pyrophosphate and sulphanilamide present in solution. However, there was no evidence that pyrophosphate had bound to DHPS together with hydroxymethyl-dihydropterin and sulphanilamide. Crystals of an *E. coli* binary complex DHPS/pterin pyrophosphate were also grown but there were no reported differences between the crystal morphologies, unlike *S. pneumoniae* DHPS. There were no reported differences between the protein main-chain atomic positions whether pterin pyrophosphate was present or not, which would suggest that in *E. coli* DHPS there is no significant conformational change detectable on the binding of pterin pyrophosphate.
In the *S. aureus* work, there were different morphologies between apoenzyme crystals and binary complexes/derivatives. [Hampele, *et al.* (1997)] There were also slight structural differences between the monomers when oxidised pterin pyrophosphate was bound. This suggests a slight conformational change in the dimer may occur on binding pterin pyrophosphate, similar perhaps to the conformational change predicted to occur in *S. pneumoniae* DHPS. [Figure 7.1] However, neither the *E. coli* not *S. aureus* enzymes change structure to any *major* extent on binding any ligand. It is possible therefore that *S. pneumoniae* DHPS operates in a different manner.

7.2 Limited-sites reactivity of dihydropteroate.

The results of the equilibrium binding experiments comparing the number of binding sites on *S. pneumoniae* DHPS occupied by dihydropteroate with those occupied by pABA suggest that dihydropteroate exhibits less than half-of-sites reactivity compared with pABA.
The *S. aureus* work concluded half-of-sites reactivity - only one of the two monomers, monomer A, had bound pterin pyrophosphate and the kinetic analysis performed suggested that additional binding of pABA to monomer B as well as A could cause a decrease in the catalytic efficiency. [Hampele, *et al.* (1997)] Unfortunately in this *S. pneumoniae* DHPS work, the possibility of half-of-sites reactivity by pterin pyrophosphate could not be investigated.

However the structural similarity between dihydropteroate and pterin pyrophosphate suggests that dihydropteroate might mimic the action of pterin pyrophosphate in binding to only one of the monomers. This is shown in Figure 7.1. Due to structural differences between the monomers, pterin pyrophosphate may be capable of binding to only one of the two monomers of *S. pneumoniae* DHPS. A conformational change could then occur, facilitating the binding of pABA.

To explain the equilibrium binding experiments in Chapter 5, dihydropteroate must be capable of high affinity binding to one of the monomers in a similar fashion to pterin pyrophosphate and pABA would have to be capable of binding with equal affinity to either monomer. From the experiments, it was clear that pyrophosphate could facilitate the binding of pABA by DHPS to more than twice the number of sites compared with dihydropteroate. If pyrophosphate mimics the action of pterin pyrophosphate in binding to only one of the monomers, pABA must be capable of binding to both monomers, one with pyrophosphate bound and one without, with an equal affinity. Dihydropteroate and pyrophosphate, the two products of the reaction, appear to be capable of binding with high affinity to the same conformational form of the enzyme as the substrates.

Another possibility is that pterin pyrophosphate, as the first substrate to be bound *by S. pneumoniae* DHPS, can bind to either monomer, causing a conformational change on binding within the DHPS dimer, rendering the other active site inaccessible to another molecule of pterin pyrophosphate. Such a conformational change would allow the binding of pABA at either active site (with equal affinity) but a reaction could only proceed at the site with pterin pyrophosphate already bound. The conformational change could be mimicked by the pyrophosphate/magnesium complex in the equilibrium binding experiments, allowing DHPS to bind pABA with a high affinity. This conformational change may also be mimicked by dihydropteroate, as an analogue of pterin pyrophosphate, allowing DHPS to bind only a single molecule of dihydropteroate at the active site of one monomer, but at a high affinity. [Figure 7.1] However if either of these cases were correct, a significant degree of product inhibition might be expected to occur, although this was not obvious from the linearity of the assay with time (until half the substrates had been converted to products) [Chapter 2]

7.3 Steady state kinetics and the monomer-dimer equilibrium.

It does not seem logical that an enzyme in a biosynthetic pathway should have such a high affinity binding site for one of its products without showing product inhibition. A possible explanation could be that the measured affinity for DHPS by the product is for binding to a conformation of DHPS that would not normally be encountered in the reaction cycle. On release of the products, DHPS may be in a different conformation than that which bound the substrates initially and the products may have little affinity for this confomation.

The kinetic experiments appeared to predict a random order of binding of the two substrates whereas the equilibrium binding experiments predicted a fixed order of binding. This apparent discrepancy can be explained in view of the monomer-dimer equilibrium for *S. pneumoniae* DHPS. Figures 7.1 and 7.2 explain in cartoon form the different modes of action observed by DHPS. In figure 7.1 the dimeric enzyme is portrayed as effecting a conformational change on the binding of a molecule of pterin pyrophosphate, and preventing the binding of a second molecule at the other site. This activity could be mimicked by dihydropteroate too, as an analogue of pterin pyrophosphate. This behaviour allows pABA to bind freely at either subunit active site with a reaction occurring at only one site. In figure 7.2 the monomeric enzyme is portrayed as capable of binding either substrate in a random fashion.

7.4 Inhibition by the sulphonamide drugs.

A range of sulphonamide drugs have been shown to effectively displace pABA from *S. pneumoniae* DHPS in equilibrium binding studies and to competitively inhibit the DHPS reaction with respect to pABA-binding. Generally the effectiveness of the sulphonamides both in displacing pABA and inhibiting the reaction increased with the increasing size and/or hydrophobicity of the R-substituent. [See Chapter 1] There has been a considerable amount of work on *Pneumocystis carinii* DHPS in the past few years, due largely to a rise in the incidence of pneumocystis pneumonia in AIDS patients, and the need for more potent drugs with less severe side effects. [Hong, *et al.* (1995 & 1996)]

Linked with this work have been reports of inhibitor constants for *Toxoplasma gondii* DHPS and *Mycobacterium avium* DHPS. [Chio, *et al.* (1996)] The first published apparent K_i values for sulphonamides with repect to pABA-binding to *E. coli* DHPS appeared in 1979. [Roland, *et al.* (1979)]

The work on *E. coli* DHPS established that sulphonamides could act as substrates of the reaction forming sulpha-pterin analogues. The authors concluded that inhibition of the DHPS reaction occurred as a result of formation of sulphapterin adducts depleting the pterin pool and that the sulpha-pterin compounds were not themselves potent inhibitors. The apparent K_i values reported were 0.035μM for STZ, 0.13μM for SMX and 5.7μM for SA. Although STZ was not one of the five sulphonamides examined in the present work, these results from SMX and SA show the same order of magnitude with the results obtained here of 0.59μM for SMX and 0.85μM for SA, and SMX as a more effective inhibitor than SA. Initial work on sulphonamides was carried out on *P. carinii* and *T. gondii* using seven sulphonamides and a sulphone - dapsone. [Voeller, *et al.* (1994)] The inhibitory characteristics of *P. carinii* DHPS had been assumed to be similar to those described for bacterial organisms but this work suggested that *P. carinii* was significantly more sensitive to sulphonamides compared with bacterial, plasmodial and *T. gondii* sources.

Following the previous work, a more detailed study of the relative inhibitory effects of sulphonamides and sulphones involving 44 sulpha-drugs was carried out on *P.carinii* DHPS. SMX and SQ were amongst the eight sulphonamides with lowest 50% inhibitory concentrations (IC_{50}s). [Hong, *et al.* (1995)] The K_i values of five of these were calculated and are summarised in the Table 7.1. The chemical structures of the compounds affected their inhibitory activities in several ways. Firstly an unsubstituted *p*-amino group was essential for inhibition, suggesting that the *p*-amino groups of both pABA and sulphonamides are involved in binding to the active site of *P. carinii* DHPS. This has now been shown to be true for the *E. coli* DHPS and evidence from the present work on *S. pneumoniae* DHPS has demonstrated the importance of the *p*-amino group, from the lack of inhibition by benzoic acid. Secondly heterocyclic substituents on the sulphonamide nitrogen atom were the most potent.

Table 7.1: K_i and IC_{50} values of the eight most potent sulphoanmides tested against *P. carinii* DHPS activity.

(Taken from Hong, *et al.* (1995))

	Mean K_i (nM)	Mean IC_{50} (nM)
Sulphamethoxazole	**7.5**	**23**
Sulphathiazole	**10.5**	**13**
Sulphachlopyridazine	**10.0**	**18**
Sulphamethoxypyridazine	**12.5**	**17**
Sulphathiourea	**16.5**	**22**
Sulphadimethoxine	**-**	**25**
Sulphaquinoxaline	**-**	**30**
Sulphisoxazole	**-**	**40**

Phenyl derivatives had IC_{50}s from 0.18-0.8μM whilst most of the heterocyclic sulphonamides had IC_{50}s lower than 0.1μM. Four of the five most effective drugs mentioned in Table 7.1 belonged to this heterocyclic group. These results again agreed with results obtained with *S. pneumoniae* DHPS with the three compounds containing heterocyclic groups - SMX, SQ and SP - much more effective inhibitors than the two which did not - SA or SAA. Thirdly, charges or substituents on the heterocyclic ring affected the inhibitory activity towards *P. carinii* DHPS, for example sulphadimethoxine and sulphadoxine vary only in a single methoxy-substituent in different positions on the heterocyclic ring, yet sulphadoxine has an IC_{50} 30-fold higher than sulphadimethoxine.

Comparing the results of Hong, *et al.* to the work on *S. pneumoniae* DHPS presented here, DHPS from *P. carinii* has a different response to sulphonamides from the *S. pneumoniae* enzyme. Whereas in the *S. pneumoniae* DHPS work, SQ was a more potent inhibitor of the reaction than SMX and more capable of displacing pABA from its binding site, in the work on *P. carinii* DHPS, SMX was a more potent inhibitor than SQ. In the *E.coli* DHPS crystal structure, the binding of sulphanilamide was accomplished by residue Ser219 hydrogen-bonding to the N1 atom and the side chain of Arg63 making a hydrogen bond to one of the sulphonamide oxygen atoms. The side chains of Phe190 and His257 are also within Van der Waals contact distance of the ligand.

These are conserved residues across all the prokaryotic and eukaryotic amino acid sequences and so may be assumed to occur for most sulphonamides binding to sulphonamide-susceptible DHPS molecules, providing the *p*-amino group is unsubstituted. However, the large, heterocyclic R-substituents of SQ and SP, for example, lie further away from the active site in the β-barrel fold and may protrude in the direction of the top of the β-strands and the loop regions extending over the core of the fold. In the *S. aureus* work there were two loop regions with poorly defined electron density in monomer B compared with the active monomer A, both of which contain conserved residues in all species.

In *S. pneumoniae* DHPS particularly, one of the loop regions (corresponding to residues Asn17-Phe30) contains three phenylalanine residues and a valine residue which may make contact with the benzoic ring systems of sulphonamides stabilising their binding. *P.carinii* also has two phenylalanine residues in that loop region and an isoleucine residue which may also provide a stabilising environment for the hydrophobic side chains of sulphonamides. In DHPS molecules from different species, the heterocyclic ring and substituents of the sulphonamide will be adjacent to different amino acid residues and so different specificities would be expected. The heterocyclic nature of the most potent sulphonamides however, suggests interactions with residues capable of providing stabilising hydrogen bonds to the ring systems.

7.5 A consideration of the mechanism of the DHPS reaction.

The question about how DHPS facilitates the reaction of pterin pyrophosphate and pABA to form dihydropteroate has not been considered for any species. A carbon-nitrogen bond is formed between the hydroxymethyl-C atom of pterin pyrophosphate and the amine-N atom of pABA, with the release of pyrophosphate as a leaving group. A bimolecular, nucleophilic substitution reaction (S_N2) could occur with a nucleophilic attack by the nitrogen on the carbon atom, proceding via a trigonal biplanar transition state, with the subsequent loss of the pyrophosphate group. [Figure 7.3] The ease with which a group could function as a leaving group in an S_N2-type reaction can be gauged by its basicity. A leaving group gains electron density going from the reactant to the transition state and the more this electron density is stabilised, the lower the energy of the transition state, and the faster the reaction. To facilitate the reaction catalysed by DHPS, the previous step in the folate biosynthesis pathway is the addition of a pyrophosphate group to hydroxymethyldihydropterin, catalysed by HPPK. Pyrophosphate is a stable anion and therefore a good leaving group, readily able to accommodate additional electron density. If an S_N2-type reaction could occur directly with hydroxymethylpterin rather than pterin pyrophosphate, it would have theoretically created a relatively unstable hydroxyl anion as the leaving group which is less able to stabilise electron density compared with pyrophosphate.

Figure 7.3: Proposed S_N2 reaction of *S. pneumoniae* DHPS.

(Taken from Streitweiser and Heathcock, (1989))

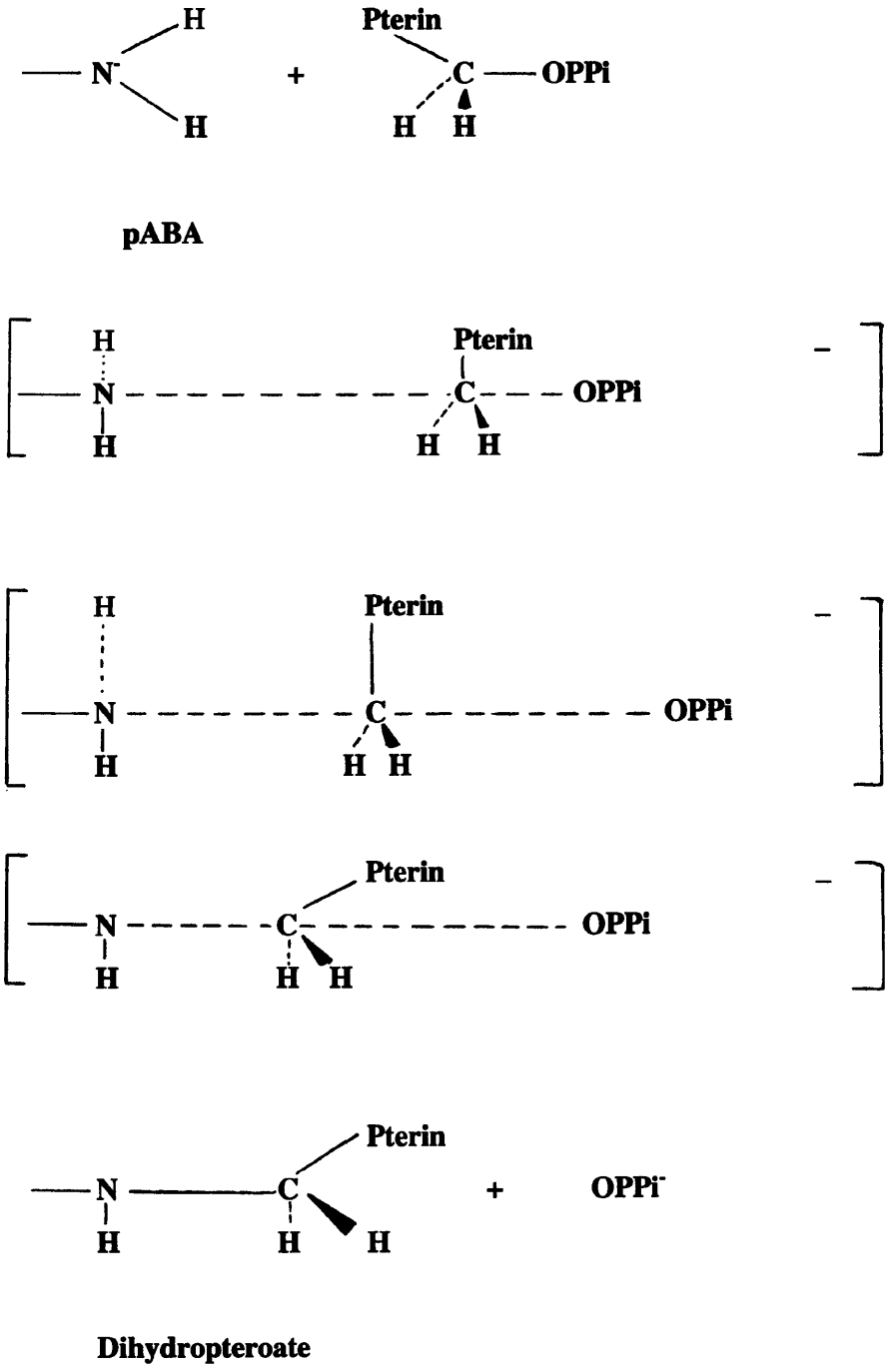

The degree to which a group can accommodate a negative charge is also related to its affinity for a proton i.e. pyrophosphate can form a more acidic conjugate acid in HOP_2O_5H than -OH in producing H_2O. An example of the use of pyrophosphate as a good leaving group in a biochemical reaction is that catalysed by Uracil phosphoribosyl transferase. The S_N2 mechanism occurs via a relatively stable oxocarbocation intermediate. [Kyte, (1995b)][Figure 7.4]

An aqueous solvent environment is not ideal for S_N2-type reactions but water molecules are excluded from the active site on the binding of the two substrates and the active site is a relatively hydrophobic environment within the protein. In order for a condensation reaction of this nature to proceed, the amino acid groups of DHPS, at or near the active site may assist in making the amine-N of the pABA molecule more reactive and nucleophilic, possibly by withdrawing electrons from the nitrogen by bonding with a hydrogen atom of the amine group or even removing one of the hydrogen atoms. From the *E. coli* DHPS crystal structure, this important amine group of sulphanilamide was estimated to be 3.5Angstroms from the reacting carbon of the pterin pyrophosphate molecule. This suggests that to facilitate the reaction, an alteration in the position of the two substrates or amino acids at the active site must occur. Until the coordinates of this *E. coli* crystal structure are available, this phenomenon cannot be studied in detail. Other amino acid residues may help to stabilise the transition state once formed, to reduce the energy barrier required to form the intermediate and stabilise the pyrophosphate leaving group.

In the *S. pneumoniae* DHPS, there is an ionisable group or groups important in the reaction - possibly one or more aspartate carbonyl-side chains or an imidazole moiety of a histidine residue. From the crystal structures of DHPS from *E. coli* and *S. aureus*, one conserved aspartate residue is involved in hydrogen-bonding to the pterin ring amine group (N6) and another in hydrogen-bonding to the pyrazine nitrogen atom (N4). [Achari, *et al.* (1997), Hampele, *et al.* (1997)] It is this second aspartate residue in *E. coli* DHPS which is believed to alter its conformation on binding of the pterin pyrophosphate. A reduced pH is therefore likely to cause a disruption to the binding of pterin pyrophosphate to *S. pneumoniae* DHPS.

Figure 7.4: The nucleophilic substitution mechanism of Uracil phosphoribosyl transferase.

(Taken from Kyte, (1995b))

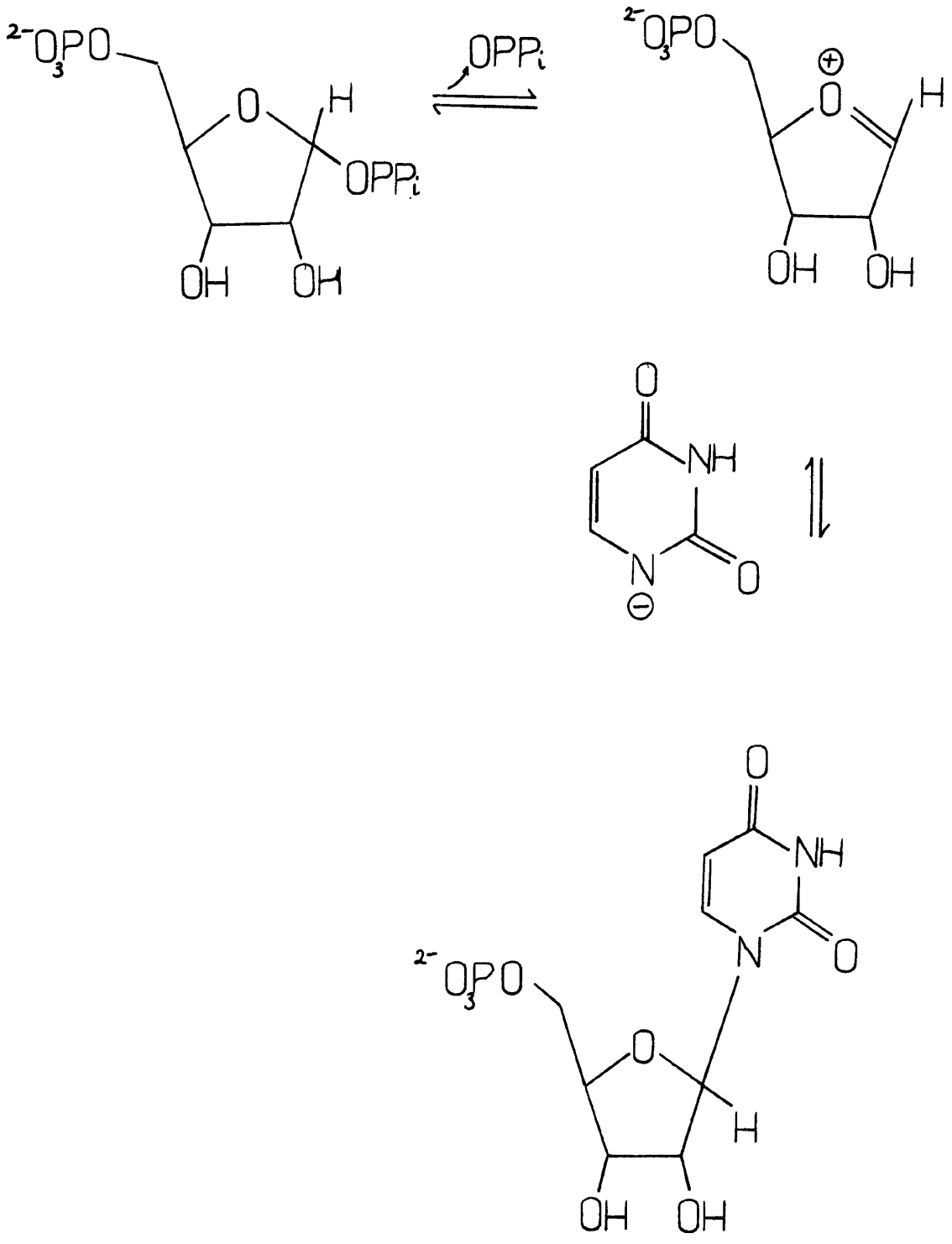

The side-chain of the conserved histidine residue stabilises one of the β-phosphate oxygen atoms of pterin pyrophosphate by hydrogen-bonding. According to the *E.coli* DHPS structure, its side-chain is also within bonding distance of the aniline -NH_2 group of pABA, along with phenylalanine and threonine conserved residues. The histidine of *S. pneumoniae* DHPS may act as a base in abstracting a proton from the amine group of pABA and subsequently act as an acid in donating that proton to the β-phosphate oxygen atom which it normally stabilises by hydrogen-bonding. The threonine side-chain hydroxyl-group makes an important hydrogen bond to the hydroxymethyl-oxygen atom of pterin pyrophosphate. As a consequence, this conserved residue may be important for the stabilisation of the pyrophosphate leaving group.

7.6 The Glutathione *S*-transferases. (E.C. 2.5.1.18)

The superfamily of Glutathione *S*-transferases (GSTs) are a group of enzymes that catalyse a similar reaction to DHPS. There are five distinct classes of mammalian GSTs discovered to date (alpha, mu, pi, sigma and theta) based on their substrate specificities and primary sequences. [Fiel, *et al.* (1996), Dirr, *et al.* (1994)]] These enzymes conjugate a wide variety of electrophilic, hydrophobic substrates to the tripeptide glutathione. This conjugation increases the solubility of the molecule, facilitating its removal from the organism. There are now crystal structures for all five classes, but as yet none reported for bacterial GSTs, although they have been identified in *Escherichia*, *Proteus*, *Pseudomonas*, *Enterobacter*, *Klebsiella* and *Serratia* species. All GSTs have a common polypeptide fold. Each monomer folds into two distinct conformations. The N-terminal domain consists of a βαβαββα module which comprises most of the hydrophilic glutathione binding site, and the mainly α-helical hydrophobic C-terminal domain is involved primarily in the binding of structurally diverse hydrophobic substrates.

Most of the highly conserved residues in the enzymes of the alpha, mu and pi classes are not retained in bacterial GSTs and therefore a considerable variation in the protein sequence can be tolerated, enabling different enzymes to perform a variety of different conjugation reactions. [Vuilleumier, (1997)]

The central features of the catalytic mechanism are that the nucleophilic species in the active site is the thiolate ion of glutathione and that the reaction is sequential with the addition of glutathione to the electrophilic substrate occurring second to form the ternary complex. [Wilce, *et al.* (1995)] The thiolate ion is about 10^9 times more reactive than its conjugate acid. There are two possible mechanisms for activation of glutathione; either polarisation of the thiol S-H bond by hydrogen-bonding to a suitable base, or ionisation to form the thiolate ion prior to conjugation. A conserved tyrosine residue in the mammalian enzymes, near the N-terminus, has been shown to have a catalytic role by donating a hydrogen bond to and stabilising the thiolate ion of enzyme-bound glutathione. The phenolic-OH group of the tyrosine residue is located in a hydrophobic environment in the active site loop. The backbone of this loop keeps potential hydrogen-bond acceptors away from the tyrosine -OH group, enabling it to function as a hydrogen-bond donor to the sulphur atom of the thiolate ion.

The best characterised bacterial GST is that from *Proteus mirabilis* which is a homodimer of 23kDa subunit molecular weight. [Di Ilio, *et al.* (1988)] It shows high sequence identity with other bacterial GSTs but less than 20% sequence identity with the mammalian GSTs. Bacterial GSTs show most similarity to the theta class of mammalian GST enzymes, but exhibit activity towards a range of compounds which are not substrates of the mammalian enzymes. Their presence in bacteria is believed to have evolved in response to toxic by-products of oxygen metabolism.The crystal structure of the theta class GST from *Lucilla cuprina*, the Australian sheep blowfly, has been reported. [Wilce, *et al.* (1995)] A deep 20Angstrom cleft forms the open, hydrophobic active site which is well separated in each monomer and lined with two leucine, two tyrosine one phenylalanine and one serine residue. The base of the pocket is lined with more polar residues including the main chain atoms of proline, glycine and the hydroxyl-group of the serine residue. A total of fifteen stabilising bonds are made with the glutathione moiety and two water molecules are also within hydrogen-bonding distance of the thiol sulphur atom. In this theta class enzyme there are tyrosine residues present at the active site but the hydroxyl group of the equivalent tyrosine residue in mammalian enzymes is 13.9 Angstroms away from the thiol sulphur atom of glutathione.

Two alternative residues may be responsible for the activation of the thiolate ion - the hydroxyl group of the serine residue (the -OH group is still 3.9Angstroms away from the sulphur atom) or one of the alternative tyrosine residues could hydrogen-bond to the thiol sulphur atom via a water molecule. There is an intricate network of potential hydrogen bonds with water molecules in the active site. Both the serine and tyrosine residues mentioned, however, are highly exposed to solvent, unlike the catalytic tyrosine of the mammalian enzymes. It is also possible that residues from the C-terminal domain may be directly involved in catalysis.

Examination of the glutathione S-transferase enzymes has revealed interesting similarities with dihydropteroate synthase. The enzyme from *P. mirabilis* is similar structurally to DHPS in that they are both homodimers with similar subunit molecular weights and the majority of their polypeptide forms extensive α/β structure. The reaction catalysed by GST centres largely around the stabilisation of a reactive nucleophile in the same manner as proposed for the DHPS reaction. The hydrogen bonds formed by the tyrosine or serine residues, demonstrated as vital for the activation of the thiolate ion, may indicate a similar role for the threonine residue (Thr62) at the active site of DHPS. There were also considerable differences between the amino acid sequences of eukaryotic and prokaryotic species of GSTs, notably also in the conserved residues. This can be clearly seen in the sequence alignments of the DHPS genes, with a higher degree of conservation within the prokaryotic species than overall.

7.7 Future prospects.

As a result of this work on *S. pneumoniae* DHPS, a lot of information has been gathered concerning the structure and mechanism of this enzyme and its inhibition by sulphonamides. Clear foundations have been laid for further crystal structures including a binary complex with pterin pyrophosphate, or a ternary complex with pterin, pyrophosphate and a sulphonamide. The application of pre-steady state kinetics will further clarify the rates of substrate and product binding to the apoprotein. This important enzyme, situated at a critical branch point of the folate biosynthetic pathway, can exist both as a monomer and a dimer, displaying different properties in each form.

One key question to be answered at the earliest opportunity must be which subunit state the enzyme adopts *in vivo*, or whether the development of these different states is an integral part of the regulation of *S. pneumoniae* DHPS activity.

Chapter 8: References.

Achari, A., Somers, D. O., Champness, J. N., Bryant, P. K., Rosemond, J. & Stammers, D. K. (1997) Crystal structure of the anti-bacterial sulfonamide drug-target dihydropteroate synthase. Nature Structural Biology, **4**(6): 490-497.

Allegra, C. J., Boarman, D., Kovacs, J. A., Morrison, P., Beaver, J., Chabner, B. A. & Masur, H. (1990) Interaction of sulfonamide and sulfone compounds with *Toxoplasma gondii* dihydropteroate synthase. J. Clin. Invest., **85**: 371-379.

Babitzke, P., Gollnick, P. & Yanofsky, C. (1992) The *mtr*AB operon of *Bacillus subtilis* encoded GTP Cyclohydrolase I (MtrA), an enzyme involved in folic acid biosynthesis and MtrB, a regulator of tryptophan biosynthesis. J. Bacteriol., **174**(7): 2059-2064.

Banner, D. W., Bloomer, A. C., Petsko, G. A., Phillips, D. C., Pogson, C. I., Wilson, I. A., Corran, P. H., Furth, A. J., Milman, J. D., Offord, R. E., Priddle, J. D. & Waley, S. G. (1975) Structure of chicken muscle triose phosphate isomerase determined crystallographically at 25A resolution using amino acid sequence data. Nature **255**:609-614.

Barton, D. H. & Ollis, W. D. Comprehensive Organic Chemistry. Elsevier Science Ltd. Volume **3**: 344-349.

Basco, L. K., Eldin de Pecoulas, P., Wilson, C. M., Le Bras, J. & Mazabrand, A. (1995) Point mutations in the dihydrofolate reductase-thymidylate synthase gene and pyrimethamine and cycloguanil resistance in *Plasmodium falciparum*. Mol. & Biochem. Parasitology **69**: 135-138.

Beynon, R. J. & Oliver, S. (1995) Protein purification protocols. Avoidance of proteolysis in Extracts.Meth. Molec. Biol., **59**(9): 81-93. Ed. by Doonan, S., Humana Press Inc. Totowa, NJ.

Birdsall, B., King, R. W., Wheeler, M. R., Lewis, C. A., Goode, S. R., Dunlap, R. B. & Roberts, G. C. K. (1983) Correction for light absorption in fluorescence studies of protein-ligand interactions. Anal. Biochem., **132**: 353-361.

Birdsall, B., Burgen, A. S. V. & Roberts, G. C. K. (1980a) Binding of coenzyme analogues to *Lactobacillus casei* dihydrofolate reductase: Binary and ternary complexes. Biochemistry, **19**: 3723-3731.

Birdsall, B. Burgen, A. S. V. & Roberts, G. C. K. (1980b) Effects of coenzyme analogues on the binding of p-aminobenzoyl-L-glutamate and 2,4-diaminopyrimidine to *Lactobacillus casei* dihydrofolate reductase. Biochemistry, **19**: 3732-3737.

Blakley, R. L. & Benkovic, S. J. (ed.) (1984) Folates and pterins , vol. 1. Chemistry and Biochemistry of Folates. John Wiley and Sons, Inc., New York.

Bloom, B. R. & Murray, C. J. L. (1992) Tuberculosis: Commentary on a Reemergent killer. Science, **257**: 1055-1064.

Bognar, A. L., Osborne, C. & Shane, B. (1987) Primary structure of the *Escherichia coli folC* gene and its folylpolyglutamate synthetase - dihydrofolate synthetase product and regulation of expression by an upstream gene. J. Biol. Chem., **262**(25):12337-12343.

Bognar, A. L., Osborne, C., Shane, B., Slinger, S. C. & Ferone, R. (1985) Folylpoly-γ-glutamate synthetase-dihydrofolate synthetase. Cloning and high expression of the *Escherichia coli folC* gene and purification and properties of the gene product. J. Biol. Chem., **260**(9): 5625-5630.

Bolin, J. T., Filman, D. J., Matthews, D. A., Hamlin, R. C. & Kraut, J. (1982) Crystal structures of *Escherichia coli* and *Lactobacillus casei* dihydrofolate reductase refined at 1.7A resolution. I. General features and binding of methotrexate. J. Biol. Chem., **257**(22): 13650-13662.

Brickner, S. J. (1997) Multidrug-resistant bacterial infections: driving the search for new antibiotics. Chemistry & Industry **4**: 131-135.

British Medical Association, Guide to Medicines and Drugs.

Brooks, D. R., Wang, P., Read, M., Watkins, W. M., Sims, P. F. G. & Hyde, J. E. (1994) Sequence variation of the hydroxymethyldihydropterin pyrophosphokinase: dihydropteroate synthase gene in lines of the human malaria parasite, *Plasmodium falciparum*, with differing resistance to sulfadoxine. Eur. J. Biochem., **224**: 397-405.

Brown, G. M. (1962) The biosynthesis of folic acid. II Inhibition by sulfonamides. J. Biol. Chem., **237**(2): 536-540.

Brown, G. M., Weisman, R. A. & Molnar, D. A. (1961) The biosynthesis of folic acid. I Substrate and cofactor requirements for enzymatic synthesis by cell-free extracts of *Escherichia coli*. J. Biol. Chem., **236**(9): 2534-2543.

Burgess, R. R. (1991) Use of polyethyleneimine in purification of DNA-binding proteins. Methods in Enzymology, **208**: 3-11.

Bystroff, C., Oatley, S. J. & Kraut, J. (1990) Crystal structures of *Escherichia coli* dihydrofolate reductase: The $NADP^+$ holoenzyme and the folate-$NADP^+$ ternary complex. Substrate binding and a model for the transition state. Biochemistry **29**: 3263-3277.

Cao, G-J & Sarkar, N. (1992) Identification of the gene for an *Escherichia coli* poly(A) polymerase. Proc. Natl. Acad. Sci. USA. **89**: 10380-10384.

Champness, J. N., Achari, A., Ballantine, S. P., Bryant, P. K., Delves, C. J. & Stammers, D.K. (1994) The structure of *Pneumocystis carinii* dihydrofolate reductase to 1.9A resolution. Structure, **2**(10): 915-924.

Chio, L-C., Bolyard, L. A. Nasr, M. & Queener, S. F. (1996) Identification of a class of sulfonamides highly active against dihydropteroate synthase from *Toxoplasma gondii*, *Pneumocystis carinii*, and *Mycobacterium avium*. Antimicrob. Agents & Chemother. **40**(3): 727-733.

Chung, C. T., Niemela, S. L. & Miller, R. H. (1989) One-step preparation of competent *Escherichia coli*: Transformation and stroage of bacterial cells in the same solution. Proc. Natl. Acad. Sci. USA. **86**: 2172-2175.

Cohen, M. L. Epidemiology of drug resistance: Implications for a post-antimicrobial era. Science **257**: 1050-1055.

Cowman, A. F., Morry, M. J., Biggs, B. A., Cross, G. A. M. & Foote, S. J. (1988) Amino acid changes linked to pyrimethamine resistance in the dihydrofolate reductase-thymidylate synthase gene of *Plasmodium falciparum*. Proc. Natl. Acad. Sci. USA. **85**: 9109-9113.

Dagan, R., Isaachson, M., Lang, R., Karpuch, J., Block, C. & Amir, J. (1994) Epidemiology of pediatric meningitis caused by *Haemophilus influenzae* type b, *Streptococcus pneumoniae*, and *Neisseria meningitidis* in Israel : A 3-year nationwide prospective study. J. Inf. Dis., **169**: 912-916.

Dale, G. E., Broger, C., Hartman, P. G., Langen, H., Page, M. G. P., Then, R. L. & Stuber, D. Characterization of the gene for the chromosomal dihydrofolate reductase (DHFR) of *Staphylococcus epidermidis* ATCC 14990: the origin of the trimethoprim-resistant S1 DHFR from *Staphylococcus aureus*? (1995) J. Bacteriol., **177**(11): 2965-2970.

Dale, G. E., Broger, C., D'Arcy, A., Hartman, P. G., DeHoogt, R., Jolidon, S., Kompis, I., Labhardt, A. M., Langen, H., Locher, H., Page, M. G. P., Stuber, D., Then, R. L., Wipf, B. & Oefner, C. (1997) A single amino acid substitution in *Staphylococcus aureus* dihydrofolate reductase determines trimethoprim resistance. J. Mol. Biol., **266**:23-30.

Dallas, W. S., Dev, I. K. & Ray, P. H. (1993) The dihydropteroate synthase gene, *folP*, is near the leucine tRNA gene, *leuU*, on the *Escherichia coli* chromosome. J. Bacteriol., **175**(23): 7743-7744.

Dallas, W. S., Gowen, J. E., Ray, P. H., Cox, M. J. & Dev, I. K. (1992) Cloning, sequencing and enhanced expression of the dihydropteroate synthase gene of *Escherischia coli* MC4100. J. Bacteriol., **174**(18): 5961-5970.

Dalziel, K. (1957) Initial steady state velocities in the evaluation of enzyme-coenzyme-substrate reaction mechanisms. Acta. Chem. Scand. **11**(10): 1706-1723.

Dieckmann, A. & Jung, A. (1986) Mechanisms of sulfadoxine resistance in *Plasmodium falciparum*. Mol. & Biochem. Parasitol., **19**: 143-147.

Di Ilio, C., Aceto, A., Piccolomini, R., Allocati, N., Faraone, A., Cellini, L., Ravaghan, G. & Federici, G. (1988) Purification and characterisation of three forms of glutathione transferase from *Proteus mirabilis*. Biochem. J., **255**: 971-975.

Dirr, H., Reinemer, P. & Huber, R. (1994) X-ray crystal structures of cytosolic glutathione *S*- transferases. Implications for protein architecture, substrate recognition and catalytic function. Eur. J. Biochem., **220**: 645-661.

Disraely, M. N. & McCann, M. P. (1964) The enzymatic synthesis of folate-like compounds from hydroxymethyldihydropteridine pyrophosphate. J. Biol. Chem., **239**(7): 2259-2266.

Dixon, M. & Webb, E. C. (1964) Enzymes. Second Edition. Longmans.

Dunn, S. M. J., Batchelor, J. G. & King, R. W. (1978) Kinetics of ligand binding to dihydrofolate reductase: Binary complex formation with NADPH and coenzyme analogues. Biochemistry, **17**: 2356-2364.

Farber, G. K. & Petsko, G. A. (1990) The evolution of α/β barrel enzymes. TIBS June ed. 228-234.

Fermer, C. & Swedberg, G. (1997) Adaption to sulfonamide resistance in *Neisseria meningitidis* may have required compensatory changes to retain enzyme function: kinetic analysis of dihydropteroate synthases from *N. meningitidis* expressed in a knockout mutant of *Escherichia coli*. J. Bacteriol. **179**(3): 831-837.

Fermer, C., Kristiansen, B.-E., Skold, O & Swedberg, G. (1995) Sulfonamide resistance in *Neisseria meningitidis* as defined by site-directed mutagenesis could have its origin in other species. J. Bacteriol., **177**(16): 4667-4675.

Fersht, A. (1977) Enzyme structure and Mechanism. Second Edition. W. H. Freeman and Company.

Fiel, S. C., Wilce, M. C. J., Rossjohn, J., Allocati, N., Aceto, A., Di Ilio, C. & Parker, M. W. (1996) Crystallisation and preliminary X-ray analysis of a bacterial glutathione transferase. Acta. Cryst., **D52**: 189-191.

Fildes, P. (1940) The mechanism of the antibacterial action of mercury. Brit. J. Exp. Path., **21**:67-73.

Filman, D. J., Bolin, J. T., Matthews, D. A. & Kraut, J. (1982) Crystal structures of *Escherichia coli* and *Lactobacillus casei* dihydrofolate reductase refined at 1.7A resolution. II. Environment of bound NADPH and implications for catalysis. J. Biol. Chem. **257**(22): 13663-13672.

Fitzgerald, P. M. D. & Masden, N. B. J. (1987) J. Crystal Growth, **76**: 600.

Foote, S. J., Galatis, D & Cowman, A. F. (1990) Amino acids in the dihydrofolate reductase-thymidylate synthase gene of *Plasmodium falciparum* involved in cycloguanil resistance differ from those in pyrimethamine resistance. Proc. Natl. Acad. Sci. USA, **87**: 3014-3017.

Friedkin, M. (1963) Assay of thymidylate synthetase activity. Meth. Enzymol., **6**: 124-129.

Futterman, S. (1957) Enzymatic reduction of folic acid and dihydrofolic acid to tetrahydrofolic acid. J. Biol. Chem., **228**: 1031-1038.

Gill, S. C. & von Hippel, P. H. (1989) Calculation of protein extinction coefficients from amino acid sequence data. Anal. Biochem., **182**: 319-326.

Greenfield, N. J. (1996) Methods to estimate the conformation of proteins and polypeptides from circular dicroism data. Anal. Biochem., **23**: 1-10.

Griffin, M. J. & Brown, G. M. (1964) The biosynthesis of folic acid. III. Enzymatic formation of dihydrofolic acid from dihydropteroic acid and of tetrahydropteroyl -polyglutamic acid compounds from tetrahydrofolic acid. J. Biol. Chem., **239**(1): 310-316.

Gutfreud, H. (1965) An introduction to the study of enzymes. Blackwell Scientific Publications. Oxford.

Hampele, I. C., D'Arcy, A., Dale, G. E., Kostrewa, D., Nielsen, J., Oefner, C., Page, M. G. P., Schonfeld, H. J., Stuber, D. & Then, R. L. (1997) Structure and function of the dihydropteroate synthase from *Staphylococcus aureus*. J. Mol. Biol., **268**: 21-30.

Henderson, G. B. & Huennekens, F. M. (1986) Membrane-associated folate transport proteins. Meth. Enz., **122**: 260-269.

Ho, R. I. (1980) Synthesis and Biological evaluation of 2-amino-4-hydroxy-6-methylpteridine pyrophosphate. Meth. Enz., **66**: 553-556.

Hoch, S. O., Roth, C. W., Crawford, I. P. & Nester, E. W. (1971) Control of tryptophan biosynthesis by the methyltryptophan resistance gene in *Bacillus subtilis*. J. Bacteriol., **105**: 38-45.

Hong, Y-L., Hossler, P. A., Calhoun, D. H. & Meshnick, S. R. (1995) Inhibition of recombinant *Pneumocystis carinii* dihydropteoate synthetase by sulfa drugs. Antimicrob. Agents & Chemother. **39**: 1756-1763.

Hong, Y-L., Hossler, P., Bartlett, M., Queener, S., Smith, J. & Meshnick, S. (1996) Evaluation of sulfa drugs against recombinant *Pneumocystis carinii* dihydropteroate synthetase and *in vivo*. J. Euk. Microbiol. **43**(5): 40S.

Hufton, S. E., Jennings, I. G. & Cotton, R. G. H. (1995) Structure and function of the aromatic amino acid hydroxylases. Biochem. J., **311**: 353-366.

Hummel, J. P. & Dreyer, W. J. (1962) Measurement of protein-binding phenomenon by gel-filtration. Biochim. Biophys. Acta, **63**: 530-532.

Huovinen, P., Sundstrom, L., Swedberg, G. & Skold, O. (1995) Trimethoprim and sulphonamide resistance. Antimicrob. Agents & Chemother. **39**(2): 279-289.

Hyunsook, L., Reyes, V. M. & Kraut, J. (1996) Crystal structures of *Escherichia coli* Dihydrofolate reductase with 5-formyltetrahydrofolate (folinic acid) in two space groups: Evidence for enolization of pteridine O4. Biochemistry, **35**: 7012-7020.

Iwai, K & Okinaka, O. (1980a) Radioassay for dihydropteroate-synthesizing enzyme activity. Meth. Enz., **66**: 560-564.

Iwai, K., Ikeda, M. & Kobashi, M. (1980b) Intracellular distribution, purification and properties of dihydrofolate synthetase from pea seedlings. Meth. Enz., **66**: 581-584.

Jancarik, J & Kim, S-H. (1991) Sparse matrix sampling: a screening method for crystallization of proteins. J. Appl. Cryst., **24**: 409-411.

Jeong, S-S. & Gready, J. E. Development of a spectrofluorimetric method for determining the pKa of pterin-analogue ligands bound to DHFR. In "Chemistry and Biology of Pteridines and Folates." 529-532. (Edited by Ayling, J. E. *et al.*) Plenum Press, New York. 1993.

Kellam, P., Dallas, W. S., Ballantine, S. P. & Delves, C. J. (1995) Functional cloning of the dihydropteroate synthase gene of *Staphylococcus haemolyticus*. FEMS Microbiol. Letters **134**: 165-169.

Koike, K., Poillon, W. N. & Feigelson, P. (1969) J. Biol. Chem., **244**, 3457-3462.

Kovacs, J. A., Powell, F., Voeller, D. & Allegra, C. J. (1993) Inhibition of *Pneumocystis carinii* dihydropteroate synthetase by para-acetamidobenzoic acid: Possible mechanism of action of isoprinosine in human immunodeficiency virus infection. Antimicrob. Agents & Chemother., **37**(6): 1227-1231.

Kristiansen, B-E., Fermer, C., Jenkins, A., Ask, E., Swedberg, G. & Skold, O. (1995) PCR amplicon restriction endonuclease analysis of the chromosomal *dhps* gene of *Neisseria meningitidis*: a method for studying the spread of the disease causing strain in contacts of patients with meningococcal disease. J. Clin. Microbiol., **33**: 1174-1179.

Kristiansen, B-E., Ask, E., Jenkins, A., Fermer, C., Radstrom, P. & Skold, O. (1991) Rapid diagnosis of meningococcal meningitis by polymerase chain reaction. The Lancet, **336**: 1568-1569.

Kristiansen, B-E., Sorensen, B., Bjorvatn, B., Falk, E. S., Fosse, E., Bryn, K., Froholm, L. O., Gaustad, P. & Bovre, K. (1986) An outbreak of group B meningococcal disease: tracing the causative strain of *Neisseria meningitidis* by DNA fingerprinting. J. Clin. Microbiol., **23**: 764-767.

Kyte, J. (1995a) Structure in Protein Chemistry. Garland Publishing, Inc. N.Y. & London.

Kyte, J. (1995b) Mechanism in Protein Chemistry. Garland Publishing, Inc. N. Y. & London.

Lacks, S. A., Greenberg, B. & Lopez, P. (1995) A cluster of four genes encoding enzymes for five steps in the folate biosynthetic pathway of *Streptococcus pneumoniae*. J. Bacteriol., **177**: 66-74.

Liu, J. & Parkinson, J. S. (1989) Genetics and sequence analysis of the *pcnB* locus, an *Escherichia coli* gene involved in plasmid copy number control. J. Bacteriol., **171**(3): 1254-1261.

Lineweaver, H. & Burk, D. (1934) The determination of enzyme dissociation constants.J. Am. Chem. Assoc., **56**: 658-666.

Lopez, P. & Lacks. S. A. (1993) A bifunctional protein in the folate biosynthetic pathway of *Streptococcus pneumoniae* with dihydroneopterin aldolase and hydroxymethyl-pterin pyrophosphokinase activities. J. Bacteriol., **175**(8): 2214-2220.

Lopez, P., Greenberg, B. & Lacks, S. A. (1990) DNA sequence of folate biosynthesis gene *sulD* encoding hydroxymethyldihydropterin pyrophosphokinase in *Streptococcus pneumoniae* and characterisation of the enzyme. J. Bacteriol., **172**(9): 4766-4774.

Lopez, P., Espinosa, M., Greenberg, B. & Lacks, S. A. (1987) Sulfonamide resistance in *Streptococcus pneumoniae*: DNA sequence of the gene encoding Dihydropteroate synthase and characterisation of the enzyme. J. Bacteriol., **169**(9): 4320-4326.

Lopez, P., Espinosa, M., Stassi, D. L. & Lacks, S. A. (1982) Facilitation of plasmid transfer in *Streptococcus pneumoniae* by chromosomal homology. J. Bacteriol., **150**(2): 692-701.

Lowry, O. H., Rosebrough, N. J., Farr, A. L. & Randall, R. J. (1951) Protein measurement with the folin phenol reagent. J. Biol. Chem., **193**: 265-275.

Mahler, H. R. & Cordes, E. H. (1966) Biological Chemistry. Harper & Row, N.Y.

Marton, A., Gulyas, M., Munoz, R. & Tomasz, A. (1991) Extremely high incidence of antibiotic resistance in clinical isolates of *Streptococcus pneumoniae* in Hungary. J. Infect. Dis. **163**: 542-548.

Martorell, G., Gradwell, M. J., Birdsall, B., Bauer, C. J., Frenkeil, T. A., Cheung, H. T. A., Polshakov, V. I., Kuyper, L. & Feeney, J. (1994) Solution structure of bound trimethoprim in its complex with *Lactobacillus casei* dihydrofolate reductase. Biochemistry, **33**: 12416-12426.

Mathis, J. B. & Brown, G. M. (1980) Dihydroneopterin aldolase from *Escherichia coli*. Meth. Enz., **66**: 556-560.

Mathis, J. B. & Brown, G. M. (1970) The biosynthesis of folic acid. Purification and properties of dihydroneopterin aldolase. J. Biol. Chem., **245**(11): 3015-3025.

McDonald, K. O. & Burke, W. F. Jr. (1982) Cloning of the *Bacillus subtilis* sulfanilamide resistance gene in *Bacillus subtilis*. J. Bacteriol., **149**(1): 391-394.

McPherson, A. (1990) Current approaches to macromolecular crystallization. Eur. J. Biochem., **189**: 1-23.

McRee, D. E. (1993) Practical protein crystallography. Academic Press. London.

Meining, W., Bacher, A., Bachmann, L., Schmid, C., Weinkauf, S., Huber, R. & Nar, H. (1995) Elucidation of crystal packing by X-ray diffraction and freeze-etching electron microscopy. Studies on GTP cyclohydrolase I of *Escherichia coli*. J. Mol. Biol., **253**: 208-218.

Neu, H. C. (1992) The crisis in antibiotic resistance. Science **257**: 1064-1073.

Nichols, B. P., Seibold, A. M. & Doktor, S. Z. (1989) *para*-Aminobenzoate synthesis from chorismate occurs in two steps. J. Biol. Chem., **264**(15): 8597-8601.

Ortiz, P. J. & Hotchkiss, R. D. (1966) The enzymatic synthesis of dihydrofolate and dihydropteroate in cell-free preparations from wild-type and sulphonamide-resistant *pneumococcus*. Biochemistry **5**(1): 67-73.

Ortiz, P. J. (1970) Dihydrofolate and dihydropteroate synthesis by partially purified enzymes from wild-type and sulphonamide resistant *pneumococcus*. Biochemistry, **9**(12): 355-360.

Otwinoski, Z. (1986) DENZO: An oscillation data processing program for molecular crystallography. Yale Univ., C.T. USA.

Pares, S., Mouz, N., Petillot, Y., Hakenbeck, R. & Dideberg, O. (1996) X-ray structure of *Streptococcus pneumoniae* PBP2x, a primary penicillin target enzyme. Nature Struct. Biol., **3**(3): 284-289.

Pawelczak, K., Makowski, M., Kempny, M., Dzik, J. M., Balinska, M. & Rode, W. (1993) Sulphonamide antifolates inhibiting thymidylate synthase: synthesis, enzyme inhibition and cytotoxicity. In Chemistry and Biology of Pteridines and Folates , Ed. by Ayling, J. E., *et al.* Plenum Press , NY. 625-628.

Pelletier, J. N. & Mackenzie, R. E. (1995) Binding and interconversion of tetrahydrofolates at a single site in the bifunctional methylenetetrahydrofolate dehydrogenase / cyclohydrolase. Biochemistry, **34**: 12673-12680.

Peltola, H. (1983) Meningococcal disease: still with us. Rev. Infect. Dis., **5**: 71-91.

Perutz, M. (1992) Protein structure: New approaches to disease and therapy. Freeman, W. H., N.Y.

Prescott, L. M., Harley, J. P. & Klein, D. A. (1990) Microbiology. Wm. C. Brown Publishers.

Radstrom, P., Fermer, C., Kristiansen, B-E., Jenkins, A., Skold, O. & Swedberg, G.(1992) Transformational exchanges in the dihydropteroate synthase gene of *Neisseria meningitidis*: A novel mechanism for acquisition of sulfonamide resistance. J. Bacteriol., **174**(20): 6386-6393.

Radstrom, P. & Swedberg, G. (1988) RSF1010 and a conjugative plasmid contain *sulII*, one of two known genes for plasmid-borne resistant dihydropteroate synthase. Antimicrob. Agents & Chemother., **32**(11): 1684-1692.

Rebeille, F., Macherel, D., Mouillon, J-M., Garin, J. & Douce, R. (1997) Folate biosynthesis in higher plants: purification and molecular cloning of a bifunctional 6-hydroxymethyl-7,8-dihydropterin pyrophosphokinase/7,8-dihydropteroate synthase localised in mitochondria. EMBO J. **16**(5): 947-957.

Reynolds, J. J. & Brown, G. M. (1964) The biosynthesis of folic acid. IV Enzymatic synthesis of dihydrofolic acid from guanine and ribose compounds. J. Biol. Chem., **239**(1): 317-325.

Richey, D. R. & Brown, G. M. (1969) The biosynthesis of folic acid.IX Purification and properties of the enzymes required for the formation of dihydropteroic acid. J. Biol. Chem., **244**(6): 1582-1592.

Roland, S., Ferone, R., Harvey, R. J., Styles, V. L. & Morrison, R. W. (1979) The characteristics and significance of sulfonamides as substrates for *Escherichia coli* dihydropteroate synthase. J. Biol. Chem., **254**: 10337-10345.

Sambrook, J., Fritsch, E. F. & Maniatis, T. (1989) Molecular cloning: a laboratory manual. Second edition. Cold Spring Harbor Laboratory Press. Cold Spring Harbor, N.Y.

Selbie, F. R. (1940) The inhibition of the action of sulphanilamide in mice by p-aminobenzoic acid. Br. J. Exp. Pathol. **21**: 90-93.

Shiota, T., Richey, D. P. & Brown, G. M. (1969) The biosynthesis of Folic Acid. IX Purification and properties of the enzymes required for the formation of dihydropteroic acid. J. Biol. Chem. **244**(6): 1582-1592.

Shiota, T., Bargh, C. M., Jackson, R. & Dillard, R. (1969) The enzymatic synthesis of hydroxymethyl-dihydropteridine pyrophosphate and dihydrofolate. Biochemistry, **8**: 5022-5028.

Shiota, T., Disraely, M. N. & McCann, M. P. (1964) The enzymatic synthesis of folate-like compounds from hydroxymethyldihydropteridine pyrophosphate. J. Biol. Chem. **239**(7): 2259-2266.

Sifaoui, F., Kitzis, M-D. & Gutmann, L. (1996) In vitro selection of one-step mutants of *Streptococcus pneumoniae* resistance to different oral β-lactam antibiotics is associated with alterations of PBP2x. Antimicrob. Agents & Chemother. **40**(1): 152-156.

Simor, A. E., Louie, M., The Canadian bacterial surveillance network & Low, D. E. (1996) Canadian national survey of prevalence of antimicrobial resistance among clinical isolates of *Streptococcus pneumoniae*. Antimicrob. Agents & Chemother. **40**(9): 2190-2193.

Slock, J., Stahly, D. P., Han, C-Y., Six, E. W. & Crawford, I. P. (1990) An apparent *Bacillus subtilis* folic acid biosynthetic operon containing *pab*, an amphibolic *trp*G gene, a third gene required for synthesis of *para*-aminobenzoic acid , and the dihydropteroate synthase gene. J. Bacteriol., **172**(12): 7211-7226.

Strauss, E.J. & Falkow, S. (1997) Microbial Pathogenesis: Genomics and Beyond. Science, **276**: 707-711.

Streitweiser, A. Jr. & Heathcock, C. H. (1989) Introduction to organic chemistry. Third edition. Maxwell Macmillan.

Swedberg, G., Fermer, C. & Skold, O. Point mutations in the dihydropteroate synthase gene causing sulphonamide resistance. in "Chemistry and Biology of Pteridines and Folates." 555-558 (Edited by Ayling, J. E. *et al.*) Plenum Press, New York. 1993.

Swedberg, G. & Skold, O. (1980) Characterisation of different plasmid-borne dihydropteroate synthases mediating bacterial resistance to sulphonamides. J. Bacteriol., **142**: 1-7.

Swedberg, G., Castensson, S. & Skold, O. (1979) Characterisation of mutationally altered dihydropteroate synthase and its ability to form a sulphonamide-containing dihydrofolate analogue. J. Bacteriol., **137**(1): 129-136.

Talarico, T. L., Ray, P. H., Dev, I. K., Merrill, B. M. & Dallas, W. S. (1992) Cloning, sequence analysis and overexpression of *Escherichia coli folK*, the gene coding for 7,8-dihydro-6-hydroxymethylpterin pyrophosphokinase. J. Bacteriol., **174**: 5971-5977.

Talarico, T. L., Dev, I. K., Dallas, W. S., Ferone, R. & Ray, R. H. (1991) Purification and partial characterisation of 7,8-dihydro-6-hydroxymethylpterin pyrophosphokinase and 7,8-dihydropteroate synthase from *Escherichia coli* MC4100. J. Bacteriol., **173**(21): 7029-7032.

Thaller, C., Weaver, L. H., Eichele, G., Wilson, E., Karlsson, R. & Jansonius, J. N. (1981) Repeated seeding technique for growing large single crystals of proteins. J. Mol. Biol. **147**: 465-469.

Thijssen, H. H. W. (1973) A simplified radioassay method for dihydropteroate synthetase activity in *Escherichia coli* and its application for an inhibition study of p-aminobenzoic acid derivatives. Anal. Biochem., **53**: 579-585.

Thijssen, H. H. W. (1980) Cell-free dihydropteroate synthetase activity - its use to investigate the relationship between structure and activity of p-aminobenzoic acid derivatives. Meth. Enz., **66**: 570-576.

Thomson, K. S., Chartrand, S. A., Sanders, C. C. & Block, S. L. (1997) Trovafloxacin, a new fluoroquinolone with potent activity against *Streptococcus pneumoniae*. Antimicrob. Agents & Chemother. **41**(2): 478-480.

Triglia, T. & Cowman, A. F. (1994) Primary structure and expression of the dihydropteroate synthetase gene of *Plasmodium falciparum*. Proc. Natl. Acad. Sci. USA., **91**: 7149-7153.

Trujillo, M., Donald, R. G. K., Roos, D. S., Greene, P. J. & Santi, D. V. (1996) Heterologous expression and characterisation of the bifunctional dihydrofolate reductase-thymidylate synthase enzyme of *Toxoplasma gondii*. Biochemistry **35**: 6366-6374.

Upson, R. H., Haugland, R. P., Malekzadeh, M. N. & Haugland, R. P. (1996) A spectrophotometric method to measure enzymatic activity in reactions that generate inorganic pyrophosphate. Anal. Biochem., **243**: 41-45.

van Duijkeren, Vulto, A. G. & van Miert, A. S. J. P. A. M.(1994) Trimethoprim/sulfonamide combinations in the horse: a review. J. vet. Pharmacol. Therap. **17**: 64-73.

Viladrich, P. F., Cabellos, C., Pallares, R., Tubau, F., Martinez-Lacasa, J., Linares, J. & Gudiol, F. (1996) High doses of cefotaxime in treatment of adult meningitis due to *Streptococcus pneumoniae* with decreased susceptibilities to broad-spectrum cephalosporins. Antimicrob. Agents & Chemother. **40**(1): 216-220.

Voeller, D. M. & Allegra, C. J. (1994) Dihydropteroate synthetase antibodies. J. Inf. Dis., **169**: 1414- 1415.

Voeller, D., Kovacs, J., Audrawis, V., Chu, E., Masur, H. & Allegra, C. (1994) Interaction of *Pneumocystis carinii* dihydropteroate synthase with sulphonamides and diaminodiphenyl sulphone. (Dapsone). J. Infect. Dis., **196**(2): 456-459.

Volpe, F., Ballantine, S. P. & Delves, C. J. (1993) The multifunctional folic acid synthesis *fas* gene of *Pneumocystis carinii* encodes dihydroneopterin aldolase, hydroxymethyldihydropterin pyrophosphokinase and dihydropteroate synthase. Eur. J. Biochem., **216**: 449-458.

Volpe, F., Dyer, M., Scaife, J. G., Darby, G., Stammers, D. K. & Delves, C. J. (1992) The multifunctional folic acid synthesis *fas* gene of *pneumocystis carinii* appears to encode dihydropteroate synthase and hydroxymethyldihydropterin pyrophosphokinase. Gene, **112**: 213-218.

Vuilleumier, S. (1997) Bacterial glutathione *S*-transferases: What are they good for? J. Bacteriol., **179**(5): 1431-1441.

Wang, P., Brooks, D. R., Sims, P. F. G. & Hyde, J. E. (1995) A mutation-specific PCR system to detect sequence variation in the dihydropteroate synthetase gene of *Plasmodium falciparum*. Molecular and Biochemical Parasitology, **71**:115-125.

Walter, R. D. & Konigk, E. (1980) 7,8-dihydropteroate-synthesizing enzyme from *Plasmodium chabaudi*. Meth. Enz., **66**: 564-570.

Webb, S. R. & Ferone, R. (1976) Inhibition of dihydrofolate synthetase by folate, homofolate, pteroate and homopteroate and their reduced forms. Biochim. Biophys. Acta., **422**: 419-426.

Weisman, R. A. & Brown, G. M. (1964) The biosynthesis of Folic Acid. V. Characteristics of the enzyme system that catalyses the synthesis of dihydropteroic acid. J. Biol. Chem., **239**(1): 326-331.

Wilce, M. C. J., Board, P. G., Feil, S. C. & Parker, M. W. (1995) Crystal structure of a theta-class glutathione transferase. EMBO J. **14**(10): 2133-2143.

Wilson, I. A., Rini, J. M., Fremont, D. H., Fieser, G. G. & Stura, E. A. (1991) X-ray crystallographic analysis of free and antigen-complexed Fab fragments to investigate structural basis of immune recognition. Meth. Enzymol., **203**: 153-176.

Wingard, L. B. (1991) Human Pharmacology: Molecular to Clinical. Wolfe Medical Publications Ltd.

Wise, E. M. Jr. & Abou-Donia, M. M. (1975) Sulfonamide resistance mechanism in *Escherichia coli*: R plasmids can determine sulphonamide-resistant dihydropteroate synthases. Proc. Natl. Acad. Sci. USA., **72**: 2621-2625.

Woods, D. D. (1940) The relation of p-aminobenzoic acid to the mechanism of the action of sulphanilamide. Brit. J. Exp. Pathol., **21**: 74-90.

Chapter 9: Appendix.

9.1 The relationships between velocity and substrate concentrations for fixed order and random order ternary complex reaction mechanisms.

Model for a fixed order ternary complex reaction.

$$[E_{free}] + [A_{free}] \overset{K_A}{\rightleftharpoons} [EA] + [B_{free}] \overset{K_B}{\rightleftharpoons} [EAB] \xrightarrow{k} \text{Products}$$

The model assumes firstly that k is slow compared the rates in the first two equilibria - K_A and K_B, and secondly that $[A_{total}] \cong [A_{free}]$ and $[B_{total}] \cong [B_{free}]$ because $[A_{free}]$, $[B_{free}] >> [EA]$, $[EAB]$

The equation describing this model is:

$v = V_{max} / (1 + K_A / [A_{total}] + K_B / [B_{total}] + K_A K_{\tilde{B}} / [B_{total}].[A_{total}])$ [Dixon & Webb, (1964)]

This equation was used to model the kinetic data in Chapter 5.

Model for a random order ternary complex reaction mechanism.

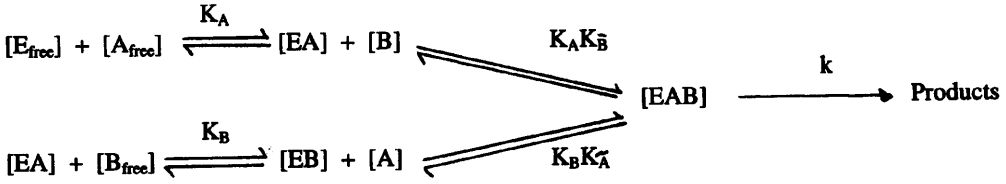

For a random order ternary complex reaction mechanism, the model assumes firstly that k is slow compared the rates in the first four equilibria - K_A, K_B, K_s^A and K_s^B, and secondly that $[A_{free}] \cong [A_{total}]$ and $[B_{free}] \cong [B_{total}]$ because $[A_{free}]$,$[B_{free}]>>[EA]$, $[EB]$ and $[EAB]$

The equation describing this model is:

$v = V_{max}/(1 + K_s^A.K_B/K_s^B.[A_{total}] + K_B/[B_{total}] + K_s^A.K_B/[A_{total}].[B_{total}])$

This equation was used to model the kinetic data in Chapter 5.

9.2 Derivation of the relationship between velocity, substrate concentrations and inhibitor concentrations for competitive inhibition of a fixed order ternary complex mechanism.

Model

$$[E_{free}] + [A_{free}] \overset{K_A}{\rightleftharpoons} [EA] + [B_{free}] \overset{K_B}{\rightleftharpoons} [EAB] \xrightarrow{k} \text{Products}$$

$$+$$

$$[I_{free}] \overset{K_i}{\rightleftharpoons} [EAI]$$

Equilibria and their respective equations:

$$[E_{free}] + [A_{free}] \overset{K_A}{\rightleftharpoons} [EA] \text{ where } K_A = [E].[A_{free}]/[EA] \text{ or } [EA] = [E].[A_{free}]/K_A \quad (1)$$

$$[EA] + [B_{free}] \overset{K_B}{\rightleftharpoons} [EAB] \text{ where } K_B = [EA].[B_{free}]/[EAB] \text{ or } [EAB] = [EA].[B_{free}]/K_B \quad (2)$$

$$[EA] + [I_{free}] \overset{K_i}{\rightleftharpoons} [EAI] \text{ where } K_i = [EA].[I_{free}]/[EAI] \text{ or } [EAI] = [EA].[I_{free}]/K_i \quad (3)$$

At equilibrium: $[E_{total}] = [E_{free}] + [EA] + [EAB] + [EAI]$ (4)

Substituting into equation (4) for $[E_{free}]$ using equation (1) and for $[EAI]$ using equation (3):

$[E_{total}] = K_A.[EA]/[A_{free}] + [EA] + [EAB] + [EA].[I_{free}]/K_i$ (5)

Pulling out $[EA]$ from the expressions in equation (5) gives:

$[E_{total}] = [EA] (K_A/[A_{free}] + 1 + [I_{free}]/K_i) + EAB$ (6)

Substituting for [EA] using equation (2), equation (5) becomes:
$[E_{total}] = K_B.[EAB]/[B_{free}] (K_A/[A_{free}] + 1 + [I_{free}]/K_i) + [EAB]$ (7)

Multiplying out equation (7):
$[E_{total}] = K_B.[EAB].K_A/[B_{free}].[A_{free}] + K_B.[EAB]/[B_{free}] + K_B.[EAB].[I_{free}]/[B_{free}].K_i + [EAB]$ (8)

Pulling out the expression for [EAB] from equation (8) gives:
$[E_{total}] = [EAB] \{(K_B.K_A/[B_{free}].[A_{free}]) + K_B/[B_{free}] + (K_B.[I_{free}]/K_i.[B_{free}]) + 1\}$ (9)

Putting the bracket contents over the same common denominator:
$[E_{total}] = [EAB]\{(K_iK_B.K_A + K_i.K_B.[A_{free}] + K_i[B_{free}].[A_{free}] + K_B.[A_{free}].[I_{free}])/K_i.[B_{free}].[A_{free}]\}$ (10)

Simplifying the bracket cancelling out the K_i values where possible:
$[E_{total}] = [EAB]\{(K_BK_A + K_B[A_{free}] + K_B[I_{free}].[A_{free}]/K_i + [B_{free}].[A_{free}])/[B_{free}].[A_{free}]\}$ (11)

Simplifying the bracket further by drawing together common terms:
$[E_{total}] = [EAB] \{(K_B.K_A + K_B.[A_{free}](1 + [I_{free}]/K_i) + [B_{free}].[A_{free}])/[B_{free}].[A_{free}]\}$ (12)

Rearranging equation (12) in terms of [EAB] gives:
$[EAB] = [E_{total}]\{[B_{free}].[A_{free}]/ (K_B.K_A + K_B.[A_{free}](1 + [I_{free}]/K_i) + [B_{free}].[A_{free}]\}$ (13)

We know from steady-state kinetics that velocity (v) = k.[EAB] (see model above). Therefore in equation (13): $v = k.[E_{total}]\{[B_{free}].[A_{free}]/ (K_B.K_A + K_B.[A_{free}](1 + [I_{free}]/K_i) + [B_{free}].[A_{free}]\}$ (14)

Also $V_{max} = k.[E_{total}]$, therefore equation (14) simplifies to:
$v = V_{max}.[B_{free}].[A_{free}]/ (K_B.K_A + K_B.[A_{free}](1 + [I_{free}]/K_i) + [B_{free}].[A_{free}]\}$ (15)

Since $[A_{total}] = [A_{free}] + [EA] + [EAB]$ and $[A_{total}] \cong [A_{free}]$ because $[A_{free}] >> [EA]$ or $[EAB]$
and $[B_{total}] \cong [B_{free}]$ because $[B_{free}] >> [EAB]$
Equation (15) for competitive inhibition of a fixed order ternary complex mechanism:
$v = V_{max}.\{[B_{total}].[A_{total}]/K_B.K_A + K_B.[A_{total}](1 + [I_{free}]/K_i) + [B_{total}].[A_{total}]\}$ (15)

Comparing this equation to that which describes the ternary complex mechanism, it can be seen that competitive inhibition changes K_B by a factor $(1 + [I_{free}]/Ki)$. If one substrate is assumed to be in excess, e.g. substrate B, the expression simplifies to:
$v = (V_{max} . A)/(K_A.(1+I/K_i) + A)$
This equation was used in determining K_i values for folate, dihydrofolate, tetrahydrofolate and methotrexate where one of the two substrates, pABA or pterin pyrophosphate was in excess.

9.3 Derivation of the relationship used to obtain the sulphonamide equilibrium binding constant for weak binding to DHPS.

An expression for the concentration of sulphonamide $[I_{total}]$ and the binding constant for the inhibitor K_i is required, in terms of the measured variables, bound pABA [EAB] and total pABA [T].

Model:

$[E_{free}] + [A_{free}] \overset{K_A}{\rightleftharpoons} [EA]$ THEN $[EA] + [B_{free}] \overset{K_B}{\rightleftharpoons} [EAB]$ OR $[EA] + [I_{free}] \overset{K_i}{\rightleftharpoons} [EAI]$ (1)

At equilibrium: $[E_{total}] = [E_{free}] + [EA] + [EAB] + [EAI]$ (2)
where A is pyrophopshate, B is pABA and I is a weakly-bound sulphonamide. One assumption made is that $[A_{total}]$ is much greater than $[E_{total}]$, therefore $[E_{total}] = [EA] + [EAB] + [EAI]$ and $[E_{free}]$ is negligible (3)
From equation (1) $K_i = [EA] . [I_{free}] / [EAI]$ (4)

which can be rearranged to give: $[EAI] = [EA] . [I_{free}] / K_i$ (5)

Using equation (5) and substituting for [EAI], equation (3) becomes:
$[E_{total}] = [EA] + [EAB] + ([EA] . [I_{free}] / K_i)$ (6)

Pulling out the expression [EA], equation (6) becomes:
$[E_{total}] = [EA] (1 + [I_{free}] / K_i) + [EAB]$ (7)

From equation (1) $K_B = [EA] . [B_{free}] / [EAB]$ (8)

which can be rearranged to give $[EA] = K_B . [EAB] / [B_{free}]$ (9)

Using equation (9) and substituting for [EA], equation (7) becomes:
$[E_{total}] = (K_B . [EAB] / [B_{free}]) . (1 + [I_{free}] / K_i) + [EAB]$ (10)

For these weakly-bound sulphonamides another assumption can be made. At equilibrium $[I_{total}] = [EAI] + [I_{free}]$ However $[I_{total}]$ is much greater than $[E_{total}]$ so [EAI] is very small compared with $[I_{free}]$. Therefore $[I_{total}] \cong [I_{free}]$ and equation (11) becomes:
$[E_{total}] = (K_B . [EAB] / [B_{free}]) . (1 + [I_{total}] / K_i) + [EAB]$ (12)

Finally, $[B_{free}]$ can be written in terms of the measured variables [T] and [EAB]:
$[B_{free}] = [T] - [EAB]$ (13)

Using equation (13) and substituting for $[B_{free}]$, equation (12) becomes,
$[E_{total}] = \{(K_B . [EAB]) / ([T] - [EAB])\} . (1 + [I_{total}] / K_i) + [EAB]$ (14)
This is an expression for $[I_{total}]$ and K_i in terms of [T] and [EAB]. Solving this equation for [EAB] involved a quadratic function. The expression became:
$[EAB] = \{([E_{total}] + [T] + K_B + K_B.[I_{total}] / K_i] \pm / ([E_{total}] + [T] + K_B + K_B.[I_{total}] / K_i)^2 - 4.[E_{total}].[T]\} / 2$

For the data fitting procedure involving the PSI-PLOT Program, the fitting equations became:
$-([E_{total}] + [T] + K_B + K_B . [I_{total}] / K_I) = X$

$[E_{total}] . [T] = Z$

$[EAB] = \{ - X \pm / (X^2 - 4 . Z) \} / 2$

9.4 Derivation of the relationship used to obtain the sulphonamide equilibrium binding constant for strong binding to DHPS.

An expression for the concentration of sulphonamide $[I_{total}]$ and the binding constant for the inhibitor K_i is required, in terms of the measured variables, bound pABA [EAB] and total pABA [T].

Model:

$$[E_{free}] + [A_{free}] \overset{K_A}{\rightleftharpoons} [EA] \text{ THEN } [EA] + [B_{free}] \overset{K_B}{\rightleftharpoons} [EAB] \text{ OR } [EA] + [I_{free}] \overset{K_i}{\rightleftharpoons} [EAI]$$

where A is pyrophopshate, B is pABA and I is a strongly-bound sulphonamide. One assumption made is that $[A_{total}] >> [E_{total}]$, therefore $[E_{free}]$ is negligible. Another is that $[I_{total}]$ is no longer equal to $[I_{free}]$ because of the strong binding and becomes $[I_{total}] = [I_{free}] + [EAI]$ (1)
At equilibrium: $[E_{total}] = [EA] + [EAB] + [EAI]$ (2)

From the model above: $K_i = [EA] . [I_{free}] / [EAI]$ (3)

Which can be rearranged to: $[I_{free}] = K_i . [EAI] / [EA]$ (4)

Substituting this equation into equation (1): $[I_{total}] = K_i . [EAI] / [EA] + [EAI]$ (5)

Pulling out the [EAI] terms from equation (5): $[I_{total}] = [EAI] (K_i / EA + 1)$ (6)

Rearranging equation (6) in terms of [EAI]: $[EAI] = [I_{total}] . [EA] / ([EA] + K_i)$ (7)

Using equation (7) and substituting for the [EAI] term in equation (2):
$[E_{total}] = [EA] + [EAB] + \{I_{total}] . [EA] / ([EA] + K_i)$ (8)

Multiplying through by ([EA] + K_i) in equation (8) gives:
$[E_{total}]([EA] + K_i) = [EA]([EA] + K_i) + [EAB]([EA] + K_i) + [I_{total}].[EA]$ (9)

Then $[E_{total}].[EA] + [E_{total}].K_i = [EA]^2 + [EA].K_i + [EAB].[EA] + [EAB].K_i + [I_{total}].[EA]$ (10)

Pulling out the [EA] terms to one side of the equation:
$[EA]^2 + [EA](K_i + [EAB] + [I_{total}] - [E_{total}]) + (K_i - [EAB] - K_i.[E_{total}]) = 0$ (11)

From the original equilibria: $K_B = [EA] . [B_{free}] / [EAB]$ (12)

Which can be rearranged to give: $[EA] = K_B . [EAB] / [B_{free}]$ (13)

An expression in terms of [T] and [EAB] is required. Since $[B_{free}] = [T] - [EAB]$ this can be substituted into equation (13) to give: $[EA] = K_B . [EAB] / ([T] - [EAB])$ (14)
Substituting for [EA] in equation (11) using equation (14):
$K_B^2.[EAB]^2 / ([B_{total}] - [EAB])^2 + K_B.[EAB] /\{([B_{total}] - [EAB])(K_i + [EAB] + [I_{total}] - [E_{total}])\} +$
$(K_i.[EAB] - K_i.[E_{total}]) = 0$ (15)

Multiplying through by ($[B_{total}]$ - [EAB]) gives:
$K_B^2.[EAB]^2 + (K_B.[EAB]).([B_{total}] - [EAB]) \{K_i + [EAB] + [I_{total}] - [E_{total}]\} + (K_i.[EAB] -$
$K_i.[E_{total}]).([B_{total}] - [EAB])^2 = 0$ (16)

With the $([B_{total}] - [EAB])^2$ term written out in full, equation (16) becomes:
$K_B^2.[EAB]^2 + (K_B.[EAB]).([B_{total}] - [EAB]) \{K_i + [EAB] + [I_{total}] - [E_{total}]\} + (K_i.[EAB] -$
$K_i.[E_{total}]).([B_{total}]^2 - 2[EAB].[B_{total}] + [EAB]^2) = 0$ (17)

Multiplying this expression out:
$K_B^2.[EAB]^2 + (K_B.[EAB].[B_{total}] - K_B.[EAB]^2) \{K_i + [EAB] + [I_{total}] - [E_{total}]\} + K_i.[EAB].[B_{total}]^2 -$
$2.[EAB]^2.[B_{total}].K_i + K_i.[EAB]^3 - K_i.[E_{total}].[B_{total}]^2 + 2.[EAB].[B_{total}].K_i.[E_{total}] - K_i.[E_{total}].[EAB])^2 = 0$ (18)

And again:
$K_B^2.[EAB]^2 + K_B.[EAB].[B_{total}].K_i + K_B.[EAB]^2.[B_{total}] + K_B.[EAB].[B_{total}].[I_{total}] -$
$K_B.[EAB].[B_{total}].[E_{total}]\} - K_B.[EAB]^2.K_i - K_B.[EAB]^3 - K_B.[EAB]^2.[I_{total}] + K_B.[EAB]^2.[E_{total}] +$
$K_i.[EAB].[B_{total}]^2 - 2.[EAB]^2.[B_{total}].K_i + K_i.[EAB]^3 - K_i.[E_{total}].[B_{total}]^2 + 2.[EAB].[B_{total}].K_i.[E_{total}] -$
$K_i.[E_{total}].[EAB]^2 = 0$ (19)

Collecting together the [EAB] terms:
$[EAB]^3\{K_i-K_B\} + [EAB]^2\{[K_B^2 + K_B.[B_{total}] - K_B.K_i - K_B.[I_{total}] + K_B.[E_{total}] - 2.[B_{total}].K_i - K_i.[E_{total}]\} +$
$[EAB]\{K_B.[B_{total}].K_i + K_B.[B_{total}].[I_{total}] - K_B.[B_{total}].[E_{total}] + K_i.[B_{total}]^2 + 2.K_i.[B_{total}].[E_{total}]\} -$
$K_i.[E_{total}].[B_{total}]^2 = 0$ (20)
This is a cubic equation describing the relationship between bound pABA and total pABA [B_{total}] and a strongly-binding sulphonamide. This cubic could not be solved using the Psi-Plot Program and so the data was fitted using a spreadsheet program. The coefficients of the cubic function were computed using a spreadsheet and the parameters were altered manually to minimise the sum of the squares.

9.5 Derivation of the relationship used to obtain the sodium pyrophosphate equilibrium binding constant.

An expression for the concentration of pyrophosphate [A_{total}] and the K_A was required in terms of both bound pABA [EAB] and total pABA [T].

At equilibrium: $[A_{total}] = [A_{free}] + [EA] + [EAB]$

Here the assumption is made that $[A_{total}] \cong [A_{free}]$ because the concentration of pyrophosphate is very large with respect to enzyme concentration, therefore [EA] and [EAB] are negligible. **In the binding experiments:**

$$[E_{free}] + [A_{free}] \overset{K_A}{\rightleftharpoons} [EA] \qquad [EA] + [B_{free}] \overset{K_B}{\rightleftharpoons} [EAB] \qquad (1)$$

where A represents the binding of pyrophosphate and B represents the binding of pABA.

From equation (1) above: $K_A = [E_{free}].[A_{free}] / [EA]$ (2)

which can be rearranged to give: $[E_{free}] = [EA]. K_A / [A_{free}]$ (3)

From the assumption described above $[A_{total}] \cong [A_{free}]$ so equation (3) becomes:

$[E_{free}] = [EA]. K_A / [A_{total}]$ (4)

At equilibrium: $[E_{total}] = [E_{free}] + [EA] + [EAB]$ (5)

Using equation (4) and substituting for $[E_{free}]$, equation (5) becomes:

$[E_{total}] = [EA]. K_A / [A_{total}] + [EA] + [EAB]$ (6)

Pulling out the expression [EA], equation (6) becomes:

$[E_{total}] = [EA](1 + K_A / [A_{total}]) + [EAB]$ (7)

From equation (1): $K_B = [EA]. [B_{free}] / [EAB]$ (8)

which can be written in terms of [EA]: $[EA] = K_B . [EAB] / [B_{free}]$ (9)

Using equation (9) and substituting for [EA], equation (7) becomes:

$[E_{total}] = (K_B. [EAB] / [B_{free}]).(1 + K_A / [A_{total}]) + [EAB])$ (10)

As stated, an expression was required in terms of [EAB] and [T]. $[B_{free}]$ can be written in terms of [EAB] and [T]: $[B_{free}] = [T] - [EAB]$ (11)

So using equation (11) and substituting for $[B_{free}]$, equation (10) becomes:

$[E_{total}] = (K_B . [EAB]) / ([T] - [EAB]) . (1 + K_A / [A_{total}]) + [EAB])$ (12)

This is an expression for the concentration of pyrophosphate [A_{total}] and K_A in terms of [EAB] and [T]. Solving this equation for [EAB] involved a quadratic function. The expression became:

$[EAB] =$

$\{([T] + [E_{total}] + K_B + K_B.K_A / [A_{total}] \pm / \{([T] + [E_{total}] + K_B + K_B .K_A / [A_{total}])^2 - 4.[E_{total}].[T]\}\} / 2$

For the data-fitting procedure involving the PSI-PLOT Program, the fitting equations became:

$- ([T] + [E_{total}] + K_B + K_B.K_A / [A_{total}]) = I$

$[E_{total}] . [T] = P$

$[EAB] = \{- I \pm / (I1^2 - 4 . P) \} / 2$

9.6 Derivation of the relationship used to obtain the *para*-Aminobenzoic acid equilibrium binding constant.

An expression for the concentration of bound pABA [EAB] and the binding constant for pABA, K_B was required in terms of the total pABA concentration [T].

Here the assumption is made that $[E_{total}] = [EA] + [EAB]$; $[E_{free}]$ is very small with respect to [EA] and [EAB] and can be omitted from the equation. In the binding experiments, it has been assumed that pyrophosphate must bind to DHPS before pABA is capable of binding. Therefore the equilibria are:

$$[E_{free}] + [A_{free}] \overset{K_A}{\rightleftharpoons} [EA] \qquad [EA] + [B_{free}] \overset{K_B}{\rightleftharpoons} [EAB] \qquad (1)$$

where A represents pyrophosphate and B represents pABA. From equation (1) we obtain the expression:

$$K_B = [EA].[B_{free}] / [EAB] \qquad (2)$$

From the assumptions described above: $[E_{total}] = [EA] + [EAB]$ (3)

Equation (3) can be rearranged to give: $[EA] = [E_{total}] - [EAB]$ (4)

Using equation (4) and substituting for [EA], equation (2) becomes:

$$K_B = ([E_{total}] - [EAB]).[B_{free}] / [EAB] \qquad (5)$$

As stated an expression was required in terms of [EAB] and [T]. $[B_{free}]$ can be written in terms of [EAB] and [T]: $[B_{free}] = [T] - [EAB]$ (6)

So using equation (6) and substituting for $[B_{free}]$, equation (5) becomes:

$$K_B = \{ ([E_{total}] - [EAB]).([T] - [EAB]) \} / [EAB] \qquad (7)$$

This is an expression for K_B in terms of [EAB] and [T].

For the data fitting procedure involving the PSI-PLOT Program, equation (7) above was solved for [EAB]. This involved a quadratic function and the expression became:

$$[EAB] = \{(K_B + [E_{total}] + [T]) \pm / (K_B + [E_{total}] + [T])^2 - 4.[E_{total}].[T]\} / 2$$

The fitting equations then became:

$$-(K_B + [E_{total}] + [T]) = I$$

$$[E_{total}].[T] = P$$

$$[EAB] = \{ -I \pm / (I^2 - 4.P) \} / 2$$

The above expression was also used to obtain equilibrium binding constants for pABA in the presence of differing concentrations of pterin. (Section 5.6.5)

9.7 Derivation of the relationsh ip used to obtain the dihydropteroate equilibrium binding constant.

An expression for the concentration of bound dihydropteroate [EAB] and the binding constant for dihydropteroate, K_B was required in terms of the total dihydropteroate concentration [T]. Here the assumption is made that $[E_{total}] = [EA] + [EAB]$ because $[E_{free}]$ is very small with respect to [EA] and [EAB] and can be omitted from the equation. In the binding experiments, it has been assumed that pyrophosphate must bind to DHPS before the dihydropteroate is capable of binding. Therefore the equilibria are:

$$[E_{free}] + [A_{free}] \overset{K_A}{\rightleftharpoons} [EA] \qquad [EA] + [B_{free}] \overset{K_B}{\rightleftharpoons} [EAB] \qquad (1)$$

where A represents pyrophosphate and B represents dihydropteroate.

From equation (1) we obtain the expression: $K_B = [EA].[B_{free}] / [EAB]$ (2)

From the assumptions described above: $[E_{total}] = [EA] + [EAB]$ (3)

Equation (3) can be rearranged to give: $[EA] = [E_{total}] - [EAB]$ (4)

Using equation (4) and substituting for [EA], equation (2) becomes:

$$K_B = ([E_{total}] - [EAB]).[B_{free}] / [EAB] \qquad (5)$$

As stated an expression was required in terms of [EAB] and [T]. $[B_{free}]$ can be written in terms of [EAB] and [T]: $[B_{free}] = [T] - [EAB]$ (6)

So using equation (6) and substituting for $[B_{free}]$, equation (5) becomes:
$K_B = \{ ([E_{total}] - [EAB]) . ([T] - [EAB]) \} / [EAB]$ (7)
This is an expression for K_B in terms of [EAB] and [T].

For the data fitting procedure involving the PSI-PLOT Program, equation (7) abovewas solved for [EAB]. This involved a quadratic function and the expression became:
$[EAB] = \{(K_B + [E_{total}] + [T]) \pm / (K_B + [E_{total}] + [T])^2 - 4 . [E_{total}]. [T]\} / 2$

The fitting equations then became:
$-(K_B + [E_{total}] + [T]) = I$

$[E_{total}] . [T] = P$

$[EAB] = \{ -I \pm / (I^2 - 4 . P) \} / 2$